The University Of Sheffield.

Department Of Mechanical Engineering

INVESTIGATING THE EFFICACY OF NOVEL ABRASIVE PARTICLES IN ORAL HYGIENE

Christopher Edward Rose

August 2015

Thesis submitted for the Degree of Doctor of Philosophy

Investigating the efficacy of novel abrasive particles in oral hygiene

Chris Rose

Summary

This thesis is concerned with the abrasive particles used within toothpastes for oral care products. The dynamic and abrasive characteristics of different particles is analysed using a variety of experimental and observational techniques, in order to discern their suitability as an abrasive agent upon sensitive human tissue such as dentine. It is of particular interest to companies working within Oral Care, to develop an abrasive formula that is both adept at removing surface detritus such as plaque, but does not cause damage to the underlying tissues of the tooth such as enamel and dentine. Further to their role as an abrasive agent for detrital removal, particles are also utilised to act as an aid against dental hypersensitity, by infiltrating and sealing off dentinal tubules. The main focus of this thesis is to study both the individual and collective behaviour of the particles in order to better understand the practicality and influence particles can introduce within oral care and why.

The efficacy of the particles is analysed from 3 key perspectives:

1. The abrasive performance of particles under a variety of tribological testing. Particular attention was paid to the wear characteristics of the particles upon key dental tissue.
2. Visualising and understanding the dynamic characteristics of the particles when motivated in an effort to relate these findings to wear observations.
3. To investigate the positive role of some key particles as an aid in dental hypersensitity.

It was found that subtle variation in particle size and shape can have a significant effect upon the magnitude of the wear. This shape can affect the abrasive properties in more than one way, either by having a more aggressive shape leading to increased scratching and material removal; or by augmenting the affinity of the particle to agglomerate and operate as an agglomeration when motivated.

Nano-manipulation techniques are employed to discern the dynamic characteristics of the particles. Being able to directly observe the particles when manipulated rather than attempt to derive suppositions from wear tracks, leads to a much improved understanding of a particles dynamic traits as well as the characteristics of particle breakdown.

A comparison is made between the occlusive efficacies of bespoke precipitated calcium carbonate versus typical ground particles. Clear differences between the particles were observed, highlighting a delicate relationship with the presence of water.

The aim of this research is to contribute further understanding of the important role that abrasive particles play within oral care, and to draw conclusions as to what factors play a key role in making a particle aggressive or sympathetic to a substrate surface.

Acknowledgements

For David and Anna Rose. Ta.

Glossary

AFM – Atomic Force Microscopy

SEM – Scanning Electron Microscopy

Plaque – An accumulated biofilm on the surface of teeth, primarily comprised of mucous and bacteria.

Calculus – Solidified plaque, hardened by mineralisation via contact with saliva.

Dentinal tubules /Dental canaliculi/ - Open pores within dentine that house the odontoblastic process. Play a key role in the transmission of stimulus to the nerve centre of the tooth.

Odontoblast - Aids in the secretion of dentine and translates external stimulus back to the dental pulp.

Buccal – Meaning of the mouth

Non-vital – The death of the pulp, unresponsive to all stimulation. Ultimately leads to necrosis of the tissue.

Vital – Healthy and living pulp material, responsive to stimulus.

Sulcus – Region where the gingival tissue meets the tooth; often referred to as the gum line.

Dentinalgia – Pain within the dentine of a tooth, synonymous with dental hypersensitivity.

Amelodentinal junction – Also known as the dentino-enamel junction it is where the dentine and enamel portions of a tooth meet.

Periodontal – Relating to the suspensory or surrounding tissues that support the tooth

Odontogenic – Relating to the formation of a tooth

Debridement – The removal of unwanted accumulated surface material, usually with the intent to let underlying tissues recover or flourish. In medicine debridement specifically relates to the removal of dead tissue. Within this thesis the term will be used from a dental perspective relating to the removal of detrital build-up, bio-film accumulation and plaque.

Erosion – Erosion discussed in this thesis will be from dental perspective rather than an engineering definition. Dental erosion is the loss of Odontogenic material through

mechanical processing with abrasives, often heightened through acid softening enamel. Erosion from an engineering process involves the gradual removal from a surface by impacting liquid of solid particles, often seen in pipework and is not appropriate within this research.

Contents

1 Historical overview of dental abrasives 1
1.1 Introduction 2
1.2 The importance of effective dental debridement and oral hygiene 4
1.3 Composition of toothpaste 6
1.4 Role of Abrasives 7
1.4.1 Particles as abrasives 7
1.4.2 Particles and tubule occlusion 8
1.5 Project objectives 9
1.6 Thesis layout 10
2 Tribology of particles 12
2.1 Surface fatigue 13
2.2 Abrasive wear 13
2.3 Particulate Erosion 14
2.3.1 Shape effect 14
2.3.2 Size effect 15
2.3.3 Hardness effect 16
2.3.4 Momentum effect 16
2.4 Review of dental abrasives 17
2.5 Summary 19
3 The Function and Structure of teeth 20
3.1 The formation of Dentine 21
3.2 Comparison of human and bovine dentine 24
3.3 Conclusions 25
4 Particle Characterisation 27
4.1 Imaging techniques 28
4.1.1 Refinement of imaging for dentine samples and preparation processes 29
4.2 Particles used in this study 31
4.3 Particle Sizing 36
4.4 Conclusions 39
5 Analysis of particle scratching 40

5.1 Scratch analysis using linear reciprocation and brush filaments 41
5.1.1 Experimental approach 41
5.1.2 Experimental results 42
5.1.3 Conclusions 54
5.2 Scratch analysis using linear reciprocation and Perspex plates 54
5.2.1 Introduction 54
5.2.2 Experimental procedure 55
5.2.3 Experimental results 55
5.2.4 Conclusions 58
5.3 Scratch analysis using rotation and Perspex 59
5.3.1 Introduction 59
5.3.2 Experimental procedure 59
5.3.3 Experimental results 61
5.4 Analysis of particle scratches on substrates of different hardness 62
5.5 Conclusions 67
5.5.1 Linear reciprocation trials 67
5.5.2 Contact plate trials 68
6 Analysis of particle friction 69
6.1 Inter-particle friction by angle of repose 70
6.2 Dynamic friction of complete contact 72
6.2.1 Friction of fixed particles 72
6.2.2 Friction of particles entrained by a brush 74
6.3 Modified Tribometer Friction analysis 76
6.3.1 Dry trials 78
6.3.2 Trials in solution 79
6.4 Conclusions 82
7 Wear of human dentine by particles 84
7.1 Hand brushed trials 85
7.1.1 Experimental apparatus 85
7.1.2 Experimental results 87
7.1.3 Conclusions 92
7.1.4 Surface damage characterisation 93

7.2 Automated brushing trials 96
7.2.1 Experimental apparatus 96
7.2.2 Surface damage characterisation 98
7.2.2.1 SEM Imaging of surface damage 99
7.2.2.2 Profilometry of surface damage 104
7.2.2.3 Vertical ball position change 108
7.2.2.4 Effect of Frequency 113
7.2.2.5 Surface roughness in relation to wear 115
7.2.2.6 Particle mixtures 117
7.3 Conclusions 122
8 Direct particle nano-manipulation 124
8.1 Background 125
8.2 Experimental procedure and sample preparation 126
8.3 Results 129
8.4 Discussion 142
8.5 Conclusions 146
9 Particle Agglomeration 148
9.1 Introduction 149
9.2 Analysis of agglomeration integrity by particle division trials 149
9.2.1 Experimental procedure 149
9.2.2 Results and discussion 151
9.2.3 Conclusions on sticky tape trials 160
9.3 Processing of particles in solution using ultrasound 161
9.3.1 Experimental procedure 162
9.3.2 Results 163
9.3.3 Conclusions for ultrasound trials 169
9.4 Summary of conclusions on agglomeration 169
10 Particle interaction with Dentinal tubules 171
10.1 Background 172
10.2 Experimental Methods 176
10.2.1 Dentine Samples 176
10.2.2 Experimental setup 176

10.3 Results 177
10.3.1 Dry Abrasive Particles 177
10.3.2 Wet Abrasive Particles 180
10.3.3 Anhydrous Paste and the Effect of Water Content 182
10.3.4 Nano-manipulation analysis 184
10.4 Discussion 187
10.5 Conclusions 189
11 Conclusions 190
11.1 Original Objectives 191
11.2 Particle conclusions 191
11.3 Review of nano-manipulation findings 192
11.4 Review of particle wear behaviour 194
11.5 Review of Dental Hyper-sensitivity findings 195
11.6 Recommendations and industrial application of findings 196
11.6.1 Key benefits of this research to end users 198
11.6.2 Critical Review of this research 199
12 References 201
13 Appendices 205

1 HISTORICAL OVERVIEW OF DENTAL ABRASIVES

Within this chapter the importance of good oral hygiene is introduced as well as a historical overview of how oral care procedures have changed over time. One of the main aims of the chapter is to both introduce common detrital materials that are found within the mouth; as well as highlight the importance of the removal of these accumulations, and the role abrasive particles play within this process. This particle role is considered from a duality of perspectives, and the primary objectives of this thesis are presented.

1.1 Introduction

The importance of maintaining good oral hygiene has been recognised throughout documented history. The process in which this was achieved and maintained has evolved from one epoch to the next and from one region to another; however the human race quickly gained an awareness of the benefits introduced through the systematic brushing and scouring of teeth and gingival regions. The Egyptians and later the Romans both recognised the importance of introducing ground abrasive material into their cleaning solutions, using materials naturally and readily available at the time. Common materials often included ground eggshells, animal bones, and ash all of which vary in the extent to which they can be milled and hardness of material. Trial and error would often be the key to developing an effective treatment to suit the dental physiology and diet of the time. Figure 1 shows examples of early Chinese toothbrushes.

Figure 1 Early Chinese toothbrushes and chew sticks [1]

The direct causes of poor dental hygiene and its physical manifestations such as caries and periodontal disease were largely unknown. The Sumerians in 5000 BC attributed such maladies to 'teeth worms', a belief which transcended into texts in ancient China and India. Despite a skewed perspective on the actual causation of these ailments they did recognise the necessity to remove dental detritus or inhibit its accumulation in order to improve their chances of maintaining good oral health. Due to the structural resilience and longevity of dental tissue we can learn a great deal about the dental practises of early civilisations and the extent of their knowledge of dental physiology through the study of archaeological finds. The surface topography of these samples can be studied, in order to analyse the degree and magnitude of scratching introduced through abrasive cleaning processes and gain and understanding of the typical abrasive additives used at the time. Figure 2 shows an image from the Bernardini F. et al study [2] of a Neolithic archaeological specimen

demonstrating a relatively proficient attempt at a cavity restoration using beeswax to seal the coronal orifice and dentinal fissure.

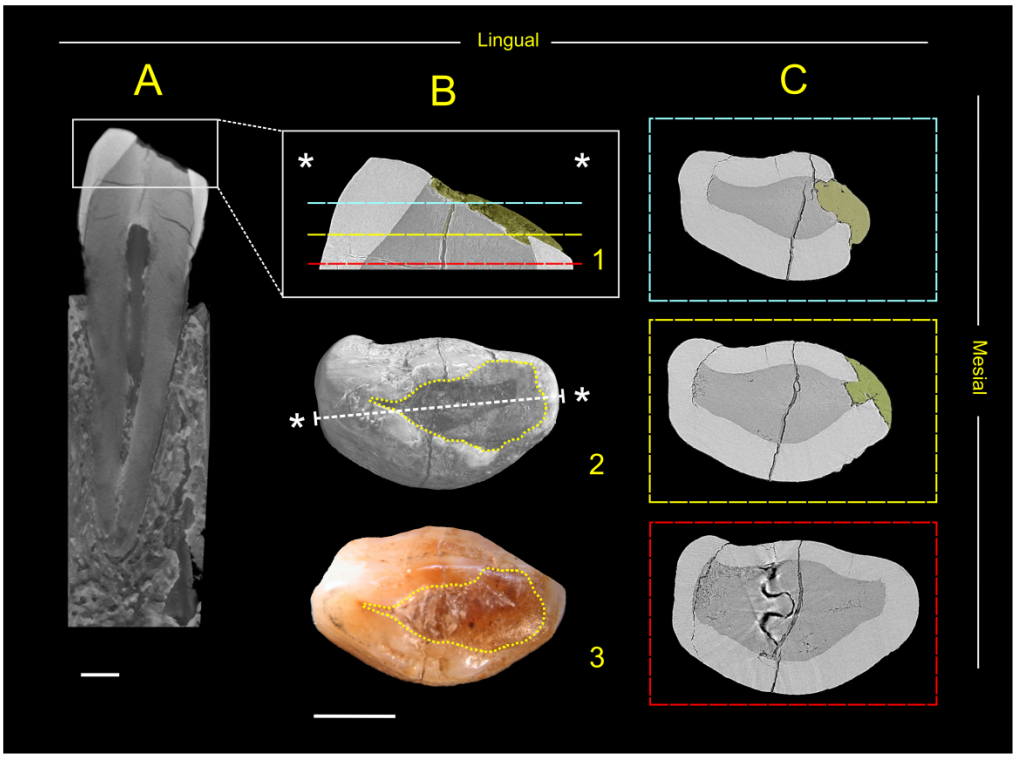

Figure 2 Distal-mesial perspective of sectioned Neolithic lower left canine using micro-CT [2]

Throughout the Middle Ages and into the 18th and 19th century great progress was made in the practical treatment of teeth. With advancements in technology and medical understanding it became easier and less invasive to remove and treat problematic areas. The focus was centred more on treatment rather than the prevention with the appearance of increasingly intricate tools for extraction and more refined composites for tooth restoration. It was not until the 19th and early 20th century that attention was shifted more to the maintenance of improved oral hygiene. During the 1930's, Frederick McKay, discovered the effects of fluoride in preventing tooth decay. As a result of this fluoride was added to water supplies, which led to a significant decrease in decay. The major advancements in toothpaste came in the early 1800's when dentifrice, more commonly known as tooth powder became more prevalent in Britain. Dentists, doctors and chemists were the main driving force behind the development of these powders which included materials which were aggressively abrasive to enamel and dentine. These powders typically included materials such as ground china and brick along with some derivatives of sea shell. The basis for most pastes was bicarbonate of soda which in later years was combined with Borax (a salt of boric acid) powder to encourage more desirable foaming characteristics. Although the importance of including these abrasive particles was known, there was no real understanding as to what made an effective abrasive additive. Often inclusive particles were outright damaging to teeth leading to significant enamel removal and gum recession.

In the early 1900's companies began to recognise the commercial opportunities in formulating competitive standardised recipes. Toothpaste began to be mass produced for the first time with more stringent considerations given to arguably more luxurious features, such as scent, flavour and foam-ability. Further to this, in order to gain a competitive edge over rival producers companies were beginning to commit more detailed thought as to the efficacy of the abrasive particles contained within their blends. Early examples of materials which are still used in oral care today (although in a refined form) were beginning to emerge, such as fine sand. Sand in essence is silica however the silica used in modern day pastes is much finer and less aggressive. Pumice, a lightweight volcanic rock was also becoming popular due to the ease with which it can be ground. Pumice consists of micro-vesicular glass and therefore could also be an aggressive material without refinement.

Despite improvements, investigations into abrasive particles largely took a backseat to analysis and refinements of aesthetic and cosmetic functions. For example there was much modification in the chemistry of toothpastes with re-mineralisation and reparation of tooth enamel of foremost interest, something that is still important today. It wasn't until there was an attention shift towards stain removal that the intricate relationship between pellicle removal by particles and whitening effects through chemical constituents and bleaching agents was acknowledged. The degree to which stain removal via mechanical erosion was achievable was heavily dependent on a multitude of variables associated with the particle itself. With a desire to remove ever more tenacious and intractable staining more understanding of the particle properties and its operational characteristics was necessary.

Commonly used materials today include calcium carbonate a chemical compound frequently found in rock as well as being the predominant constituent in the shells of marine organisms and eggs. Aluminium oxides and hydrated silica which is a form of silicon dioxide (often found in nature as the gemstone opal) are also regularly used. With the advancements in processing technology we are no longer constrained to materials that are easy to grind into fine particles. We now have at our disposal a plethora of materials all offering different characteristics and leading to different performance capabilities within the cleaning process.

1.2 The importance of effective dental debridement and oral hygiene

The importance of maintaining good oral hygiene is fairly well understood today. We can attribute poor dental health to a number of factors, the predominant three of which are listed below and shown in Figure 3.

a. Erosion – Often affected by diet. Acids in the food and drink we consume can lead to gradual thinning of the tooth enamel. Eventually this can lead to dentine exposure

and dental hypersensitivity. Other causes of erosion can be through teeth grinding and excessive tooth brushing.

b. Caries - More commonly known as tooth decay, this is a bacterial infection that results in the breakdown of the hard dental tissues. This is achieved by demineralisation of the surface via bacterial fermentation of unmoved detritus.
c. Periodontal disease – Also known as gum disease is usually a result of plaque being allowed calcify in the presence of saliva over time, turning the plaque into much harder calculus. This inhibits the removal of bacterial build-up in and around gingival regions, leading to localised infection and bone loss.

Figure 3 Images showing dental erosion [3], caries [4] and periodontal disease [5]

With the exception of dental erosion we can see that the majority of these issues are brought about through the ineffective removal of detritus. In general it is accepted that with frequent brushing we can hope to maintain good oral health but the complexity of the relationship between particle entrainment, abrasive material removal and the mode in which this is achieved is often taken for granted.

Plaque is essentially a biofilm, which accumulates upon teeth, primarily through the adsorption of bacteria and proteins. The plaque is able to adhere to teeth as a result of the Van der Waals and electrostatic forces present, encouraging further accumulation by forming intermolecular bonds with secondary colonisers. According to Wilkins [6], "Formation time means the average number of days required for the primary soft deposit to change to the mature mineralized stage. The average time is about 12 days, within a range from 10 days for rapid calculus formers to 20 days for slow calculus formers. Mineralization can begin as early as 24 to 48 hours". With the mineralisation process potentially commencing as early as within 24 hours, the importance of recurrent and effective dental scouring is clear. The hardness of calculus is significantly higher than that of its predecessor plaque and its removal requires specialised equipment usually operated by a dental professional. Abrasive particles therefore are designed for processing detrital materials of a similar composition to that of plaque and there is inherent commercial value in the efficacy of this removal process by abrasives.

Although the swift removal of surface pellicle is essential in as comprehensive a manner possible, it is important not to lose sight of the fact that abrasives can be damaging to the substrate surface.

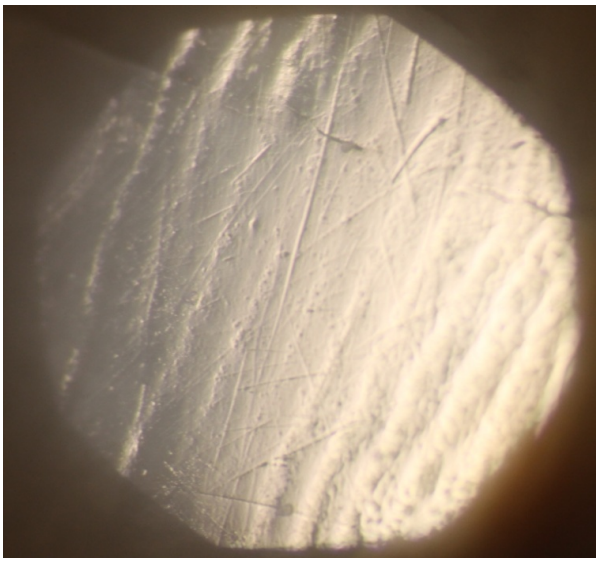

Figure 4 Optical microscope image at 10x magnification of buccal face of upper incisor

Designed to protect teeth from damage, enamel is an especially hard material. Covering the crowns of the teeth it is comprised of highly calcified prisms of apatite arranged in columns. With a Vickers hardness of around 290 kgf/mm^2 (measured using a load of 196N) it is a very tough material, however as can be seen in Figure 4 the surface can become scratched by abrasive particles. Vickers hardness is often presented as a number only, for example 290 HV rather than the units Kgf/mm^2. Alternatively these can be multiplied by the acceleration due to gravity (g) to present these figures in MPa. Dentine on the other hand is much softer at around 60 kgf/mm^2 and is therefore much more susceptible to damage through abrasive cleaning. These hardness values were acquired by conducting Vickers indentation testing on samples collected by the experimenter (the author), the acquisition and preparation details of which are discussed in detail later in this thesis. Dentine can become exposed through a number of factors including dental erosion discussed above and gum recession. It is for this reason the abrasive particles adopted must be meticulously investigated and scrutinised so as to ensure they pose no threat to dental tissue. Chapter 7 studies in more detail dentinal wear and material loss through abrasive processing.

1.3 Composition of toothpaste

There are a number of component parts that comprise modern day toothpastes. Arguably the most proactive ingredient in the removal of plaque and consequently the maintenance of good oral hygiene is the abrasive particle. It is important however to recognise the other constituents and the synergistic relationship they share. These ingredients are as follows:

- Abrasives – The driving force behind detrital material removal. Particles are designed to be effectively entrained by brush filaments and abrasively remove plaque and bacterial build-up. Their effectiveness is dependent on many factors making them the subject of rigorous study. They are the subject matter for this thesis.

- Binder – Often derived from seaweed colloids and natural gums, the role of the binder is to stabilise the mixture by preventing the separation of liquid and solid phases. They achieve this by swelling in the presence of water and are sometimes referred to as hydrophilic colloids.
- Humectants – These are included to prevent the paste from drying out by inhibiting the loss of water when exposed to air for prolonged periods. Sorbitol and Glycerol are common examples of humectants.
- Detergent – An important working aid to the abrasive particles, detergents have a dual purpose. One role is to lower surface tension thus helping to loosen detritus and ultimately help emulsify the material removed by particles. A secondary role of detergents is to contribute to the foaming nature of the paste, which is considered desirable to users.
- Preservative – to maximise the shelf life of the toothpaste
- Flavour – Principally a variation of mint flavouring added to improve the brushing experience for the user.
- Therapeutic agent – In most cases the 'therapeutic agent' introduced is fluoride. Discussed earlier in this chapter fluoride has many beneficial effects within oral healthcare including reducing the incidence of periodontal disease and dental caries.

There is considerable variation in the respective proportion of these inclusions from manufacturer to manufacturer. Eric C. Reynolds, summarises a typical formulation as follows in Table 1 [7]:

	Component						
	Abrasive	Binder	Humectant	Detergent	Preservative	Flavour	Therapeutic agent
Proportion	10-40%	1-2%	20-70%	1-3%	0.05-5%	1-2%	0.1-0.5%

Table 1 Typical proportion of component parts for toothpaste formulations [7]

1.4 Role of Abrasives

1.4.1 Particles as abrasives

The efficacy of modern day toothpastes is heavily dependent on the abrasive particles contained within, which typically contribute a large proportion of the paste constituents. The range in abrasive performance and dynamic characteristics from one particle to another is considerable and is reliant on a number of different factors. The primary role of the particle is to aid in the abrasive removal of plaque and surface staining whilst inhibiting the formation of calculus. When dental detritus develops upon teeth and around gingival regions over prolonged periods of time, calcium salts within the saliva progressively mineralise plaque into calculus [8]. This tough layer traps bacteria and food particles

beneath, whilst at the same time preventing effective irrigation of the area by manual brushing. Effective removal of build-up is therefore important in the first instance.

Particle characteristics such as size, shape, affinity to agglomerate and material hardness all contribute to cleaning efficacy and effective pellicle removal. Particles are often selected based upon its position on the Mohs hardness scale. As a general principle a harder material will scratch and remove material from a softer material [9]. It is desirable therefore for particles to fall within a window of hardness that makes it harder than the detritus to be removed, but softer than the tooth surface that it is important to remain sympathetic to. The value of abrasive particles within toothpaste can be plainly observed when brushing regions of pellicle or staining with the abrasive grains removed. There is little resultant material removal and it is evident that filament upon tooth brushing is not enough for satisfactory dental irrigation.

Studies have been conducted to better understand the interaction behaviour of different particles with brush filaments as well as how resultant material removal is achieved. Lewis and Dwyer-Joyce et al investigated particle motion and stain removal during simulated abrasive tooth cleaning [10]. Using a combination of visualisation studies and tribological abrasive testing the efficacy of particle capture was analysed alongside quantitative results from abrasive stain removal experimentation. Other studies have adopted computer simulation technology in order to model three-dimensional abrasive particles. De Pellegrin and Stachowiak [11] use such an approach to computationally represent and geometrically quantify features such as particle sharpness for particles used within industrial cutting processes.

The way in which this study aims to develop these ideas and further the dynamic understanding of the abrasive particles is by using direct in-situ nano-manipulation technology to directly observe and attempt to understand the dynamic behaviour of abrasive particles under stimuli and relate this to tribological laboratory experimentation. Within this study more extensive bespoke particle geometry, developed through tailored precipitation processes, are analysed in order to try and acquire an understanding of the effect this has on the mechanism for particle movement and inter-particle relationships.

1.4.2 Particles and tubule occlusion

Further to the active cleaning of teeth particles can serve a dual purpose in combating dental hypersensitivity. Discussed in more detail in chapter 3.4 the predominant cause of dentinalgia (the generation of pain through the internal stimulation of dentinal tubules) is through the hydrodynamic effect. A key avenue of study within this thesis is the potential of bespoke particles in interacting with dentinal tubules so as to provide a protective barrier against nerve stimulation. Arrais et al [12] investigates the obstruction of dentinal tubules

using different operational mechanisms. The blocking of tubules via the presence of abrasive particle which have managed to infiltrate the lumen is compared with that achieved indirectly via the formation of a smear layer and through the use of active agents within the dentifrice slurry. Further studies have been conducted [13] investigating the use of active agents which are key features in the well known toothpaste brand Sensodyne®. These agents include the bioactive glass calcium sodium phosphosilicate, which has been linked with dental remineralisation, and Strontium acetate, which has similar properties to calcium and is used to replenish lost dentinal tissue and block tubules by deposition and expansion.

The fundamental difference between these aforementioned techniques for achieving dentinal occlusion and that investigated within this study is the mechanism for lumen occlusion. This study focuses on the affinity of bespoke tailored particles in forming efficient and strong physical barriers without the aid of active agents. The interaction and impregnation of these particles within tubule orifices is not purely a result of particle size and random chance.

1.5 Project objectives

The aim of this project was to evaluate the physical attributes, understand the dynamic behaviour and determine the efficacy of novel abrasive particles for use in toothpaste. The project was sponsored by Unilever and the particles studied were developed for potential inclusion in the next generation of Unilever's oral care range.

The key objectives were thus:

1. Particles were to be studied using a number of different analytical techniques in order to gauge their competency and discern any potential competitive characteristics regarding abrasive cleaning
2. To understand and characterise the dynamic behaviour of a range of novel abrasives using conventional and bespoke tribological testing
3. To investigate properties relating to particle entrainment through filament capture during the brushing process
4. To understand the collective properties of the particles and investigate how they interact each other.
5. To investigate the efficacy and suitability of the particles as a sensitivity aid by studying particle interaction with dentinal tubules under varying operating conditions and environments
6. To highlight any potential adverse effects particles might introduce to dental tissue and understand the reasoning behind it

1.6 Thesis layout

Chapter 1 discusses of the role of the abrasive particle within oral healthcare and provides an overview of the thesis, its aims and objectives. The tribology of abrasive processes and mechanisms is considered within chapter 2. Chapter 3 studies the function and structure of dentine and highlights why this tissue is of significance within the field of dental debridement. It is in this chapter the origins of dental hypersensitivity are explained and the role of particles as a treatment examined.

Chapter 4 introduces the abrasive particles to be studied within this thesis. Using SEM imaging this chapter aims to familiarise the reader with the dimensional and aesthetic properties of the particles.

Particle abrasive scratch properties are studied in chapter 5. Using a variety of linear reciprocation techniques the characteristics of particle capture and entrainment, as well as substrate surface degradation are studied under varying operating conditions. Chapter 6 expands upon these findings with more detailed examination of cumulative particle friction. Using more specialised tribological technology particle behaviour is evaluated using both laboratory and more representative setups.

Chapter 7 considers the dentinal wear properties associated with each particle under different operating conditions. Using a variety of post processing techniques such as profilometry and atomic force microscopy, alongside optical and scanning electron microscopy; the aggressive or passive nature of the particles upon key dental tissues is investigated.

In chapter 8 the dynamic characteristics and mechanistic properties of particles are studied. Using in situ nano-manipulation SEM technology, the mechanisms for movement of motivated particles can be directly visualised. A key chapter in this thesis, this area of the research provides visual support for findings and data derived in other chapters. Using this technology we are not only able to discern the modes of movement but also other particle properties such as characteristics of fracture under loading and affinity to agglomerate.

Chapter 9 explores the agglomerative properties of the abrasive particles. Further to analysis of individual particle behaviour the likelihood of particles operating as larger agglomerations, the shape of these agglomerations and their structural resilience is investigated.

Chapter 10 investigates the efficacy and suitability of different particles as an aid against dental sensitivity. Using nano-manipulation in conjunction with SEM analysis, the affinity of particles to interact with, penetrate and seal dentinal canalinculi is investigated.

Conclusions are summarised and discussed in Chapter 12.

All work conducted for the purposes of this thesis was done so with the direction of the sponsor company, with the aim of deriving the optimum amount of information on the particles relevant to the most important products utilised at that time. The importance of the different particles and their implementation was often shifting throughout the duration of the project, and for this reason in some trials particles are omitted from study and sometimes not revisited. Despite careful consideration being applied to particles of notable value to the sponsor company (for various reasons including accessibility, cost and recent results), all results are considered to provide an overview of findings for particles in general.

2 TRIBOLOGY OF PARTICLES

Tribology, or “The study of friction, wear and lubrication; the science of interacting surfaces in relative motion” [14] encompasses the main domain of this thesis. Within this chapter, the interaction of particles both with each other and with the odontongenic materials of the tooth is considered. Common tribological principles are presented with particular attention paid to wear, which is defined as the loss of material from a surface caused by a contacting counterface [15]. The nature of each interaction evidences itself by observation of the wear scars left behind after the surfaces have contacted. Within this chapter various wear processes are all discussed from a Tribological perspective and are not to be confused with like dental terminology which can sometimes hold different meanings.

2.1 Surface fatigue

Otherwise known as delamination wear, surface fatigue involves the propagation of sub surface cracks which nucleate until the contact region delaminates [16] [17]. It is most often found in metal contacts but can be found elsewhere. Evidence of surface delamination has been observed with dentine, likely a result of its potentially brittle nature and laminar structure. The full sequence of events is shown in Figure 5 involves:

- The transmission of normal and tangential loads through asperity contact by adhesion and ploughing leading to the smoothing of the softer surface. (a)
- Cyclic loading of the smoothed plane by asperities (b)
- Subsurface deformation and nucleation of cracks (c)
- Crack extension and propagation parallel to the surface
- Shear at the surface removing long thin sheets of material (d)

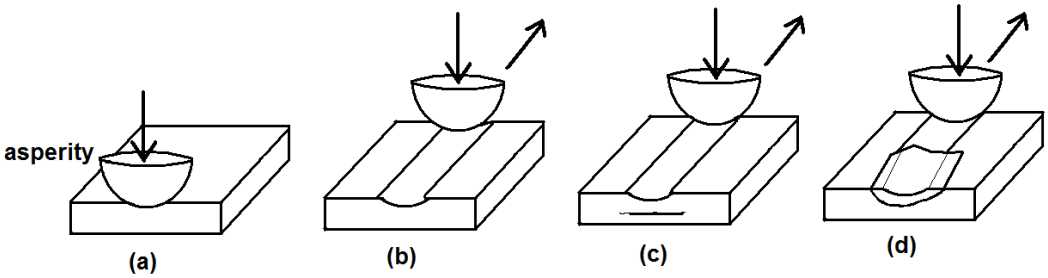

Figure 5 Surface fatigue mechanism of wear

2.2 Abrasive wear

There are two wear situations that give rise to abrasive wear; two-body and three-body abrasion. In both cases, a softer surface is ploughed by harder materials. The classification describes whether the abrasive particles are constrained (two-body) or free to roll (three-body) [18].

Various mechanisms have been proposed by which abrasive wear occurs including ploughing, cutting and fragmentation [19]. The most commonly accepted form of two body abrasion describes how the asperities of the harder surface remove those of the softer surface (Figure 6)

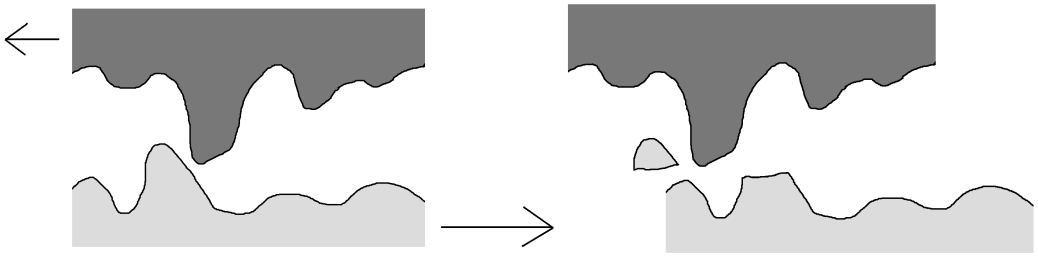

Figure 6 Mechanism of two-body abrasion

In three body abrasion particles between the contacting surfaces cause the removal of material by ploughing (Figure 7)

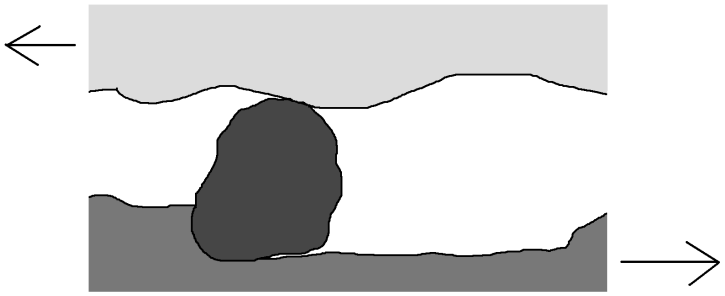

Figure 7 Mechanism of three-body abrasion

Often during contact, material removal by two-body abrasion forms into a three-body abrasion regime as the debris becomes trapped within the contact area.

Abrasive wear is normally characterised by long parallel grooves in the contact direction, which can vary in extremity from light scratches to heavy gouging. Various parameters are known to influence the wear rate of materials by abrasion including ductility, relative hardness, contact relative speed and moisture level. Generally abrasive wear is an unwanted side effect of sliding contact in the presence of abrasive particles however, in certain cases, such as the topic of this thesis, controlled three body abrasion with particulates can be desirable.

2.3 Particulate Erosion

Particulate erosion describes the progressive removal of small amounts of material from a surface by particles. This is comparable to 3-body abrasion however characteristics or 'effects' of the body in question can affect the efficacy of the body in the material removal process. Various properties of particles are known to have an effect on the ultimate wear regime and wear rate of a substrate. These include particle shape, particle size, hardness, angle of impact and velocity. There is also a difference in wear mechanism between ductile and brittle substrates, all of which is discussed below.

2.3.1 Shape effect

The angularity of particles has a strong effect on the wear rate of materials although it is difficult to define precisely and quantify. Since particle shapes are generally complex three-dimensional geometries they are often not measured quantitively [15]. Description of a two-dimensional projection is often used to give a qualitative assessment of a particles shape. Figure 8 shows a scanning electron microscope image of particles of differing angularity. With all other properties remaining constant, it would be expected that the more angular particles develop a significantly higher wear rate of a substrate than the rounder particles.

We will see throughout this thesis however that subtle variations in these other particle properties can have a dramatic affect on the aggressive nature of the abrasive particle.

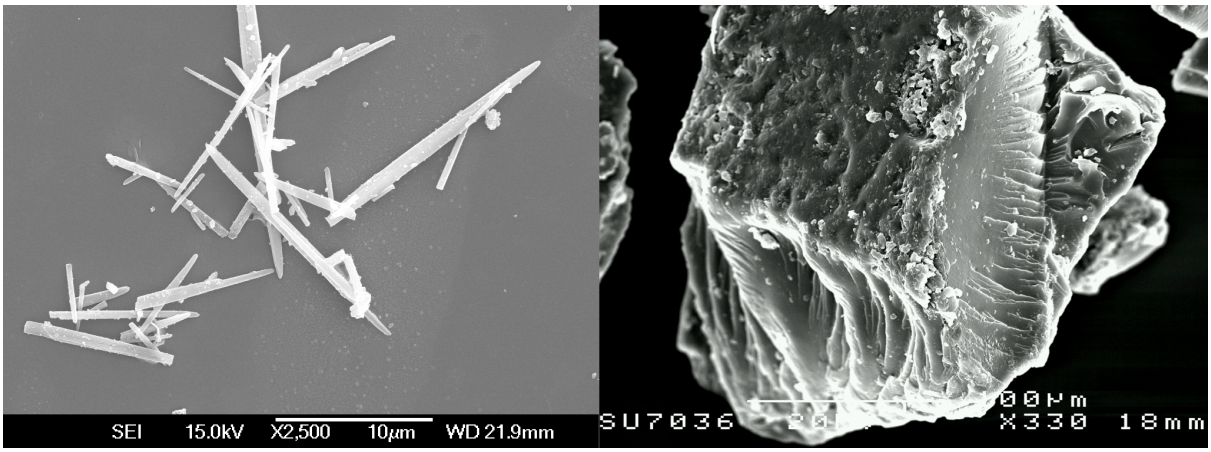

Figure 8 Electron micrograph of more angular particles (Left – Maruo Rods) and rounder particles (Right – Polyester Resin)

The mechanism by which particle angularity affects wear rate is due to the pattern of plastic deformation and proportion of material displaced by each indentation [20] [21]. Angular particles tend to form a rim or lip whilst more rounded particles have less localised deformation leading to an increase in the number of contacts required to generate wear. The roundness of a particle or body is most commonly attributed to how closely the shape of that body approaches that of a circle. It may be that a particle has many small-scale angularities or projections, however it is the large scale overall features that dictate the roundness of the object. For example in Figure 8, it could be said that the needle like Rod particles have a relatively smooth and spherical cross section whereas the larger Omya particles are quite rough in appearance with increased jagged projections. When gauging the geometry of the particles on the whole however it is easy to determine that the Omya particles are rounder than the needle like Rods due to their more obvious spherical nature. The roundness of particles throughout this thesis is judged according to these guidelines.

2.3.2 Size effect

The size of particles is known to affect the wear rate during abrasion. The mechanism may vary depending on particle size from polishing by sub-micrometre particles to gouging by millimetre-sized particles. In addition the severity of the wear is likely to decrease as particle size decreases below 100µm [22]. This is most likely a result of larger particles being more readily entrained and motivated along with a potential change in dynamic behaviour of larger particles compared to smaller (sliding potentially becoming rolling with an increase in size). The particles responsible for the most aggressive abrasive wear are generally between 150µm and 500µm [15]. The increase in wear rate with increasing particle size is thought to be due to a size effect in the strength of the material.

2.3.3 Hardness effect

Particles with hardness lower than that of the surface with which they contact cause less wear than harder particles. Wear rate is more sensitive to the ratio of particle/surface hardness when the abrasive hardness is lower than the surface hardness. This condition is due to the plastic deformation of either the particle or the surface depending on which is harder (see Figure 9).

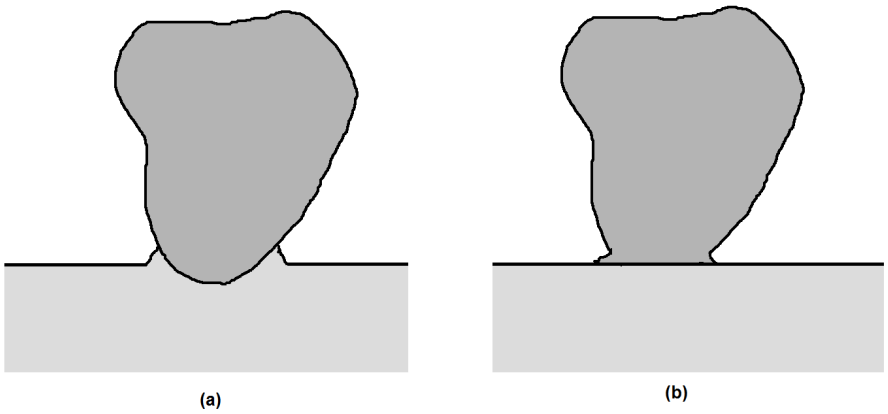

Figure 9 Particle indentation under normal load in which (a) the particle has higher hardness than the surface and (b) the surface has higher hardness than the particle

Deformation in this instance (figure 9) can be both plastic or elastic depending on the properties of the particle and the counterface it is contact with. Elastic deformation may be less damaging to the surface in the first instance however the way in which this could potentially augment the dynamic behaviour of the particle (potentially initiating a rolling motion) could still lead to notable damage.

2.3.4 Momentum effect

Many forces can act upon a particle in contact with a surface; inter-particle contact forces, drag forces, gravity, surface forces and fluid flow. The deceleration of a moving particle is primarily done by contact force with the surface. The energy transferred into the surface by the particle leads to wear, and therefore particles travelling with higher energy (momentum) lead to larger energy transfer and higher wear rates. In this way, a heavier particle and a particle moving more quickly lead to a more rapid wear of the surface. It should be considered however that particles have the ability to operate both in isolation and form (potentially large) agglomerations. Thus smaller particles could, if acting in an agglomeration, cause greater wear. The agglomerative behaviour of particles is studied in more detail in later chapters. It should also be noted, that for a given mass of particles, if the particles are small there are many more present per unit volume compared to if they are large. This means that a mass of small particles can be greatly more abrasive than the same mass of large particles.

2.4 Review of dental abrasives

A good abrasive is one that is adept at removing unwanted material from a surface effectively and efficiently. This can be affected by a number of different factors such as:

- The size of and shape of the abrasive grain
- The difference in hardness between the abrasive particle and the abraded material
- The efficacy of entrainment and the transfer of the applied load through the particle to the substrate

Although the abrasive processes are similar, there are differences in the requirements for particles adopted for conventional abrasive cleaning processes compared to those used as dental abrasives. The most obvious of these is the delicate nature of the human tissue the abrasive process is being conducted upon.
It is important that dental abrasives balance the duality of performance requirements in both removing surface build-up and polishing the substrate surface. In principle a large number of small scratches is visually subtler than a single large scratch, which may imply that small particles may be most useful within oral care. R.L.Aghan et al looked into the mechanistic behaviour behind abrasive polishing. Here they showed that fine abrasive polishing operations could occur by a mechanical mechanism in which very small chips are cut. The difference between polishing and abrasion in this respect is only one of degree [23]. This study provides evidence to show how the abrasive particles are held so that they may act as planing tools

In reality the efficacy of the abrasive process is more complex, large particles are likely to be more adept at removing surface build-up. Also it cannot be assumed that particles operate solely in isolation, but potentially as agglomerates. The most common material used within toothpastes are Calcium Carbonate, Silicas and Perlite. Calcium Carbonate ($CaCO_3$) occurs naturally under three crystal structures: Aragonite, Valerite, and Calcite; the latter being the most commonly occurring. The hardness of Aragonite is conveniently placed lower than calcite however due to its lower prevalence in nature precipitated carbonates are often considered [24]. More detail on the structure and composition of these materials can be found in Chapter 4.

Lewis and Dwyer-Joyce [25] investigated the interaction between abrasive grains and substrate in cleaning processes. They highlighted the effects of the formation of a fluid layer in facilitating the transit of particles through the filament-substrate contact. The trials discussed here were all conducted without the presence of fluid and therefore the behaviour of particle entrainment cannot be affected by the formation of a boundary layer. Particles are analysed with a fluid presence later in this thesis. Lewis and Dwyer-Joyce carried out visualisation trials using modified optical equipment to show that the majority of

particles become trapped at the filament tip, with only a small minority of the scratched particles (circa 10%) contributing surface damage in the form of scratching.

There are multiple considered mechanisms for the abrasive behaviour of particles.; these mechanisms can change with a change in particle size and shape. H.Sin et al investigated the effect of size upon the abrasive wear mechanism. They concluded that the grit size effect is a consequence of the transition from a cutting mechanism to a sliding wear mechanism. The wear coefficient in this case was shown to be less than that predicted by a cutting model owing to the plastic deformation of the surface being worn [26].
E. Rabinowicz et al showed that, for any system, there exists a minimum abrasive particle size which allows maximum abrasive action. They suggested that this critical abrasive size corresponds to the size of adhesive wear fragments of the material being abraded. Their experiments showed good agreement between the postulated and measured critical abrasive sizes [27].

There has been much investigation into the abrasive performance and mechanistic properties of dental abrasives when administered using alternative (often powered) apparatus. L. Yin et al investigated the material removal mechanisms of dental ceramics using a dental hand piece and burs impregnated with different grit sizes. The material removal rates were measured as a function of total machining time. It was found that, as the grit size was increased from ultrafine to fine and coarse, the removal rate and the resulting surface roughness for each material increased substantially. The mechanisms of material removal were found to consist of a combination of ductile and brittle-type chip formation processes. The occurrence of brittle fracture increased as the grit size was increased. While the material removal process in porcelain was dominated by brittle fracture, zirconia was primarily subjected to ductile cutting. Four wear processes were identified on the burs in prolonged cutting tests: grit micro fracture, grit pullout, wear flat generation, and matrix abrasion [28].

Although trends and observations can be defined through experimentation (similar to the aforementioned), such as the effect of grit size on the expected behavior of the particle, the complexity of filament entrainment as well as other factors makes understanding the characteristics of particles in oral debridement difficult. Chapter 4 highlights the wide variety of abrasive particles adopted within the industry, with a multitude of shapes, sizes and material properties. Experimentation is carried out within this thesis in an effort to observe possible trends between materials and shapes and also to reveal the aggressive or sympathetic nature of different abrasive particles.

2.5 Summary

There are a number of different mechanisms in which an abrasive particle can operate, each with different characteristic properties. The requirements for abrasive particles within oral care are multifaceted. It is necessary to remove surface build-up as quickly as possible, however with regards to the substrate (enamel or dentine) it is desirable for particles to act as more of a polishing agent. This is desirable not just for aesthetic purposes but also to minimise the potential foundation for future plaque reformation brought about by scratch prevalence. As calculus is formed by nucleation and pearlisation, any remaining plaque deposits would usually encourage re-growth and propagation; a smoother surface should stave off the reformation of plaque for longer by presenting less nucleation sites. An abrasives formula could therefore be employed which is capable of introducing more subtle micro-scratches with the intention of making the tooth surface more 'plaque phobic'. This would a useful claim for prospective manufacturers in oral care.

The abrasive process involved within oral care using brush filaments to motivate particles introduces a significant number of variables. The loading and entrainment of particles is inconstant as well as the delicate nature of the substrate and particle breakdown potentially leading to third-body abrasion. It also cannot easily be known the extent in which particles are operating as individuals or as part of an agglomeration. Some of these questions can be answered through experimentation and analysis of wear tracks. Although mechanistic characteristics can be defined this way it does not necessarily explain completely how particles interact or move. In order to more directly observe the dynamic properties of abrasive particles in-situ analysis is required. Both of these approaches are explored within this thesis.

3 THE FUNCTION AND STRUCTURE OF TEETH

This chapter introduces the primary material adopted as a substrate within this thesis, dentine. The material makeup of dentine is introduced along with its function and location within the tooth. There are different classifications of dentine, which are discussed, with consideration as to the most suitable for experimentation in this case. The reason dentine is of particular concern during the teeth cleaning process is because of its reduced hardness when compared with the protective layer enamel. As mentioned in Chapter 1 dentine can easily become exposed via a number of processes; it is very common for individuals to have a notable incidence of exposed dentine at any point in time. Not only can dentine be at risk of painful stimuli when brushing but also abrasive material removal. Within this chapter consideration is given to the use of bovine dentine as a suitable substitute for human dentine, for the purposes of wear experiments.

3.1 The formation of Dentine

Dentine is a calcified tissue and is one of the four major components of teeth along with cementum, pulp and enamel. The predominant constituent of teeth, it is covered by enamel on the crown and cementum on the root and surrounds the entire pulp. Approximately seventy percent of dentine consists of the mineral hydroxyapatite, twenty percent is organic material and ten percent is water.

Figure 10 shows the basic layout and morphology of a typical human tooth. The sample shown is a 3rd molar (commonly known as a wisdom tooth) and was sectioned and studied within 24 hours of extraction. The darkened appearance of the pulp chamber is a result of necrosis of the nerve, after it became non-vital through impact; ultimately leading to the removal of the tooth. No caries or other manifestations of poor dental health were present in the sample.

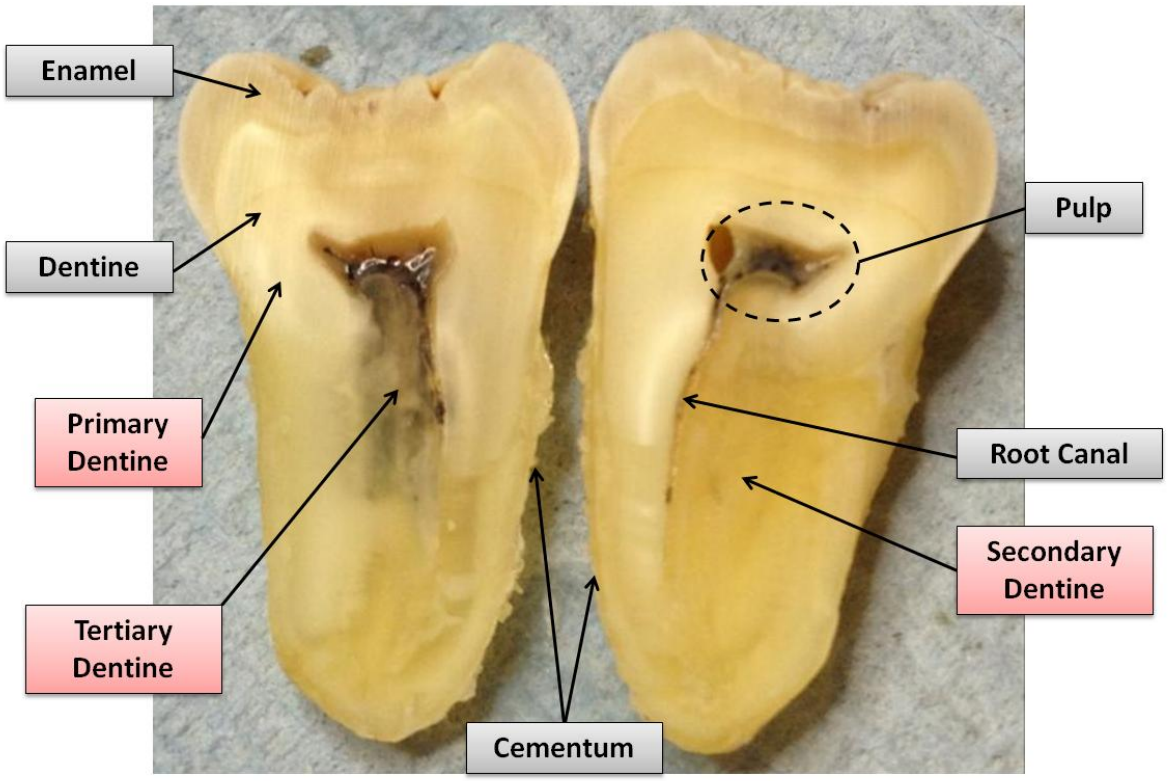

Figure 10 Sectioned 3rd molar from human female

A specialised type of bone, dentine is created by odontoblasts. Dentine differs from comparable tissues in that it is comprised of cellular extensions rather than complete cells; these projections are cytoplasmic extensions from the odontoblast. These extensions span the entirety of the dentine originating from the cell body located at the boundary between the dental pulp and the dentine through to the dentine-enamel junction. These tubular processes are referred to as dental canalinculi or dentinal tubules and are talked about in more detail later in this chapter. The formation of dentine is a multi-stage process. Firstly the odontoblasts form the organic matrix known as predentine. Over time, within this

matrix spherical masses are developed initiating calcification. These spheres fuse as they develop in size leading to the formation of the darker more familiar mineralised dentine.

As shown in Figure 10 there are three different classifications of dentine present within the structure of a tooth; primary, secondary and tertiary dentine. Within these classifications there are differently titled examples of dentine however these are largely titled specific to location and are generally not of a dramatically different composition or structure. Primary dentine is largely comprised of mantle dentine and circumpulpal dentine. Mantle dentine is located immediately adjacent to the border with enamel whereas circumpulpal dentine forms the inner portion of dentine adjacent to and surrounding the pulp. This distinction is necessary as although the density and consistently are generally similar, there are some subtle differences between the geometry and layout of tubules due to the conditions and rate with which the tissue was formed. When investigating the interaction of particles with dentinal tubules it is important that the dimensions and proportions of these features be representative of those that would be involved in typical everyday brushing scenarios. For this reason work concerning particle-tubule interaction was conducted upon mantle dentine as this is dentine which would become exposed through the depletion of enamel. General tribological and wear experiments were extended to both mantle and circumpulpal dentine due to the similar nature of their mechanical and frictional properties.

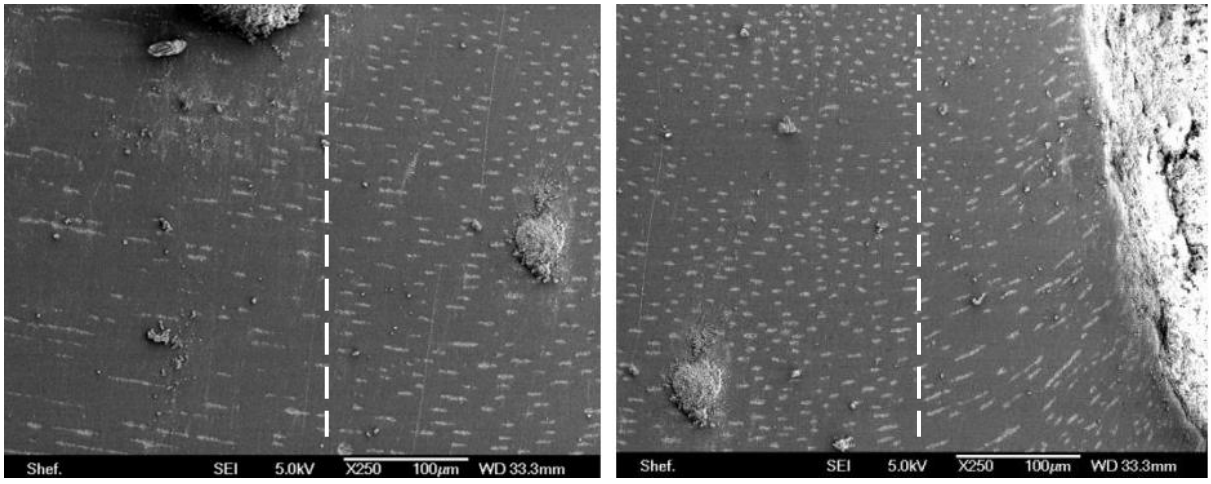

Figure 11 Electron micrographs showing the variation in tubule orientation across transitions in dentine type.

Figure 11 demonstrates how it is not unusual for changes in the consistency of dentine, when passing from one grade to another, to affect the trajectory of tubules. Both images are taken from the second molar of a middle aged male.

Secondary dentine is formed throughout the functional life of the tooth and over time its gradual deposition leads to a narrowing of the pulp chamber. Tertiary dentine on the other hand, often referred to as reparative dentine is formed as a pulpal response to trauma. As a result of the increased rate in which it is formed tertiary dentine differs from primary and secondary, having a more irregular structure. Figure 12 shows a presence of tertiary

dentine, which was likely initiated by the impact the tooth incurred. Tertiary dentine is not used in any laboratory testing throughout this study.

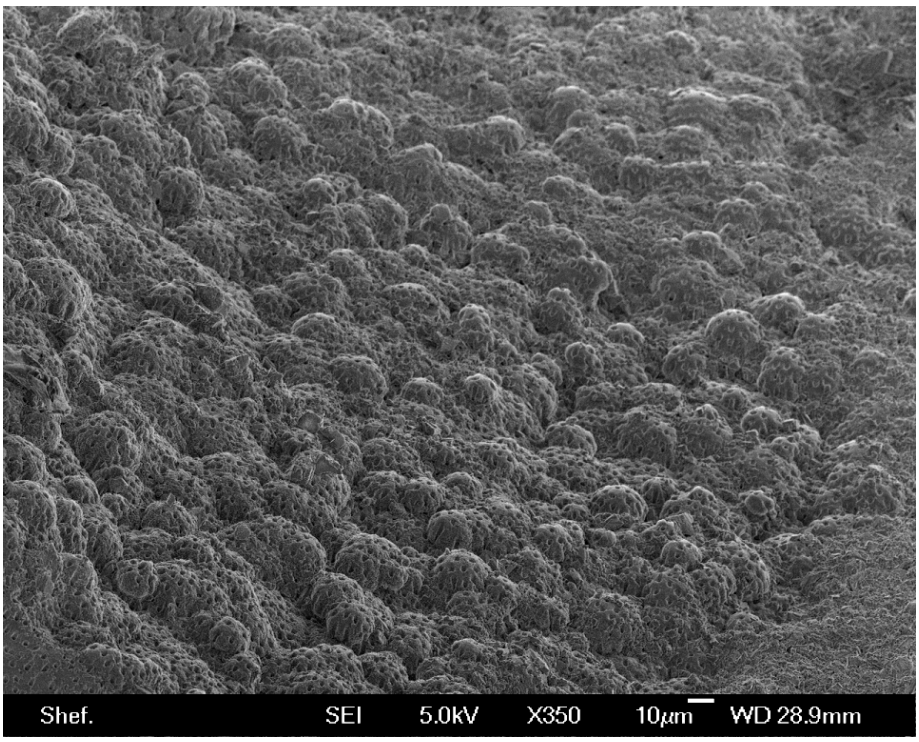

Figure 12 SEM micrograph of inside of pulp chamber showing development of secondary dentine

The secretion of the dentine matrix by odontoblasts during the formation of dentine is carried out in discrete increments. As this calcifies the mineralisation phases remain visible and are referred to as the contour lines of Owen. A similar process occurs in the development of enamel and these are referred to as the lines of Retzius. Figure 13 below shows these features respectively.

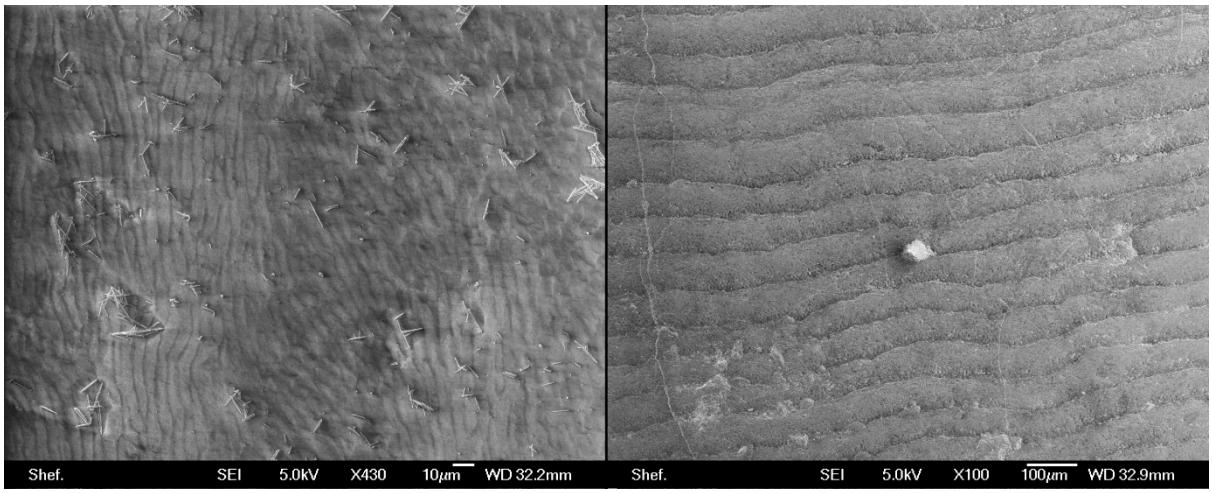

Figure 13 SEM micrographs of human dentine and enamel showing the lines of Owen (spanning vertically) and Retzius (spanning horizontally) respectively

3.2 Comparison of human and bovine dentine

Due to its availability and low commercial cost bovine dentine is often studied as a substitute for human dentine. There are many similarities in the structure and morphology of both tissues however it is important, particularly with trials concerning particle-tubule interaction, that tubule geometry be highly representative. A good deal of literature has been produced investigating Bovine dentine as a substitute for human dentine however much of these comparative studies have been focussed upon the characteristics of the two materials as a foundation for adhesive dental restorations. Within these studies, different regions and different grades of dentine are often analysed. Schilke et al reports that:
"Corresponding coronal dentine layers of human deciduous and permanent molars, and of bovine central incisors, are not significantly different in the number of tubules per mm2 and their tubule diameter; whereas tubule density in bovine root dentine is significantly higher. These results suggest that provided standardized preparations are used, bovine incisor crown dentine is a suitable substitute for human molar dentine in adhesion studies"[29].

Initial trials were undertaken to investigate the suitability of bovine dentine as a substitute in experimental trials. Samples of both bovine and human dentine were analysed using scanning electron microscopes to image and statistically compare the frequency, density and geometry of dentinal tubules.

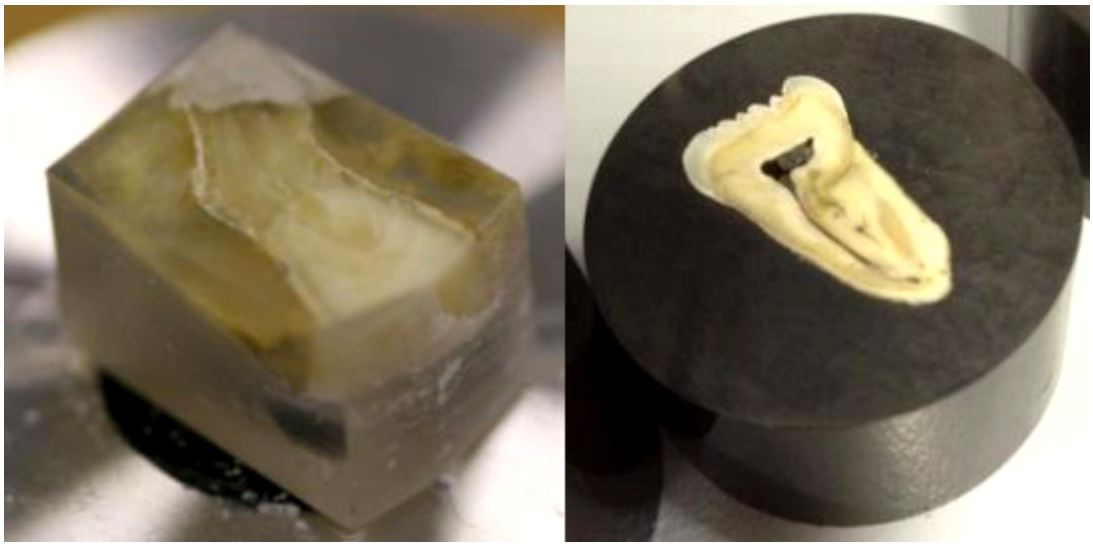

Figure 14 Left: Coronal bovine dentine, Right: Bisected human molar set in Konuctomet phenolic compound

Figure 14 shows the prepared dentine ahead of SEM imaging; samples remained uncoated. Figure 15 shows comparative micrograph images of the tubule arrangement.

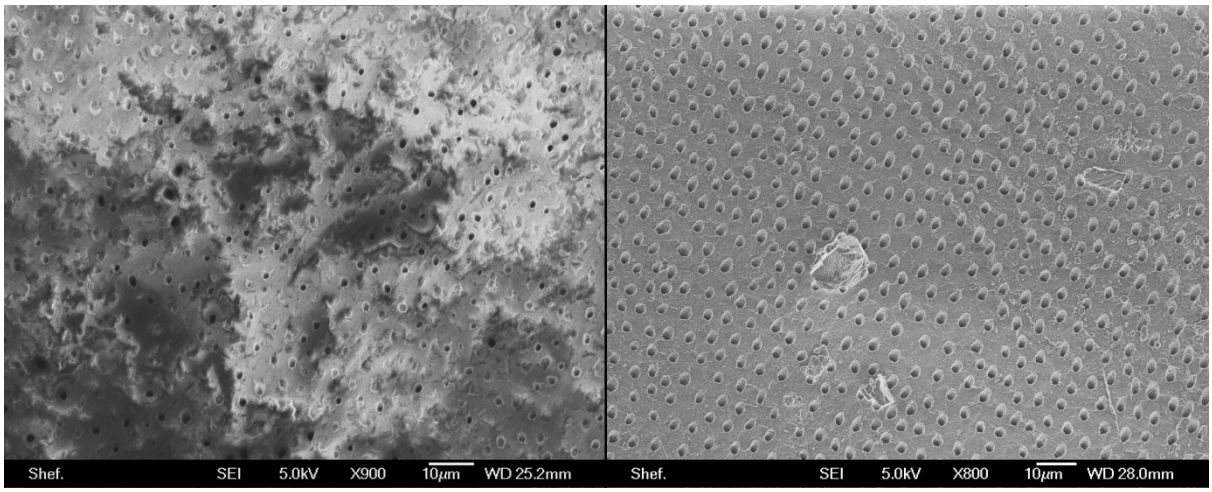

Figure 15 SEM micrographs of coronal bovine and human dentine respectively

Measurements were made regarding tubule width and density. Lumen diameter was measured according to the shortest distance to negate any effects of potential oblique tubule trajectory. Data was processed using Student T test statistical analysis, the details of which can be seen in appendix 1. As a result of this statistical analysis combined with analytical microscopy it was deemed that with both tubule density and lumen diameter there was significant difference between data sets. For this reason all dentine and enamel tissue featured in this study is of human origin.

Sample tissue used throughout this study was universally acquired as a result of dental overcrowding or for orthodontic purposes. Any samples that showed evidence of caries or dentinal deterioration were discarded. Tissue was stored at representative buccal conditions and tested within 48 hours of extraction.

3.3 Conclusions

This chapter introduces the various forms of dentine as the major constituent of teeth, providing an overview of its formation and function. Enamel is a vital tissue, important for both the provision of structure and as a medium for synaptic communication; however due to its hardness it is not susceptible to significant wear like the softer dentine. For this reason dentine and synthetic substrates of similar characteristics to dentine, are employed as the primary focus for substrates within this thesis.

Within this chapter the modes in which dentine can become exposed are discussed. The most likely regions for dentine exposure occurs are around gingival regions in close proximity to the sulcus. When the gum level recedes the dentine becomes exposed. This exposed dentine is mantle dentine, which has subtle differences to circumpulpal dentine (found deeper within the tooth surrounding the pulp chamber). These differences are mainly attributed to the geometry and frequency of the lumen of dentinal tubules. Because

of this, all experimental work conducted within this study investigating the interaction of particles with dentinal tubules is conducted on mantle dentine.

General tribological and wear experiments are extended to both mantle and circumpulpal dentine due to the similar nature of their mechanical and frictional properties. These similarities are justified through a combination of research into past investigations within oral care [8, 30] and feedback from trials conducted for the purpose of this thesis which are discussed in more detail in later chapters.

Further to analysis of both bovine and human dentine samples it was decided that only human dentine would be used throughout this study so as to maintain a representative substrate within sensitive nano-manipulation trials.

4 PARTICLE CHARACTERISATION

This chapter introduces each of the particles analysed within this study and, using a number of different analytical techniques, compares and contrasts the physical properties of these particles. The efficacy and suitability of an abrasive particle is reliant upon a number of factors ranging from size and shape, to material porosity and affinity to breakdown. Subtle changes in these characteristics can lead to significant differences in particle performance. Particles introduced in this chapter were selected and developed based upon a multitude of factors including ease of manufacture, accessibility of source material and production cost. As a result of the aforementioned manufacturing considerations there is a progressively changing hierarchy of particle importance.

4.1 Imaging techniques

A large portion of the analytical work undertaken within this thesis is achieved using scanning electron microscopy (SEM). An SEM works by mapping or tracing a sample surface using an electron beam. The scanning of the sample using a beam of electrons can introduce one of the most common problems associated with SEM image acquisition, sample-charging effects. If the samples being analysed are not naturally conductive this can lead to a increase in static electric charge within the sample. This can have a dramatic effect upon the image acquisition by affecting the behavior and directionality of secondary electrons. Figure 16 shows charging effects from early analysis of abrasive particles within this thesis. We can see from this image that the charging issues have led to a notable deterioration in image quality, with unrepresentative and illegible regions of brightness. Most of the materials analysed within this thesis are naturally insulating, such as Calcium Carbonate and dentine, which are limited in conductivity and therefore it was necessary to take steps to minimise the incidence of sample charging.

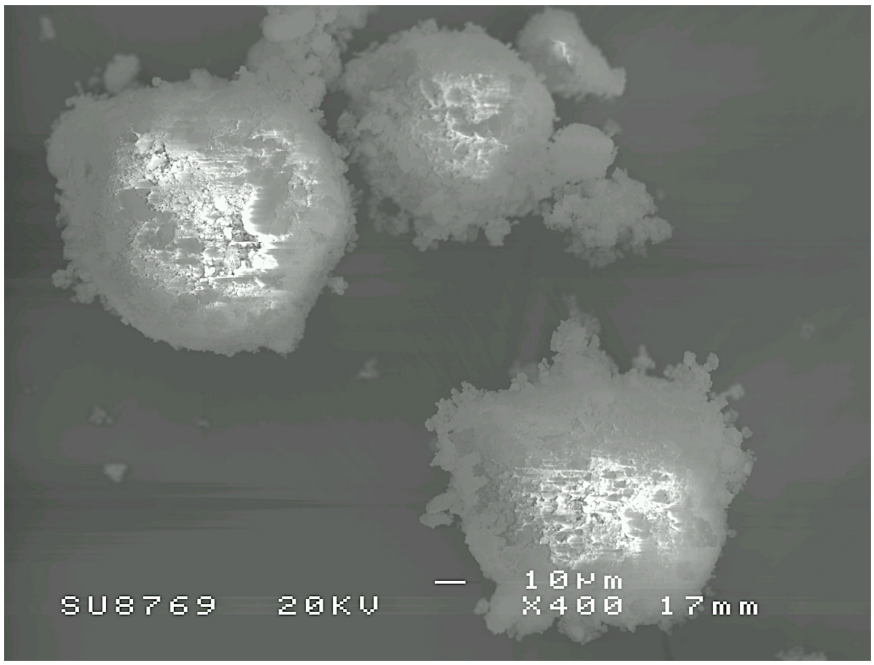

Figure 16 Scanning Electron Micrographs of Hubersorb 250 particles demonstrating notable charging issues

Imaged particles shown above were acquired using a Jeol JBM-6500F at 20kV accelerated voltage. Due to the relatively low conductive nature of the samples, in order to minimise charging effects and optimise image clarity steps were taken to address charging issues:

1. Samples were coated using an Emscope SC-500 gold sputter coater (Figure 17). By introducing a conductive layer to the outside of the feature items, negative charges can continually pass to the ground or SEM stage minimising the occurrence of static build-up. Samples were coated for deposition duration of 1 minute at 15 milliamps.

2. The particles were staged on adhesive carbon tabs to both limit sample movement and maximise contact with the conductive sample stage.
3. Dedicated charge pathways were introduced for Dentine samples using conductive silver paint, discussed in more detail in the next section.
4. Lower accelerated voltage can be adopted in some cases however, despite lowering noise and charging effects, this can compromise the clarity of the image in other ways. This was administered on a trial and error basis.

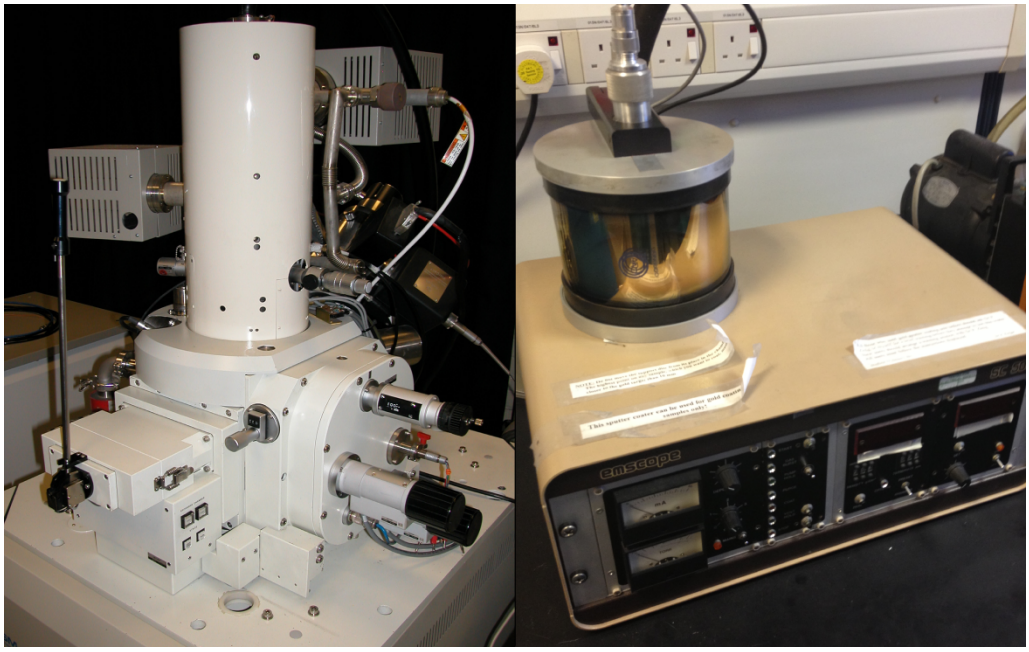

Figure 17 Images of Jeol JBM-6500F and Emscope sputter coater respectively

Further to this SEM analysis relies upon the use of a vacuum resulting in the dehydration of samples. This is not an issue for particle analysis however care must be taken to avoid degradation or denaturing of dentine components. It has been proposed by W. G. Matthews et al in 'Air blast-induced evaporative water loss from human dentine, in vitro'[31]:

"S*ustained air blasts may remove enough fluid from the pulp dentine complex to cause disruption of odontoblasts and changes in pulpal blood flow*".

Using short air blasts to encourage evaporative water loss from dentinal tissue they found that the acute removal of moisture can lead to the collapse of demineralised collagen. For this reason, all dental samples analysed using scanning electron microscopy were allowed to dry at ambient conditions for 24 hours after bisection and further sample preparation. Samples were then evacuated of any remaining moisture using a Pfeiffer DN40 vacuum chamber over several hours.

4.1.1 Refinement of imaging for dentine samples and preparation processes

Much experimentation within this thesis required the use of dentine as a substrate, which demonstrated itself as vehemently isolating material. Atomic force microscopy (AFM) is a

commonly used instrument for the purpose of studying dentine, due to it being less susceptible to the aforementioned charging effects introduced through SEM analysis. This is due to imagery and topography plots being derived via the close proximity of a stylus rather than a beam of electrons, which can lead to charging. For the purposes of this work however it was important to be able to study very fine visual detail of a number of different features of dentine including nano-scale imagery of surface roughening from abrasive processes, internal detail of dentinal tubules (see chapter 3), as well as analysis of the fine individual components of both enamel and dentine. For this reason a preparation process was continually refined in order to give the best ultimate image quality. Figure 18 shows the resultant image quality of dentine both before and after the sample preparation refinement process.

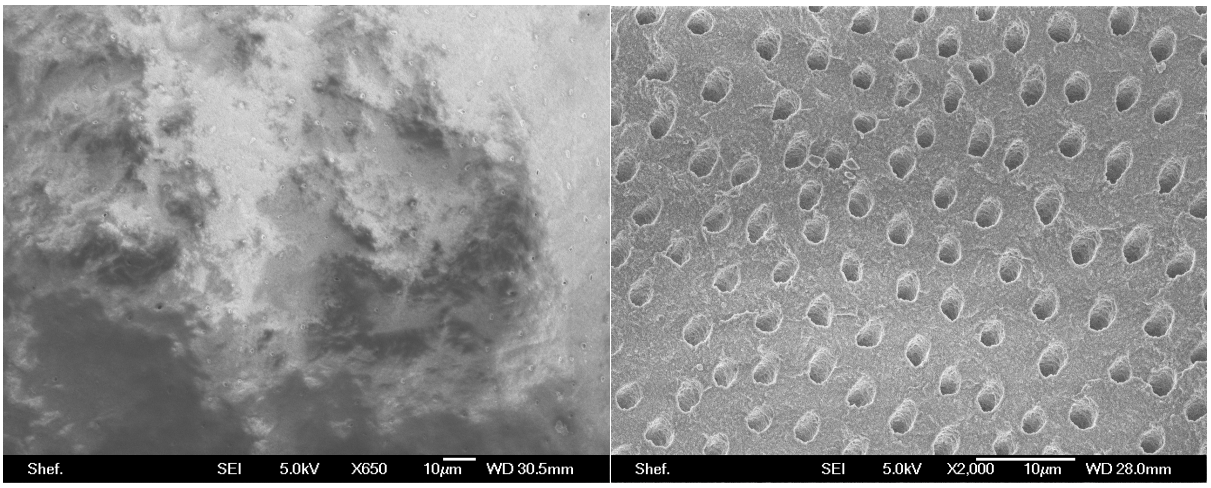

Figure 18 Above: Dentine imaged after simple bisection, Below: Dentine prepared according to more stringent preparation process

The following sample method was adopted for the preparation of dentine for all experiments featuring analysis involving dentine within this thesis:

- Samples were acquired only from adult humans all above the age of 18. Sourced teeth were removed for orthodontic purposes and were free of caries and of sound oral health.
- Samples were sealed and stored in a 10% neutral buffered formalin solution immediately after extraction. All samples were prepared within 2 weeks of extraction and ultimately analysed within 24 hours of preparation.
- Teeth were sectioned mesio-distally using a Well 3241 180 micron diamond coated wire saw isolating palatal, lingual and buccal faces. The cutting process was water cooled throughout to minimise temperature fluctuation. The Maximum measured temperature measured during cutting processes was 19°C with a mean temperature of 16°C.
- Isolated dentine samples were staged within Konductomet phenolic mounting compound (20-3375-016) and wet ground using a 'Bueler Automet 250' for 2

minutes using a pile coarseness of 120 microns, with a touch force of 20N, a head speed of 50 RPM and a platen speed of 240 RPM.

- Further to this samples were polished using a 0.5 micron diamond polishing slurry for 4 minutes; using a 20N touch force, head speed of 50 RPM and a platen speed of 140 RPM. The polishing process was repeated using a 0.25 micron diamond solution.
- Samples were ultrasonicated in distilled water for 5 minutes to evacuate the tubules of any remaining diamond particles and to remove any manifestations of smear layer.
- Samples were then gold coated using the aforementioned Emscope SC-500 gold sputter coater for a deposition duration of 2 minutes at 15 milli-amps.

Due to the porous nature of the prepared materials, samples were introduced into a vacuum chamber overnight to remove any remaining moisture from the preparation process, which might impede analysis within a scanning election microscope environment. This was done before the gold coating process so as to avoid potentially trapping moisture. A prepared human sample is shown in Figure 19.

Figure 19 Prepared human sample

4.2 Particles used in this study

Table 2 introduces all particles contained within this study. Particles marked with an asterisk (*) are considered a primary particle of interest and subject to increased scrutiny and testing. This project was sponsored by a company with dynamic and changing interests dependent on a number a different factors. For this reason some particles are studied in more detail or exposed to more dedicated investigations, depending on the needs of the sponsor at the time.

The value of a particle can be attributed to a number of factors:

- Low cost to manufacture
- Easy or fast to manufacture
- Be of novel or bespoke geometry
- Posses potentially desirable traits such as minimal surface damage to substrates
- Fit with desirable marketing claims (for example be derived from a naturally growing source)

Particle	Description	Image
Omya 5av* Ground calcium carbonate (GCC) Avg size: 7µm	Large variance in particle shape as a result of the unpredictability of the milling process. Significant range in particle size. Omya 5AV is often referred to a 'standard' within this thesis due to its commonality within abrasive cleaning products.	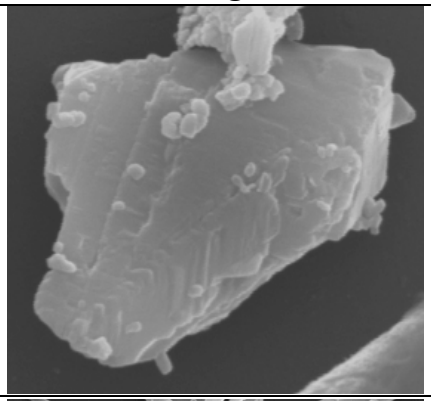
Maruo Rods* Precipitated Calcium Carbonate (PCC) Avg size: 6 x 0.5µm	Created through a series of heating and impurity removal. The precipitation process allows for increased control of shape development and size distribution. Rod particles have a much higher aspect ratio and appear relatively delicate.	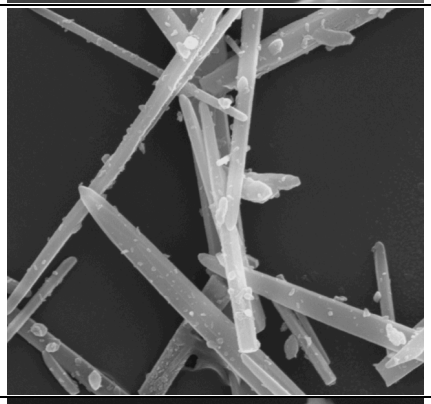
S2E* Precipitated Calcium Carbonate (PCC) Avg size: 3.8µm	PCC of the scalenohedral calcite family. Tend to generally follow the form of a polyhedron consisting of 12 sides following the profile of a scalene triangle. Analysis has shown that the S2E particles take on a slightly more baguette shape, with a wider middle and tapering tips.	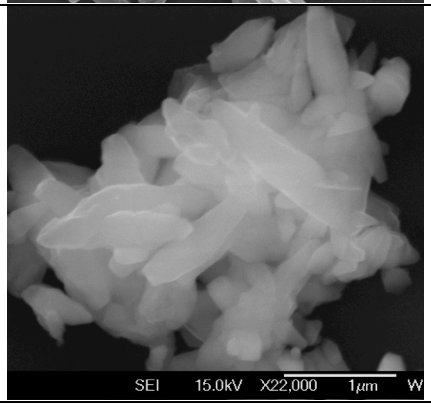

Vicality Albafil* Precipitated Calcium Carbonate (PCC) Avg size: 3.6µm	A small PCC its shape is that of a prismatic calcite. Due to the small nature of the particle the variance in particle size appears small. Less needle like than S2E and Rods, the prismatic shape of Albafil makes it appear more rounded; it is in fact polygonal.	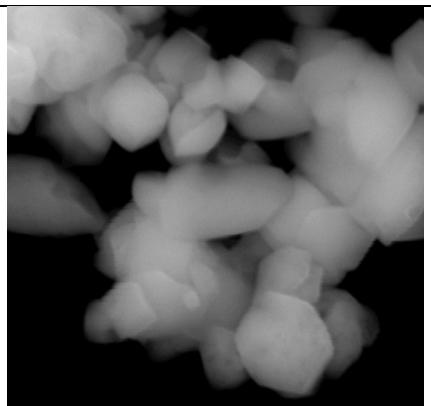
Perlite* Amorphous alumina silicate Avg size: 33µm	An amorphous alumina silicate often derived from volcanic glass. Naturally occurring, it often features in cleaning products and is relatively cheap to source. Its typical flat shape makes it theoretically well suited for entrainment by cloth or brush filaments during the cleaning process.	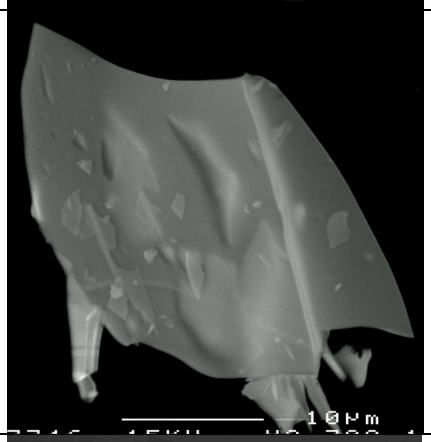
Sturcal L* Precipitated Calcium Carbonate (PCC) Avg size: 7µm	Similar to S2E, Sturcal L falls within the category of a scalenohedral calcite. Modal particle sizing using laser diffraction suggests a size of 7µm however SEM analysis suggests a size closer to 2 microns. It is likely agglomeration plays a part readily with this particle when sizing.	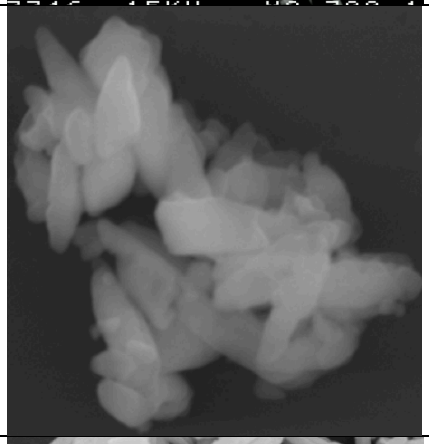
Sturcal F* Precipitated Calcium Carbonate (PCC) Avg size: 1.3µm	Sturcal F is an aragonite derived from naturally occurring acicular aragonite crystals. The crystal lattice of aragonite is different from standard calcite promoting an orthorhombic arrangement based upon a rectangular prism, which is mutually orthogonal.	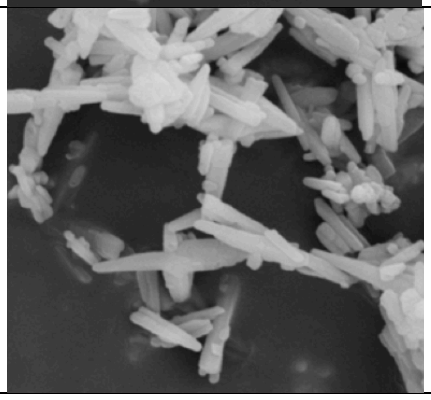

Polyester Resin Resin Avg size: 255µm	Manufactured via a condensation reaction between glycerol and both unsaturated and saturated dicarboxylic acid. Derived via grinding process the geometry of the particles is varied. Mechanical properties can be modified by varying the glycol or acid content.	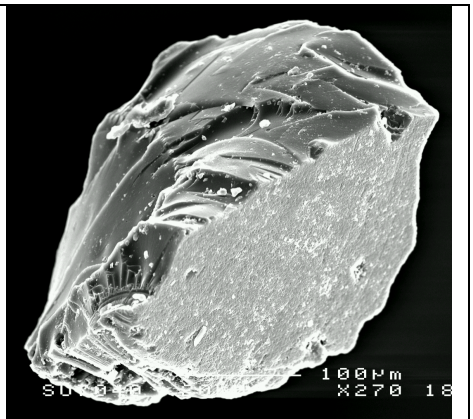
Bamboo Bambusa Arundincea Avg size: 345µm	These particles have no known hazardous or irritant properties. The elastic nature of material make it difficult to industrially refine to a fine particle (likely to be responsible for the sizable nature of the particle). Significant range in size and shape; particle geometry varies from polygonal to rounded geometries and faces.	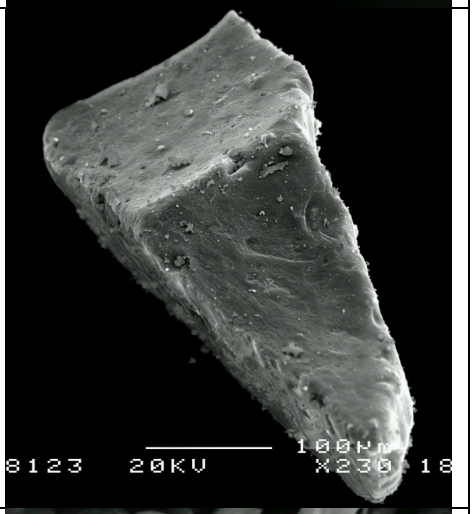
B200 Prologite Micah Magnesium Mica Avg size: 11.04µm	A magnesium mica formed as a hydrated silicate of magnesium and potassium. Commonly adopted for its chemical inertness and reinforcing properties. The material is desirable due to its widely accepted non-toxic properties and is comprised of a hexagonal crystal structure.	
5C103 Attapulgite clay Palygorskite and smectite components Avg size: 2.47µm	Comprised of palygorskite and smectite components. The former of these appears fairly needle like in appearance and resistant to expansion when in the presence of water. When in suspension attapulgite readily forms a lattice structure with neighbouring particles via hydrogen bonding.	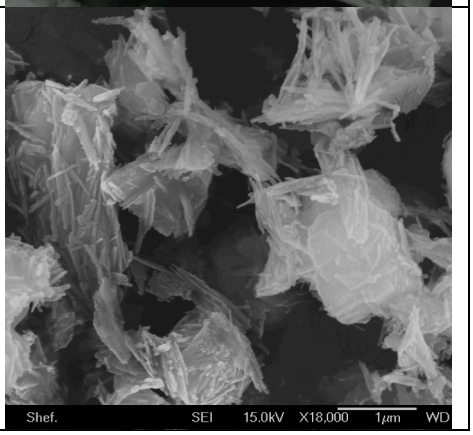

S20 Talc Soapstone derivative Avg size: 11.04µm	These particles are often used within industries such as food additives and pharmaceuticals. Produced via a grinding process thus demonstrating a increased range in particle shape and size. Somewhat similar in appearance to Omya 5AV however can be more easily produced in smaller particle sizes.	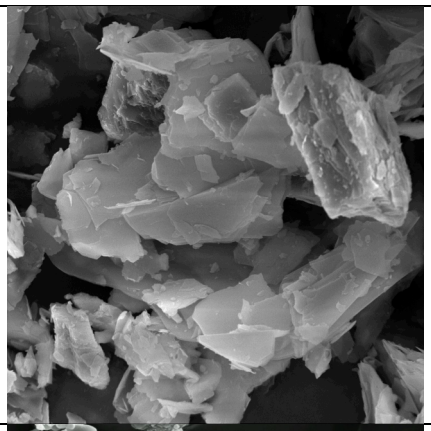
FM1000 Calcium Silicate Avg size: 7µm	A particle often used in the pharmaceutical industry in the production of placebo tablets. It is usually mixed with mannitol and microcrystalline cellulose however particles analysed within this study was segregated calcium silicate.	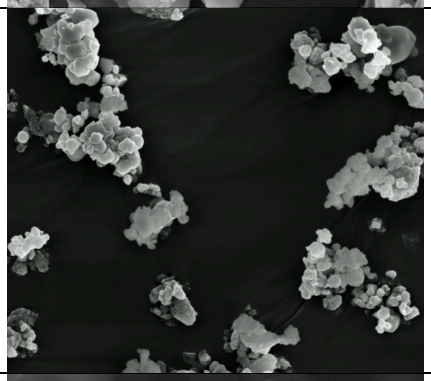
Baralev CA Calcareous calcium lime, predominantly calcium carbonate Avg size: 5.2µm	A calcareous calcium lime predominantly comprising of calcium carbonate. Often derived through the processing of chalk and limestone. Particle size and geometry is a result of progressive grinding.	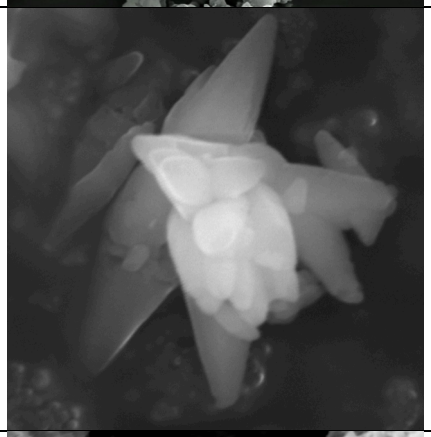
Hubersorb 250 Calcium silicate Avg size: 83µm	Calcium silicate is produced through a reaction between silica and calcium oxide. Each grade of Hubersorb is based upon the variation in the size of the resultant particle. Particles are processed using progressive grinding to achieve the desired grain size.	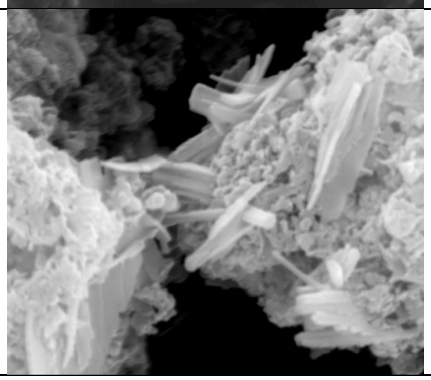

Hubersorb 600 Calcium silicate Avg size: 6µm	More spherical in shape than 250, 600 particles are more fibrous in appearance.	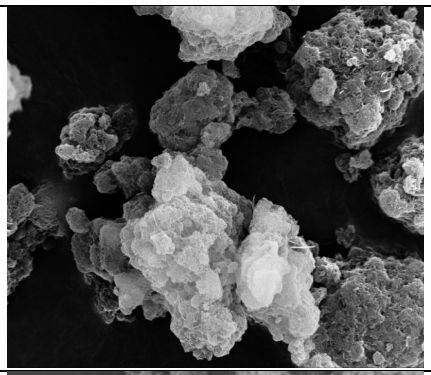
Hubersorb 5121 Calcium silicate Avg size: 125µm	These particles when measured using laser diffraction, show a modal size that appears larger than SEM imagery would suggest. Particles appear to be comprised of smaller sub particle fragments.	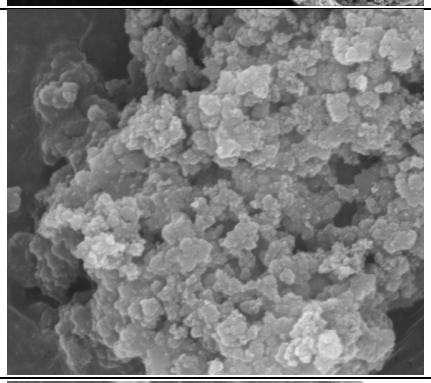
MEV Vermiculite Aluminium-iron-magnesium silicate Avg size: 28.15µm	Manufactured by the hydrothermal processing of biotite, vermiculite is the geological name attributed to a range of hydrated laminar materials. A result of the variability of the manufacture process, the hardness and density of the particles are difficult to ascertain.	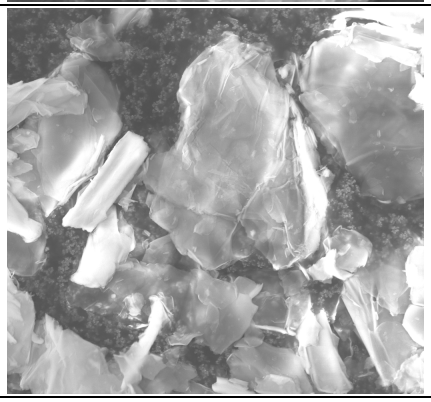

Table 2 A comparison of abrasive particles analysed within this study

A geometric overview of the seven crystal systems is shown in appendix 2.

4.3 Particle Sizing

Particle size can be determined using laser technology (Figure 20) to produce size distributions for different particles. Whilst not providing information about shape, it does allow for the comparison of grain size to a reasonably high degree of accuracy. This process uses laser diffraction as a means of calculating the mode particle size based upon the angle of scattered light from a propagating beam.

Figure 20 Images showing a Malvern Instruments Mastersizer 2000

Figure 21 shows a typical size distribution plot compiled from the raw data produced using a Malvern laser diffraction particle sizer. This particular data set represents a sample of bamboo particles which, within the dental abrasive industry, are at the upper end of the scale regarding size. Figure 22 compares the range in mode size of analysed particles. In order to try and minimise the likelihood of particle agglomeration a teepol surfactant was added.

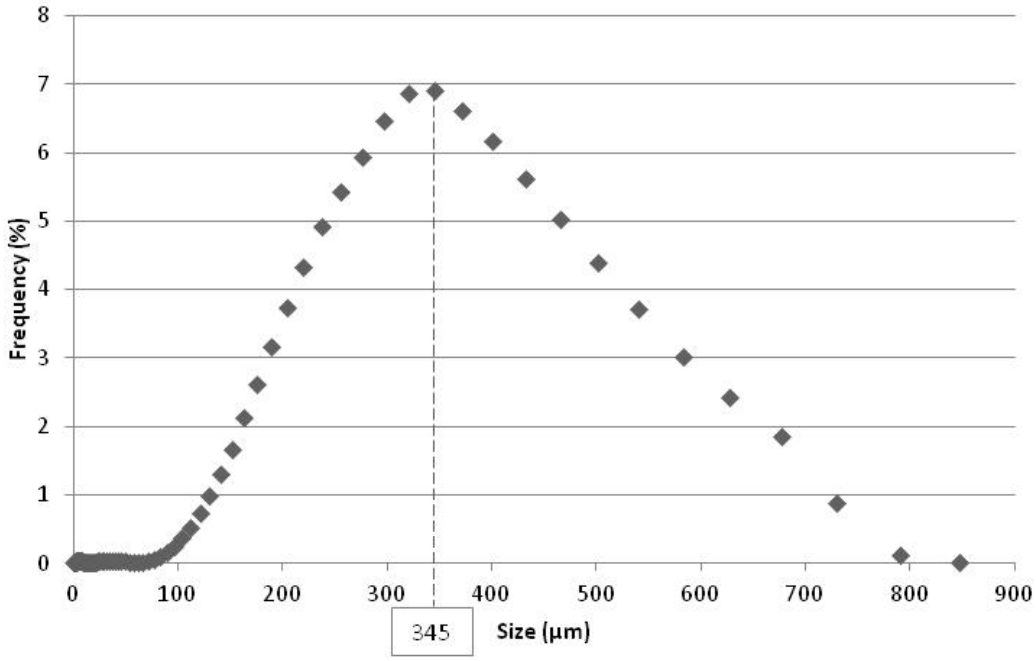

Figure 21 Frequency plot of particle size for bamboo particles

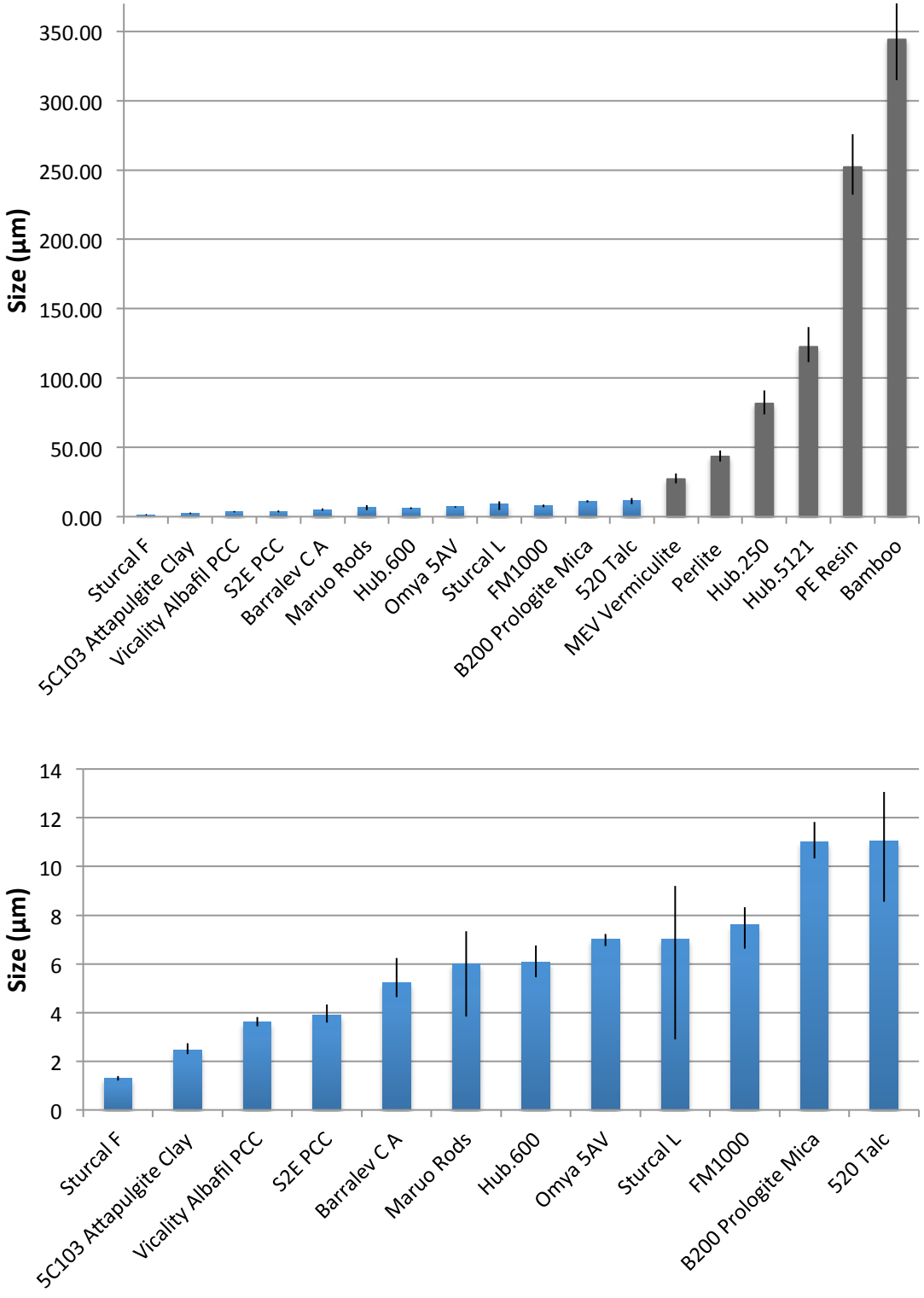

Figure 22 Comparative plots showing modal particle frequency

Figure 22 shows the comparative particle sizes derived through laser diffraction measurements. A separate sample of each particle type was measured on three separate occasions. Each time a trial was conducted a modal particle size was derived from the frequency plot, as seen in Figure 21. Each bar within Figure 22 represents the mean value of these three modal particle sizes. The error bars represent the range in the modal values.

Particle sizing using laser diffraction is a convenient way to formulate particle size distributions however it the technology is not able to discern between individual particles and particles agglomerations. Although steps are taken to encourage homogenisation of the suspension before analysis misrepresentations can be made for particles with a high affinity to agglomerate.

4.4 Conclusions

As can be seem from SEM imaging there is significant variation in particle geometry and form. It is not clear the effect that the inherent crystal structure has upon the natural particle shapes when manufactured through grinding processes. It is likely that these processes lead to more varied particle geometries via these manufacturing methods and that the effect of crystal shape is eclipsed. These structures may play more of a key role in the fracture characteristics of individual particles. This is investigated in more detail in Chapter 8.

A clear difference in the appearance of Calcium Carbonates manufactured through precipitation processes compared to those produced through grinding can be seen. The overall quality and integrity of the precipitates appears more complete with a notable improvement in size control. The size and shape of ground particles is significantly more varied whereas there is a improved uniformity to the precipitates which may have an effect on their structural integrity and fracture characteristics. This improved control uniformity does come at cost, however, with precipitation process being notably more expensive that grinding.

The largest particles considered are Bamboo particles shortly followed by Polyester Resin particles, with the smallest Sturcal F and Attapulgite Clay. It is of interest within these investigations, to examine the relationship between particle size and the aggressiveness of that particle towards material removal. It could be said that a larger particle does not necessarily suggest that it will be more adept and detrital removal or more likely to cause substrate damage.

Particles were sized using laser diffraction technology, which does not take account of possible agglomerative behaviour. For this reason additional sizing and more detailed analysis is carried out using SEM analysis. What cannot be discerned from basic SEM analysis of particle shape is the mechanistic behaviour in which particles move. These dynamic properties are reliant on factors such as density, surface friction properties, agglomerative behaviour, affinity to break down, as well as overall geometry. All these attributes are studied in the following chapters.

5 ANALYSIS OF PARTICLE SCRATCHING

It is desirable for the abrasive nature of toothpaste particles to form a balance between being aggressive to potential detrital build-up and sympathetic to human tissue. It is therefore important to compare and contrast the scratch characteristics of different particles in an effort to gauge both their aggressiveness and to try and discern potential mechanistic and dynamic characteristics. In this chapter scratch analysis is undertaken using linear reciprocation under varying conditions. The resultant scratches are compared and contrasted using optical microscopy and scanning electron microscopy to observe resultant damage on a micro-scale.

5.1 Scratch analysis using linear reciprocation and brush filaments

5.1.1 Experimental approach

Preliminary scratch trials were conducted using a linear reciprocation rig, which incorporated a flat-trim toothbrush with 8mm Nylon bristles (standard Unilever toothbrush) as the motivated contact (shown in Figure 23). The setup allowed for the control of test variables such as brush stroke length and load throughout trials. Trials were conducted on perspex without water for 3 minutes per particle. Dry particles were administered to the Perspex surface sufficient to cover the brush strike zone. Throughout the test particles were continually reintroduced into the path of the proceeding brush, using controlled airflow by the operator. The brush head was loaded to 3.92N (400g) and processed at 0.925m/s. A brush stroke length of 60mm was adopted as this distance allowed for the full development of filament angle; each trial was run for 3 minutes. Although these experimental conditions are not accurately representative of common hand brushing conditions for the general public, the focus of this experiment was to try and determine whether a change in the angle of the brush filament can have a dramatic effect on the brushing activity; primarily through efficacy of particle capture. In order to achieve a noticeable change in filament angle a higher load was adopted, and higher brush speeds were implemented in order to encourage the resultant motion of the armature to rise on the reverse stroke so as only to process the particles in one direction (with the correct filament angle).

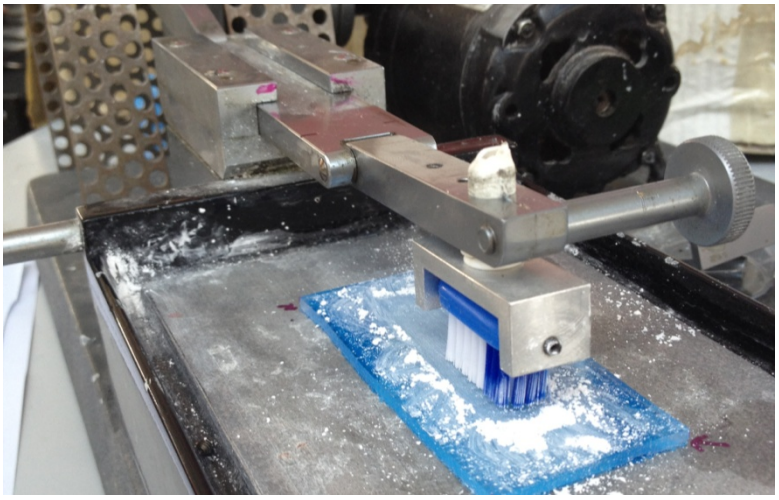

Figure 23 Linear reciprocation setup with standard Unilever brush head upon Perspex

Perspex samples were processed with the setup highlighted in Figure 23. Perspex is often used as a useful tool within scratch analysis trials within oral care due to its similar hardness properties to that of dentine; the comparative physical properties between dentine and perspex are discussed in more detail in later chapters. In conjunction with this setup high-speed video capture was taken with a Phantom V210 ultra-high frame rate camera, to study the progression of the brush. Although not capable of observing propagating particles directly due to their small size, it does allow for the understanding and measurement of

filament angle and various points of the brush stroke. Figure 24 below shows both the video capture setup and typical frames captured from trials.

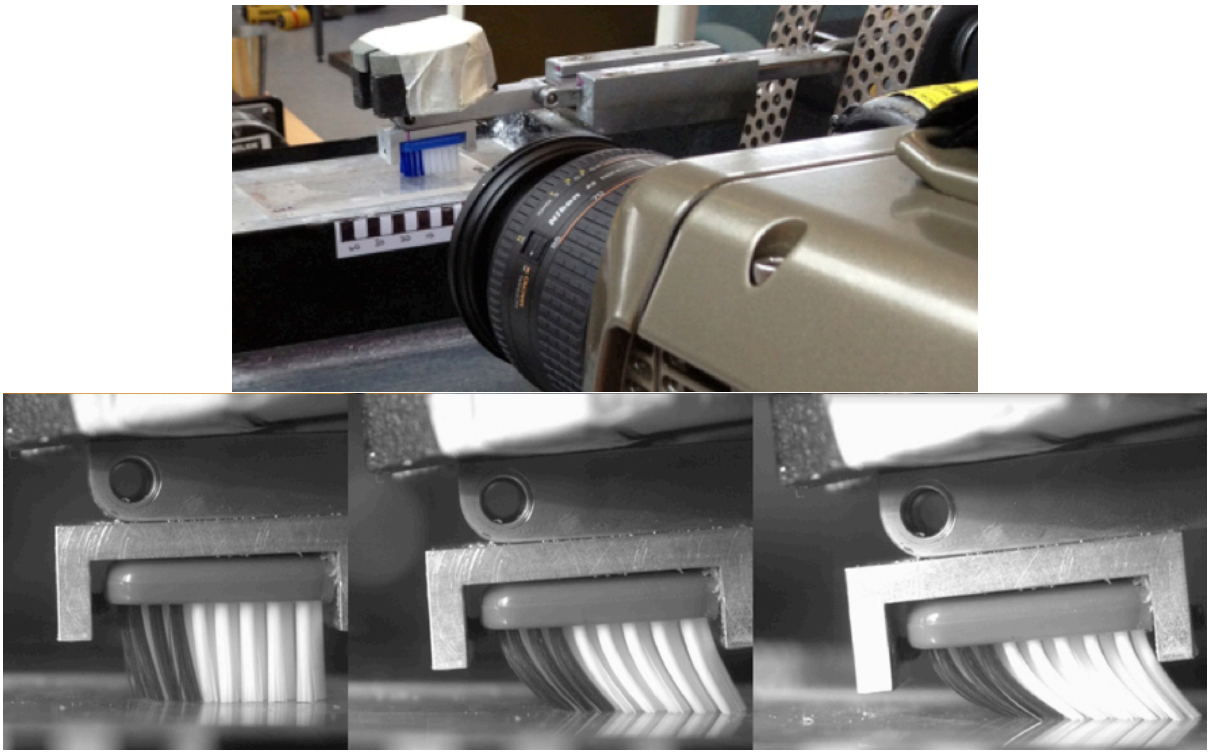

Figure 24 High speed camera setup and stills from calibration trial (without particles)

By understanding the arrangement of filaments at different locations upon the scratched surface it is possible to observe the behaviour of a particle (from analysis of scratches) relative to the angle of the filament itself. It is possible that particles have different aptitudes for entrainment at different filament angles relative to the individual particles size and geometry.

Post trial Perspex samples were studied using optical microscopy and Atomic Force Microscopy (AFM) to map the surface topography of the scratched region. An AFM uses a small probe tip in conjunction with a cantilever to move in close proximity to the surface being analysed. Subtle deflections in the cantilever are brought about and measured as the undulations of the studied surface introduce forces to the probe tip. This surface characterisation method is quite detailed and accurate to 1.5nm. Three Regions of the wear scar were studied at the same locations on each sample, resulting in filament entrainment angles of: 'Start' - 70°, 'Middle' - 35° and 'End' - 20°. All AFM scans were conducted over a 50x50µm region, and the resultant scratch data recorded.

5.1.2 Experimental results

Figure 25 shows optical microscope images of scratch characteristics from a few of the particles tested. Apparent is the high degree of variance in both the frequency of scratches

and the width and severity of scratches. Sliding direction for the brush is horizontal across each image. Some of these images appear black and some lighter, this is a result of trials being conducted on different coloured plastics due to availability. The material properties of all the plastics were identical and measured to verify.

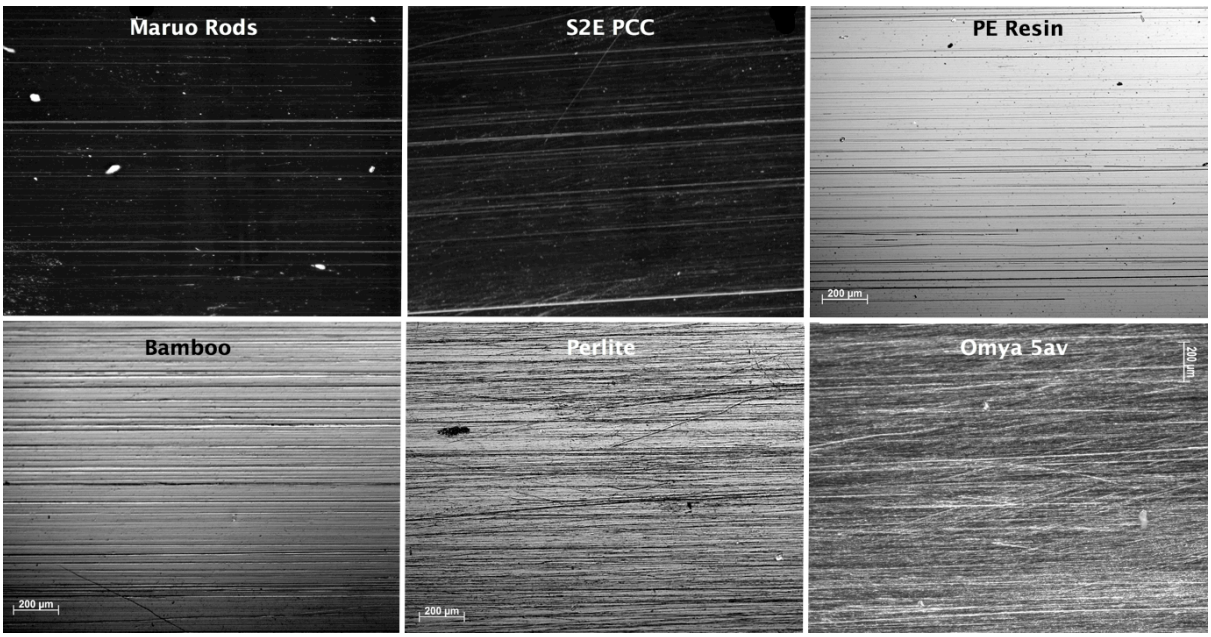

Figure 25 Optical microscopy images of scratches left by motivated particles upon Perspex

Maruo Rod particles appear sympathetic to the substrate surface with relatively few scratches present, fewer so than S2E PCC which is recognised for its sensitivity properties. The larger particles, Polyester Resin and Bamboo, do introduce seemingly deep scratches with an increase in scratch frequency; this is potentially a result of improved ease of particle entrainment due to their larger size. The uniformity of the scratches for Bamboo and PE Resin are consistently parallel and uninterrupted. This would suggest that the security of entrained particles is high, with particles unlikely to slip laterally out of, or slide entirely through filament contact. Omya 5AV and Perlite particles displayed aggressive scratching. Particularly with Omya there appears to be little uniformity to scratch direction. Particles appear to have notable directional freedom with the frequency of scratches significantly high. Comparing the apparent aggressive nature of Omya and Perlite particles with Maruo Rods and S2E PCC it would appear that Omya and Perlite would be adept at removing surface build-up, which is a desirable trait, however this does seem to come at a price. The low presence of scratching with other particles, namely Rods, does not necessarily imply that they are ineffective in processing surface detritus; only that their dynamic characteristics when motivated are not detrimental to the perspex.

AFM analysis allows us to quantitatively compare the scratch characteristics of particles as well as produce informative plot data based upon surface measurements. Figure 26 shows

comparative three-dimensional output plots from a selection of particles. The orientations of each plot are rotated so as to provide the optimum perspective, highlighting surface markings. Different colour filters are adopted for different plots to effectively illustrate surface topography. Whilst these plots do not provide detailed information as to the magnitude and specific characteristics of surface topography, which is provided in two-dimensional profile plots such as figure 27; they do allow for a physical appreciation and understanding of the general damage and surface markings that can be introduced using different particles. Figure 26 provides a qualitative overview of the aesthetics of the substrate surface after using different particles whilst figure 27 provides quantitative information.

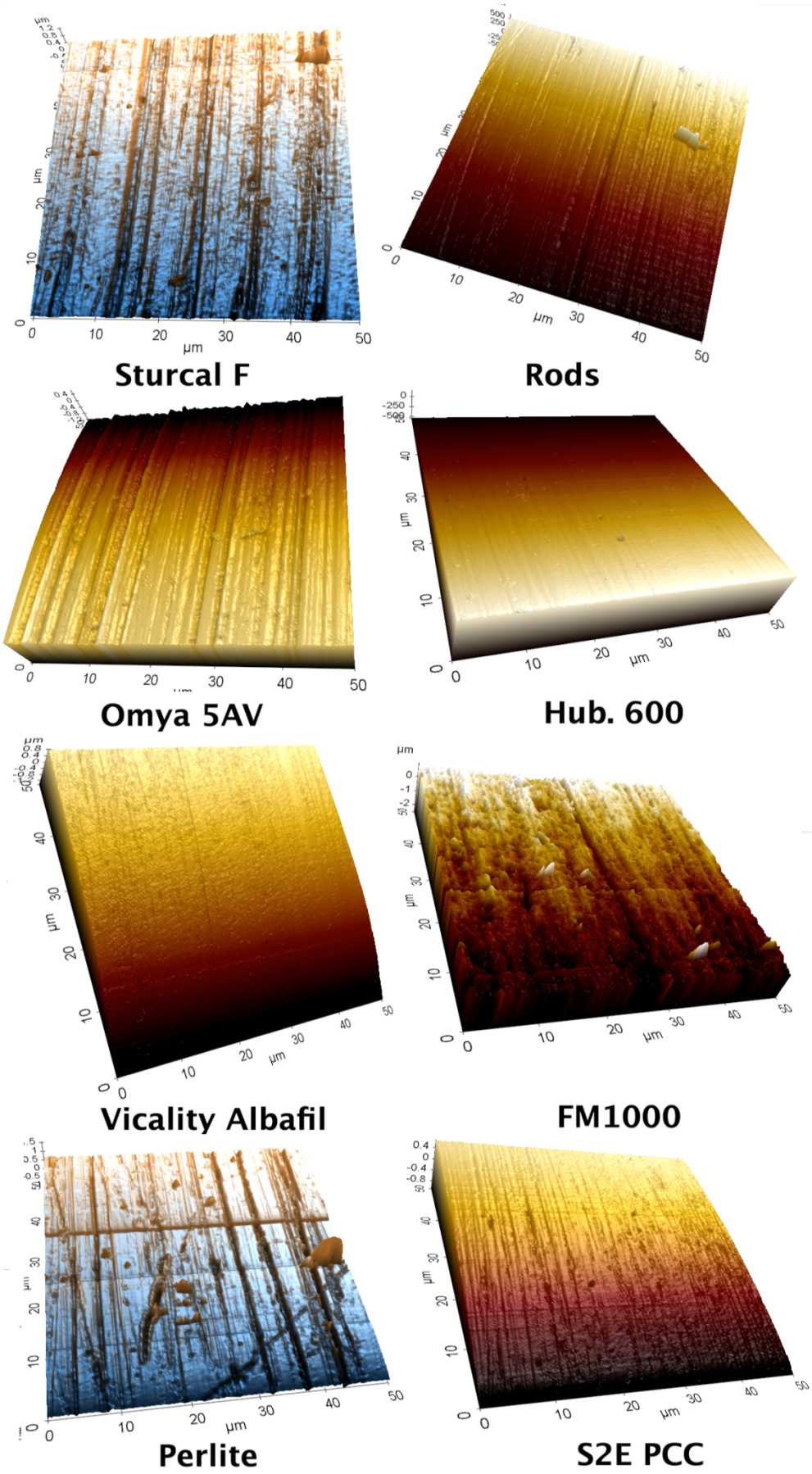

Figure 26 3D AFM plots of scratched Perspex using different particles

Infrequent instances of erroneous spikes are seen in the surface of the plots. These are likely to be a result of a combination between external vibration, static build-up and occasional contamination.

Omya 5AV has consistently deeper scratches than the other particles including Sturcal F which was expected to be more aggressive. Sturcal F demonstrated more widespread and chaotic surface markings with a combination of both deep and shallow scratches along with intermittent pock marking in the material surface. As outlined in Chapter 4 Omya 5AV particles are typically quite varied in size due to being manufactured by a grinding process but have an average size around 7 microns. This is notably larger than Sturcal F, which are less than 2 microns and show increased consistency in particle size. Initial analysis of the surface damage would suggest that the scratches caused by Omya 5AV are from individual particles, which do which do not appear to operate as agglomerations. The magnitude of observed scratches with Sturcal F is notably larger that than the size of the particles which caused them. This would suggest that particle agglomerations are responsible which would also explain the variance in scratch width for Sturcal F. The intermittent pock marking of the material surface may be a result of spherical agglomeration presenting projecting particle tips, which gouge the surface upon entrainment.

Figure 27 shows an example of the data obtained by AFM to determine scratch frequency and depth. For reference the particle sizes for Omya 5AV and Sturcal F are 7 microns and 2 Microns respectively.

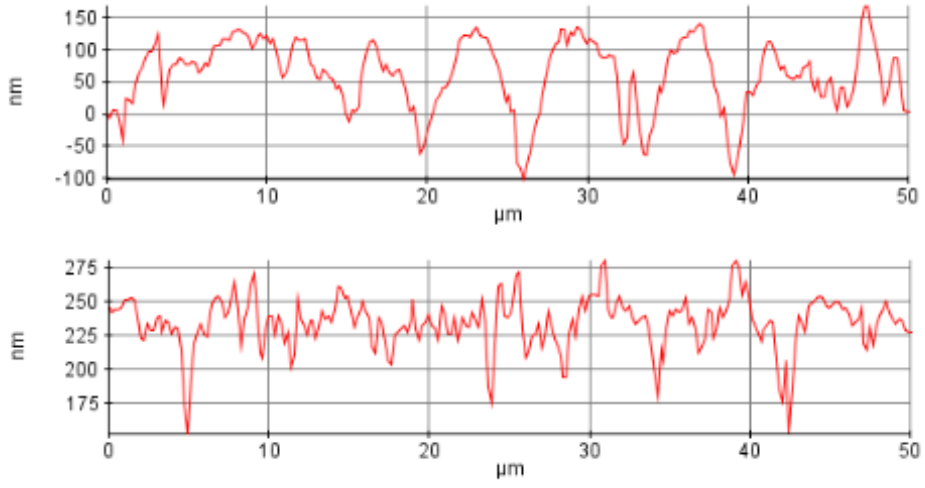

Figure 27 Profile plots showing the magnitude of scratch depth and frequency for Omya 5AV (above) and Sturcal F (below)

It can be seen that Omya has a lower scratch frequency than sturcal however showed 38% deeper scratches with an average depth across all analysed scratches of 225nm. Scratch frequency was derived as an average of distinct scratches observed within a 50X50µm plotted region. Multiple sections were studied with repeat scans to increase reliability.

Sturcal F particles produced an average scratch depth of 139nm. Comparing the roughness values across all scratched regions for Omya and Sturcal F, Omya produces a rougher finish with an R_a value of 37 compared to 22 for Sturcal F. It can be seen that some of the scratches are notably wider than the size of the particle in question. In each case, a scratch is defined as a legible undulation from the substrate baseline, sufficient to be distinct from other undulations and greater in magnitude than asperities. Appendix 3 shows a tabulated comparison of all measured values derived from AFM surface scans of scratches analysed within these trials.

Figure 28 compares the relationship between particle size and the depth of resultant scratches for all particles.

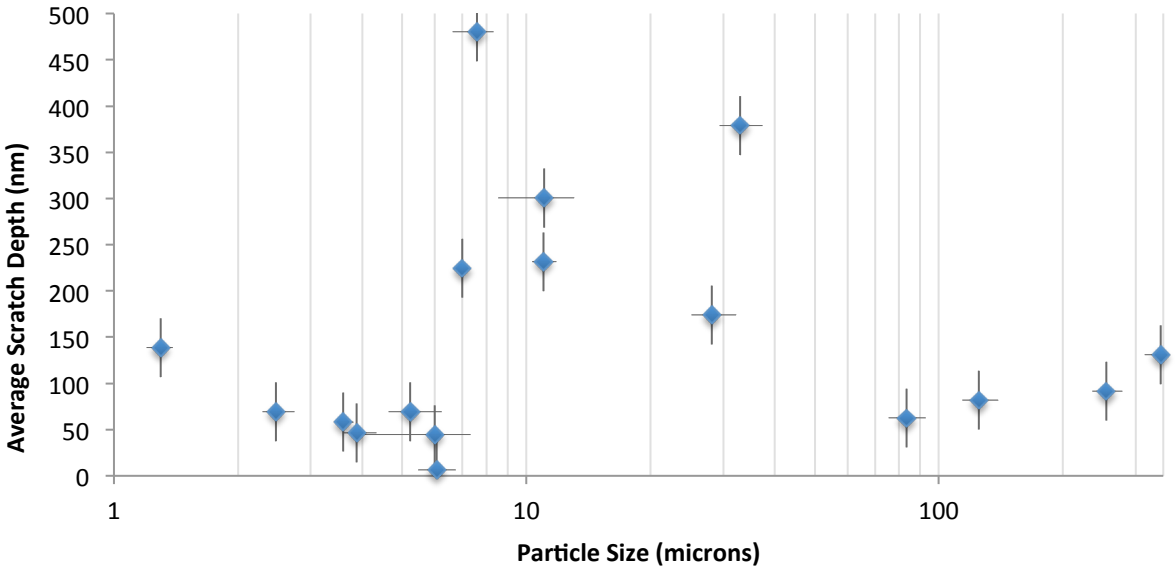

Figure 28 A comparative plot of particle size vs. average scratch depth

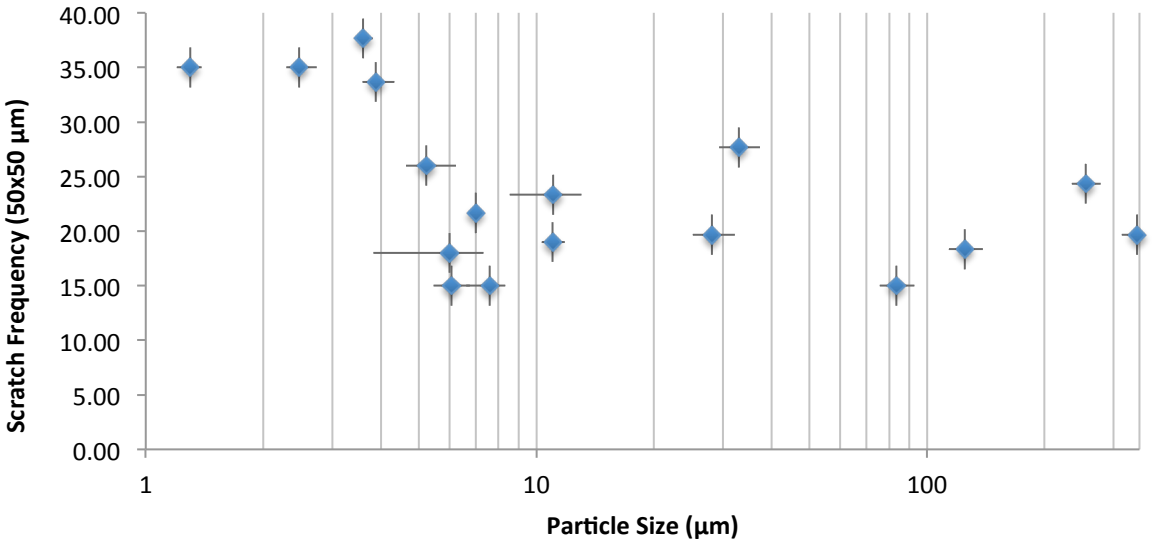

Figure 29 A comparative plot of particle size vs. scratch frequency

Maruo Rod particles and Sturcal F are both manufactured via a precipitation process and have relatively similar geometries. Rod particles are however larger in size and it was of interest to see how these two particles compared in terms surface damage. There is a notable decrease in surface degradation with Rods with Sturcal F having both a higher average scratch frequency and depth. Even the deepest scratches observed with Rods were relatively shallow, with an average scratch depth of 18µm (vs. 35µm for Sturcal F). It would be expected then being of relatively similar shape but Rods being more sizeable, that the Rods would be more readily entrained by filaments and thus scratch frequency and depth would be greater with Rods; this was not the case. As previously discussed this could be a result of the possible affinity of Sturcal F to agglomerate compared to Rods. SEM analysis of loose dry particles undertaken in Chapter 4 would support this, with imaged Rods tending form loose assemblies. Sturcal F on the other hand is often seen forming more tightly arranged agglomerations.

The particle most sympathetic to the substrate surface was Hubersorb 600, which demonstrated both the lowest average scratch frequency and depth despite being similar in size to Omya 5AV. The average scratch depth for Hubersorb 600 was 6µm which is significantly lower than other particles. The particle which led to the greatest scratch depth was FM1000. This particle appears aggressive to the substrate surface resulting in significant material removal. At around 7µm FM1000 is a relatively small particle at but it would appear that an increase in particle size does not necessarily lead to an increase in scratch depth or frequency.

Contrary to expectation there does not appear to be a discernable relationship between particle size and the resultant scratch depth. As can be seen in Figure 29 there is no obvious trend with some of the deepest scratching being introduced by relatively small particles. One might expect that the larger the particle the higher the likelihood of entrainment under filament and conversely the greater the potential for the introduction of deep scratching relative to the particles geometry. This is mainly a result of the increased ease with which propagating filaments can gain purchase on the particles when they interact. There is also argument that larger particles, being derived more commonly through grinding processes, have more sharp edges and remain in isolation more readily; this is discussed in more detail in Chapter 8. It appears however, there is a greater number of variables affecting the affinity of the particle to scratch the substrate surface. There is however a weak trend between particle size and scratch frequency for the smaller particles below 10 microns. In this case as the size of the particles increases, the frequency of scratches decreases. Although there is the potential for an increased presence of individual particles within the filament-substrate contact zone when the particles are small, this does not necessarily increase the chances of successful entrainment.

It is difficult to discern the dynamic characteristics of particles within the filament-substrate complex using AFM scans however Chapter 8 looks at this in more detail. From the above results it can be concluded that a subtle variation in particle shape can have a dramatic effect upon both its likelihood of entrainment and how damaging it can be to the substrate surface. This may be a result of the particle having a more aggressive shape in isolation but is more likely to be a result of a change in the way like particles interact; augmenting the agglomerative properties for that particle.

Analysis of the brush filaments using slow motion video showed the angle of the filaments to fall predominantly within 3 regimes. These brushing regimes are referred to as 'Start (70°), Middle (35°) and End (20°)' with each occurring for a similar duration. All angles are measured relative to the substrate surface and not from the normal to the substrate surface as shown in Figure 30.

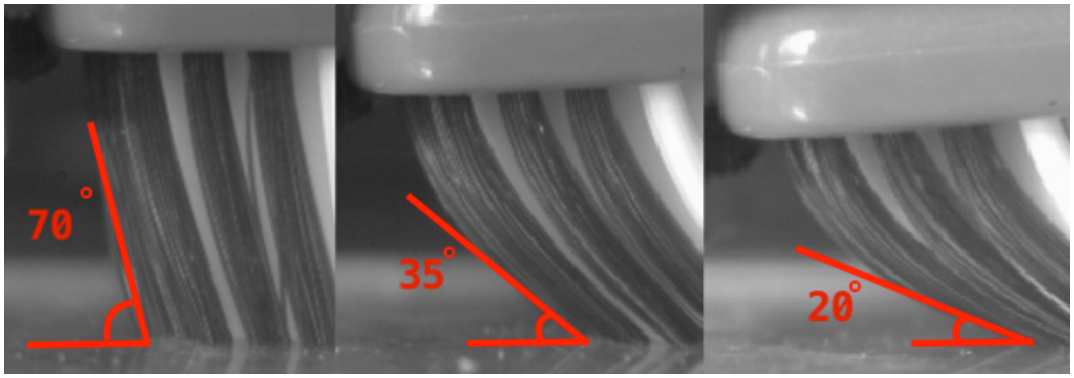

Figure 30 Illustration of three brush angles adopted

Regional analysis of the tested samples showed that there was not significant variance in the scratch frequency between zones for each particle. There was however a discernable difference in scratch depth from one zone to the next with the middle brush stroke zone (filament angle 35°) leading to the highest scratch depth and roughness. Figure 31 compares the measured scratch depths for the three filament angles.

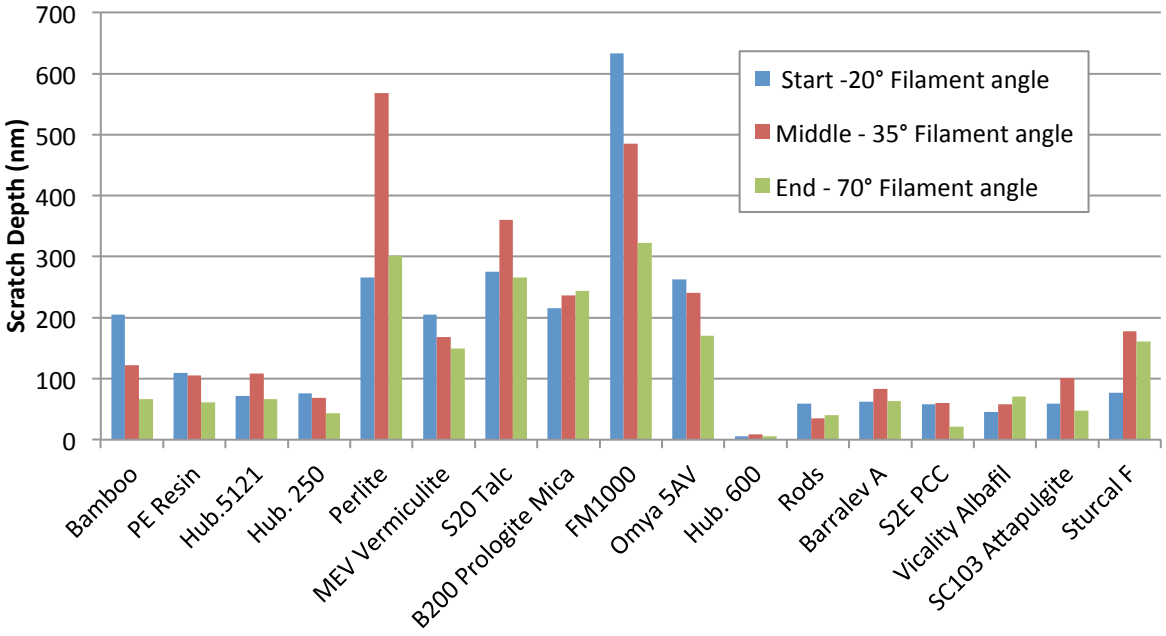

Figure 31 Comparative plot of Scratch depths incurred adopting different filament angles

It can be seen that largely there is little comprehensible difference between the filament angles for the start and end zones which the observed scratch depths being similar. There does appear to be an increase in scratch depth for the middle zone however this is not significantly higher. The particles in Figure 31 are listed in order of decreasing magnitude. Clearly the most prominent surface damage was not observed with the largest particles but was considered 'middle sized particles in the region of 10-33 microns. Following the trends from FM1000 to Hubersorb 600 there is a significant drop in scratch depth to almost no perceivable surface damage.

We can see that the most prominent scratch depth was caused by FM1000 particles. It is thought that in this case it is a result of high particle friction coefficient, which is discussed in more detail in Chapter 5.

As can be seen in Figure 31 there is not a convincing relationship between filament angle and scratch depth, however there is a marked increase in the magnitude of scratching for the centremost particles of the plot. This seems to work synergistically with the filaments half flexed at 35°. It could be that steeper or shallower filament angles are less effective for different reasons. The shallow filament angle could allow the passage of particles through the contact zone quite readily, whereas too steep an angle results in a smaller surface area presented to the particle and thus less effective entrainment.

Lewis and Dwyer-Joyce [25] observed a relationship between filament deflection and particle entrainment highlighting the key role of filament bundle configuration and filament deflection. They proposed that particles are more likely to become trapped at the tip of the

filament at low deflection whereas at high deflection the bent shaft of the deflected filament is more likely to entrain the particle. In the visualisation studies they conducted it was apparent that it was the filament tip region responsible for entrainment, which was only readily infiltrated by the smaller particles. It could be that there is a window of particle size that is notably more adept at becoming entrained, with particle size above and below this either forcing their way through the contact zone or sliding though relatively unimpeded. In this case this would be particles from perlite through to FM1000. Within this setup it is difficult to know for certain whether particles are prone to operating in isolation or as an agglomeration. Chapter 8 and Chapter 9 investigate the collective and individual properties of particles in more detail. It would appear however that the relationship between particle size and shape and its affinity to become entrained by a filament is quite delicately balanced. There is a marked increase and decrease in scratch depth from Hubersorb 250 to Perlite and FM1000 to Omya5AV respectively; the change in particle size in both cases is marginal. It appears this is not solely a result of a change in the shape of a particle augmenting the efficacy of particle to become entrained, as this would likely lead to erratic modifications in scratch behaviour rather than a continuous step increase across a number of particles within a particular size bracket.

In the study 'Fluid/Solid Interactions in Abrasive Teeth Cleaning [32], Lewis and Dwyer-Joyce also study the effect of load and thus filament deflection on the number of particles present at the point of entrainment. By varying the applied load on the filaments they saw a difference in the number of particles able to find their way to the filament terminus and become entrained. As load increased and thus the filament deflection angle decreased fewer particles were observed at the filament tips. Although the load on brush (in the experiments conducted as part of this thesis) was fixed, the acceleration and deceleration of the brush head as it changed direction led to a variance in filament angle resulting in three distinguishable zones; 'Start' - 70°, 'Middle' - 35° and 'End' - 20°. Within the Lewis study non-uniformity of filament length as a result of low load was shown to be a notable contributing factor in allowing particles to frequently pass over filament tips, which did not fully contact the substrate surface.

In the study 'Interaction of Perlite Particles and Toothbrush Filaments in a Tooth Cleaning Contact' [33] Lewis and Dwyer-Joyce observed increased non uniformity in Perlite scratches than the standard comparative Silica particle they employed. Scratches brought about using Perlite were lower in frequency, shorter and shallower. In comparison with Dwyer-Joyce et al. Perlite particle scratches were relatively deep and reasonably frequent; however similar to Lewis and Dwyer-Joyce' findings the scratch durations were notably short (see Figure 31). The reason there could be a notable difference in scratch depth could be a result of a variance in load between studies. Although the loading scenario is relatively comparable the flexural rigidity in the bristle filaments could be quite different. It could be that the shape of Perlite (Figure 33), being subtly convex, lends itself to effective capture at the filament tip.

However as this entrainment appears to be short lived and as the angle of the filament progresses the particle capture does not appear to be effectively maintained. The results observed in Figure 32 would support this with Perlite showing a notable increase in scratch depth for filaments in the middle of stroke with the start and end of the stroke being similarly low. Looking at the roughness data we can see that there was considerable increase in surface damage within this middle region. Table 3 compares the roughness value for Perlite for different filament angles with a particle of similar size but more generic shape, MEV Vermiculite.

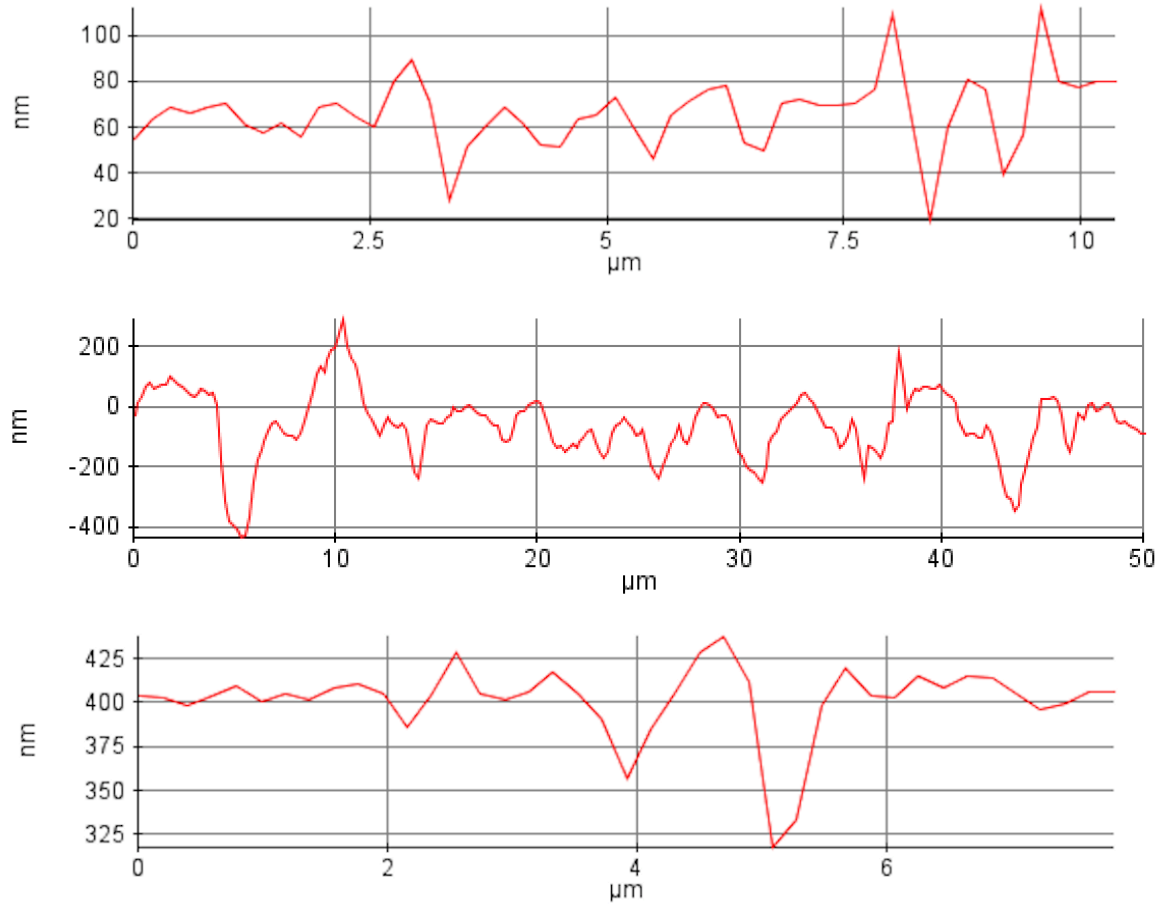

Figure 32 Profile plots showing the typical magnitude of scratch depth and frequency for Perlite particles. (Above: Start of stroke, Middle: Middle of stroke, Below: End of stroke)

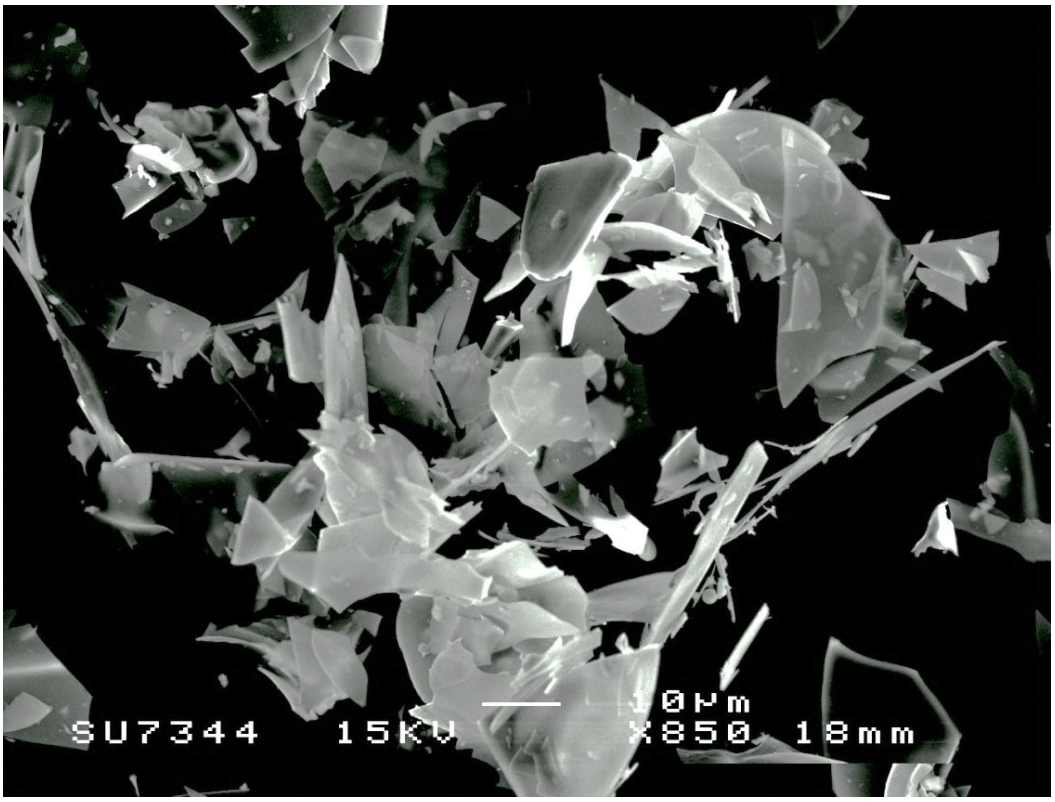

Figure 33 Scanning Electron Micrograph of loose Perlite particles

	Roughness (Ra)		
Particle	Start	Middle	End
Perlite (33µm)	28	89	26
MEV Vermiculite (28µm)	29	30	11

Table 3 Comparative Ra values for Perlite and MEV Vermiculite particles

Stability of the trapping process, as expected, is closely related to the particle shape and plays an important role in the entrainment of the particle both in terms of the likelihood of capture, but also the depth and duration of the resultant scratch. Lewis et al proposed this might be a beneficial contributive action as the particle is less likely to damage the substrate surface but it could be said that this makes it an inferior abrasive if it is not capable of effectively removing surface detritus. It is possible that there is an operational mechanism by which some particles may be relatively adept in both detrital removal and remaining sympathetic to the substrate surface. The roughening of a substrate surface via abrasive scratching is often accentuated (in some cases visually) by the shoulders of these scratches. Some particles with appropriate geometry may be able to find a compliant position relative to the substrate surface and remove these surface projections (shoulders) when motivated, resulting in a smoothing effect.

5.1.3 Conclusions

Attempting to generalise the shape of the particles and correlate these findings to generically predict scratch characteristics is not practical. From the results above there appears to be no distinct relationship between the shape of a particle, and its affinity or aggression towards scratching a substrate surface that can be derived using post trial analysis of scratched surfaces. There are many variables at play here, the subtle modification of which can have a dramatic affect on the particles behavior.

Further, taking the particles analysed using Atomic Force Microscopy here and assigning them an objective roundness value in order to arrange the particles in a hierarchy from sharp to round particles; shows that there is little correlation between the scratch behavior and the 'roundness' of the particle in these cases. A graph shown in Appendix 4 demonstrates this lack of correlation for both scratch frequency and depth. Particles were assigned a roundness value from one to ten, one being the most pointed and ten the most rounded particles.

This is not to say that particle shape does not affect the abrasive characteristics of the particle, it is likely that it does, however the relationship cannot easily be generalised or summated. Chapter 9 uses nano-manipulation tools to analyse individual particles dynamically, in an effort to better understand the effect of shape on the abrasive and physical properties of the particles.

5.2 Scratch analysis using linear reciprocation and Perspex plates

5.2.1 Introduction

It was thought that with particles introduced between plates of a suitable substrate of representative hardness (Perspex) and of a high quality surface finish to ensure the meticulous osculation of the surfaces; a known load could be applied. Substrates could then oscillate with abrasive particles pressed and contained between the two plates and the resultant surface damage and particle breakdown can be analysed accordingly.

It was thought that the inconsistent means in which particles are loaded via brush filaments can sometimes introduce irregular observations. It is of interest to study the continuous loading of particles, where the entirety of the load is conveyed through the particles with no likelihood of particles escaping contact.

The entrainment of particles by brush filaments is an inherently difficult parameter to control, with the reliability and efficacy of particle capture highly variable. In order to study the scratch characteristics of trapped particles constrained to remain in contact, trials

adopting contacting plates were undertaken. To demonstrate that comparable results could be obtained, the experimental setup initially consisted of two contacting Perspex plates, a lower fixed plate and a reciprocating upper plate. The upper plate was integrated into the aforementioned linear reciprocation rig used in filament entrainment trials as shown schematically in.

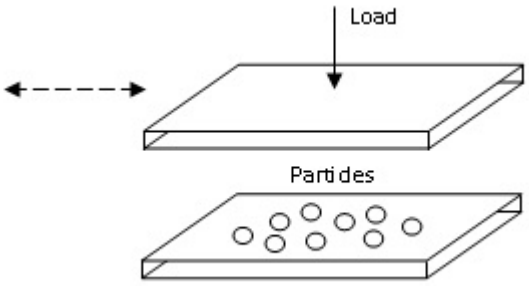

Figure 34 Reciprocating Perspex contact plate setup

It was important to ensure the plates remained flush throughout the progression of the stroke. The reciprocating arm was coupled so as to allow the upper plate to be free to hinge appropriately when motivated. Three particles of particular interest to the sponsor company were selected for analysis within contact plate trials, these were Maruo Rods, S2E PCC and Omya 5AV.

5.2.2 Experimental procedure

Scratch trials were constrained using the same linear reciprocating rig described in the previous section, allowing for the control of contact speed and load. The particles were introduced dry using a speed of 0.925m/s, loaded at 400g (3.92N). Scratches analysed after processing were assessed on both the scratch frequency per unit area ($3mm^2$) and scratch depth using scanning electron microscopy. Particles were studied without the presence of water to observe their interactive behaviour both with each other and with the surface of the perspex, without the influence of water.

5.2.3 Experimental results

Figure 35 shows the scratches obtained by Maruo Rods using optical and scanning electron microscopy.

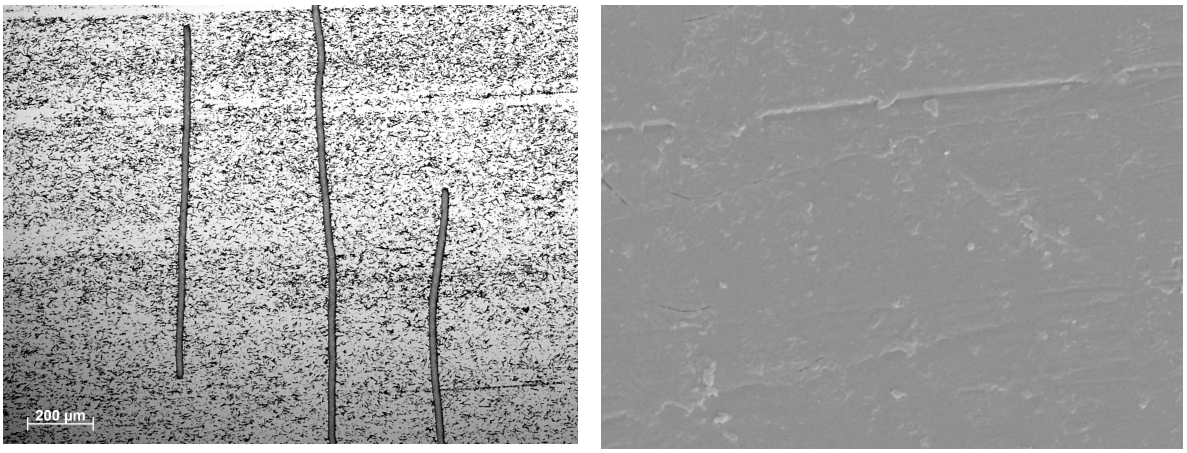

Figure 35 Scratches for various materials by Maruo Rods using optical microscopy (left) and SEM (right) – plate sliding direction was horizontal

The scratches generated are generally unidirectional but significantly wider than individual particles. The rod particles are seen to behave in a unique manner, forming long thin agglomerations.

Figure 36 particle agglomerations with individual particles in the background showing the scale of the clusters. It is not known for certain why the Rod particles have an affinity to agglomerate in this fashion. It is likely a result of the unusual slender geometry of the precipitated calcium carbonate. These particles are particularly adept at interlocking with surrounding particles as they propagate which can lead to particles gathering under a moving load. As the lattice moves more particles are collected and the agglomeration begins to roll. The dynamic behaviour of this and other particles is examined in more detail in chapter 8.

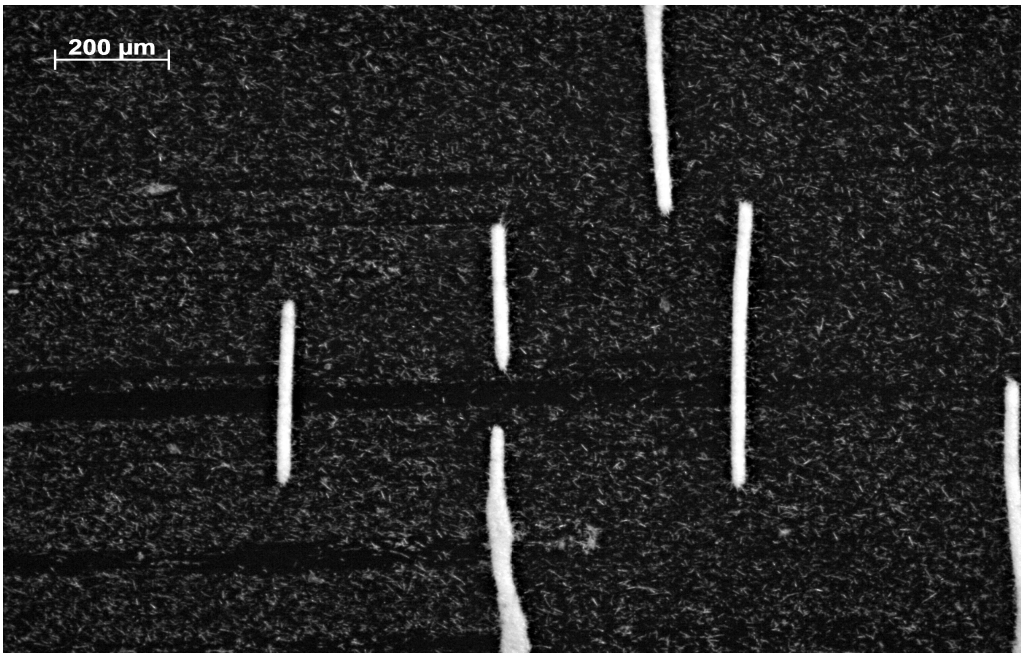

Figure 36 Rod particle agglomerations from contact plate trials - plate sliding direction was horizontal

Figure 37 shows the arrangement of some of the projecting particles from one of the formations. It is thought that the rods do not become significantly more damaging to the substrate surface because these particle tips are very fragile in nature and are easily broken off observable by the increased prevalence of small particle fragments of similar size to the particle tips on the substrate surface after testing. This is discussed in more detail in Chapter 8.

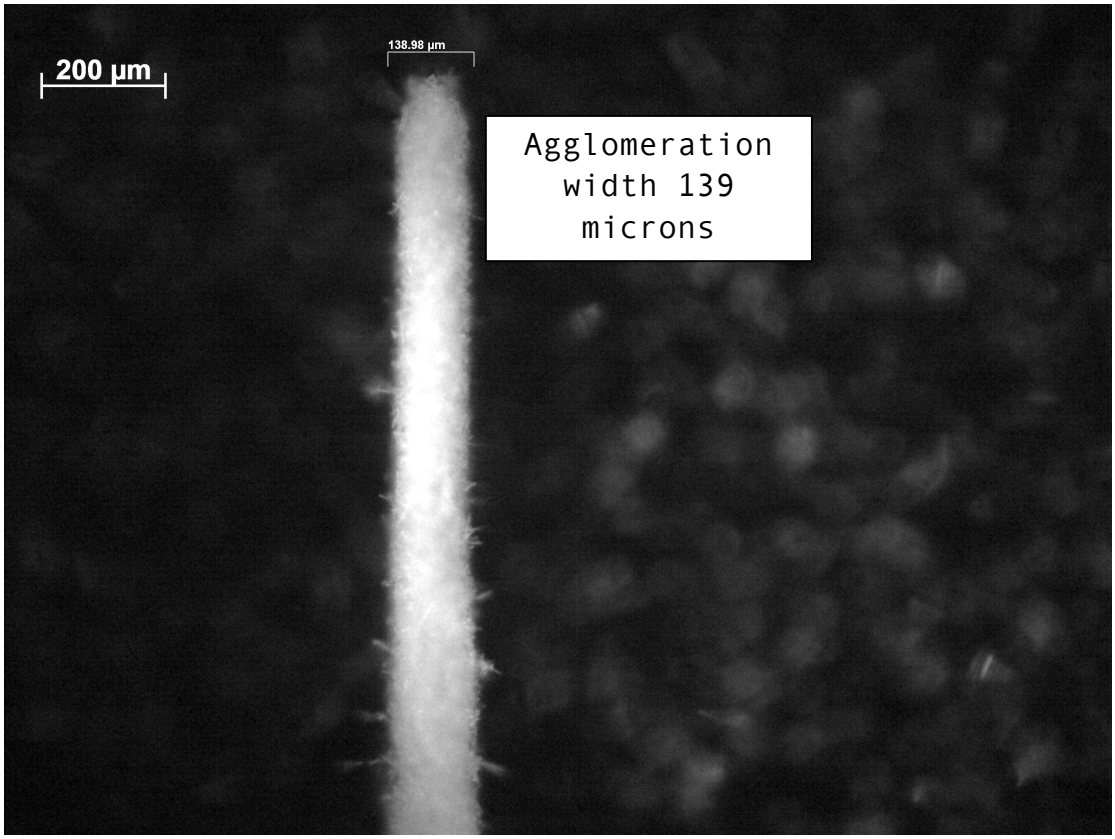

Figure 37 Protruding Maruo Rods under SEM

Figure 38 below shows the scratches obtained by S2E PCC particles.

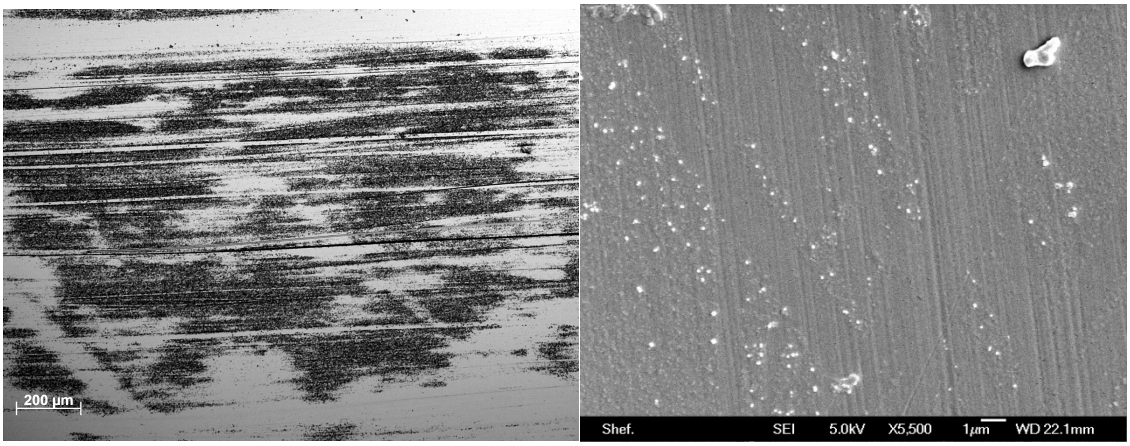

Figure 38 Scratches for various materials by S2E PCC particles using optical microscopy (left) and SEM (right)

The above scratches show more aggressive behaviour than Maruo Rods particles with deeper and more frequent scratches. The particle motion is still linear with long straight scratches indicating that particles are likely to be sliding rather than rolling in the contact region. This is interesting as S2E PCC particles are much less angular than Maruo Rods and often suggested/proposed within oral care as a candidate for a gentle abrasive particle for non-aggressive toothpastes. For this behaviour however Maruo Rods appear much more suitable.

Figure 39 below shows the scratches obtained by Omya 5AV.

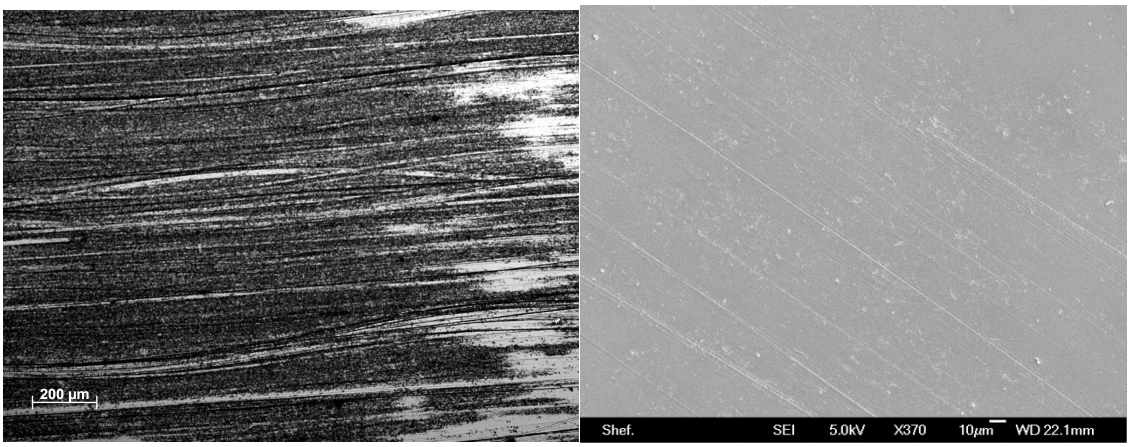

Figure 39 Scratches for various materials by Omya 5AV particles using optical microscopy (left) and SEM (right)

Scratches by Omya 5AV particles are deep and frequent showing aggressive material removal.

The wear scars shown above demonstrate the aggressiveness of this particle with material being ripped from the grooves. For Maruo Rods particles the wear track edges parallel and uniform whilst for Omya 5AV some gouging is evident indicating a more aggressive behaviour.

5.2.4 Conclusions

When comparing the results above, Omya 5AV particles are the most aggressive showing the deepest and most frequent scratches. Since the results are comparable, it has been demonstrated that useful data can be derived from flat plate testing such as this. However, testing using this reciprocating rig has limitations. Load control is difficult and limited in terms of both evenness and accuracy. With a more controlled loading, it was thought that it may be possible to observe the ability or resistance of particles to break down or cause damage to the substrate under a known constrained load.

5.3 Scratch analysis using rotation and Perspex

5.3.1 Introduction

The CETR offers improved control in terms of greater aptitude for data recording along with load and speed control. The reliability of initial tests for reciprocating plate trials were somewhat questionable since, despite efforts to keep the plates flush in contact, the true extent of this contact could not be easily known and it was the case there were areas of suspected non-contact and bias. Further to this there was a range in speed occurring in initial trials due to the reciprocating nature of the setup. For this reason unidirectional trials were employed with rotating components at uniform speed.

5.3.2 Experimental procedure

The CETR tribometer has been set up as below in Figure 40

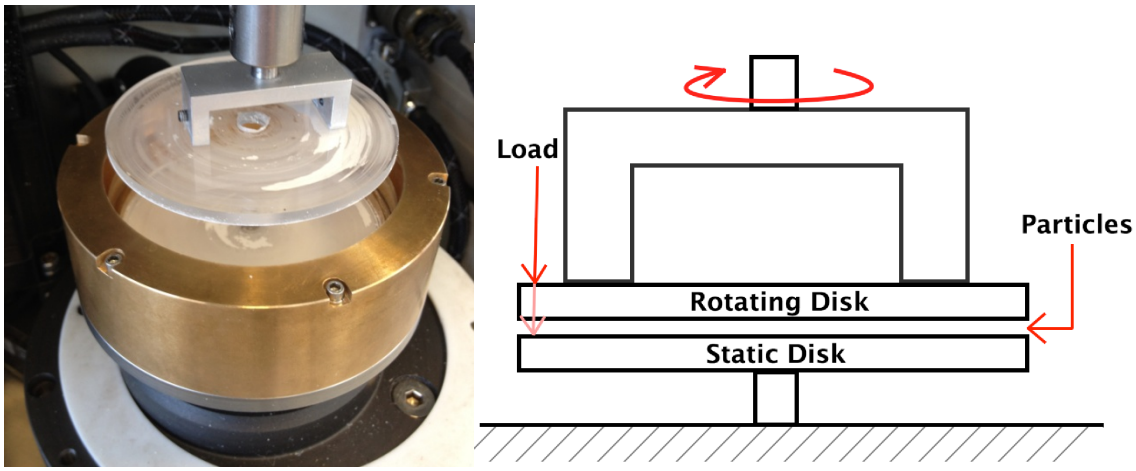

Figure 40 CETR tribometer set up for plate trials

To give a good range of particle behaviours and characteristics, those selected for this test regime are given below:

- Hubersorb 600
- FM1000
- Baralev A
- Hubersorb 5121
- Bamboo
- PE resin
- Hubersorb 250
- Perlite

An example of a plate post-test is shown below in Figure 41. It can be seen that particles often agglomerate or clump together however scratch generation appears unaffected by this.

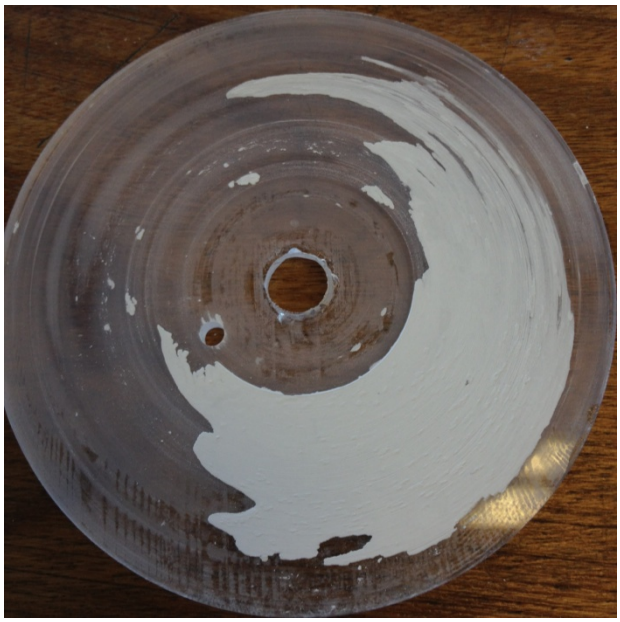

Figure 41 Example of particles and scratches following a test

Using high resolution surface metrology and a form measurement system it is possible to map the topography of the substrate surface in order to derive a better understanding of the scratch characteristics. Scratch depth and frequency for the various samples has therefore been measured using Atomic Force Microscopy (AFM) within a 3mm square area on each worn surface. An example of the computational surface generated using AFM for acrylic worn by Hubersorb 600 is shown in Figure 42.

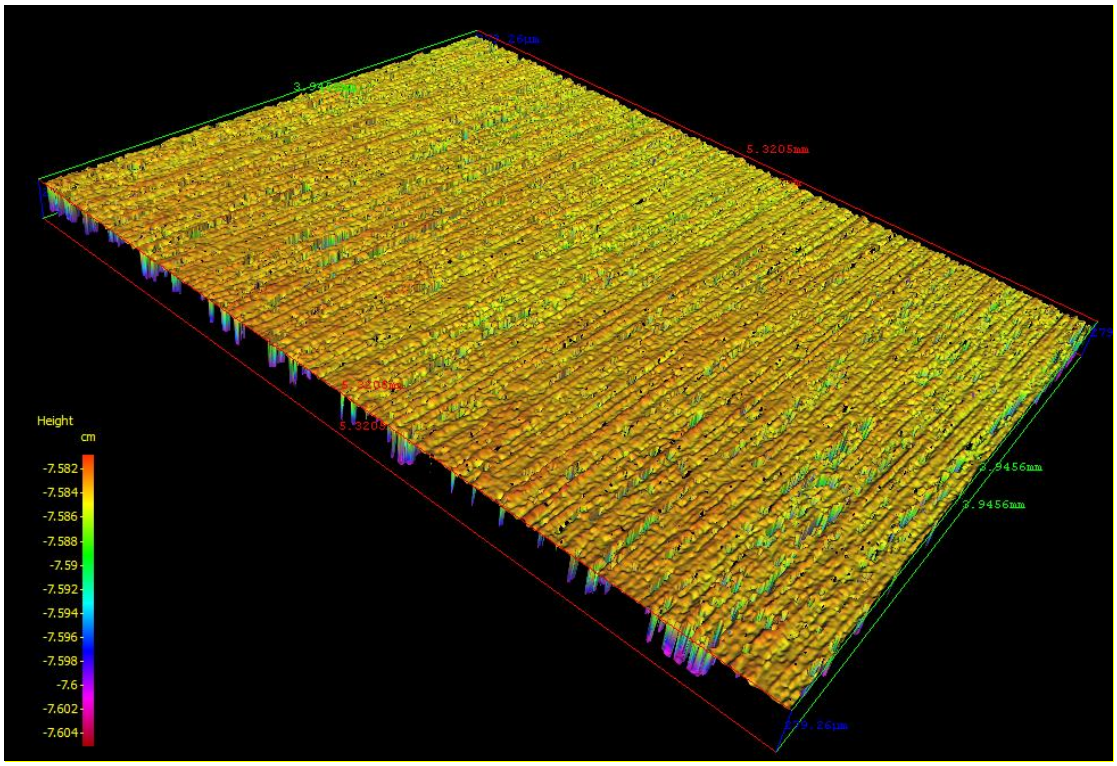

Figure 42 AFM measurements for Perspex worn by Hubersorb 600 particles

Further to visualisations of the substrate such as in Figure 42, which represents a matrix of topographical measurements, detailed plots on specific regions can be explored to derive the frequency and depth of scratches and surface features.

5.3.3 Experimental results

When compared with filament loading trials, the results show that there is a tangible difference between the resultant scratching derived from linear reciprocation trials using brush filaments and those yielded from the plate trials for the same particle (see Figure 43)

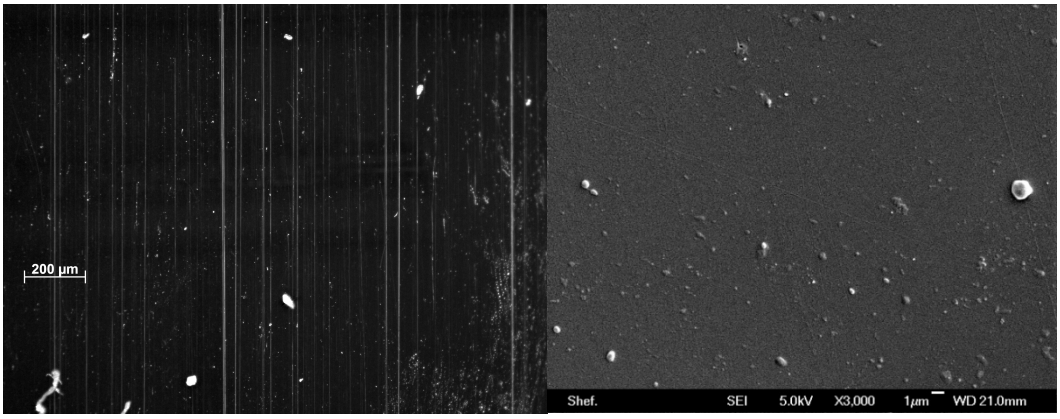

Figure 43 Scratch analysis of post processed Perspex from brush and plate trials (respectively) using Rod particles

Images from plate trials (Figure 43, right) show a significant decrease in scratch frequency, even when analysed by scanning electron microscopy. Particle breakdown also appears more complete with little presence of debris above 0.5 microns. This is most likely a result of larger particles being more easily entrained by filaments but not necessarily being more adept at penetrating the substrate surface.

Similarly, other particles are seen to exhibit potentially unrealistic behaviour by testing between two plates. Maruo Rods agglomerations for instance are seen to form into long strands that are not seen in filament trials. It is interesting to note that the aggressiveness of particles generally correlates between plate and filament trials, with aggressive particles such as Omya 5AV remaining aggressive and gentle materials such as Maruo Rods particles remaining gentle.

5.4 Analysis of particle scratches on substrates of different hardness

In addition to the scratch analysis above, work has been carried out to determine the full suitability of Perspex as a substrate material. Further to this, determining the hardness of a microscopic body can be problematic. It was hypothesised that it is possible to gain a representative understanding of hardness based upon a test similar to the Mohs hardness scale. Since a harder material will scratch a softer material it was thought possible to rank particle hardness by scratch testing against the various hardnesses of the substrates above. It was expected that a particle softer than the substrate it is tested against would not induce scratching whilst a particle the same hardness or harder would lead to scratching. Since the different substrate hardnesses have been determined, an estimate of particle hardness was thought to be possible in this manner. Further to this, the basic nature of the interaction of the particles with the different plastics could be observed.

During analysis of particle behaviour, it is not always appropriate to use human dentine samples for contact. There are various reasons for this including the difficulties associated with obtaining human samples and variability between different teeth. In order to make results fully comparable, a uniform surface should be used in trials. The surface hardness must be such as to allow the particles to behave as they would on genuine dentine samples. Perspex is generally selected for its similar hardness to dentine (for reasons discussed within this thesis), however other materials have been investigated and are discussed below.

Plastics have been selected for testing as they initially provide a reliably uniform scratch free surface which under a microscope reveals only the damage done by the particles with no granular structure like that of metals or other materials. Various different plastics have been tested in order to determine the one most suitable for the bulk of the testing within this thesis.

Hardness was gauged comparatively using ocular readings from a Vickers indentation testing. Figure 44 compares the ocular readings derived from indentation testing for each of the 7 substrate materials tested.

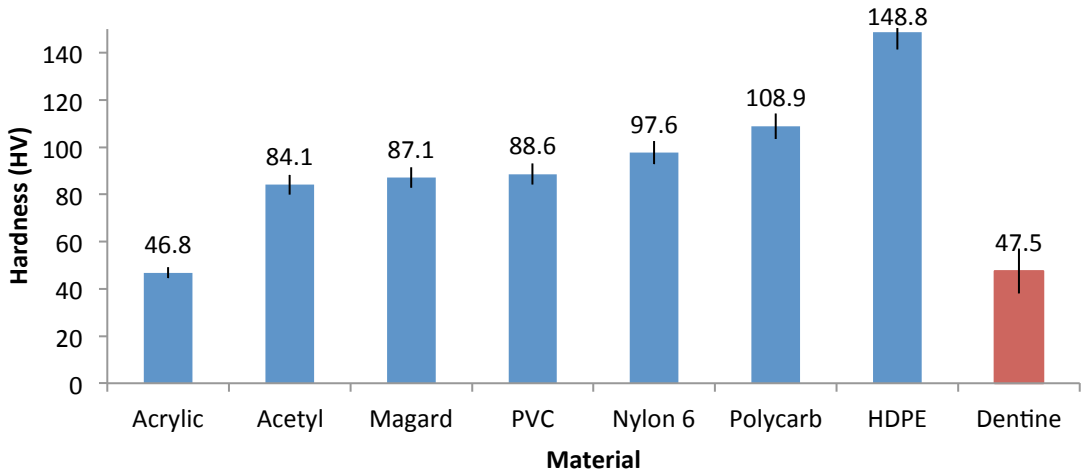

Figure 44 Substrate hardness by Vickers test

Whilst it can be seen that the hardness of Acrylic (Perspex) is the closest to that of dentine (approximately 45 – 50 HV [34] [35], there may be some value in using a different plastic. This range in hardness values for dentine varies a little from the figure introduced earlier in this thesis (60 HV) and was proposed by a different study [35], which utilised a greater range of samples from which the hardness values were acquired. Unfortunately being a natural material there can be notable variety in material properties across different ages, lifestyles and the also the location within which the hardness test is conducted (across different types of dentine). Although the earlier mentioned figure is higher, it was considered worthwhile including the data from this study [35] due to their arguably more representative sample collection.

If particles are seen to interact with the plastics in different ways, then it is possible that there is a more suitable substrate (that more closely matches particle behaviour against dentine samples), despite the difference in hardness. Further, it is hypothesised that it is possible to use the various different plastics to determine the hardness of particles as described below.

From the AFM data for these trials, measurements can be averaged for each repeated trial and then compared with material hardness for each of the plates. An example of scratch depth and frequency relative to the plastic hardness for Hubersorb 600 is shown below (Figure 45). Scratch frequency was calculated within a width of 1mm using basic static imaging software to help highlight and count individual scratches.

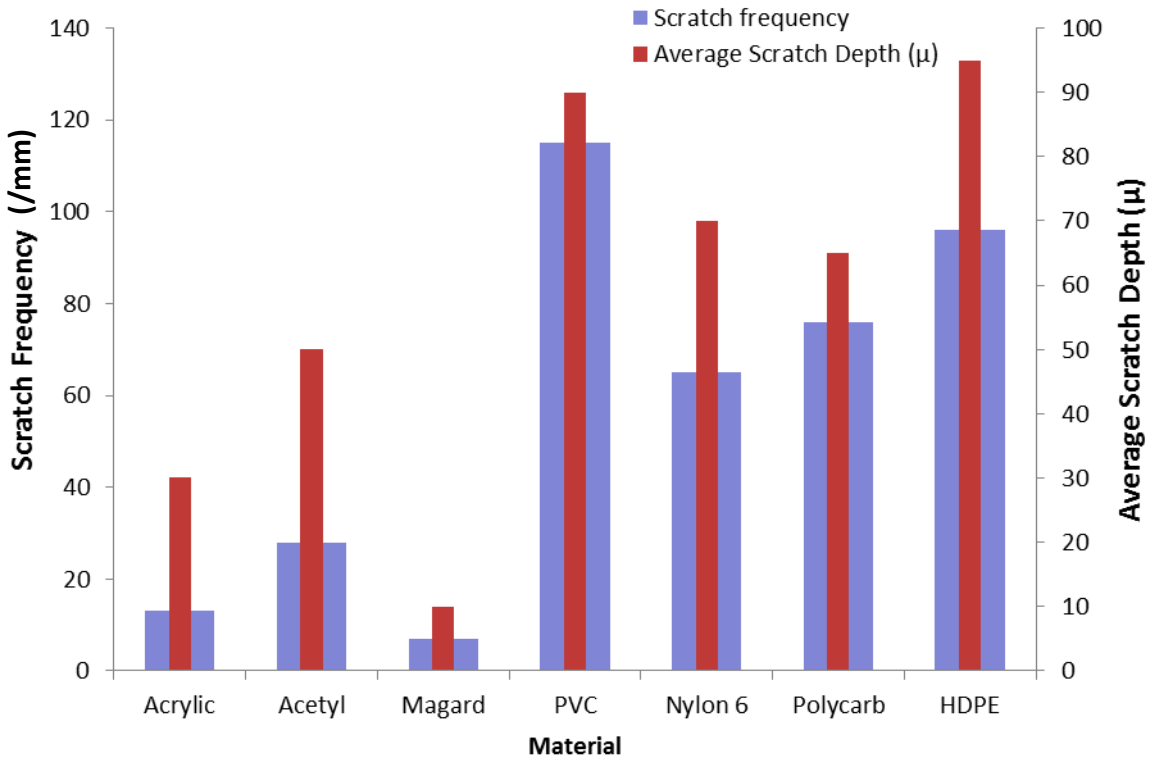

Figure 45 Scratch frequency and depth for Hubersorb 600 against various different plastics

It can be seen that there is a general correlation in scratch depth and frequency relative to each other however the aggressiveness of the scratches has little relationship with the hardness of the plastic. In this case, Magard for instance shows the least scratching despite being only the third hardest material. Similarly, all surfaces showed some degree of scratching and this test process has therefore been shown to not be useful in determining particle hardness. 'Aggresiveness' in this case is a qualitative term, which summates the affinity of a particle to cause damage to the substrate surface.

A ranking of each particle in terms of aggressiveness can however be made and scratches compared by microscopy. The matrix shown below in Figure 46 gives least to most aggressive particles by scratch frequency (horizontally) relative to the softest to hardest plastics tested.

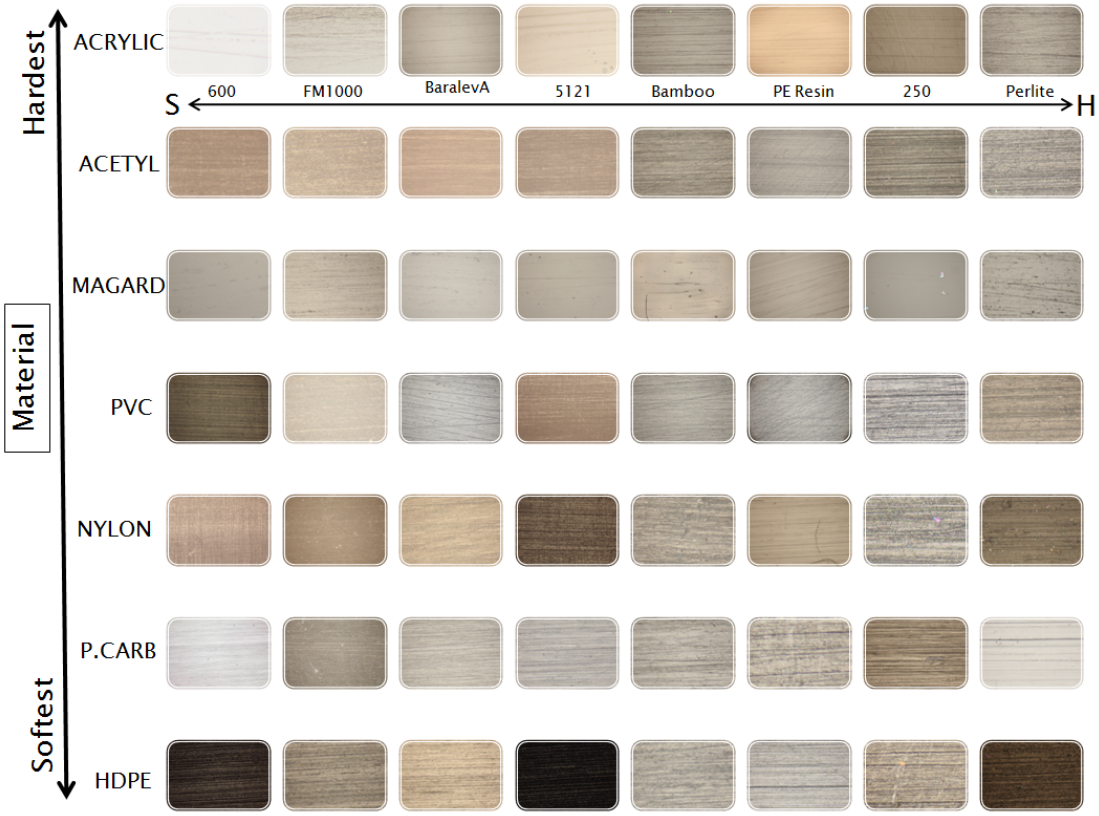

Figure 46 Scratch analysis of various plastics with least to most aggressive particles left to right

In each case however, there is only tenuous similarities found between the various plastics tested and the characteristics of the scratches observed. It is possible that this indicates that the particles are all harder than even the hardest substrate tested (46.8HV) or that under loading, they break down and size effects artificially elevate the perceived particle hardness. Here my findings suggest that size effects (as the particles break down) may artificially raise the perceived particle hardness. This may appear to contrast with earlier claims within this thesis regarding smaller particles and that it was expected in many cases that as size decreases, wear would also decrease. It could be argued that there are multiple variables are at play here and the two claims are not mutually exclusive. It may well be that a breakdown in particles can modify its perceived hardness, however the hardness of the particle is only one factor affecting the affinity of the particle to scratch or damage the substrate surface. Likelihood of filament entrainment, geometry and how the particles interact with each other (operating in isolation or as agglomerates) are all important factors affecting the aggressive nature of each particle. This is investigated in more detail in Chapter 8.

It is also possible that there is non-uniformity of particle hardness within a sample leading to some individual particles capable of scratching harder surfaces with others unable to. This may feature more with non-precipitated particles derived through a grinding process. The results of this testing therefore cannot be used to determine particle hardness as predicted, however the differing breakdown behaviours observed are an interesting result.

When scratch depth is compared with particle size, a correlation is more subtlety apparent (Figure 48). With the exception of Baralev A and Perlite, an increase in particle size led to an increase in scratch depth. Although this relationship appears stronger than that observed with scratch frequency vs. particle size, it is not in itself a convincing relationship.

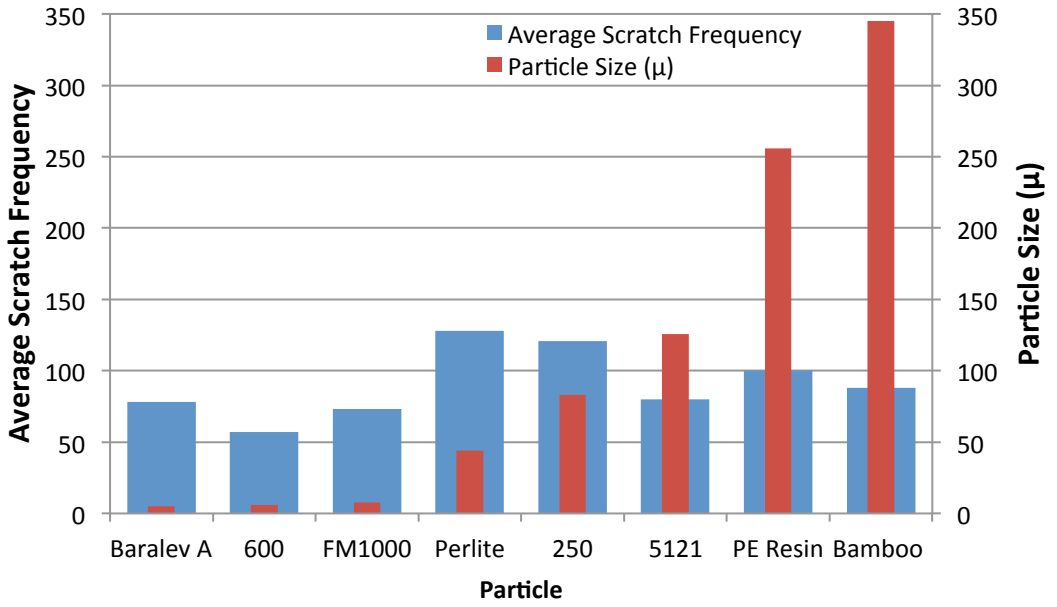

Figure 47 Scratch frequency vs particle size (averages of the scratches across all substrates)

The correlation is not apparent when compared with scratch frequency however (shown in Figure 47)

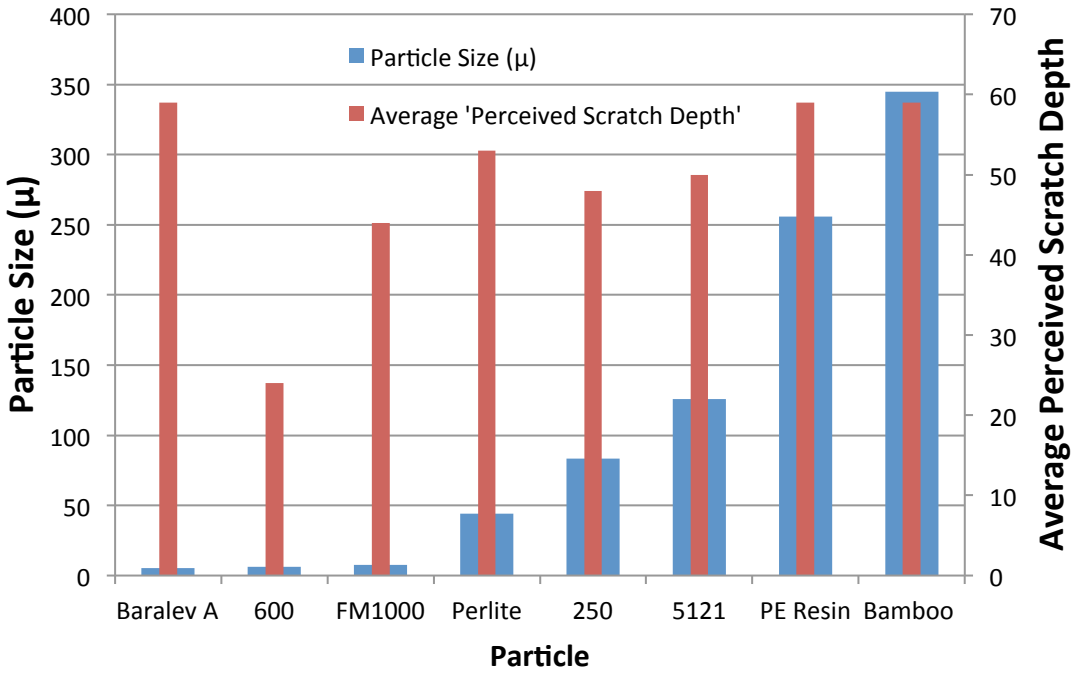

Figure 48 Particle size and scratch depth (averages of the scratches across all substrates)

Clearly, larger particles generate deeper scratches when tested in this manner however this does not correlate with the frequency of these scratches. Whilst this is an interesting result, it is worth noting that the interaction of particles with the surface may be limited.

5.5 Conclusions

5.5.1 Linear reciprocation trials

Observation of some particles within linear reciprocation trials demonstrated low scratch frequency and depth suggesting they are sympathetic to the substrate surface; this does not mean they cannot operate as an effective abrasive however. The geometry and dynamic characteristics of these 'gentle' particles when motivated may well make them adept at removing surface detritus and macroscopic asperities without marking the substrate surface.

It is apparent that a subtle change in size or shape can have a dramatic effect on the aggressiveness of the particle to the substrate surface. This could be attributed to a number of factors including a change in the in the agglomerative behaviour of the particle. There was little relationship between particle size and scratch frequency above 10µm, however there was a more legible relationship between particle size and scratch depth observed.

The largest particles are not necessarily the most likely to pose a threat to the substrate surface. The results in the case of these particles (which were notably larger than others) within these trials, suggest they were not abrasively aggressive to the substrate. In some cases they demonstrated quite low abrasive wear.

Analysing scratches from one filament angle zone to another did not lead to obvious trends. There was however some notable change in individual particle behaviour with a change in filament angle. The middle brush stroke zone (filament angle 35°) lead to the highest scratch depth and roughness

There is no distinct relationship between the roundness of a particle and its scratch behaviour in terms of scratch depth and scratch frequency. It is very likely that particle shape does indeed have an effect upon the abrasive performance of the particle however this is subject to a number of different variables and is not easily discernable from the analysis of scratches.

5.5.2 Contact plate trials

The hardness of various plastics has been determined and flat plate trials undertaken in order to determine the effect of substrate hardness on particle aggression. Simple reciprocating trials have demonstrated that it is possible to gain comparative results by suspension of particles between two flat plates.

Maruo Rods don't appear to scratch as aggressively as Omya 5AV particles and are relatively sympathetic to the surface. This fits with what has been observed in filament trials and other trials. Arguably particle breakdown is less than that observed with filament motivation since instead particles form thin elongated agglomerates. The true mechanism behind this is not certain, however it is known that rods have an affinity to lie flat to the surface due to their uniform and level faces. It is possible that the asperities of the plates provide a much more evenly distributed load when motivating compared to the unpredictable nature of the filaments and so the rods are potentially quite resilient under compression but fragile with eccentric loading due to their thin elongated geometry.

A general correlation in scratch depth and frequency has been found in tests with greater control offered by the CETR Tribometer, however the aggressiveness of the scratches only loosely correlates to the hardness of the plastic substrate. It could be the case that the particles are all considerably harder than the plastics tested however the hardness of the particles is difficult to determine directly. Considering there was a range of materials used comprising the particles, likely introducing a range in hardness values for these particles, it is possible that the aggressiveness of particles is attributed to other factors; such as dynamic behaviour, shape, fracture characteristics and agglomerative behaviour. These characteristics are explored in more detail in later chapters. Scratch testing on a range of substrates therefore is not a reliable method for determining particle hardness by inference. It does however give a means of determining particle aggressiveness irrespective of surface hardness.

When compared with filament loading trials results show tangible differences between scratches generated for the same particle however the ranking of aggressiveness of particles remains the same.

6 ANALYSIS OF PARTICLE FRICTION

Frictional contact of particles can be split into two distinct interactions. Those of the particles contacting other particles, and those in which they form a third body mechanism with another surface or surfaces. Inter particle friction can be significant since it will partly determine the ease with which particles move past each other and hence the granular material as a whole. This frictional interaction can be determined statically through measurement of the angle of repose. The frictional interactions of the particles as a three body mechanism must however be measured dynamically and various methods have been adopted to this end and are described in detail in this chapter.

6.1 Inter-particle friction by angle of repose

The angle of repose of a conical pile of granular material is approximately equal to the static coefficient of friction of the particles [36].

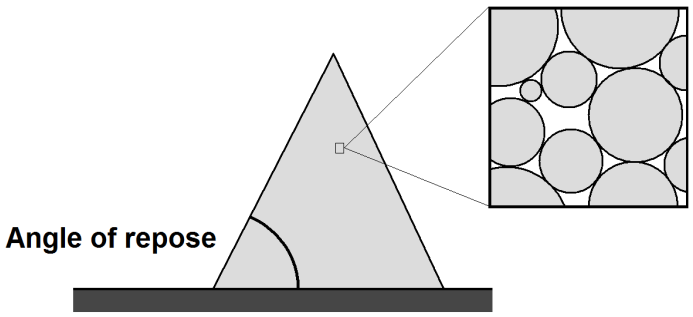

Figure 49 Angle of repose of a conical pile of granular material

Figure 49 shows how frictional contact between the particles allows for steeper angles in high friction cases, or shallower angles as in low friction cases.
To determine the static coefficient of the particles, the following experimental set up has been used (Figure 50).

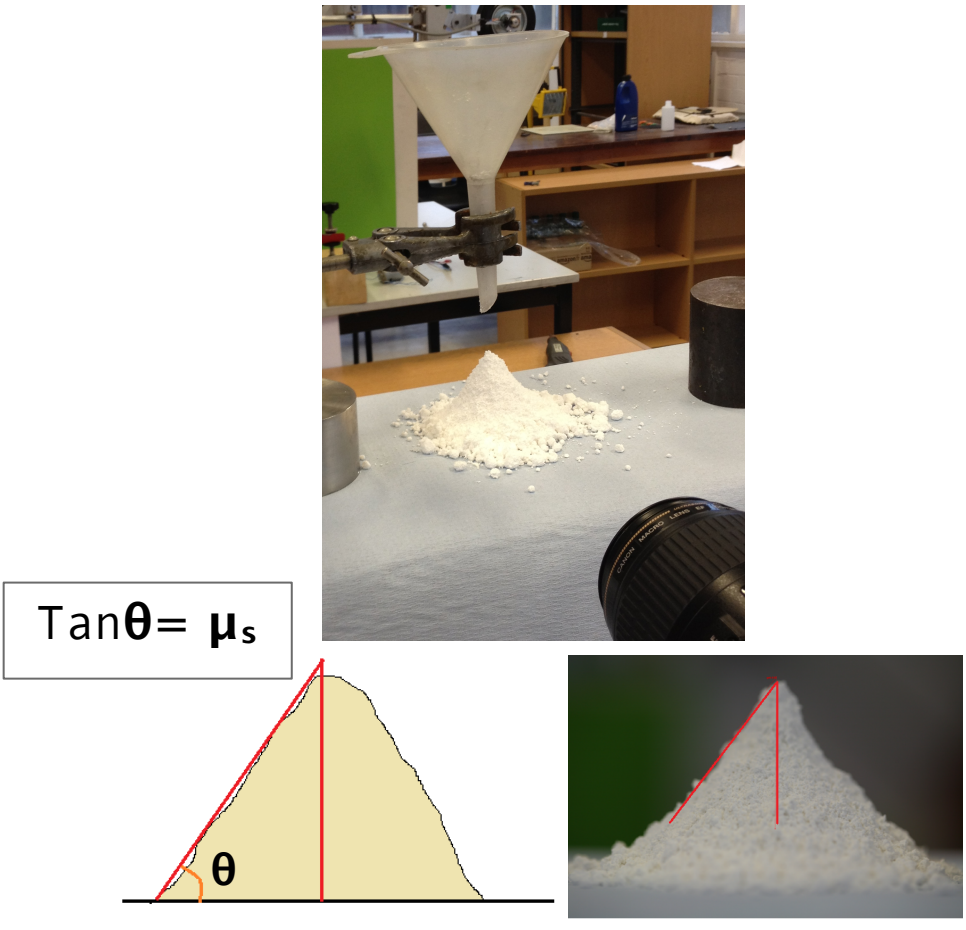

Figure 50 Experimental set up for angle of repose measurements

A funnel has been used to drop the particulates onto a flat surface. A camera has been used to image the conical pile and calibrated so that measurements can be made from the resulting images. The procedure was run 6 times for each particle and the results are shown below in Figure 51. The error bars in this case indicate the range in measurements across the 6 trials.

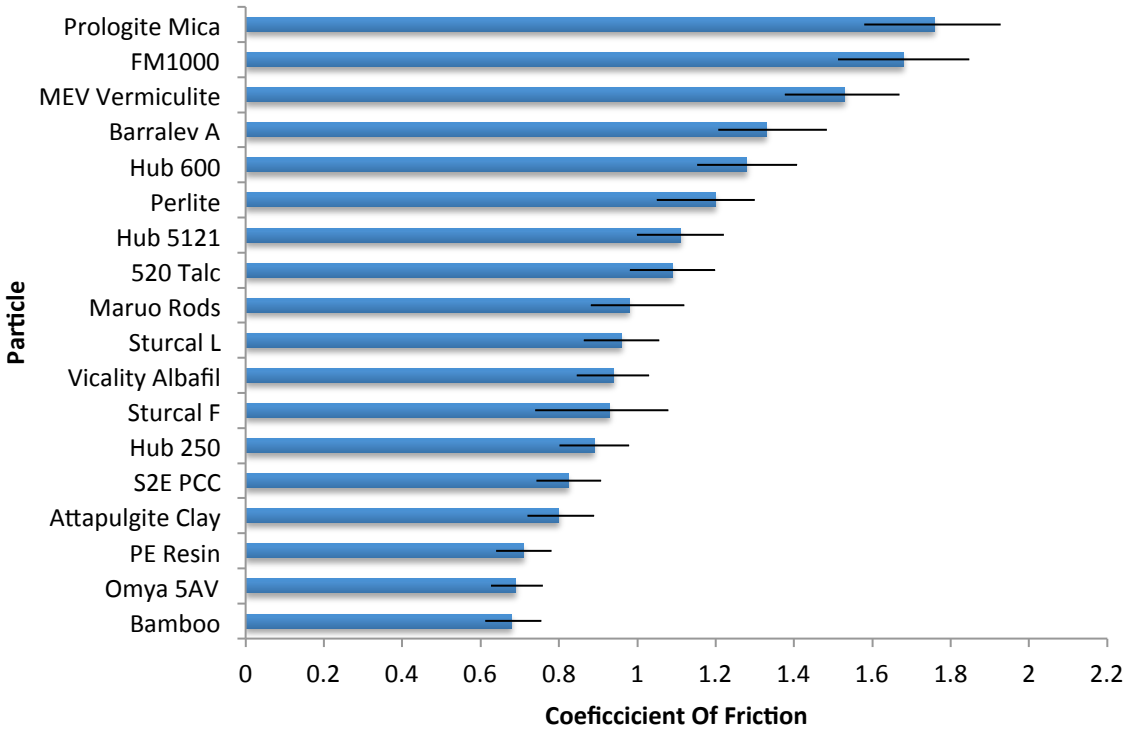

Figure 51 Particle's coefficient of friction from angle of repose trials

The mean angle of repose of the Prologite Mica was shown to give the highest coefficient of friction of the particles tested (1.74) whilst Bamboo and Omya 5AV showed the lowest coefficient of friction (0.71). Standard deviations were in the range of 0.036 to 0.073. Whilst COF is effectively measured as a bulk material in this manner particle interlocking due to shape will most likely have an effect on the results which may artificially promote certain particles (such as Maruo rods) to a higher ranking in terms of COF. Similarly, the COF data for all particles appears relatively high. It is thought that this is also an effect of particle agglomeration due to shape and other forces of attraction. Although particle shape is the predominant driving force behind the angle of repose formed, it cannot be claimed with total certainty that there is not a small degree of inherent moisture content associated with the different particles. This in theory can vary from particle to particle depending on the material characteristics. Any moisture present may introduce electrostatic attraction of the water to particle surfaces. This in theory could affect both the COF in general for the particles and the angle of repose; however the latter may be more sensitive to this as a result of the delicate and static nature of how it is measured (particles gently poured into

contact whereupon they remain unmotivated). If the particles clump together to form an unrepresentative peak this can potentially quite dramatically alter the measured angle of repose, making this process more unreliable. For this reason each particle was measured 6 times and averages taken.

6.2 Dynamic friction of complete contact

In an attempt to gauge the 'aggressiveness' of the particles, systemic frictional properties have been analysed for a full contact scenario. The aim was to be able to interpret a difference between the outputs from the various abrasive particles for the system as a whole, indicating that despite the seemingly insignificant particle dimensions a cumulative and notable difference in friction could be observed. The following experimental set up has been used to determine cumulative frictional properties of the various particles (Figure 52)

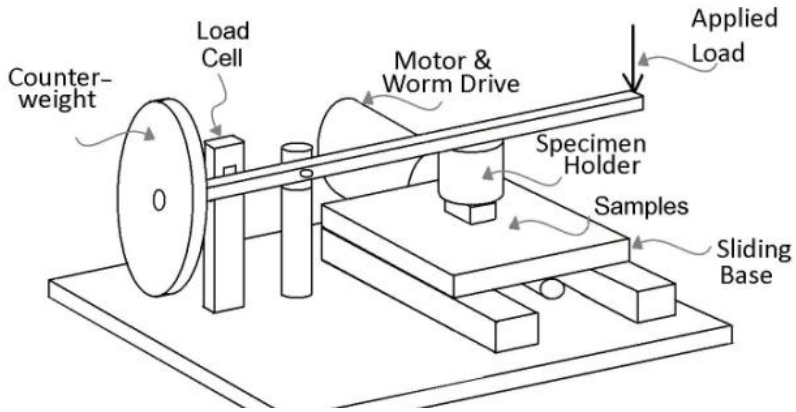

Figure 52 Schematic of experimental set up for cumulative friction measurements [37]

As the motor is engaged the sliding base beneath the specimen holder moves at a constant speed causing the armature to rotate about a pivot point, ultimately applying a force to the load cell. Two experimental approaches have been used. The first involves fixing the particles in position whilst the second uses a brush head. In both cases the particles are in contact with a Perspex plate.

6.2.1 Friction of fixed particles

The particles were initially fixed to Agar adhesive Carbon SEM tabs (Figure 53), which was then introduced to the specimen holder on the armature and loaded to 0.2 kg. These tabs are very flat and uniform as they are a common feature in scanning electron microscopy technology. This allowed for the introduction of a replicable region of particles; the tabs were sufficiently coated such that no adhesive substrate was in direct contact with the moving base (excess particles were removed with a blast of air).

Figure 53 Adhesive Agar 15mm SEM Tabs used to mount particles

An example result is shown below in Figure 54.

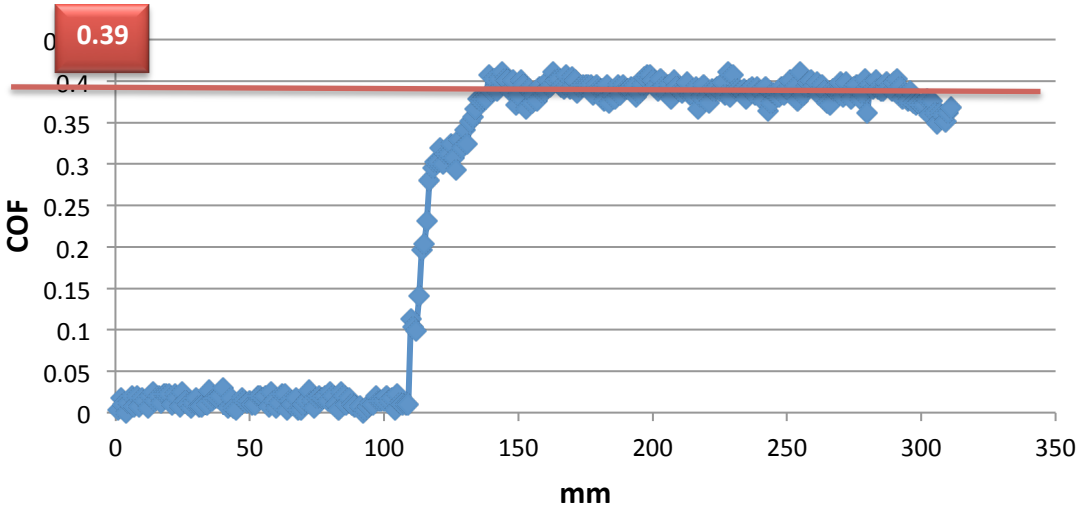

Figure 54 B200 Prologite Mica raw friction rig data

Initial data points show little or no coefficient of friction due to the sample moving unimpeded with the dynamic base. As the armature contacts the load cell the coefficient of friction rises to a nominal value at which point slipping occurs and the contacting surfaces move relative to each other. This nominal value is seen to be relatively steady and can be used to compare the various particles.

Figure 55 gives an example of the COF values of different particles tested on carbon tabs.

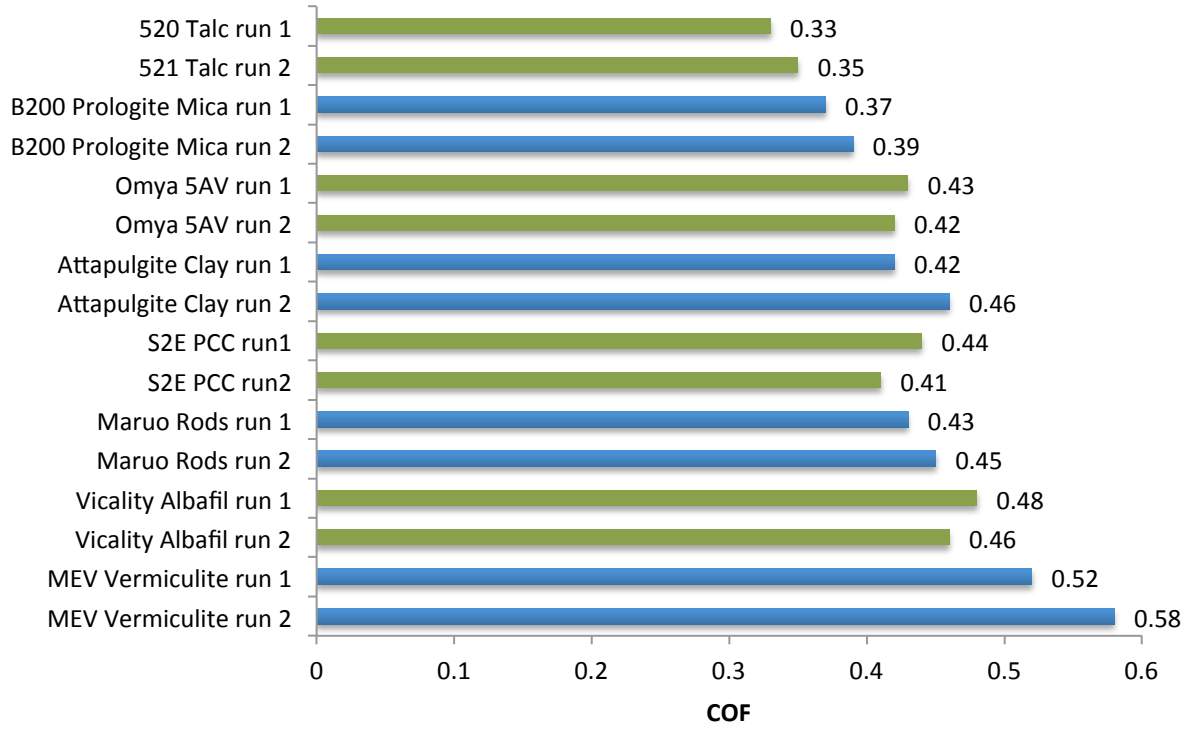

Figure 55 Comparison of COF values from friction trials

In these trials the highest COF was observed with MEV Vermiculite and the lowest S20 Talc.

There is sufficient variance between particles to suggest that useful comparative friction data can be determined from particle to particle, however it is important to distinguish if this is still the case using the more representative interface of a brush head. Despite there being a step difference in the overall magnitude of the COF values derived by each method, there does appear to be a correlation in the ranking of the particles from low to high COF. Despite the similar rankings of particles, the angle of repose is seen to yield significantly higher COF than dynamic trials. For example, MEV Vermiculite shows a COF by angle of repose of 1.52 and dynamic COF of 0.56. This indicates that the particle-particle interactions are stronger than between particle and Perspex substrate.

6.2.2 Friction of particles entrained by a brush

The above experimental procedure has been repeated using a standard Unilever brush head (Figure 56). The purpose of this test was to demonstrate the validity of the methods used, including mounting, particle preparation and entrainment before moving on to more advanced experimental equipment meaning the reduction of particle types to two examples. Full results are shown in Figure 57. The brush head in this experiment was used in trials both with and without the presence of water. In wet trials the minimum amount of water was added so as to just saturate the particles, and ensure that no freestanding water was present. Further to trials with filaments passing through particles in the path of the

brush, trials were also conducted where the brush head was motivated from a static position amidst a small pile of dry particles.

Figure 56 Friction rig analysis with brush head interface

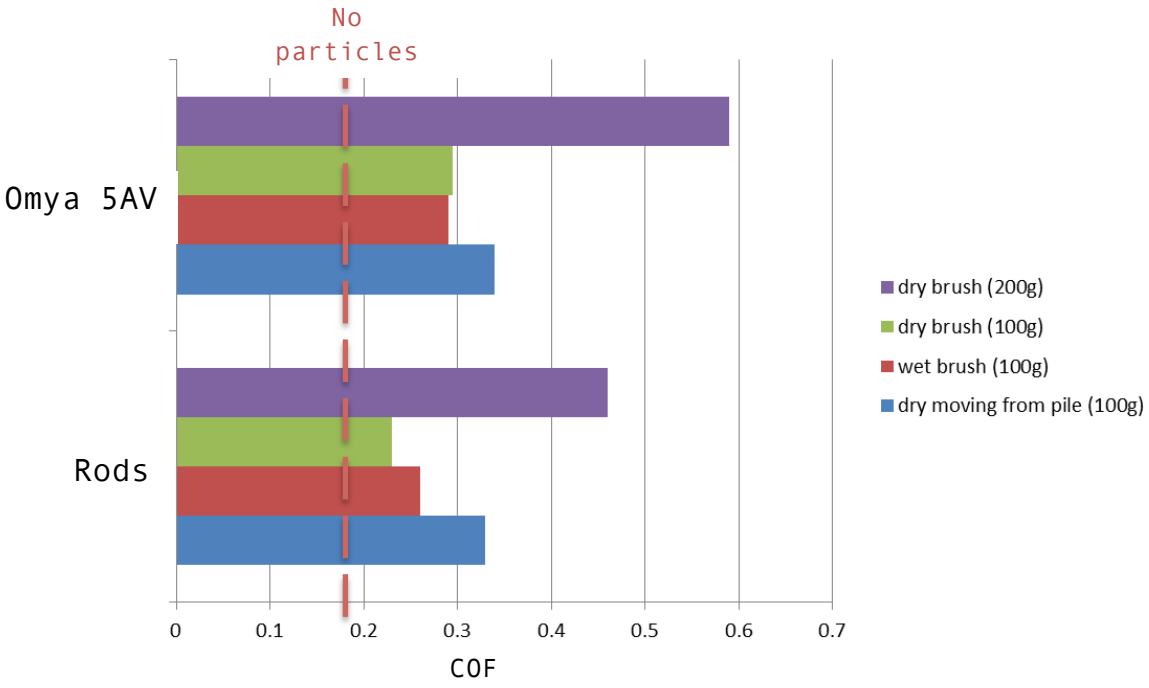

Figure 57 Comparative plot of Friction Rig data for brush head on Perspex

The baseline friction between the dry brush filaments and the Perspex substrate was found to be 0.18, significantly lower than on addition of particles. Particle COF remained comparable between trials using carbon tabs and trials using a brush interface. Omya 5AV particles appeared to have a higher COF than that of Rods, which became more apparent at higher loads. It can be seen that with the dry trials, that COF is load dependent; at higher loads there is almost twice the COF – possible at these higher loads there is a higher number of filaments in contact and particles are more likely to remain entrained.

In some trials, a spike in the COF can be observed (such as in Figure 58), in this case around the 200 data point mark. This appears to be from the sudden and momentary increase in resistance produced as many of the filaments change their orientation and align in uniform formation.

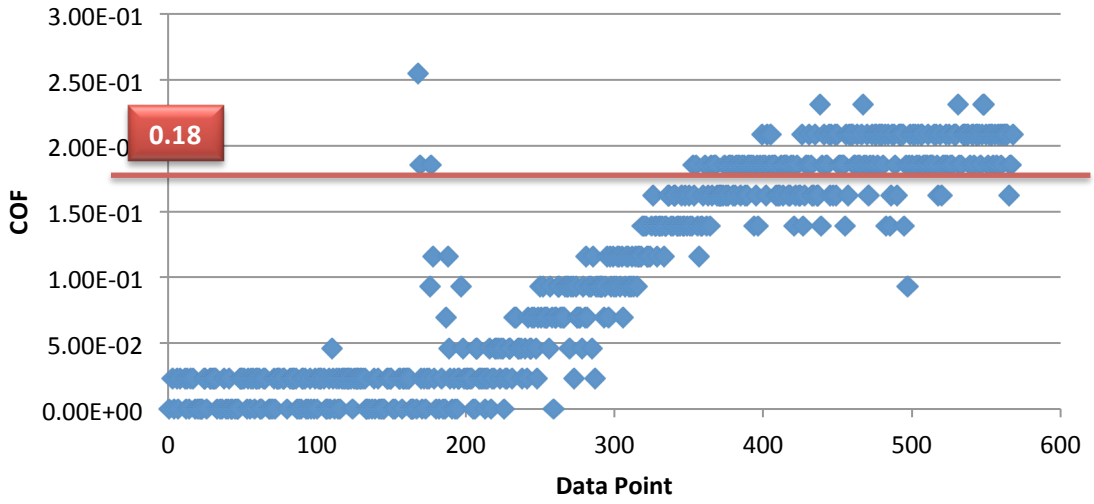

Figure 58 Raw Friction Rig data for brush head upon Perspex with no particles present

Despite the introduction of a flexible filament interface leading to a reduction in the succinctness of the trend, observable differences in COF are present. Particle COF also remains comparable between trials using carbon tabs and trials using brush interface. Omya 5AV particles appeared to have a higher COF than that of Rods, which became more apparent at higher loads.

6.3 Modified Tribometer Friction analysis

Following on from the cumulative friction trials above, a wear and friction Tribometer (Figure 59) has been modified in order to further analyse and understand the variance in particle friction.

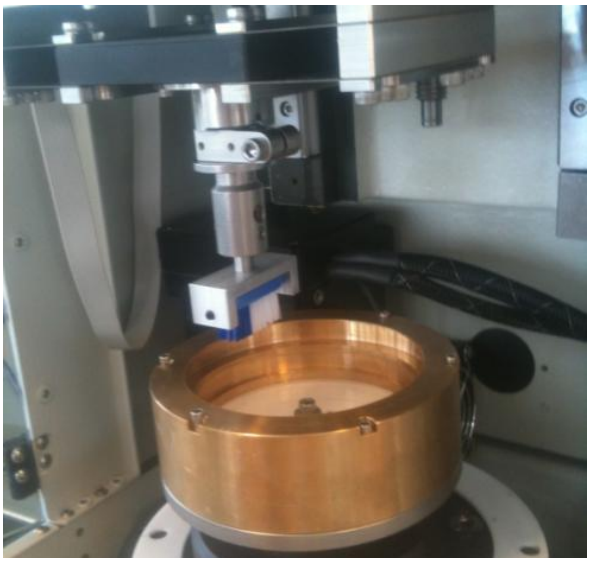

Figure 59 Experimental set up of precision wear and friction tribometer

A brush head is contacted with a rotating Perspex disk and controlled in speed, position and load. This approach is capable of much higher degrees of accuracy whilst also being computer controlled allowing for stringent operation and the introduction of detailed operational program scripts. Initial scripts were constructed to analyse the effect upon the COF introduced by a change in load or brush speed. Sequences dictating incremental changes in both the load applied through the brush head and the rotational velocity of the substrate disk enables reliable and replicable data between particles and trials. Particles were analysed both dry and suspended in distilled water.

Figure 60 plots baseline data for friction between the brush filaments and Perspex substrate without the presence of particles. This value remains reasonably constant at around 0.325 despite the continual increase in brush speed. This figure is higher than the observed baseline friction value for the previous friction rig at 0.18. This could be a result of the improved loading mechanism of the computer controlled Tribometer setup, which continually attempts to maintain a constant load as the filaments move and deform.

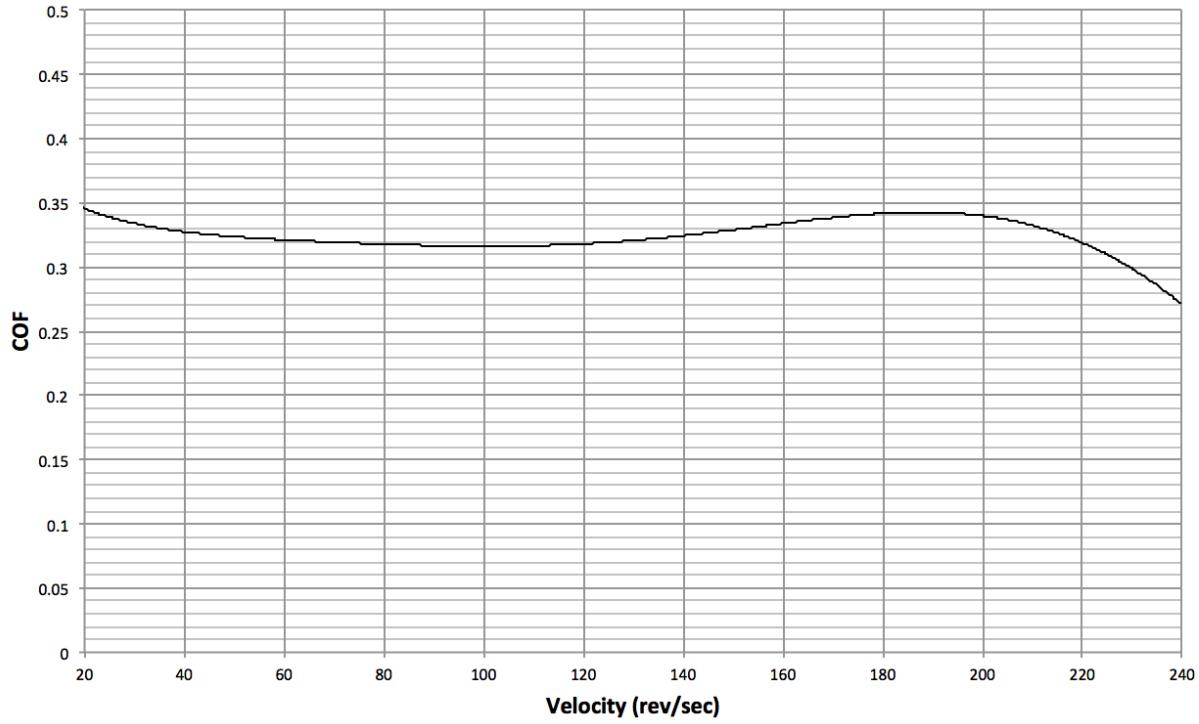

Figure 60 Raw Tribometer data for COF vs. Brush Velocity without particle presence

Close inspection of the plot in figure 60 reveals a subtle cyclic frequency, which may best be described as 'noise'. The amplitude of this noise is small enough that it does not contribute sufficiently to confound results. This is potentially a result of the load control system which attempts to modify the applied load on the brush as the Z position of the interface subtly changes.

6.3.1 Dry trials

The introduction of any particles is seen to increase the COF substantially. As an example, the inclusion of dry Perlite in the contact region is seen to more than double the baseline COF value for brush filament-Perspex contact alone.

The behaviour of the particles does not appear to be uniform across the spectrum of velocities unlike the COF values yielded from the filament upon substrate trial which remained constant. Perlite displays a considerably higher COF from the outset, however this increases further still as brush speed rises. A 30% increase in speed results in an 18% rise in the COF and arguably the 'aggressiveness' of the particle. Figure 61 compares the trends in COF of dry particles as the velocity is increased.

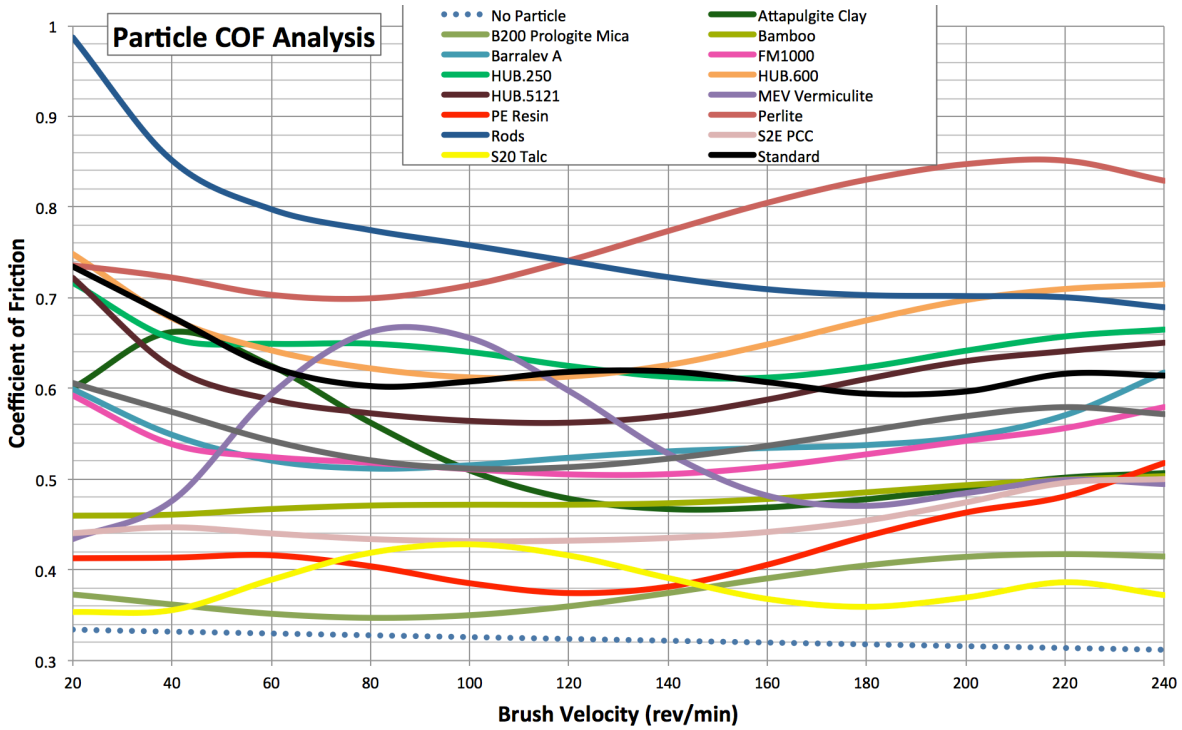

Figure 61 Comparative plot of COF vs. Velocity for all dry particles

As can be seen from Figure 61 there is considerable variance in the COF between particles. Particles appear to be affected by speed in different ways, whilst some appear relatively impervious to brush velocity. Generally particles appear to start and finish with higher levels of friction whilst commonly experiencing a lull in aggressiveness around central velocities. This could be a result of low speed providing an increased capture time in which the particles are directly entrained between the filament and substrate. Higher speeds might encourage the agglomeration of particles due to the speed at which particles are being introduced to the filament-substrate interface. The highest recorded COF was from Rod particles; however this was only prominent at lower speeds (with increase in velocity the frictional affects of Rod particles decreased). Perlite exhibited the most positive increase in COF with increased brush speed whereas S20 Talc and Prologite Mica showed the lowest general COF and appeared not to be affected by speed. Omya 5AV particles despite being of similar length to Rod particles are significantly more cumbersome and stout compared to the sleek and needle like geometry of the Rods. It was expected that filaments would be able to acquire an improved purchase upon these particles than would be attainable with Rods. Despite this Omya 5AV had a lower COF than Rods across the board.

6.3.2 Trials in solution

The so-called 'aggressiveness' of particles is integrally linked to the frictional attributes of that particle. These frictional characteristics can be heavily modified by the environment in which the particle exists. Trials were therefore carried out to study the effects of brush speed on the COF of particles in full suspension (all particles suspended in distilled water).

Figure 62 plots the COF against the brush velocity with the introduction of only distilled water (no particles presence). The resultant trend is fairly constant at 0.33 with a small amount of additional resistance as the setup initially accelerates. As expected the introduction of water alone does not augment the COF value as speed changes, similar to the dry filament upon substrate test with no particle presence. The small isolated data spikes, due to their cyclic location, are likely a result in the step up transition in operational speed according to the control script. Although these are an unfortunate occurrence they do not detract from the legibility of the overall trend.

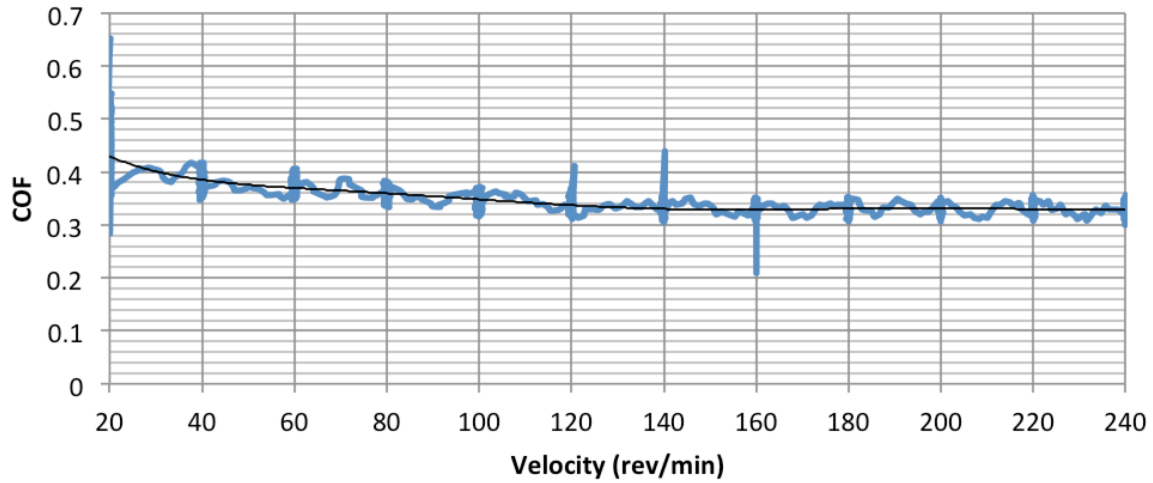

Figure 62 Raw Tribometer data for COF vs. Brush Velocity with distilled H2O present, no particle introduced

As can be seen in Figure 63, the introduction of particles in suspension causes a distinct increase in COF at lower speeds. This was observed in nearly all the particles tested.

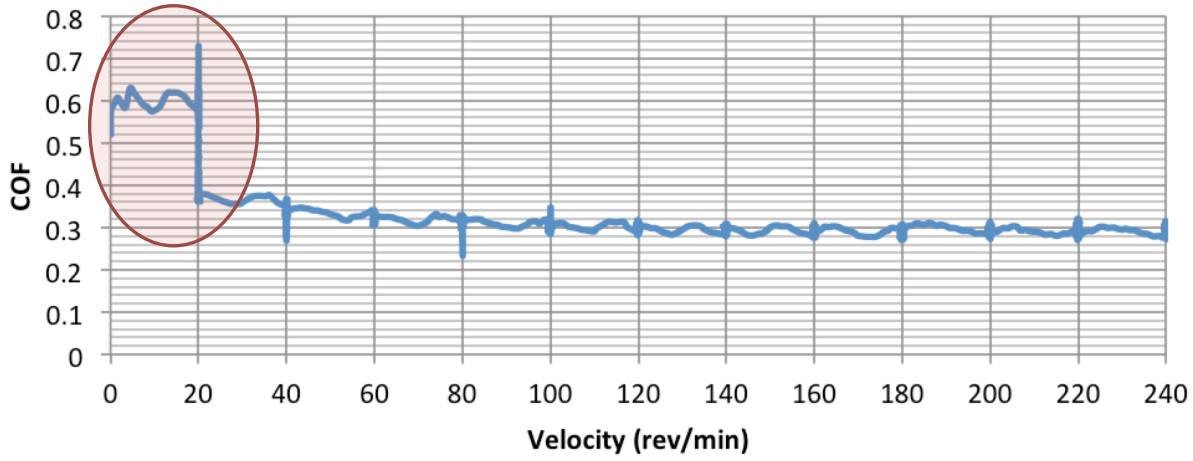

Figure 63 Raw Tribometer data for COF vs. Brush Velocity with the introduction of Atapulgite Clay in solution

Figure 63 illustrates typical behaviour of particles in solution for this setup. At low speed the particles cause a substantial increase in the COF. However, COF reduces to a more stable

value of approximately 0.33 at higher speeds, which is the same value as when no particles are present.

This suggests the formation of a fluid film layer at higher speeds, which causes the abrasive particles to be ineffective when passing through the contact. The fluid film appears to form at around a 50cm/sec (20 rpm) brush speed; whereas at slower speeds the particles are in full contact with the counterface. This has the effect of reducing COF at higher speeds.

This would suggest that wear would be reduced at higher speeds. In later test on dentine (chapter 7 figure 105) test have been done using the same number of brushing strokes, but at different frequency. Unfortunately the picture is not clear, sometimes, the wear reduces with frequency and sometimes it increases – depending on the particle used. Clearly, the process is complex.

Although these speeds are rather higher than in conventional brushing, it is helpful to observe the behaviour of the particles during accelerated testing, as the duration of these tests at only conventional speeds would take a significantly long time

Figure 64 compares the magnitude of COF value at this initial step across all tested particles.

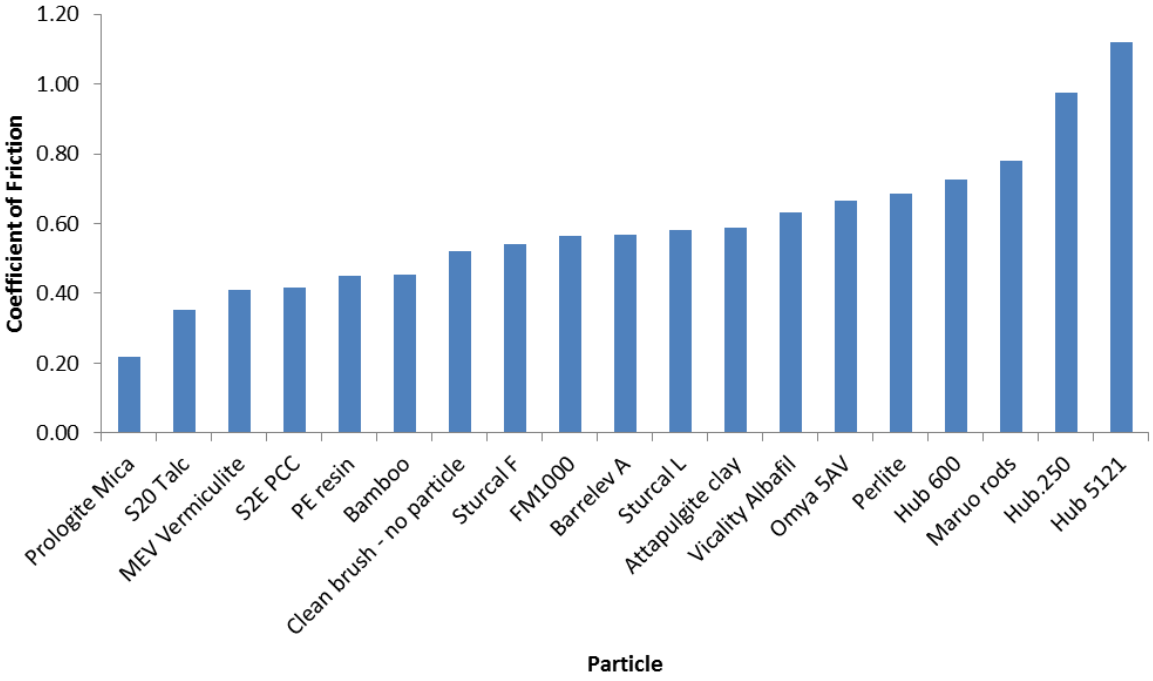

Figure 64 Comparison of initial COF values for particles in suspension before supposed fluid film formation

Immediately obvious is the generic increase in COF brought about by the particles being in solution (at this slow speed only). Three particles display significantly high COF (Maruo Rods, HUB.5121, HUB250), increasing the resistance of the brush head upon the substrate considerably. The results are summarised in Table 4.

			Modified tribometer - Dry COF			Modified tribometer - In solution COF		
Particle	COF angle of repose	Dynamic COF - fixed particle	20 rpm	120 rpm	240 rpm	20 rpm	120 rpm	240 rpm
Clean brush - no particle	NA	NA	0.40	0.31	0.30	0.52	0.34	0.33
Bamboo	0.71		0.45	0.48	0.50	0.46	0.29	0.26
Omya 5AV	0.71		0.77	0.63	0.63	0.67	0.37	0.37
PE resin	0.72		0.40	0.36	0.50	0.45	0.28	0.26
Attapulgite clay	0.80	0.43	0.61	0.50	0.55	0.59	0.30	0.28
S2E PCC	0.85	0.43	0.45	0.43	0.49	0.42	0.28	0.29
Hub.250	0.88		0.82	0.64	0.68	0.97	0.33	0.37
Sturcal F	0.92		0.51	0.41	0.47	0.54	0.37	0.36
Vicality Albafil	0.94	0.47	0.70	0.52	0.56	0.63	0.32	0.30
Sturcal L	0.96		0.58	0.51	0.49	0.58	0.34	0.39
Maruo rods	0.98	0.44	1.13	0.73	0.69	0.64	0.38	0.41
S20 Talc	1.10	0.34	0.38	0.43	0.39	0.35	0.23	0.21
Hub 5121	1.12		0.79	0.58	0.65	1.12	0.38	0.34
Perlite	1.18		0.78	0.75	0.84	0.69	0.35	0.34
Hub 600	1.26		0.79	0.61	0.71	0.73	0.36	0.30
Barrelev A	1.33		0.64	0.52	0.64	0.57	0.35	0.32
MEV Vermiculite	1.52	0.56	0.41	0.63	0.50	0.41	0.32	0.33
FM1000	1.66		0.68	0.52	0.59	0.56	0.36	0.33
Prologite Mica	1.74	0.38	0.38	0.36	0.43	0.22	0.24	0.23

Table 4 Summary of coefficient of friction data

6.4 Conclusions

In this chapter frictional qualities of the various particles have been observed.
Inter-particle friction has been measured by angle of repose leading to a ranking of particles by static coefficient of friction. This method showed a range of coefficients from 0.7 to 1.7 with standard deviations between 0.03 and 0.07. The scatter of the data gives a reasonable validation of the method and indicates that the ranking is fair.

Dynamic analysis of a complete system has been progressed from simple fixed particle trials to full filament entrainment trials. Again it has been found to be possible to rank the particles clearly by these methods. The results show that MEV Vermiculite has the highest COF whilst S20 Talc had the lowest. The baseline friction between the brush filaments and

the Perspex substrate was found to be 0.18. Particle COF remained comparable between trials using carbon tabs and trials using brush interface. The results obtained from these trials are also comparable with the COF rankings obtained by angle of repose. COF by angle of repose is seen to be higher than in dynamic tests indicating that inter-particle interactions are stronger than those between particle and Perspex substrate.

Particles appear to be affected by speed in different ways, with some appearing relatively unaltered by brush velocity. Generally particles appear to exhibit higher friction at low and high velocities whilst commonly experiencing a lull in aggressiveness around central velocities. Omya 5AV particles, despite being of similar length to Rod particles showed lower coefficient of friction. It is thought that this is because the Omya 5AV particles are significantly more cumbersome and stout compared to the sleek and needle like geometry of the Rods.

7 WEAR OF HUMAN DENTINE BY PARTICLES

This chapter looks directly at the wear characteristics and bulk material removal of odontogenic material by abrasive particles. Dentine as a natural material is rougher than acrylic, which could modify how particles interact with it. Similarly, dentine has tubules which form open pores within the substrate surface, which may affect wear performance. The specific characteristics of how particles mechanistically move are studied in more detail in Chapter 8. The primary objective of this chapter is to gain an understanding of the resultant material removal and wear properties of the different particles upon representative substrates. This chapter focuses directly on the wear of human dentine by particles in an effort to quantify and compare the aggressiveness of the particles in contact with this substrate. Experiments have been carried out using both hand and automated brushing trials, to relate dentine abrasion to operating conditions and particle morphology.

7.1 Hand brushed trials

Preliminary wear testing of dentine has been undertaken by hand brushing and scratch observation. Wear analysis has been conducted on human samples using linear reciprocation to constrain brushing activity to better understand the affinity of particles to abrade and remove dental tissue.

7.1.1 Experimental apparatus

Dentine samples have been prepared as discussed previously in Chapter 4 by hot mounting and wire cutting. Half of each sample has then been masked off by adhesive copper tape with the remaining half exposed to the brush and particles (see Figure 65)

Figure 65 Sample preparation for hand brushed trials

Initially trials were conducted with dry particles, following which tests have been carried out in solution. For these, water has been saturated with particles and administered as a slurry. The samples were then hand brushed for 30 minutes to determine whether material removal was observable. Samples have also been weighed before and after testing using digital scales accurate to 1µg.

Further to testing, attempts have been made to use atomic force microscopy (AFM) as a means of analysing the surfaces post test. Figure 66 and Figure 67 below show example images obtained by AFM surface mapping.

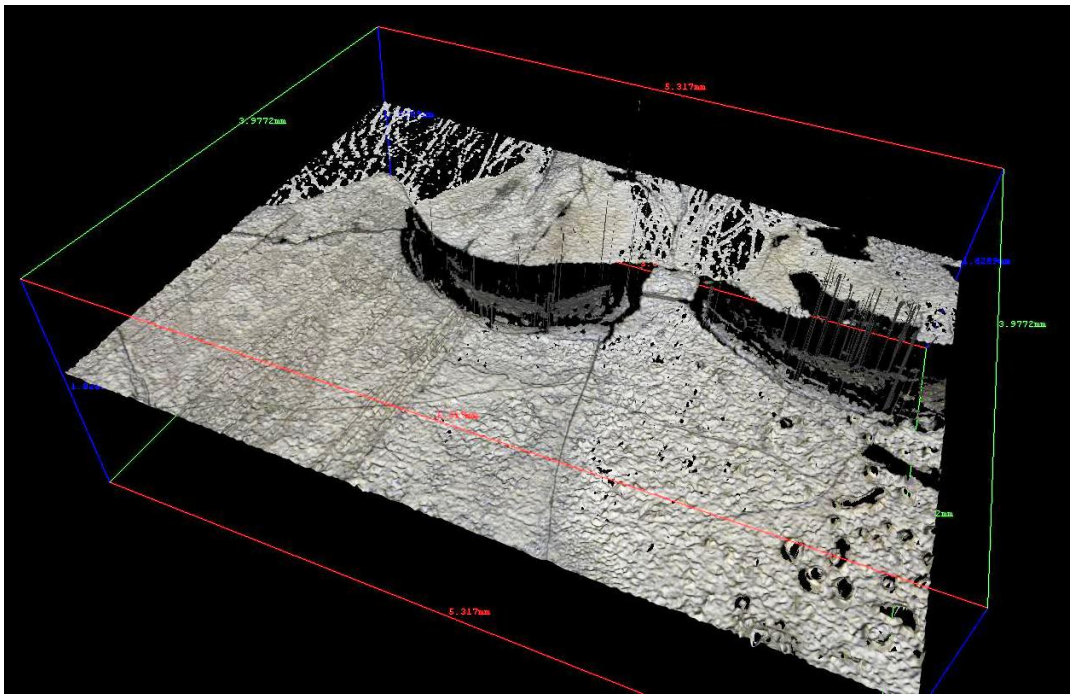

Figure 66 AFM 3d image of dentine abraded without particles (water only)

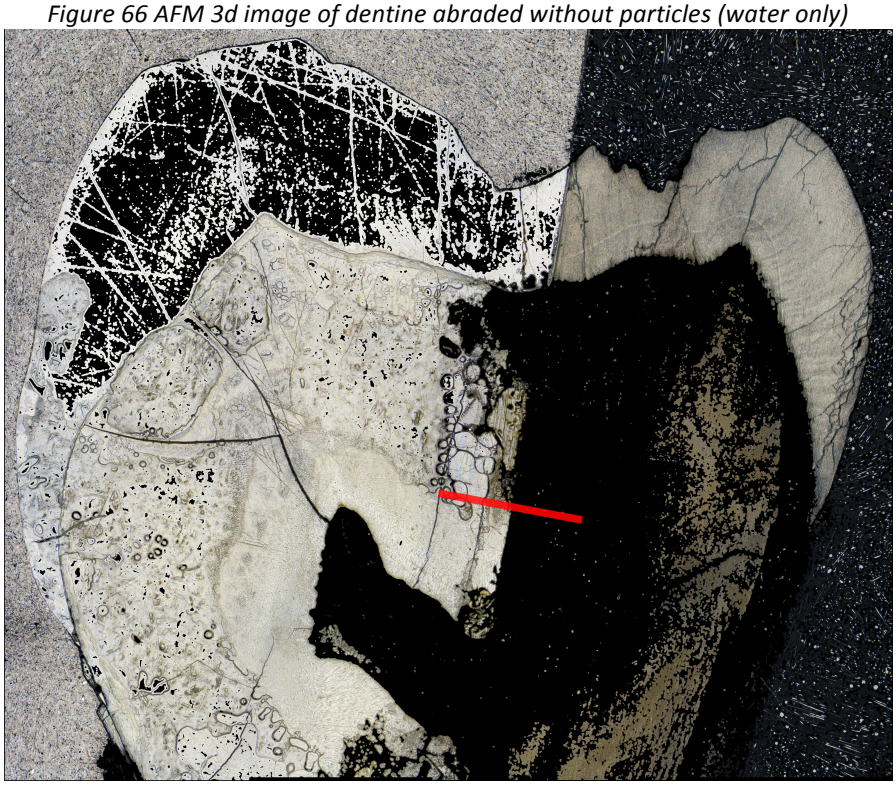

Figure 67 AFM of dentine masked and abraded with Omya 5AV particles

Whilst the images obtained by this technique are interesting, the limitations of the AFM make it an unrealistic analytic tool for this work. The primary limitation is that any steep drops or overhangs in a profile are not measured, leading to inaccuracies in the image produced. Further to this, as outlined in Chapter 8, non-contact surface profiling (such as AFM) is more susceptible to erroneous measurements through surface contamination, surface reflectance and charging effects than contact based analysis. Although useful results

in Chapter 5 'Analysis of Particle Scratching' were obtained, the samples in that instance were Perspex, which is a reliably homogenous material, which is easy to clean. The human tissues studied in this section however contain many instances of surface pores and are a naturally permeable material; particularly the circumpulpal dentine. As a result it is difficult to entirely limit the moisture presence on the surface, despite efforts to effectively clean and dry all samples before analysis. For this reason AFM surface analysis was not taken forward for these trials.

7.1.2 Experimental results

The following results have been obtained from the trials in solution. Four trials have been conducted to determine whether comparable and distinguishable results can be obtained. The trials conducted were:

- Water only (no particles)
- Omya 5AV
- Perlite
- Sturcal F

Water only (no particles)

Firstly, an example of dentine brushed in water without particles is shown in Figure 68.

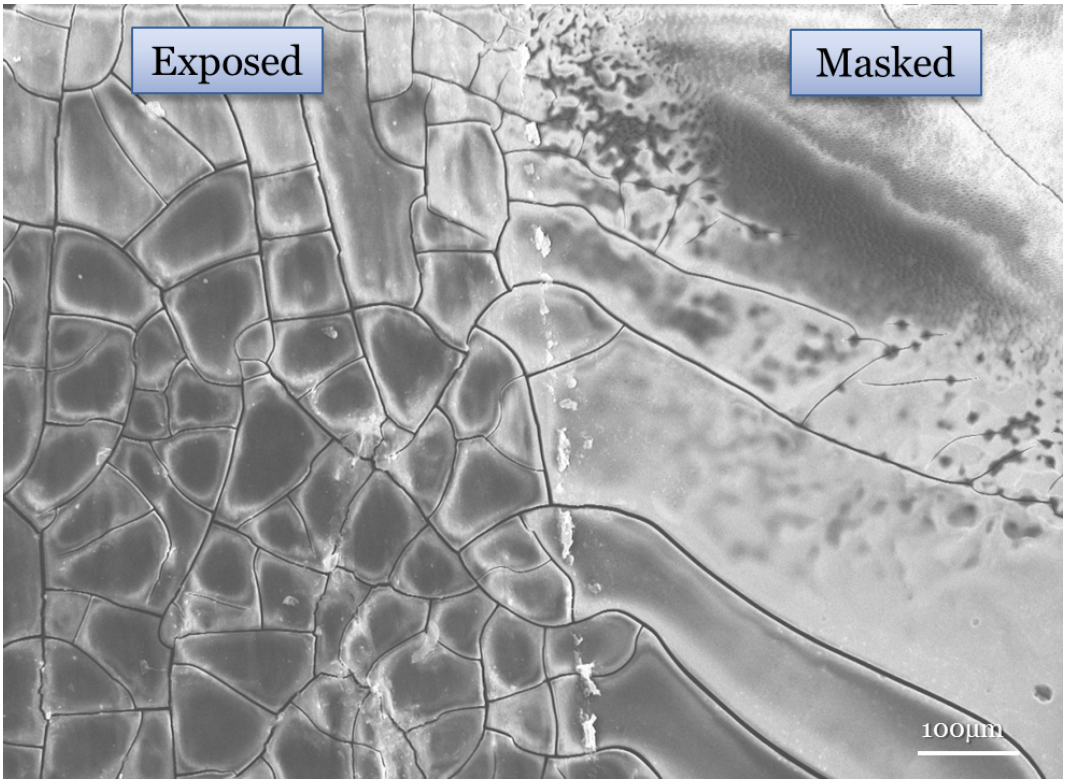

Figure 68 SEM image of exposed and masked dentine abraded by brushing with water without particles

It is clear that brushing with water alone has little effect on material removal for dentine. The SEM image shows a slight cracking of the surface layers of the dentine leading to a similar appearance to dried mud however there is no observable material removal. There is also an associated small material loss of 0.00126g (equivalent to 0.006%) by this brushed sample. This shows that without particles presence, the brush filaments alone with water pose virtually no threat to the dentine. There is some cracking of the surface where the brush has caused distress the dentine however this is likely to be a result of the tooth drying out since its removal from the patient. Although efforts were taken to ensure that the samples were stored in representative conditions to that of the mouth, and stored only for as short amount of time possible before testing, all samples are unique and the permeability to water of some of the Odontogenic material can vary.

This drying out of Odontogenic tissue is not an occurrence solely observed in extracted material. Kishen [38] studied the mechanical changes in endodontically treated teeth with particular focus upon the increased susceptibility to fracture. Along with five other factors (chemical, microbial, structural, restorative, and age) Kishen attributes moisture loss as a major contributor to the increased brittleness of dentine. Historically, the importance of moisture content is a widely purported claim. Helfer et al [30] pioneered investigations into the affects of moisture content in dentine showing that endontically treated teeth had a moisture content typically 9% less than those with a vital pulp. Shuichi Ito et al [39] studied the relationship between water content and stiffness in both caries affected and non-caries human dentine. Their work revealed a significantly inverse relationship between stiffness and water content, and stiffness and shrinkage.

Considering the findings of these studies two suppositions could be proposed:

1. That the change in brittleness of dentine is not limited to solely extracted teeth and can readily be observed in vivo.
2. The mechanical changes in dentine as a result of loss of moisture are subtle and progressive. Based upon observations from microscopy and surface analysis It is considered unlikely that the friction properties and wear resistance of the samples tested in this section be unrepresentative of those found in the human mouth.

Omya 5AV.

With the addition of particles, more extreme changes are visible in the unmasked portion of dentine. Below is an SEM image of dentine (Figure 69) brushed with Omya 5AV particles and an optical microscope image of exposed enamel (Figure 70).

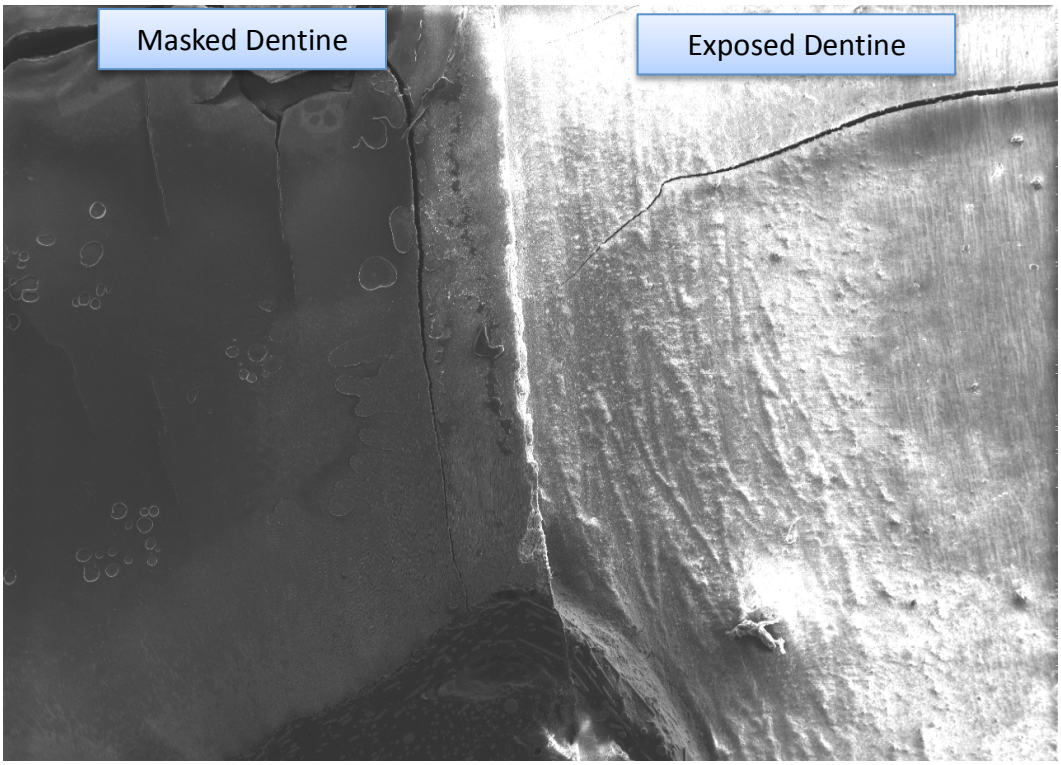

Figure 69 SEM image of sample brushed with Omya 5AV in solution for 30 minutes by hand

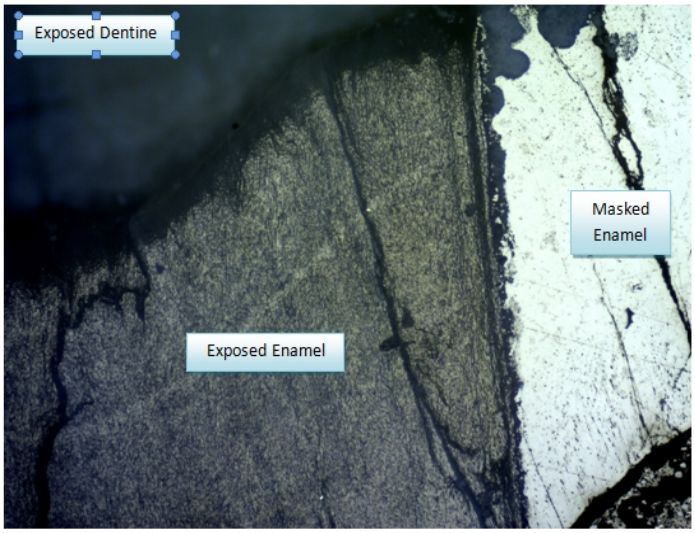

Figure 70 Optical microscope image of sample brushed with Omya 5AV in solution for 30 minutes by hand. Left: Enamel exposed to particle brushing, Right: Protected Enamel.

The above images show the relatively aggressive wear of dentine by Omya 5AV particles with notable material removal and a large degree of roughening. Although the wear surface has the appearance of macroscopic galling occurrence, this is usually associated with adhesion (which is less likely between particle and substrate). It is more likely that abrasive ploughing and surface (as well as particle) fracture has occurred; which will ultimately contribute to three-body abrasive processes. Figure 70 highlights the removal of dentine below the Amelodentinal junction (visible in the top left corner of the image). Although the enamel appears to be somewhat worn from optical microscope images this is predominantly an exaggerated effect from the roughening of the tissue surface, changing

the reflectivity of the sample. Analysis using contact profilometry showed material removal for enamel to be negligible.

Perlite

Figure 71 below shows an SEM image of a sample brushed with Perlite particles in solution for 30 minutes.

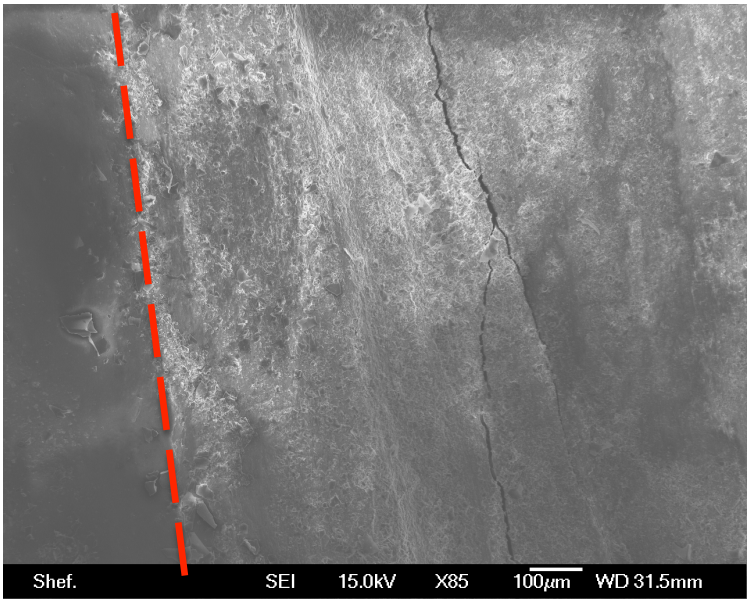

Figure 71 SEM image of sample brushed with Perlite particles in solution for 30 minutes by hand with masked area on the left and unmasked on the right

Much less severe wear is observed by perlite particles when compared to Omya 5AV yet still more material removal can be seen than with water alone. This can be seen in optical microscopic images also (Figure 72)

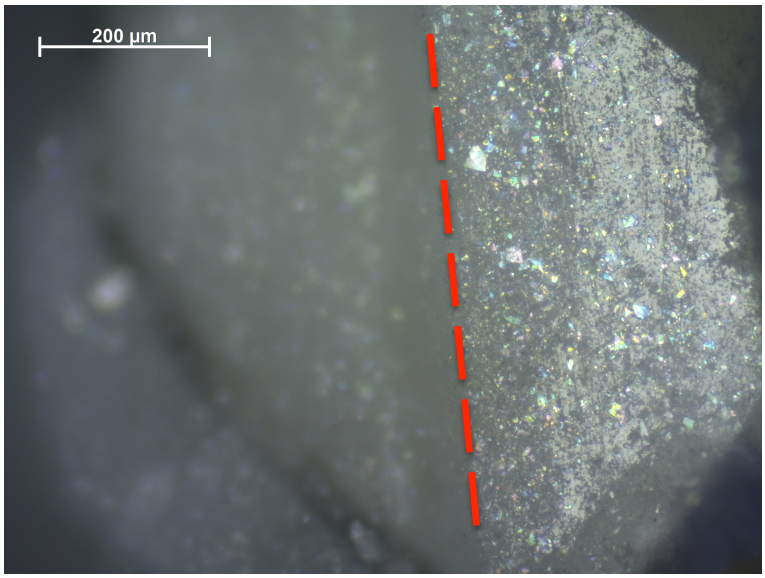

Figure 72 Optical microscope image of dentine brushed with Perlite particles for 30 minutes in solution with masked area (left) and unmasked area (right)

Sturcal F

Figure 73 shows a dentine sample hand brushed with Sturcal F particles in solution for 30 minutes.

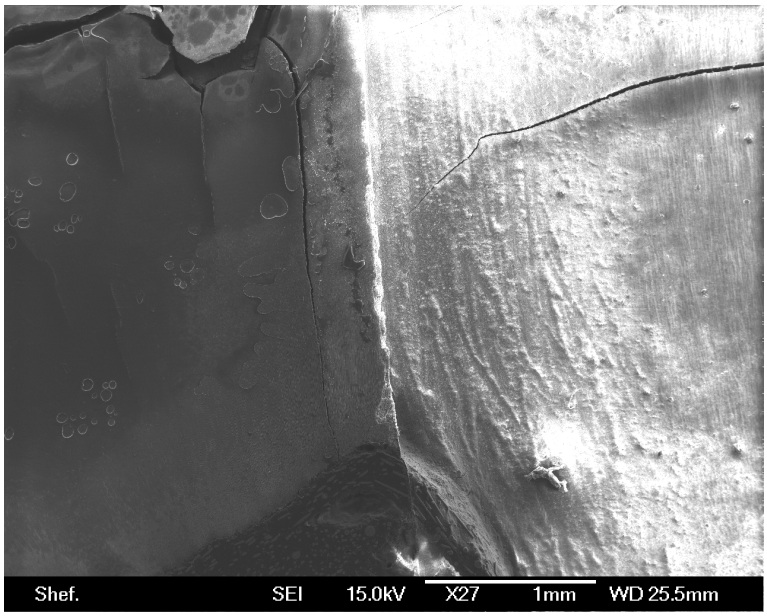

Figure 73 SEM image of dentine brushed with Sturcal F particles in solution for 30 minutes with masked area (left) and unmasked area (right)

The aggressive nature of the material removal can be observed in the unmasked regions. There is a large degree of roughing and surface gouging with long deep scratches observable. The optical microscope images complement these observations (Figure 74)

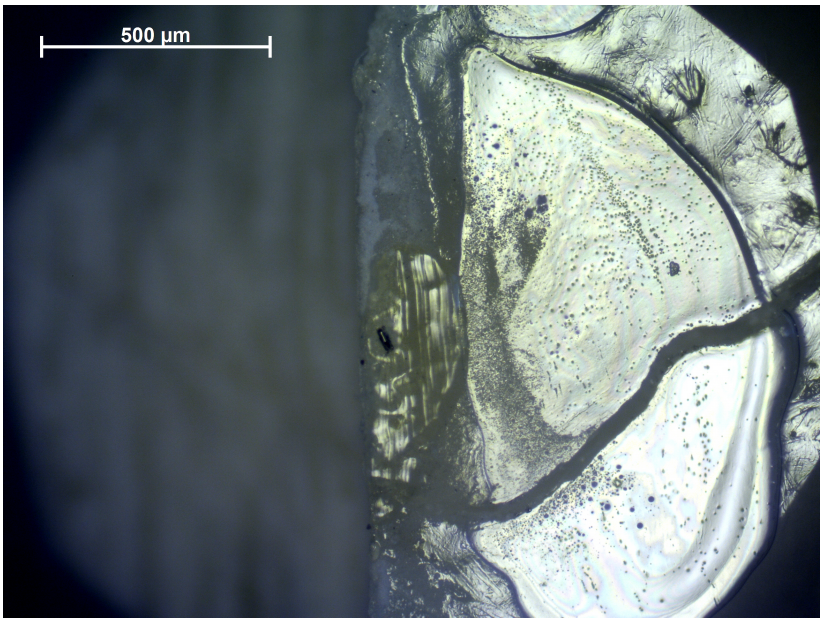

Figure 74 Optical microscope image of human sample brushed with Sturcal F particles in solution for 30 minutes (Left: unmasked region, Right: masked region)

Immediately obvious is the extent of the material removal upon dentine. As can be seen in Figure 73 the remaining dentine (right hand side) is notably marked with numerous striations from wear tracks. Figure 74 demonstrates the extent of material removal, with the exposed left hand portion out of focus as a result of being considerably lower than the right.

Even with these particularly aggressive particles, the enamel region is not seen to have significant material removal during these tests. The substantial hardness of enamel meant that material removal was minimal, however there was observable surface roughening from brushing with particles for this duration. The mechanism for the roughening is difficult to determine without detailed understanding of the dynamic behaviour, and interactive properties of the particles. This is investigated in Chapter 8. Comparative images of brushed enamel for each particle are shown in Figure 75 in the next section.

7.1.3 Conclusions

Little material loss is visible to exposed enamel in all cases although there is some evidence of surface roughening. This surface roughening does give the appearance of notable material loss however profilometry confirms that this is not the case.

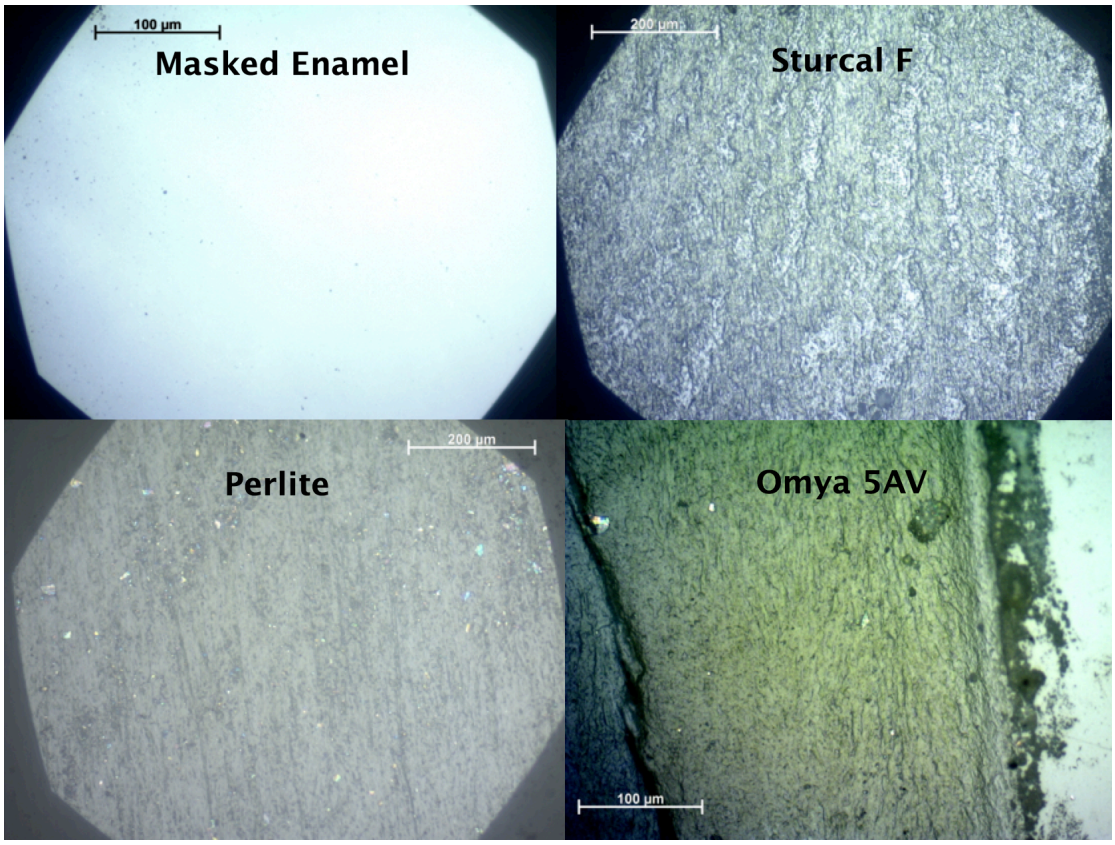

Figure 75 Optical microscope images of enamel brushed with Sturcal F, Perlite and Omya 5AV particles in solution for 30 minutes

Dentine shows signs of significant material loss in the 30 minutes of brushing with various particles. Mass loss during the tests is shown below in Table 5. These scales were capable to 10^{-5} of a gram and to maximise accuracy each sample was measured three times and an average taken (the discrepancy was minimal if present at all).

Particle	Material Removed (g)
No Particle	0.00126
Perlite	0.01068
Sturcal F	0.01828
Omya 5AV	0.02625

Table 5 Material loss during brushing with particles in solution by hand

The material mass loss, even though small compared with the overall sample mass, was significant and so was useful in ranking aggressiveness of the particles

7.1.4 Surface damage characterisation

Further to attempts to characterise the surface damage by AFM techniques, analysis of surface damage can be achieved by contact profilometry. In this case using contact

profilometry has the added benefit of remaining less affected by surface contamination than non-contact methods. As seen in Chapter 5 it is not uncommon for surface contaminants to register exaggeration anomalous results within the profiling process. As the stylus makes mechanical contact with the sample surface the following results are significantly less likely to be affected by colour or surface reflectance.

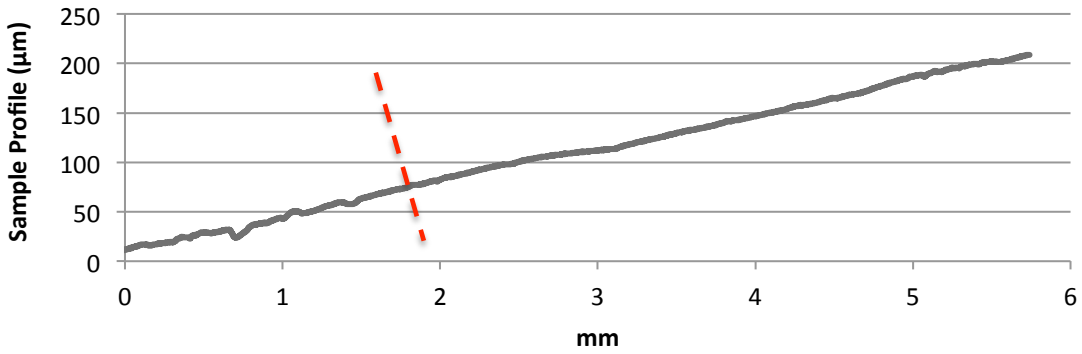

Figure 76 Profile across dentine centre, sample brushed with water with no particle presence for 30 minutes (LHS: Exposed, showing increased roughness. RHS: Masked, remaining smoother)

As can be seen from Figure 76 above there is very little observable wear from the action of the filaments alone in the brushing process. Any material removal is less significant than the natural roughness and undulations already present in the sample surface. The gradient of the graph is a reflection of how level the sample is when measured. This can often be difficult to constrain particularly when measuring on this scale, as very subtle misalignment of the sample can appear dramatically exaggerated when viewed macroscopically. For the purposes of observing material removal however, as is the case here, this is not an issue.

Some example profiles are shown below for Omya 5AV across the masked area after 30 minutes of brushing.

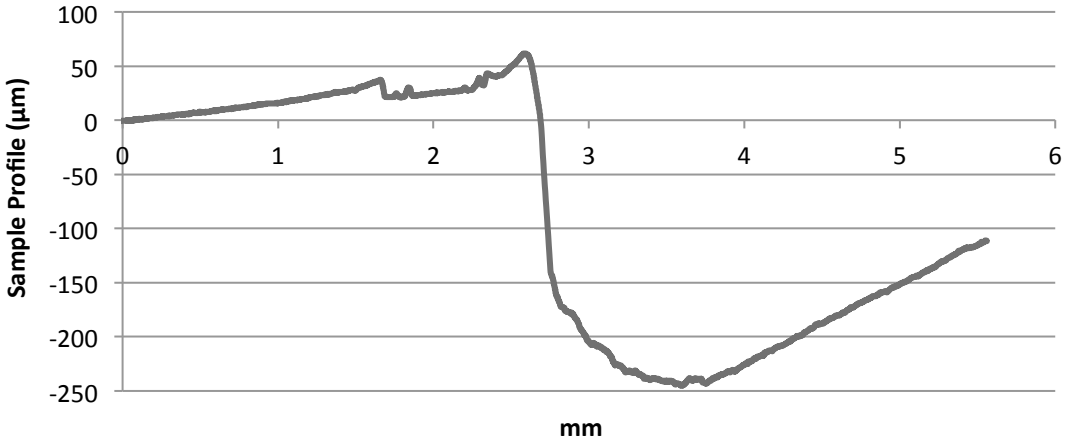

Figure 77 Profile across dentine centre, sample brushed with Omya 5AV particles in solution for 30 minutes

Figure 77 above shows the profile across a masked dentine region brushed by Omya 5AV particles. Clear evidence of wear of the unmasked region is visible (right hand side) with scratch depth around 300µm. Below, Figure 78 shows the profile generated across the masked enamel region by Omya 5AV particles.

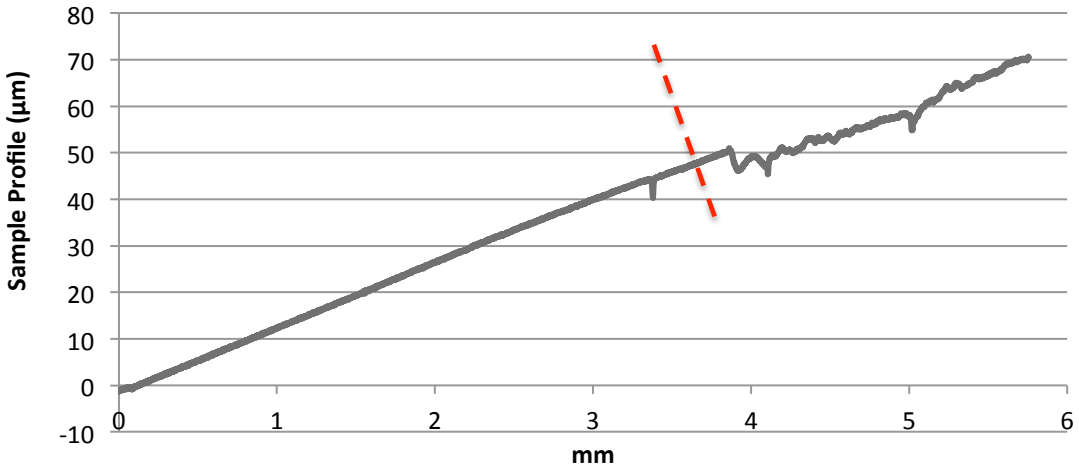

Figure 78 Profile across masked enamel, crown region, sample brushed with Omya 5AV particles in solution for 30 minutes

It is clear when comparing the above two figures that the enamel region does not exhibit the same magnitude of wear as the dentine (as expected). This follows predictions based on the relative hardness of each region.

We can see from comparison of Figure 77 and Figure 79 that Sturcal F is similarly as aggressive as Omya 5AV. Although Omya particles led to the deepest wear scar, considering the relative size of Sturcal F to Omya 5AV (approximately 1.3 vs. 7 microns) it can be said that Sturcal F is an aggressive abrasive.

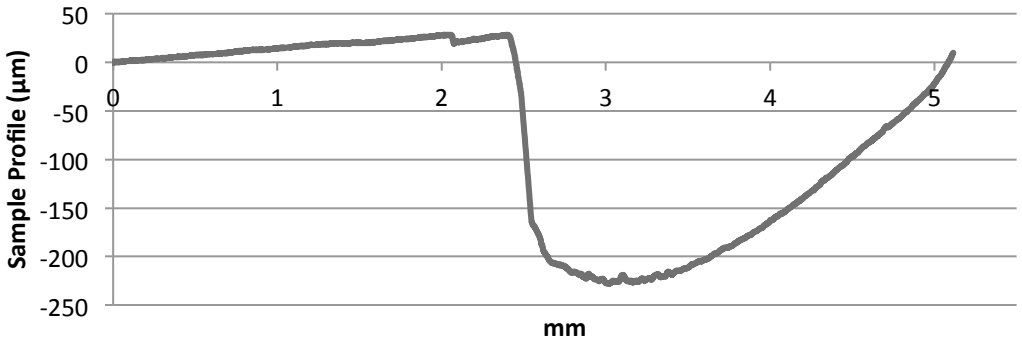

Figure 79 Profile across dentine centre, sample brushed with Sturcal F in solution for 30 minutes

Figure 80 shows the profile generated after brushing with Perlite particles. We can see that there is a contrast in profile shape when compared to Omya and Sturcal plots. Both Omya and Sturcal F demonstrate a more rounded trench-like profile whereas Perlite led to an even step down in material removal. This difference was observed at different locations on the

wear scar and also across different samples. This could suggest a difference in the ability of the particle to break down. It could be that perlite particles break down due to their seemingly fragile nature (as gauged from SEM imagery). It could be that particles that find themselves entrained within a biased portion of the wear scar, perhaps near the masked boundary where particles may initially butt-up against and gather, break down. The more resilient nature of Omya and Sturcal F particles could lead to more significant wear in this area from trapped particles, which are less likely to break down. We know from Chapter 9 on Agglomeration affinity and Integrity analysis, that Sturcal F particles form very tight spherical agglomerations, which lends some explanation as to their significant wear characteristics. The breakdown characteristics of the particles are studied in detail in Chapter 8.

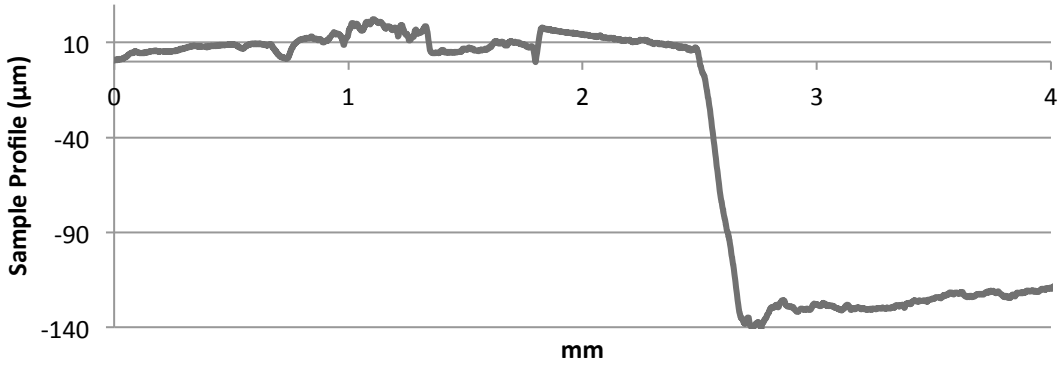

Figure 80 Profile across masked dentine root region, sample brushed with Perlite particles in solution for 30 minutes

7.2 Automated brushing trials

Although great care was taken in an attempt to brush all samples evenly and with equal force, it is not possible to process each sample identically. As such, a CETR tribometer has been used to apply an even load and speed for a number of cycles in order that valid, comparable results can be obtained for wear caused by the various particles.

7.2.1 Experimental apparatus

Trials were conducted on a Bruker UMT 3 tribometer test rig. A linear reciprocation module is used along with a 6.1mm diameter nylon ball. A nylon ball has been selected as it is more controllable than a brush head (since filament change at each end of the stroke is unlikely to be identical every time). The ball in these trials has comparable material properties to those found in brush filaments. Although the structural properties are different it provides a replicable and representative (in terms of friction and hardness) substitute. The ball is mounted into a specimen holder as shown below in Figure 81.

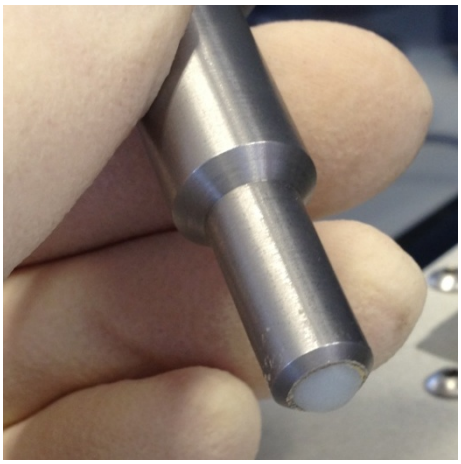

Figure 81 Ball holder for CETR trials

The tooth samples are mounted and cut as described previously and shown in Figure 82.

Figure 82 Prepared teeth samples mounted in phenolic compound

The surfaces are brought into contact and the CETR base reciprocated with a 7.5mm stroke length with particles suspended in solution at the point of contact. Particles were continually replenished within the contact zone. The duration of each test was 30 minutes and various frequencies and loads have been applied to determine the effect of these variables on wear rate.

The particles selected for analysis using this technique are as below and have been selected based upon the interests and requirements of the sponsor company at the time of testing.

- Water only
- Omya 5AV
- Maruo Rods
- Sturcal F
- Sturcal L
- S2E PCC
- Vicality Albafil

Various loads and conditions have been tested to replicate the speed and loads during manual brushing. These conditions were selected according to what would compliment the brushing speeds deemed suitable by the sponsor company. The frequencies and loads of each test scenario are as follows:

- 1.25Hz and 0.3N
- 2.5Hz and 0.3N
- 5Hz and 0.3N
- 2.5Hz and 0.45N
- 2.5Hz and 0.6N
- 2.5Hz and 0.3N with the addition of a binding agent

In the latter case the binding agent was an Agar derivative introduced to see the effect of modifying the viscosity of the solution on the particles abrasive behaviour.

Further to these tests, it was thought that the shape and size of various particles might complement each other in some way leading to synergistic differences in the wear rate of the substrate (beneficially or negatively). This hypothesis has been tested by the addition of Omya 5AV particles in equal ratio with each of the other particles. Omya 5AV particles were selected because it is considered the standard accessible abrasive in this field as a result of its ease of manufacture and low cost.

7.2.2 Surface damage characterisation

Below, the various particles are discussed following testing using SEM imaging, and surface profiling. Position of the ball in the vertical direction is used to estimate the wear rate of the particles (since the CETR attempts to apply a constant load, Z position relates to material removal). Optical and SEM analysis of the nylon ball post trial showed there to be no material removal from the ball itself, therefore the change in Z position was representative of solely dentine removal.

Roughness measurements have been taken from three locations on the wear scars by contact profilometry. These locations are shown below in Figure 83.

Figure 83 R_a roughness locations from profilometry measurements

Although three surface roughness measurements have been made, only 'Middle' Ra is compared since this represents the material removal by the particles best.

7.2.2.1 SEM Imaging of surface damage

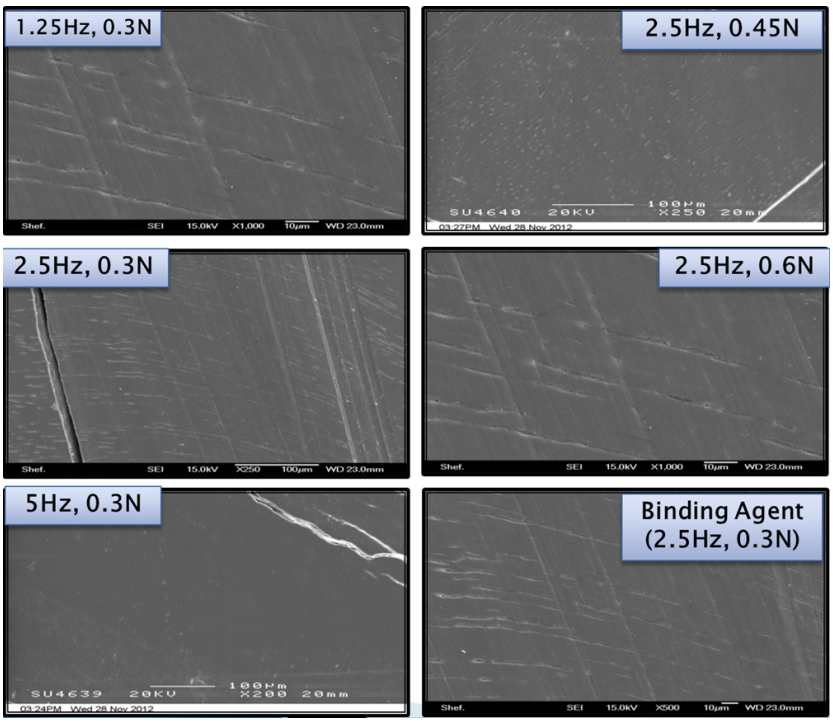

Figure 84 SEM images of surface abraded by water only with no particles at various loads and frequencies. Stroke direction is vertical.

The above SEM images in Figure 84 show the scratches observed after 30 minutes at various loads and speeds when no particles are present. Very little wear of the surface is visible at any load or frequency. Some mild scratching can be seen in the direction of travel but there is no further evidence of abrasion of the surface. Comparing the infrequent scratches that can be found on the surface post-testing with the horizontal dentinal tubules spanning the sample, we can see that the magnitude of these scratches is very low and could be a result of third body abrasive from loose microscopic dental material. It should be noted that not all SEM images are at the same magnification. Dentine is a difficult material to image at high magnification. For some samples charging effects are seen quite strongly, which can be minimised or removed by altering both the accelerated voltage and, more effectively, the magnification. In some cases this was only necessary to a small variance in magnification, however occasionally required a larger variation in magnification.

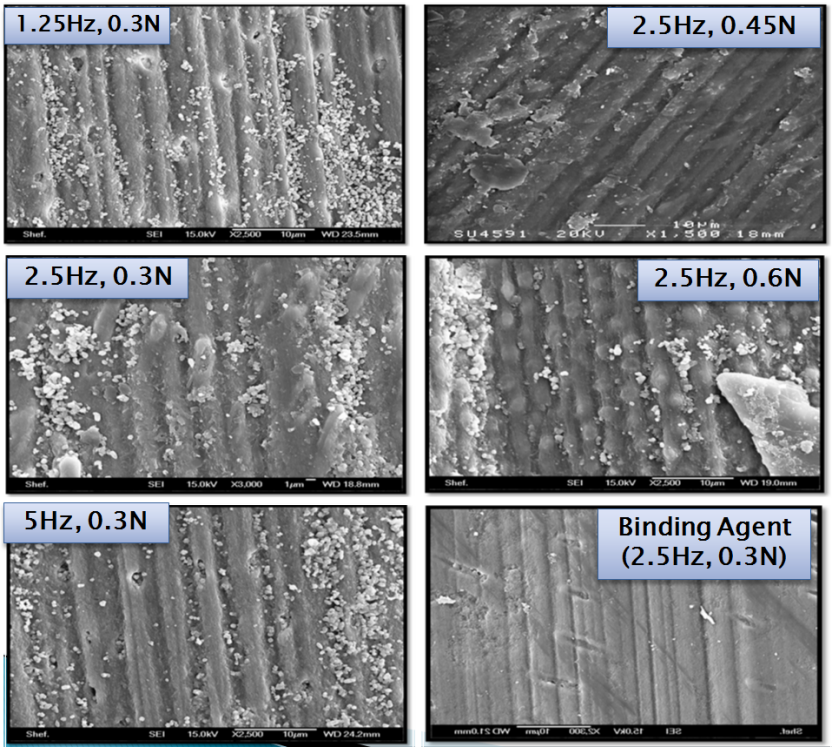

Figure 85 SEM images of surface abraded by Vicality Albafil at various loads and frequencies

The SEM images above in Figure 85 show the scratches observed after 30 minutes at various loads and speeds for Vicality Albafil particles. Visually, scratch depth appears to increase dramatically with increase in frequency. Increasing loads led to the development of nodules and irregularity of the scratches. This suggests that there is mechanistic variation when load is altered most likely due to the freedom of the particles to rotate in the contact region. It is also possible that with increasing load the fluid film operates at a higher pressure, squeezing particles and rotating them within the existing grooves. The introduction of a binding agent significantly reduces the severity of the scratches reducing both frequency and depth.

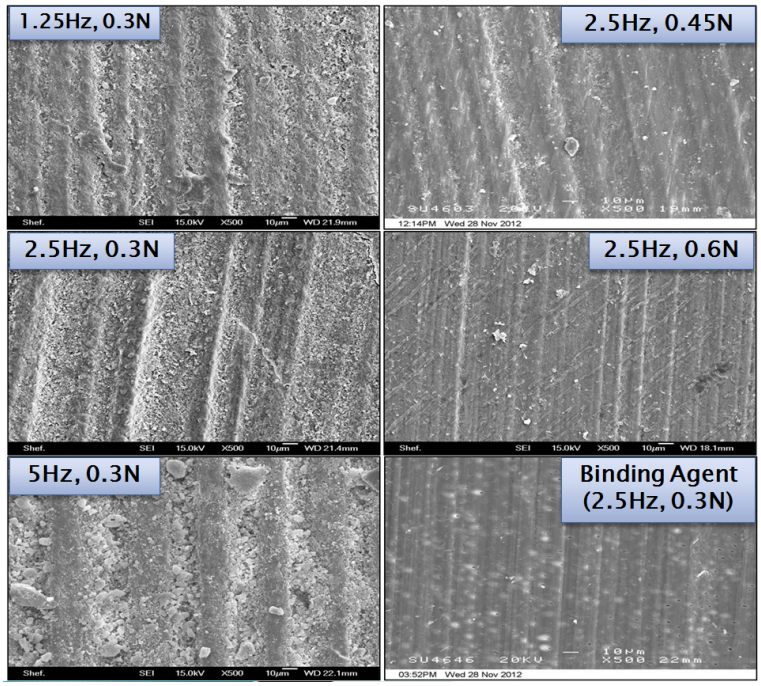

Figure 86 SEM images of surface abraded by Omya 5AV at various loads and frequencies

The SEM images above in Figure 86 show the scratches observed after 30 minutes at various loads and speeds for Omya 5AV particles. Since the wear scars are significantly wider than individual particles it is likely that wear tracking is occurring. Wear tracking is an occurrence where a scratch or groove forms in a substrate surface and particles find themselves entrained within the groove throughout reciprocation trials. This can lead to exaggerated wear effects greater in magnitude than the size of the individual particles. Figure 87 below illustrates how wear tracking occurs.

In this case an increase in scratch frequency leads to greater aggression in terms of scratch width and depth visually whilst an increase in load shows a decrease in material removal. Again, the introduction of a binding agent reduces scratch appearance. Despite being a larger particle, the Omya 5AV samples showed much shallower scratches than the Vicality Albafil in the presence of a binding agent.

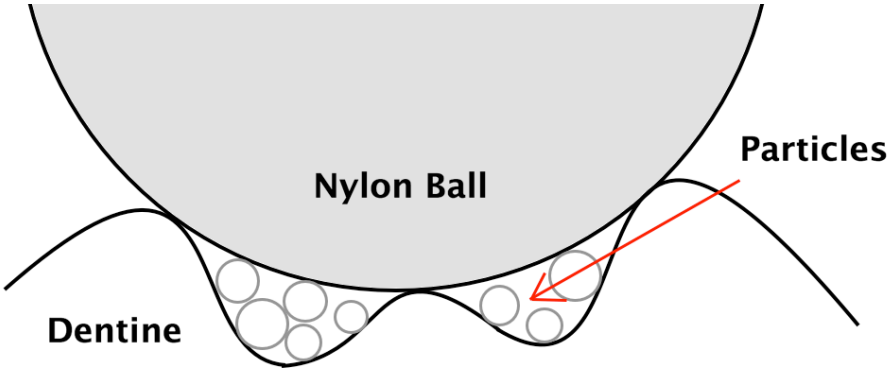

Figure 87 Illustration of wear tracking

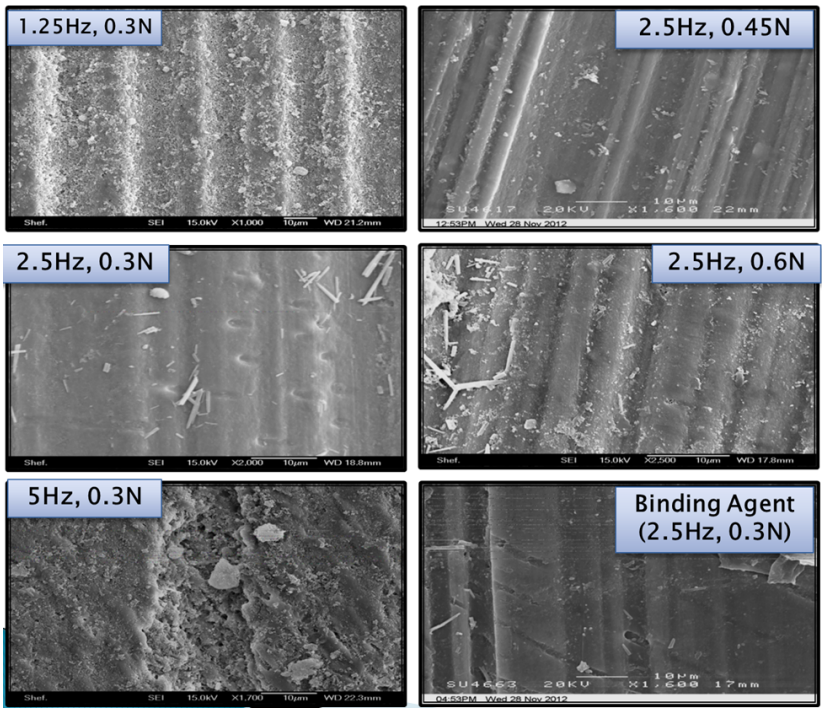

Figure 88 SEM images of surface abraded by Maruo Rods at various loads and frequencies

The SEM images above in Figure 88 show the scratches observed after 30 minutes at various loads and speeds for Maruo Rods particles. It can be seen that increasing speed (1.25Hz to 2.5Hz) significantly reduces scratch depth and frequency. Evidence for particle fracture and breakdown in this case is notably reduced. Increasing speed further still leads to infrequent but deep and aggressive scratches. Increase in load does not appear to lead to greater material removal or surface roughening but instead leads to deeper and more uniform scratches. The addition of a binding agent appears to have an arguable polishing effect, presenting some of the deepest and neatest scratches with smoothed intermediate substrate between the scratches. The largest scratch widths are seen at the lowest speed indicating wear tracking.

Wear depth and observations on scratch severity are made qualitatively by examination of SEM images for the various experiments. Whilst these do not provide quantifiable data it does allow for reasonable comparison between the scenarios. Data support is presented later in this chapter by measuring the two-dimensional area of profile plots

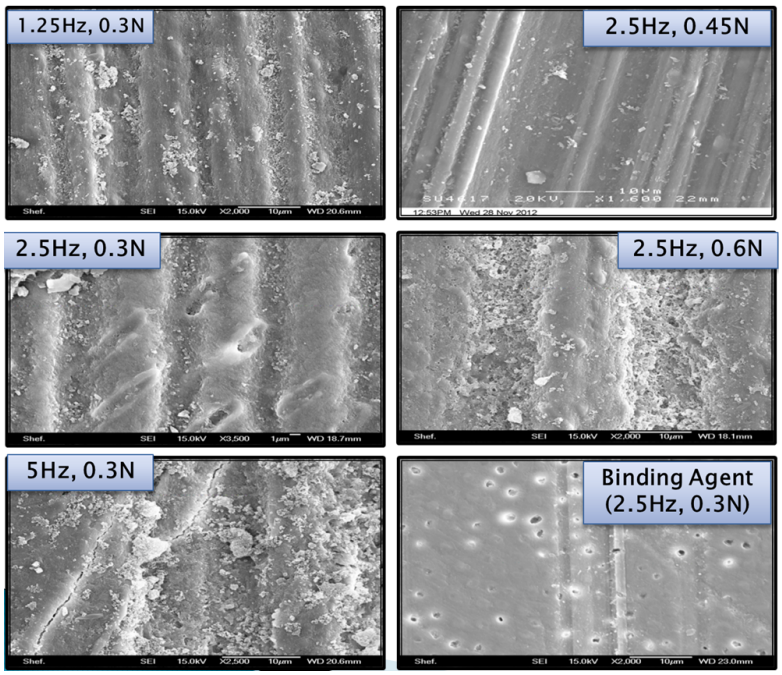

Figure 89 SEM images of surface abraded by S2E PCC at various loads and frequencies

The SEM images above in Figure 89 show the scratches observed after 30 minutes at various loads and speeds for S2E PCC particles. Scratch occurrence in terms of frequency, continuity and uniformity increased from 1.25Hz to 2.5Hz suggesting an improved security of particle entrainment. There was also an increase in surface degradation and macroscopic galling observable at 5Hz. Increase in load (0.45N) led to smaller more uniform individual scratches. The highest load generated much larger scratches whilst the binding agent greatly reduced scratch frequency and observable depth.

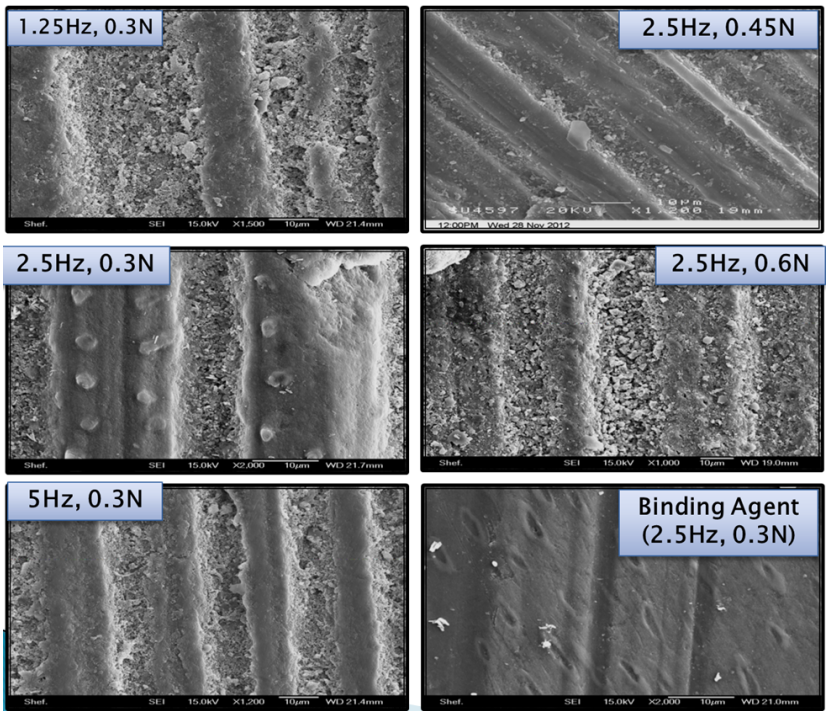

Figure 90 SEM images of surface abraded by Sturcal F at various loads and frequencies

The SEM images above in Figure 90 show the scratches observed after 30 minutes at various loads and speeds for Sturcal F particles. The images show deep scratches with a large presence of particle fragments within them after testing. It is known from Chapter 9 where the agglomeration properties of particles are discussed, that Sturcal F particles demonstrate strong spherical agglomerations with projecting particle tips. This may be responsible for the presence of particles seemingly embedded (with some loose) within the walls of wear scars. The dentine between the scratches is relatively smoothed. An increase in load is seen to dramatically decrease the regularity and consistency of scratches whilst increased surface degradation is apparent. The binding agent trials appear to produce deeper scratches than with other particles.

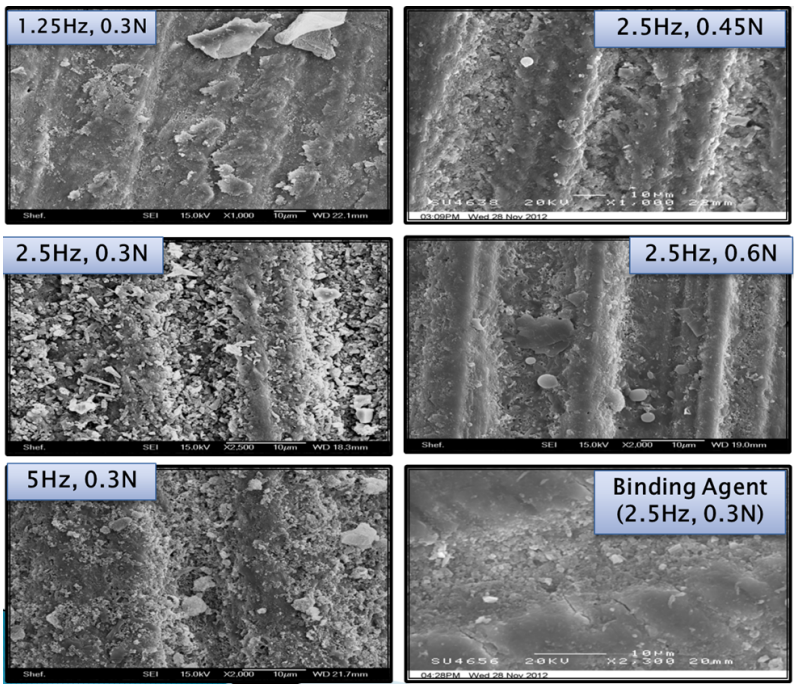

Figure 91 SEM images of surface abraded by Sturcal L at various loads and frequencies

The SEM images above in Figure 91 show the scratches observed after 30 minutes at various loads and speeds for Sturcal L particles. The low frequency trials are seen to create dramatically raised scratch boundaries whilst increased speed leads to an increase in particle breakdown. The higher load trials show more aggressive material removal within scratches although the macro scratch width appears similar between the various test conditions.

7.2.2.2 Profilometry of surface damage

Mean scratch dimensions have been measured from the SEM images for the various materials and scenarios.

Figure 92 below shows the change in area of material removal with respect to increasing frequency for all of the samples. The 'area' in this case was the two-dimensional area of the

cross section of measured profile plots. In each scenario the overall area of the substrate-penetrating trough for each wear scar is calculated and presented in terms of $\mu m^{2"}$. Cross section profiles of the wear scar were measured using a profilometer. The cross sectional area of the wear scar was estimated from these plots (by determining the area of material removed below an unworn surface datum). Figure 42 shows the variation of this wear scar cross sectional area with frequency for each of the particles tested.

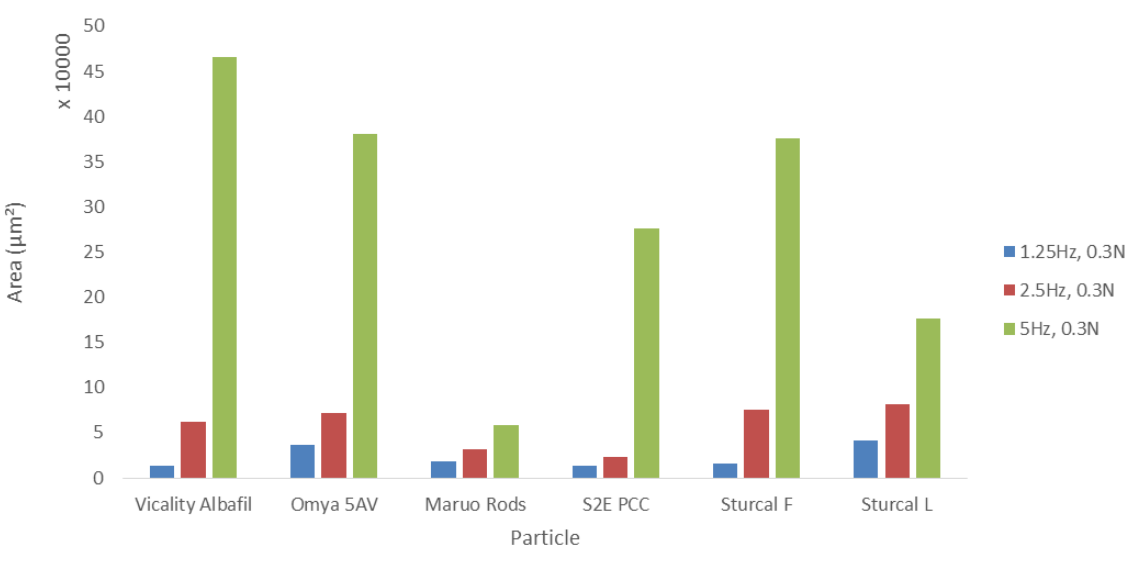

Figure 92 Material removal for the particles at various frequencies

Clearly, with increasing frequency, material removal is greater, though in each case it is not simply doubled for a doubled frequency. It is likely that these changes correspond to a change in particle dynamics (rolling or sliding). The effect of frequency is discussed fully below in 7.2.2.4

Figure 93 below shows the change in area of the wear scar with respect to change in loading condition.

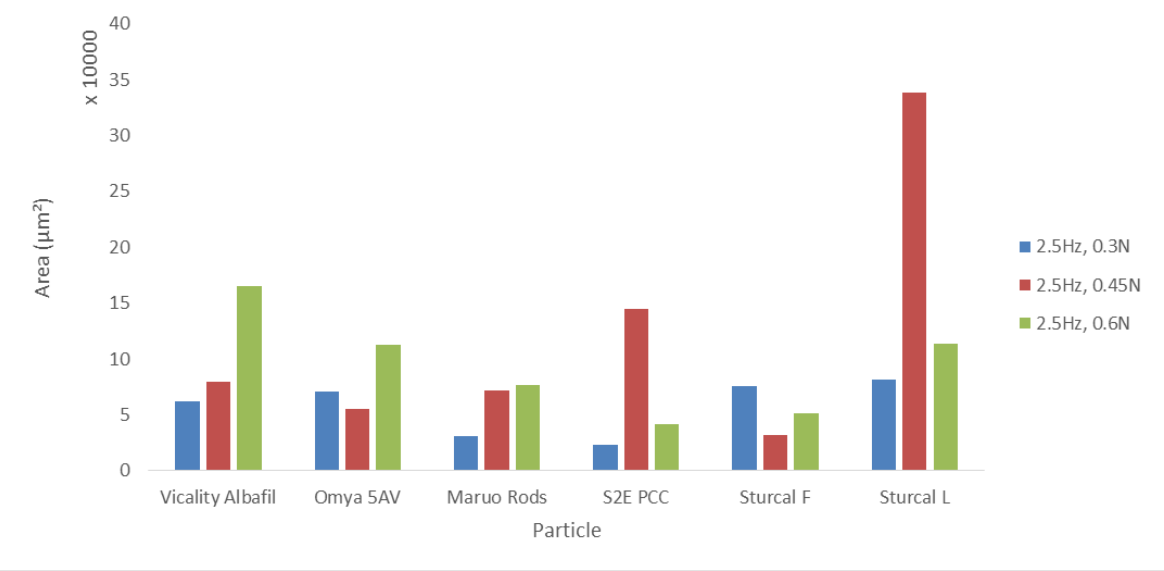

Figure 93 Material removal for the particles at various loads

Whilst there is a general increase in material removal for higher loading, it is much less marked than for increase in frequency. The most significant change in material removal occurred for Sturcal L particles at 0.45N, which was much larger than at lower or higher load. S2E PCC particles showed the same trend. Vicality Albafil particles showed a direct increase in material removal with increasing load, as did Maruo Rods.

Figure 94 shows the effect on material removal by the addition of a binding agent.

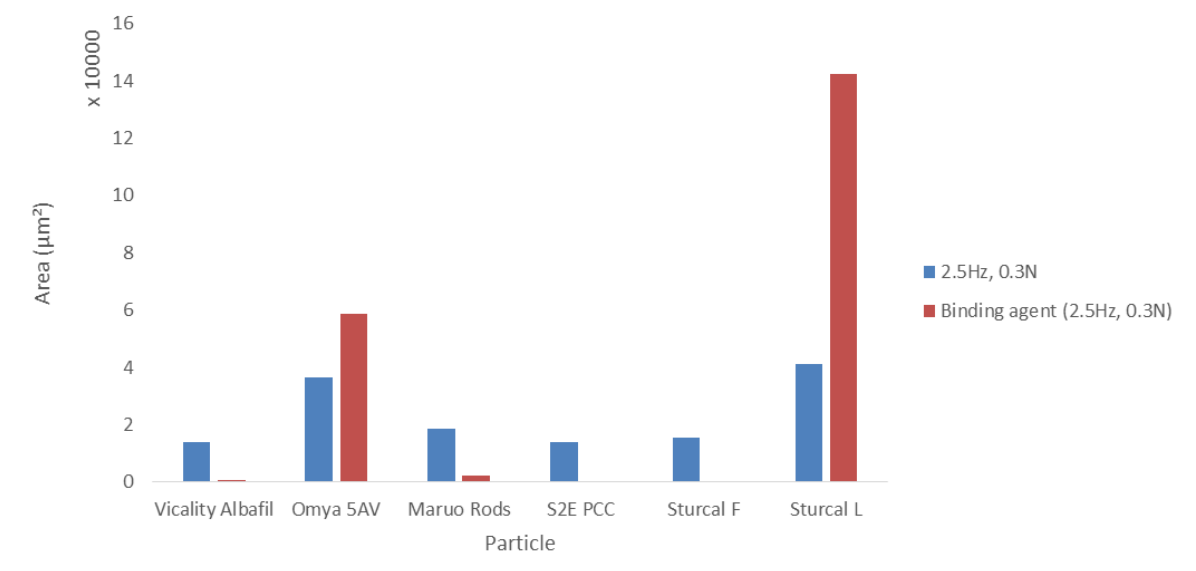

Figure 94 Material removal for the particles with and without binding agent

The binding agent in general has the effect of significantly reducing material removal with the exception of for Omya 5AV and for Sturcal L particles.

Figure 95 below shows the change of roughness with respect to increasing frequency for all of the samples.

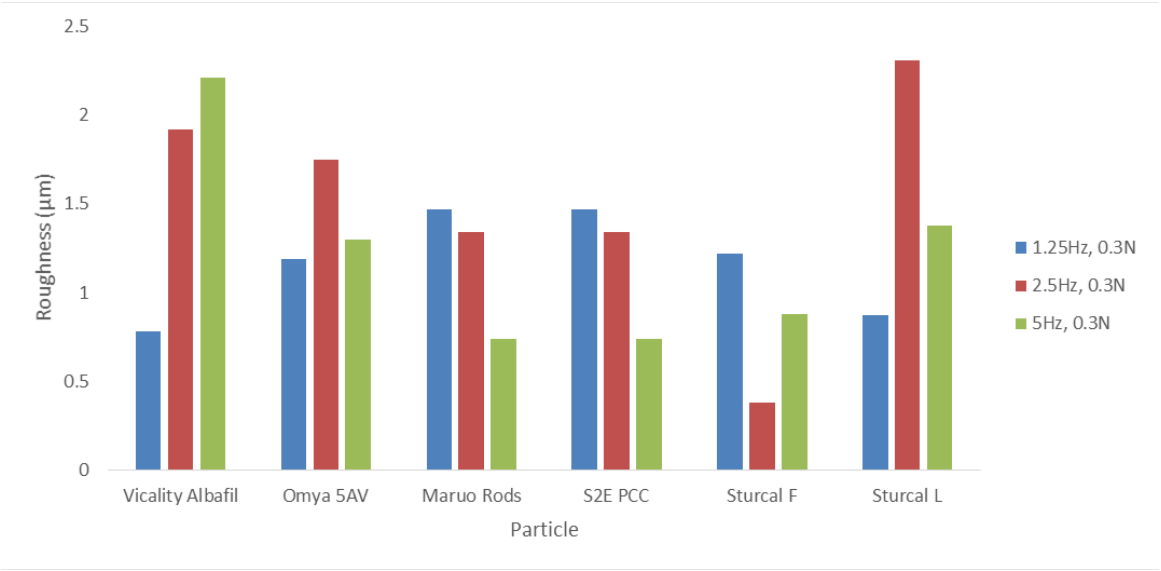

Figure 95 Roughness of wear scar for the particles at various frequencies

Whilst there are clear differences between the different particles, some tend to become rougher with increasing frequency whilst others diminish.

Figure 96 below shows the change of roughness of the wear scar with respect to change in loading condition.

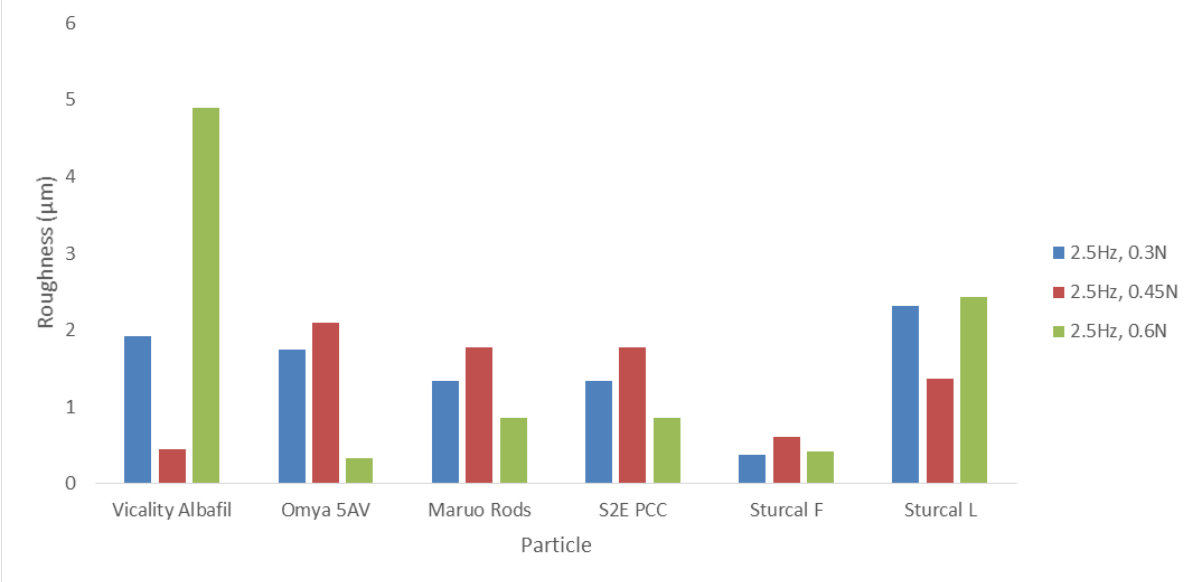

Figure 96 Roughness of wear scar for the particles at various loads.

In this case, no pattern can be determined for variation in roughness with respect to a change in load.

Figure 97 shows the effect on roughness by the addition of a binding agent.

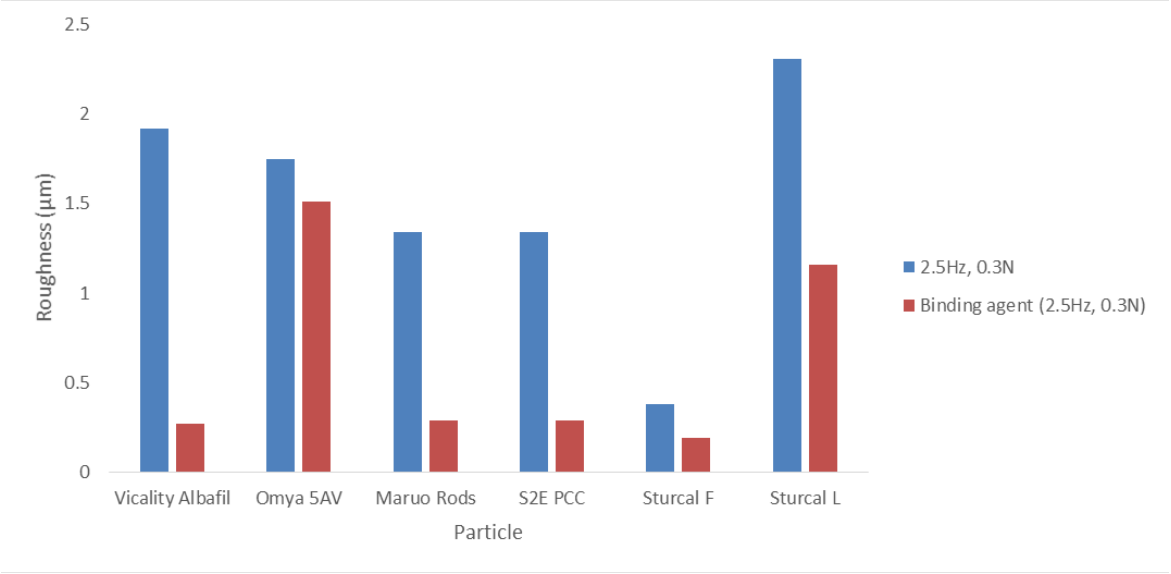

Figure 97 Roughness of wear scar for the particles with and without binding agent

The binding agent in general has the effect of significantly reducing the roughness of the wear scars.

7.2.2.3 Vertical ball position change

The vertical position of the ball during tests gives a good indication of the rate of material removal from the substrates. As material is removed the Z position of the ball will change. The shape of each plot allows for the comparison of material removal and how this changes over time between particles.

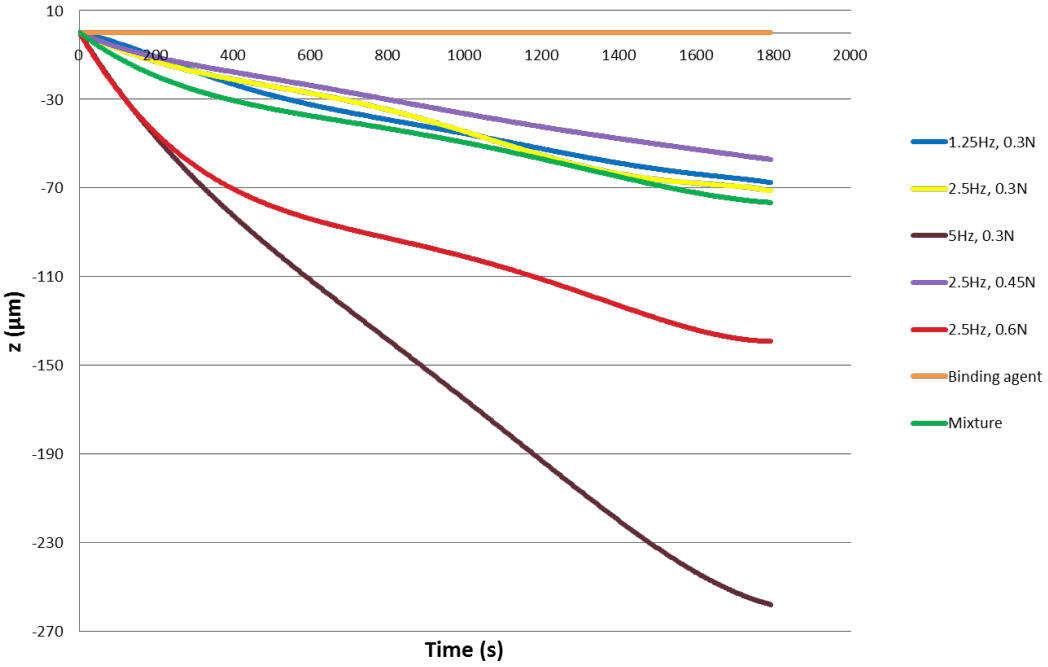

Figure 98 Change in vertical ball position over test duration for Vicality Albafil tests

Figure 98 above shows how the vertical ball position changes with test duration for Vicality Albafil tests. It is clear that higher frequencies develop a faster material removal rate although interestingly, initial rate of material removal at higher loads and lower frequencies is comparable. Whilst at a higher load, wear rate appears to stabilise and reduce for the higher frequency (5Hz) wear rate remains relatively rapid for the entire test duration. For lower frequencies and lower loads, wear rates are seen to remain comparable and the addition of a binding agent is again seen to lead to extremely low rates of wear.

Figure 99 shows the change in vertical position over the test duration for Omya 5AV particles in different scenarios.

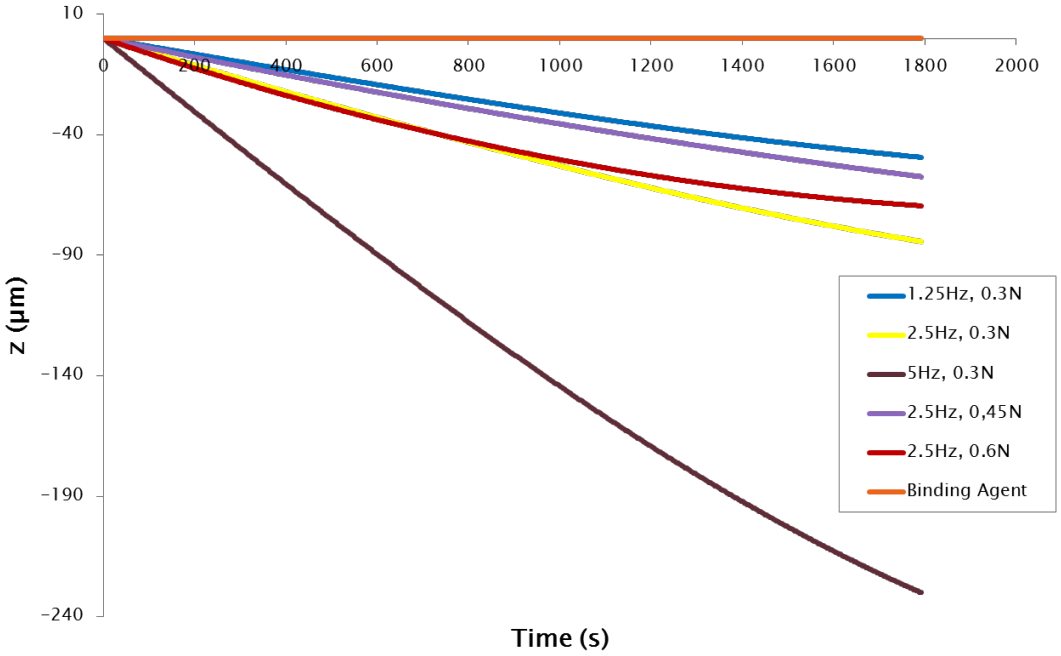

Figure 99 Change in vertical ball position over test duration for Omya 5AV tests

As with Vicality Albafil, the highest frequency (5Hz,0.3N) had most significant effect on Z ball position (substrate penetration). Increase in speed led to a greater increase in material removal than load whilst introduction of a binding agent significantly reduced scratch prevalence and overall wear.

The vertical ball position over the test duration is shown for the various scenarios with Maruo Rods below in Figure 100.

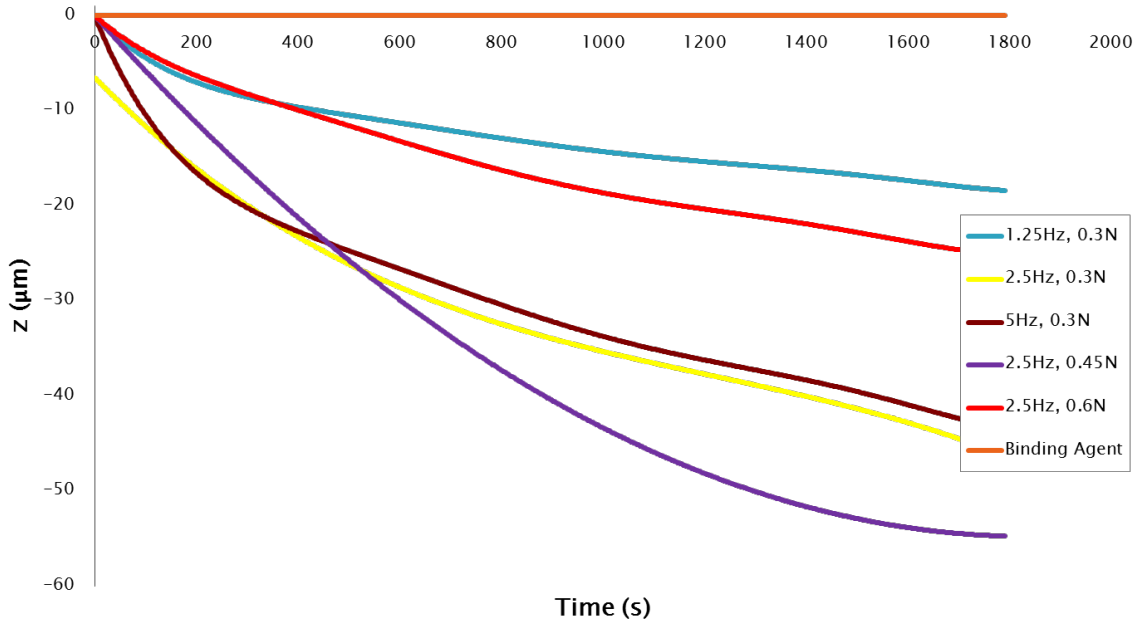

Figure 100 Change in vertical ball position over test duration for Maruo Rods tests

Increasing frequency from 2.5Hz to 5Hz is not seen to have an effect on substrate penetration. At the lower frequency of 1.25Hz the wear rate is reduced. The largest change in material removal is seen with increasing load.

Below, Figure 101 shows the displacement of the ball in the vertical direction over the course of the tests for S2E PCC particles. The highest frequency shows the most rapid displacement whilst the intermediate load (0.45N) showed a more rapid wear than other loads.

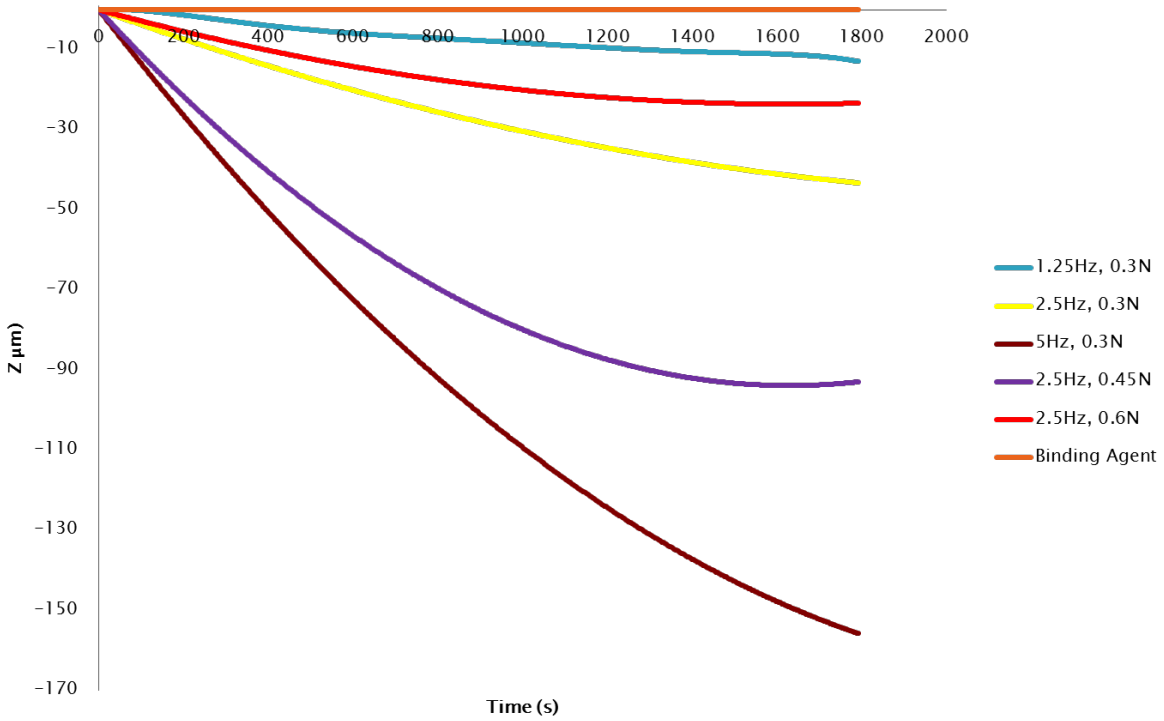

Figure 101 Change in vertical ball position over test duration for S2E PCC tests

It is interesting that the most vertical displacements correspond more closely with minimum scratch widths than with maximum or average. It was found that the highest loads created much wider scratches although the penetration depth is less deep. It is possible that this effect could be due to particles being distorted (flattened) or forming agglomerations, which have the effect of spreading the load at higher loads reducing the depth of scratches whilst increasing their width.

Below, Figure 102 shows the change in vertical position over the test duration for Sturcal F particles.

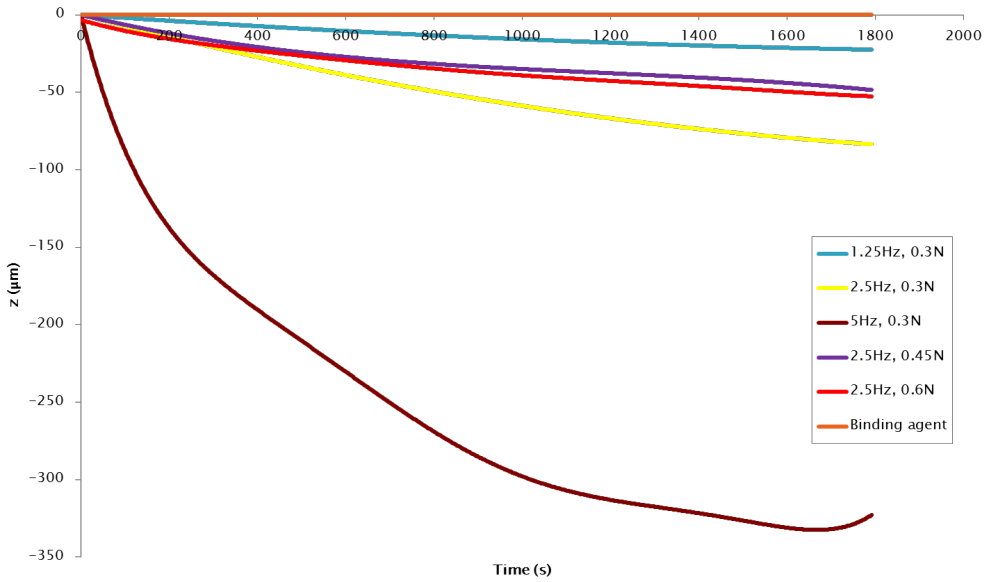

Figure 102 Change in vertical ball position over test duration for Sturcal F tests

It can be seen that there is relatively little surface penetration for the majority of scenarios whilst testing at 5Hz has resulted in a rapid wear rate. There is a significant contrast in this case with notable accelerated wear from the outset. Comparing ahead to Sturcal L we can see that although aggressive behaviour is demonstrated by both, we do not see such notable and isolated penetration depth at higher processing speeds with Sturcal L. We have seen in Chapter 9, that Sturcal F particles form smaller agglomerations that are less densely arranged than Sturcal L. It could be the case that at the higher processing speeds Sturcal F particles are prone to breakdown leading to dual wear mechanisms involving both particles in isolation and as agglomerates. In some trends we can see a subtle change to a positive gradient at the end of a plot for the penetration depth of the ball. This would suggest that the ball is actually rising a little towards the end and does not occur in all trends. Experimentation suggests that no fluid absorption occurs into the ball, which could lead to swelling. It could be the case that as the trial progresses particle breakdown and potentially fragments of the dentine breaks down and forms slurry within the contact zone, which eventually begins to lift the ball in some cases.

The ball penetration for the various trials with Sturcal L particles is shown below in Figure 103.

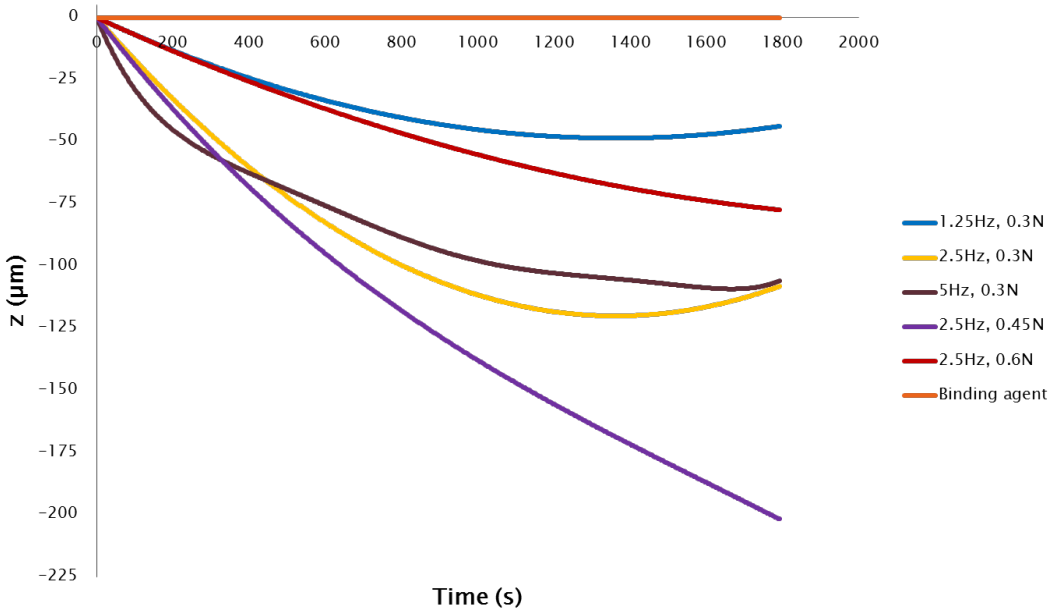

Figure 103 Change in vertical ball position over test duration for Sturcal L tests

The largest ball penetration is seen at the intermediate load (0.45N) whilst the other trials give no apparent relationship between ball penetration and load/frequency. Despite the more aggressive wear seen in SEM images and by measurement, the ball position for the binding agent trial is seen to remain relatively low. It is thought that whilst material removal was taking place, the binding agent had the effect of supporting the debris and hence the ball resulting in the low displacements seen.

- At this point the wear depth has been presented as both a calculated area from profile plots and as a change in the vertical position of the nylon ball. It can be seen that there is no convincing correlation between the two methods. For the following reasons the change in ball position is considered the more accurate and representative way of comparing wear depth:
- The accuracy of the ball position, for a calibrated CETR, is to within 500nm (calibration was carried out between each trial).
- There was no observable wear on the ball itself, which could contribute to the change in ball height (every ball was examined under SEM).
- When measuring the profile plots there is a margin of error for choosing the exact start and end for the wear scars.

The profilometer measurement may be misrepresented by the presence of wear debris pressed into the wear scar.

7.2.2.4 Effect of Frequency

The testing above has shown clear differences which allow for comparison of the different particles. Firstly, to observe general trends between frequency and surface penetration, the

samples should be compared at the same number of strokes. Since the end of 1.25Hz tests is equal to 2250 strokes, a comparison line has been drawn as shown below in Figure 104

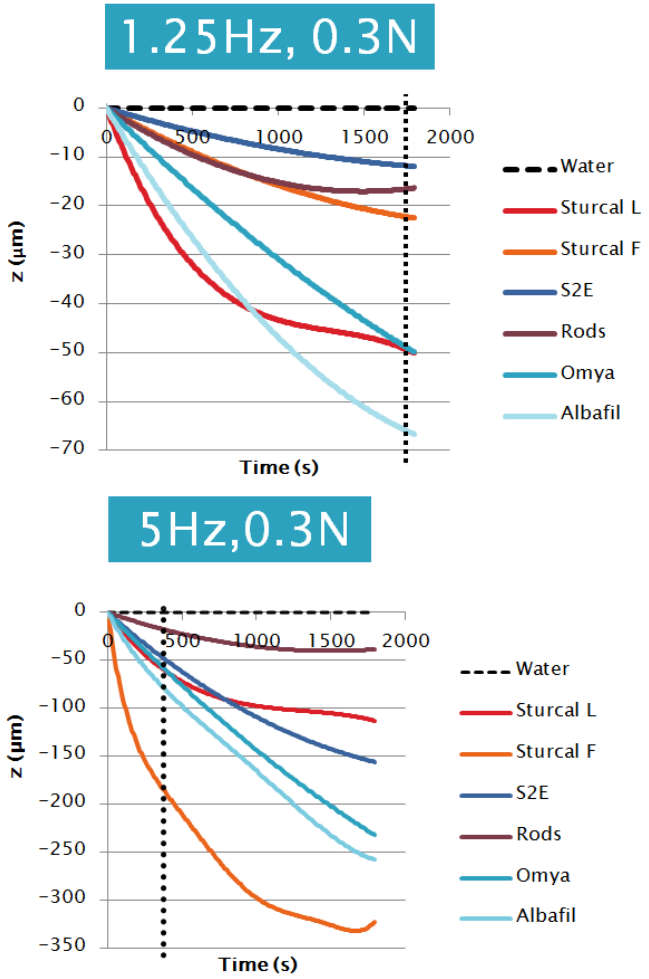

Figure 104 Comparison sample surface penetration at frequencies of 1.25Hz and 5Hz

By this method it can be seen that higher frequencies generally lead to higher wear rates. However, it should be noted that the relationship is not linear in that doubling the frequency does not lead to twice the wear. The wear of each surface after 450 strokes and 1800 strokes is shown below for the various particles in Figure 105.

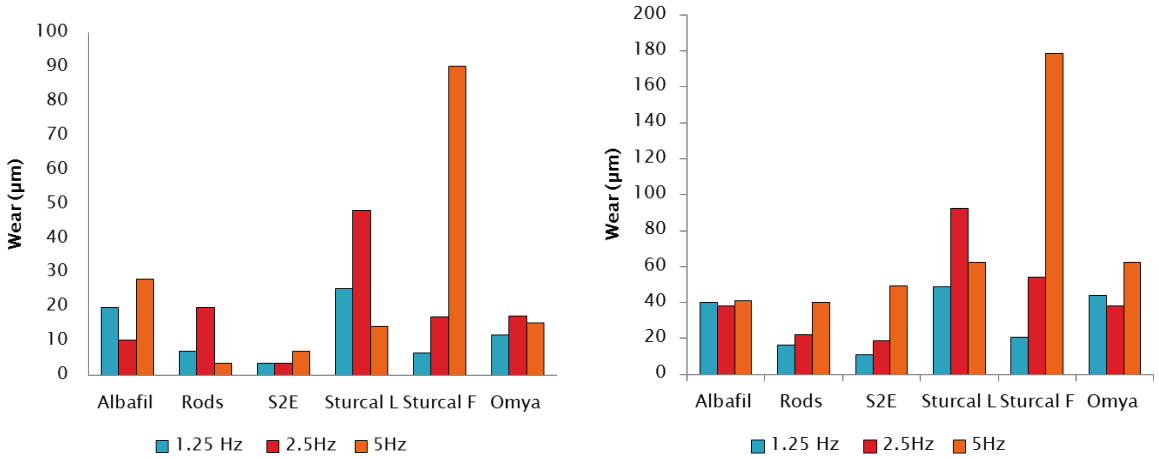

Figure 105 Wear after 450 strokes (left) and 1800 strokes (right) for the substrates interacting with various particles

After the same number of passes there is a significant difference in material loss for different frequencies and between the different particles. This demonstrates that there is something intrinsically different about the particle behaviour at different speeds. Clearly, at higher speeds Sturcal F particles lead to the most aggressive wear whilst Sturcal L particles show highest wear at intermediate speed (2.5Hz).

7.2.2.5 Surface roughness in relation to wear

Surface roughness can be compared directly to profile depth for the various particles. Shown below are the different test conditions with the measurements of overall region Ra and profile depth (Figure 106 to Figure 111).

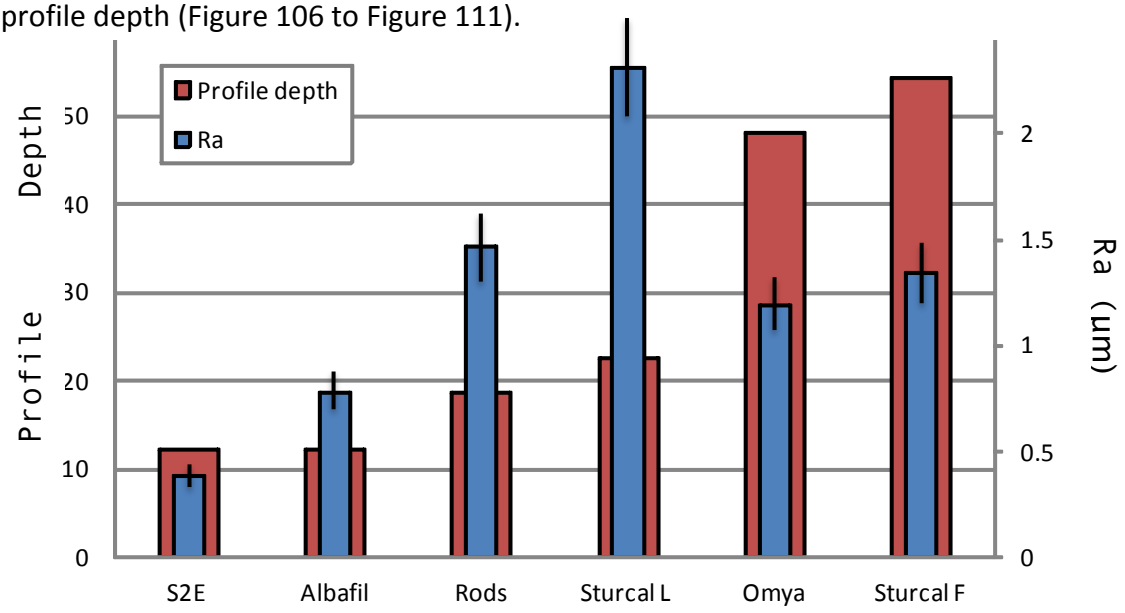

Figure 106 Comparison of overall Ra and profile depth for various particles at 1.25Hz, 0.3N

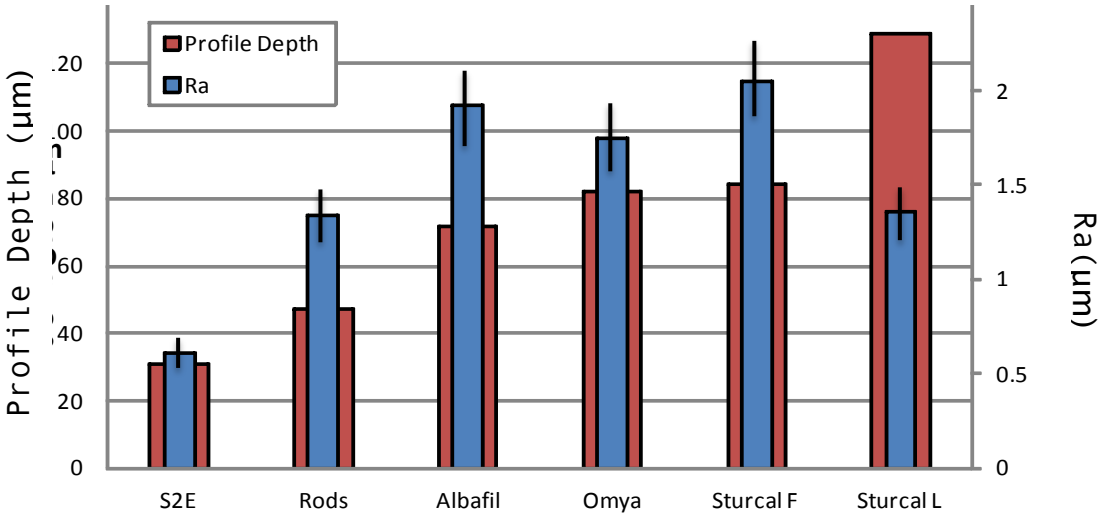

Figure 107 Comparison of overall Ra and profile depth for various particles at 2.5Hz, 0.3N

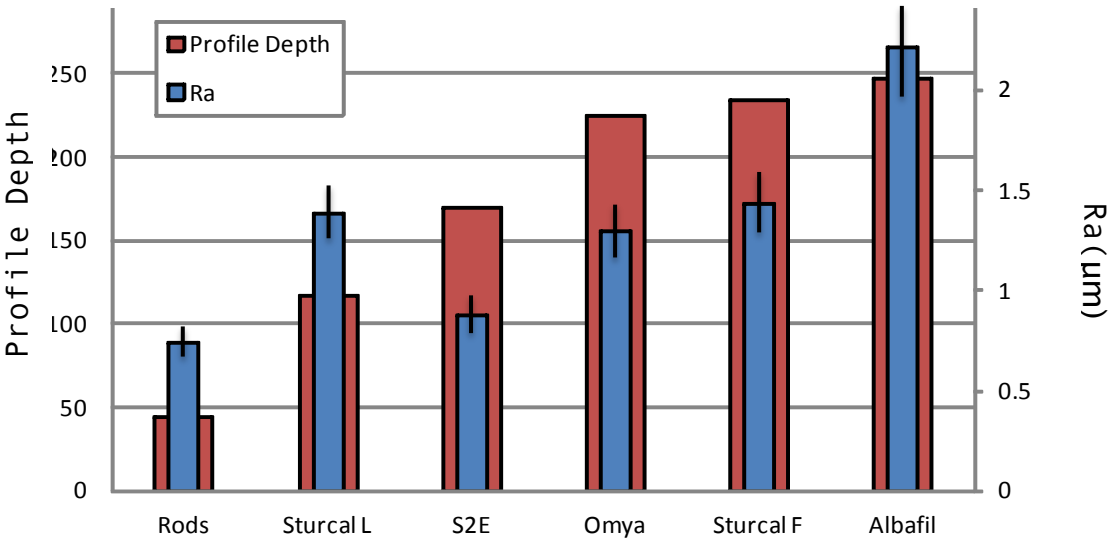

Figure 108 Comparison of overall Ra and profile depth for various particles at 5Hz, 0.3N

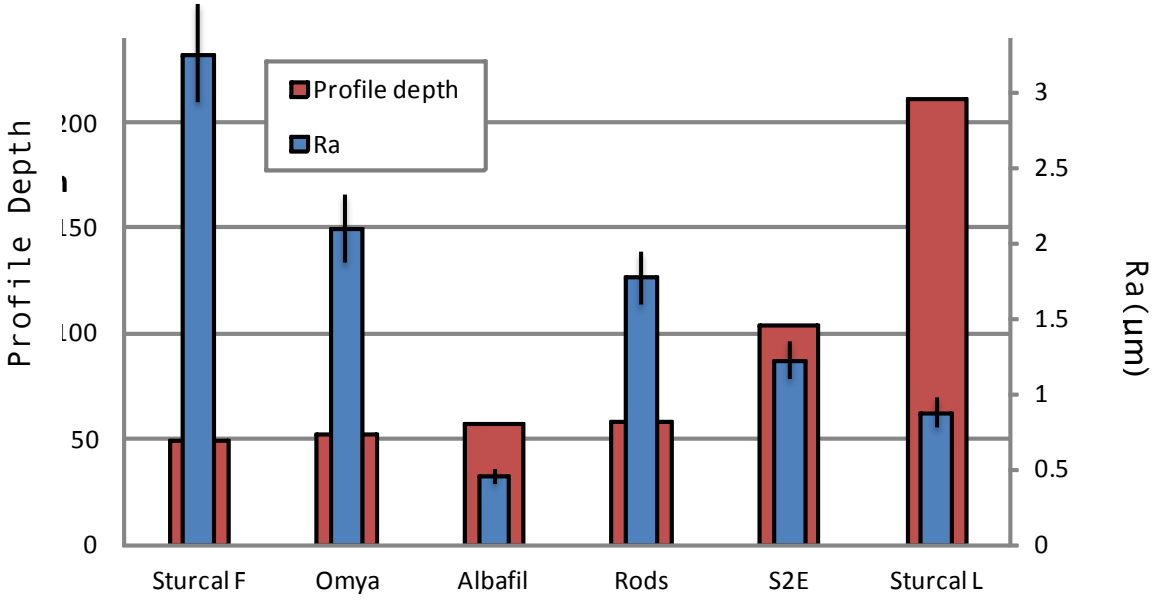

Figure 109 Comparison of overall Ra and profile depth for various particles at 2.5Hz, 0.45N

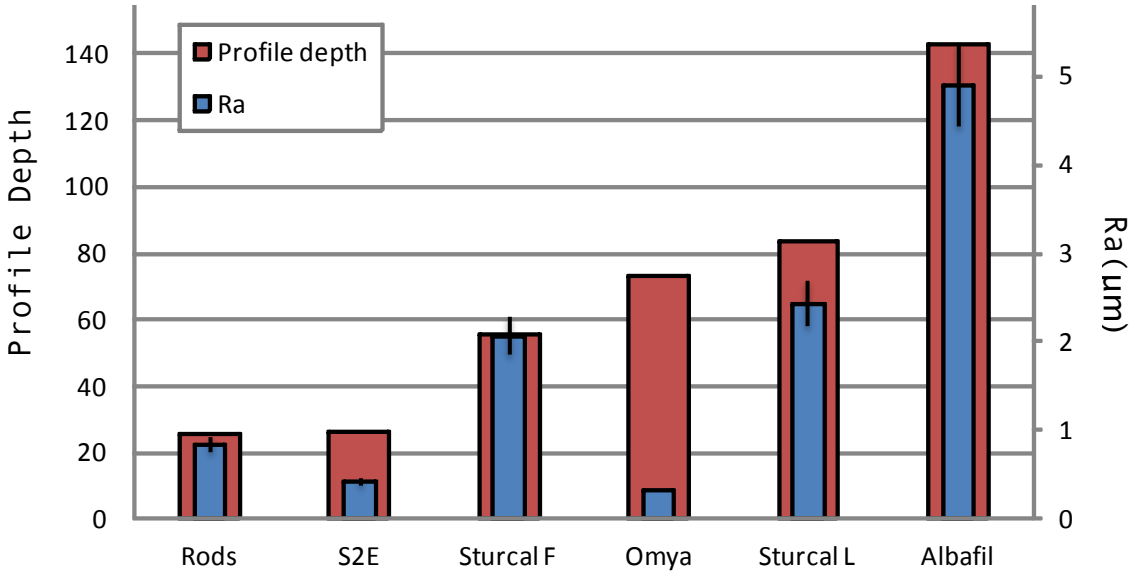

Figure 110 Comparison of overall Ra and profile depth for various particles at 2.5Hz, 0.6N

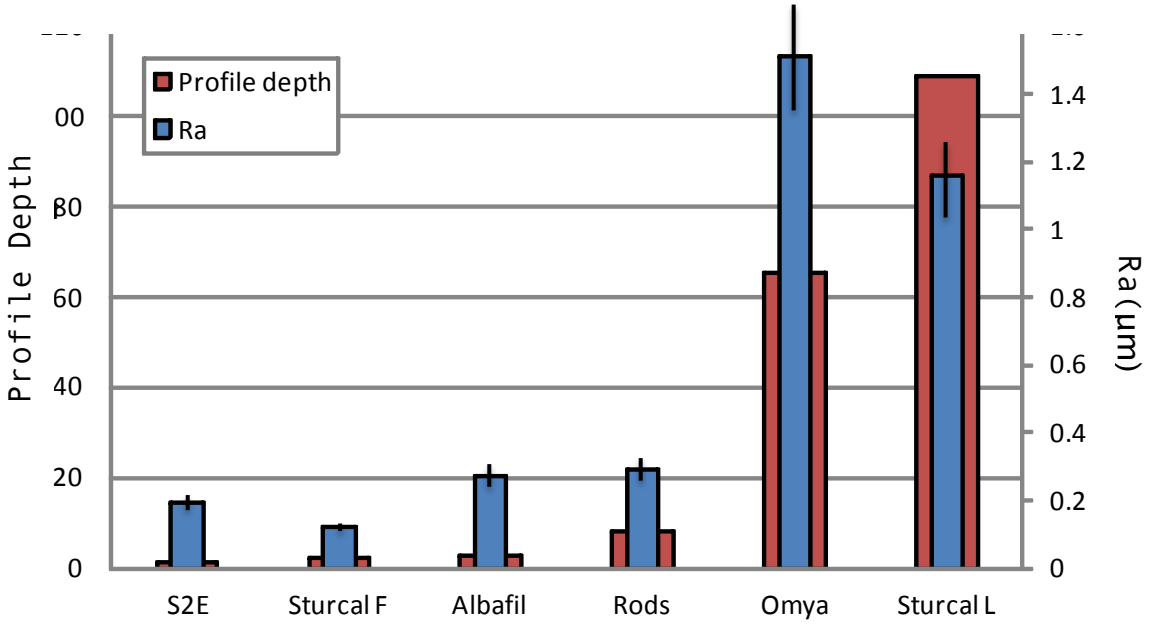

Figure 111 Comparison of overall Ra and profile depth for various particles with the addition of a binding agent

There appears to be little correlation between Ra and profile depth in most cases, based upon figures 106 to 111. It is thought that particle breakdown leads to shape changes and variation in the distribution of the load leading to wider or deeper scratches than would otherwise be observed. To determine this the dynamic particle behaviour must be observed directly, this is investigated in Chapter 8.

7.2.2.6 Particle mixtures

Since particle shape and size along with particle breakdown is thought to affect the aggressiveness of the wear observed above, the tests have been repeated using particles combinations. It has been observed that subtle changes in particle shape and size can have

dramatic affects on wear behaviour. It was of interest to explore whether, by combining each particle with a standard particle (Omya 5AV), there was a synergistic change in the results we previously observed for the particles in when run in isolation. Omya 5AV was selected as the 'standard particle' as it is an accessible and cheap particle to produce through grinding processes and common to basic oral care products. The particles have been mixed in equal measure before being applied to the contact region by the same method discussed previously.

Figure 112 below shows SEM images taken of the wear surfaces following testing of mixtures of the various particles with Omya 5AV.

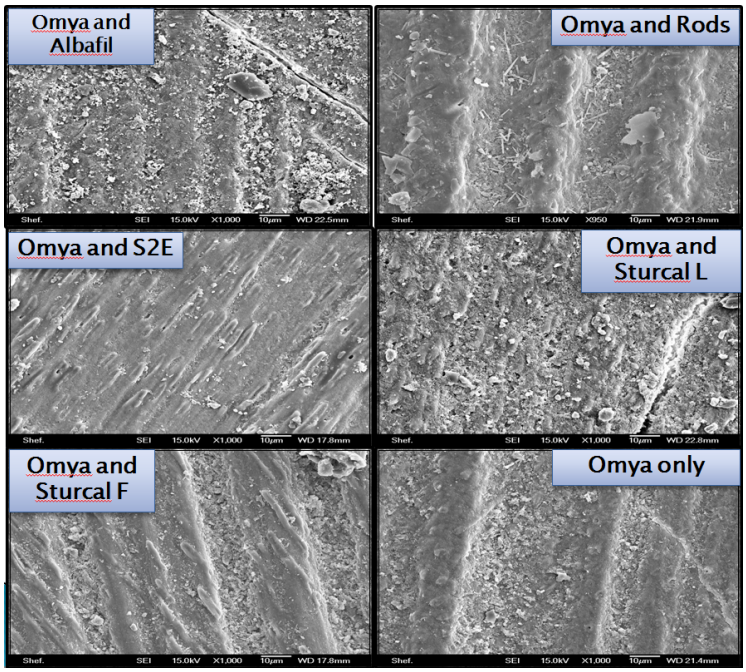

Figure 112 SEM images following testing of mixtures with Omya 5AV particles

The SEM images above show that wear has been affected differently depending on the mixture. The most notable effect was that the introduction of Maruo Rod particles to Omya 5AV did lead to smoother surface finish within and around wear scars. It has been proposed from the results of other experimentation within this thesis that Rod particles do indeed posses polishing properties when used. Figure 114 below compares in more detail SEM micrographs of dentine processed with solely Omya 5AV and Omya 5AV with the introduction of Rod particles. Figure 113 shows a simplified overview of this proposed smoothing process with Rods.

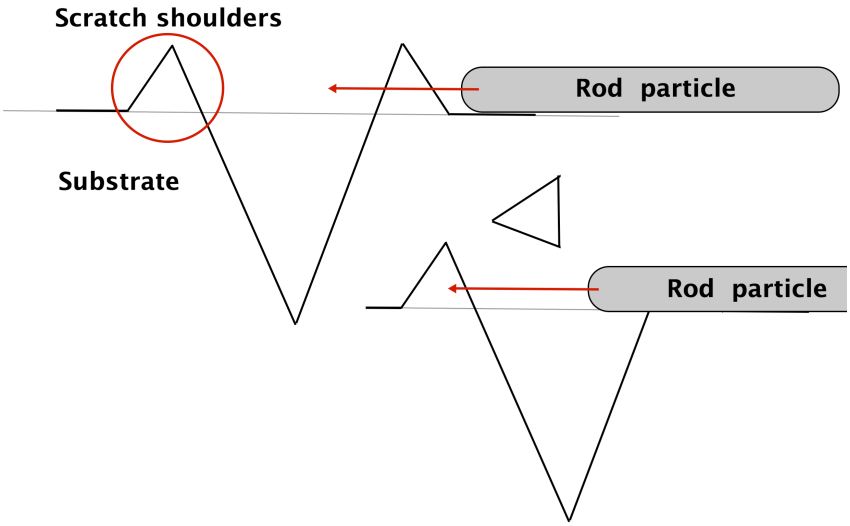

Figure 113 Mechanistic diagram for proposed Rod smoothing effect

The majority of data in this case would not be susceptible to skewness or kurtosis with the claim that there is a potential polishing affect introduced with Rods. This is not thought to have an effect on the material removal process (most likely promoted by the smaller sub particles – see Chapter 8) but rather has the added benefit of asperity movement based upon the movement of large intact particles which can potentially remove projecting shoulders and asperities from the substrate surface via the characteristic movement of the larger particle (discussed more in Chapter 8). This smoothing process would be limited to the depth of a single particle, which would be insignificant compared to the macroscopic data. There is the potential for skewness to become more apparent within the roughness data. In order to perceive this bias however would require substantial numbers of trials to be carried out in order to populate normal curves demonstrating a plethora of values for each experimental scenario. This was not possible due to the limited nature of the real teeth samples used and the preparation time required in polishing each one before experimentation. This would be an interesting statistical exercise to carry out and my prediction would be that positive skewness would be demonstrated by the Rod particles as a result of them lowering the mean roughness in general. Since the distribution in this case would no longer be normal the Kurtosis would be a moot point, however if Kurtosis were to present itself it would more likely be of platykurtic characteristics rather than leptokurtic, as the polishing effects of the Rods are relatively broad due to the unpredictable mix of intact and fractured particles.

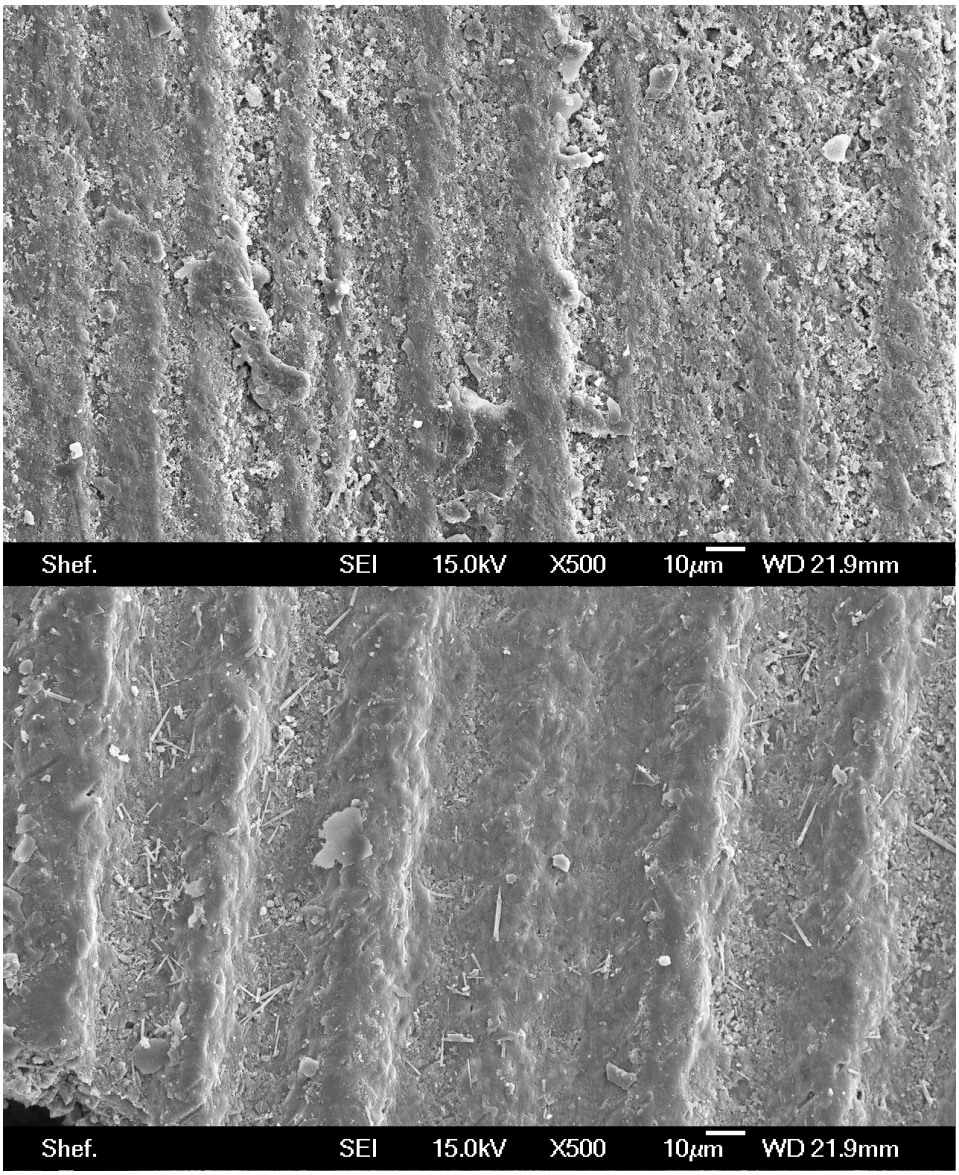

Figure 114 Above: Dentine brushed we Omya 5AV particles. Below: Dentine brushed with Omya 5AV and Rod Particle combined (2.5Hz, 0.3N)

In the case of Sturcal L, particle mixtures appear to also lead to a reduction in the aggressiveness of the scratches. It could not be said however that the scenario has led to any examples of substrate smoothing. It could be that, due to the significantly aggressive nature of Sturcal L particles, the introduction of Omya 5AV leads to reduction in material loss merely because there is a lowered presence of Sturcal L particles.

Figure 115 below shows the surface penetration for various mixtures relative to the Omya 5AV particles alone.

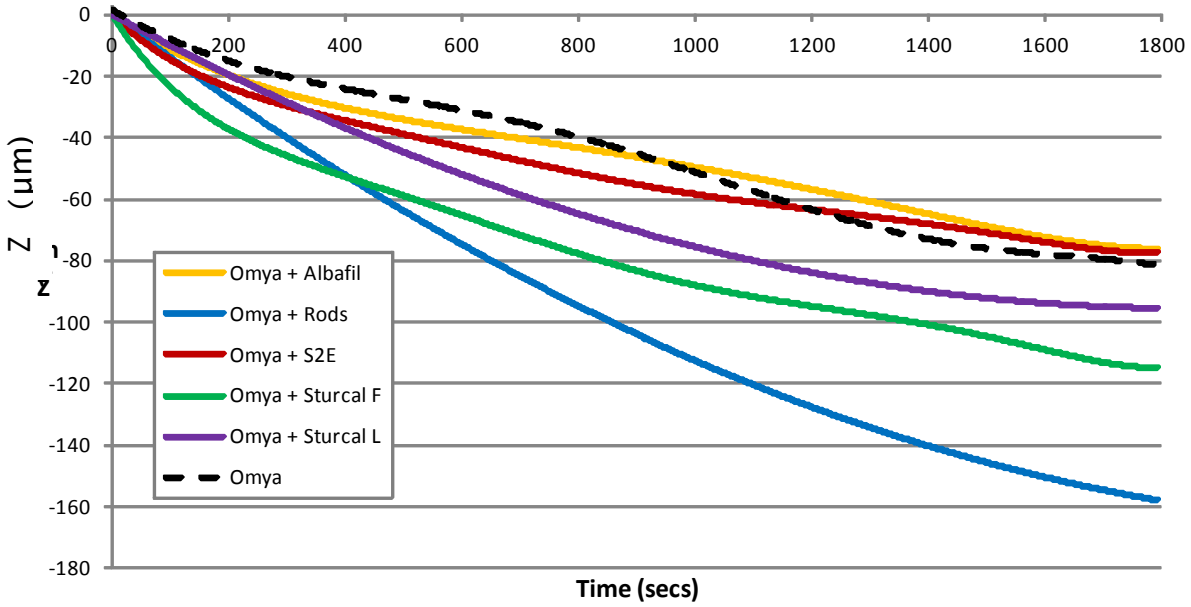

Figure 115 Surface penetration for test duration for various particle mixtures with Omya 5AV at 2.5Hz, 0.3N

It can be seen that an increase in surface penetration can be achieved by particle mixture. In particular, mixture with Maruo Rods has led to a greatly accelerated wear rate (almost double). This is interesting as although we observed aesthetically a smoothing effect through the introduction of particles by SEM analysis; we can see a significant increase in material removal through the introduction of Rod particles than with Omya 5AV on there own.

Profile depth has been compared for particles only and particles mixed with Omya 5AV. This is shown below in Figure 116.

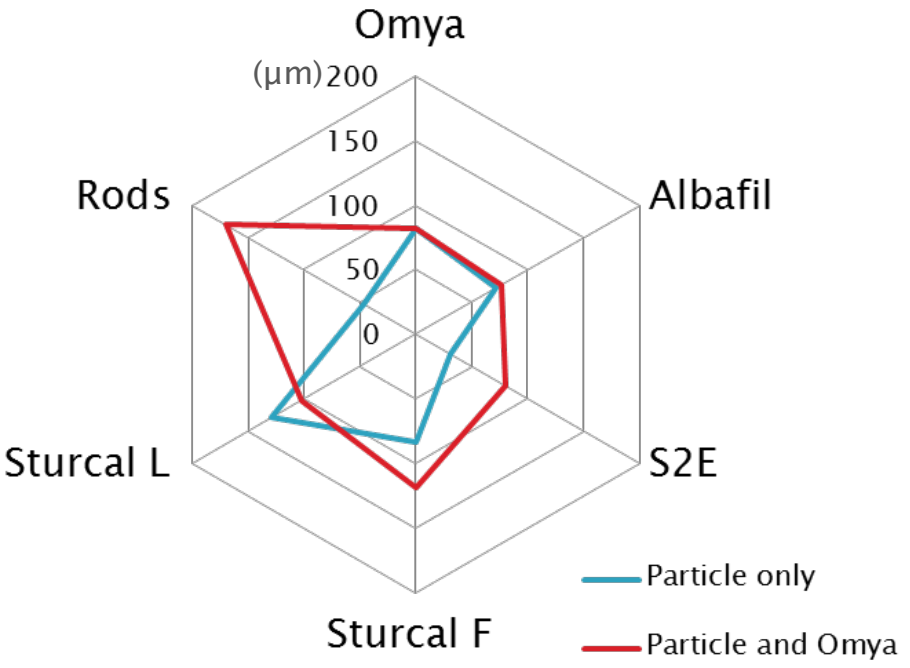

Figure 116 Comparison of particles only and particles mixed with Omya 5AV by profile depth in microns

Whilst some particles such as Vicality Albafil show little change in profile depth with the addition of Omya 5AV particles, other such as Maruo Rods show a significant change. This is consistent with the surface penetration profiles seen above. It is thought that Vicality Albafil particles are relatively similar in size and shape to Omya 5AV and so the effects of the mixture are lessened.

It should also be noted that whilst in some cases the mixing of particles has led to a synergistic change in wear performance (Maruo Rods for instance show a larger increase in wear than the two particles combined in isolation), in other cases, such as Sturcal L particles the mixture has led to a reduction in wear.

7.3 Conclusions

Various observations can be made from the testing undertaken above. Firstly, it is significant that particle behaviour is seen to vary depending on the speed and load applied since this enables mechanistic traits to be suggested along with the ranking of particle aggressiveness.

With hand brushing trials, although material removal from enamel was minimal with all particles (as shown with contact profilometry) there was observable surface roughening. This extent of this roughening did show variance in severity from particle to particle with perlite remaining the most sympathetic to enamel, showing the least severe roughening effects.

It has been noted that speed has a greater effect on wear than load, even when taken independently of the number of strokes. It is thought that the differences seen in behaviour at various speeds are due to some particles being more prone to tracking. Omya 5AV decreases incidences of tracking with increasing load whilst Maruo Rods show evidence of tracking only at low speed. Sturcal F particles consistently show evidence of tracking throughout the various trials. Maruo Rods and Sturcal L particles were observed to be the only samples with which speed had little effect on wear rate.

S2E PCC had the greatest variation in scratch characteristics between the different test conditions. Sturcal F showed an increase in surface degradation with load whilst Sturcal L showed the most aggressive material removal, particularly at high load. Trials without particles at the contact (water only) produced no noticeable wear demonstrating that it is the effect of the particles that is being observed during this testing.

In some cases, the mixing of particles led to a synergistic change in wear performance, most significantly with Maruo Rods, where the wear was greater than for the two individual particles combined. Other particles such as Sturcal L in mixture however led to a reduction

in wear. When introduced with Omya 5AV particles, Maruo Rods showed polishing effects on the small scale scratching.

It may be that the introduction of a binding agent be useful in improving the abrasive performance of a particle. Review of the COF data for the particles showed that in many cases the introduction of a binding agent increased the friction properties whilst reducing the observed surface damage. It could be that this may make for an effective balance between stain removal and remaining sympathetic to the substrate surface. Sturcal L is the only particle that led to an increase in scratch magnitude with the introduction of a binding agent.

8 DIRECT PARTICLE NANO-MANIPULATION

Subtle differences in particle characteristics such as size and shape can have a dramatic effect on the mechanisms associated with dynamic particle movement. This in turn can lead to considerable modifications of inter-particle relationships, as well as how the particle interacts with a substrate surface. The dynamic behaviour of particles is often studied by post mortem analysis of surface scratching in an attempt to discern traits of particle motivation via surface markings. There are inherent problems with this as an experimental method due to the difficulty in verifying the direct cause of surface marking and the lack of control of confounding variables. This chapter uses nano-manipulation in an SEM environment in order to directly influence microscopic bodies in-situ and observe the associated dynamic behaviour. Motivation of five different $CaCO_3$ particles was brought about using Nickel-Chromium nano probes. The main focus of this nano-manipulation analysis is to better understand the mode of particle movement in isolation, the effect of this dynamic mechanism upon the substrate and the affinity of particles to agglomerate. The characteristics of particle breakdown under loading, both in isolation and as a cumulative agglomeration was also analysed.

8.1 Background

There is significant focus upon the efficacy of abrasive particles and their affinity to remove surface detritus from, or cause damage to, a substrate surface. The dynamic mechanism in which a particle moves can contribute significantly to the aggressive nature of that particle. The characteristics of particle movement can be dictated by a number of factors including particle size and shape, the affinity of the particle to agglomerate or remain in isolation as well as the characteristics of particle breakdown. The combination of these factors can have potentially positive or negative synergistic effect upon the likelihood of a particle to cause damage. A small particle can potentially be more damaging to a substrate surface than a much larger particle depending upon the combination of other dynamic and interactive traits; such as the affinity of the particle to operate as an agglomeration or in isolation. It is for this reason that the dynamic behavior of abrasive particles is meticulously studied.

There have been numerous studies investigating nano-manipulation technology as a practical motivational tool for a variety of applications. Sitti et al [40] investigated the robotic nano-manipulation of nano-scale particles on a substrate under ambient conditions. In contrast to the source of manipulation discussed in this chapter, Sitti adopted an atomic force microscope (AFM) setup as the method for manipulation. AFM technology is primarily used as a means for micro and nano-scale imaging, however it can be adopted to provide a cost effective approach to small-scale manipulation. Sitti et al experiment with latex upon a silicon substrate, with the focus on the study less about the observed dynamic characteristics of the particles and more about the validation of the proposed experimental setup as a system of nano-manipulation. In order to appreciate the dynamic properties of manipulated bodies it is important to have real-time visual feedback of manipulation events. For this reason AFM controlled manipulation is not as adept as the systems used within this study, as they introduce certain operational limitations. Firstly using AFM as a motivational tool does not allow for the increase in range and intuitive control available with operator controlled probes. One of the more significant limitations with the AFM setup is that real-time monitoring of the manipulation process cannot be achieved as a result of the operational systems being devoted to either an imaging or motivational process at any one given time. Using an offline analytical system areas can be studied where a motivational event has occurred, however the dynamic features of the operation cannot be known [40]. Atomic force microscopy utilises interatomic force interaction to derive topographical information and thus are limited to analysing particles which are semi or fully-fixed to a substrate surface. This can impede the natural dynamic characteristics of unrestrained particles, which are central to this study. Jing Hou [41] examined the terminus of the AFM setup within the contact zone in an effort to minimise instances of slip and particle bisection. As AFM setups contact the particle to be manipulated at a single point with a

small contacting area this can be a common occurrence. To address this they introduced a 'nano-hand strategy', which aimed to introduce informed planning of pushing location, speed and step length by developing the kinematics model of the nanoparticle. Using this system does provide a reasonable solution for the limitations of the AFM however it does not compensate for the continued lack of real-time visual feedback.

Lixin Dong et al [42] adopted similar probe-based manipulation technology to that used within this chapter. A nano-robotic manipulator with 10 degrees of freedom was operated via piezoelectric ceramics (PZT) in an SEM. Dong highlights the benefits of operator controlled probe technology compared to AFM. Particular attention is paid to the susceptibility of AFM technology to drift and hysteresis, as well as the limits of the directional freedom of the setup. Manipulating nano-scale bodies within a three dimensional domain relies on the introduction of rotational command of the motivational source. Dong demonstrates the precise control achievable using three-dimensional nano-robotic cantilever, rather than an investigation into the behavior of manipulated bodies this was an informative validation of the nano-manipulation setup. Sitti et al [43] surveyed a number of nano-manipulation setups in an effort to compare and contrast their strengths and weaknesses. One of their conclusions was that one of the most confounding variables of the nano-manipulation process is sample preparation. Non-uniformity in substrate preparation and dispensation of particles can have notable effect on the ultimate manipulation properties of said particles. For the purposes of this study stringent environmental standards are adopted to ensure no inter-trial bias is introduced between particle and substrate and from particle to particle.

8.2 Experimental procedure and sample preparation

Within this study 5 Calcium Carbonate particles were analysed: Maruo Rods, Sturcal L, Sturcal F, S2E PCC and Omya 5AV. With the exception of Omya 5AV which is derived through grinding, these particles are the result of a precipitation process. Maruo Rods and Sturcal F are Aragonite particles whereas Sturcal L and S2E are Scalendrohedral. More information and images of these particles can be found in table 2 in Chapter 4.

The primary experimental apparatus used for visualisation was a Jeol-6500 scanning electron microscope in-conjunction with two Kleindick MM3A manipulation probes (Figure 117).

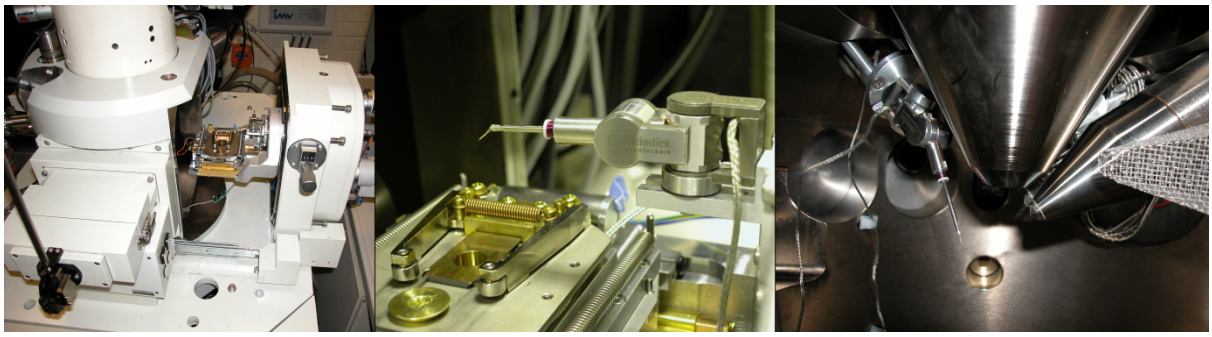

Figure 117 Left: Jeol 6500, Right: Nano-manipulation probes within SEM chamber

The probing of microscopic bodies requires very precise positioning accuracy together with a reliably stable control system. The nano-manipulation probes act as an extension of the operator's movements, allowing for the intuitive and controlled movement of introduced items. The probes are moveable according to three modes outlined in Figure 118, the combination of which allows for fluid and sweeping probe movements.

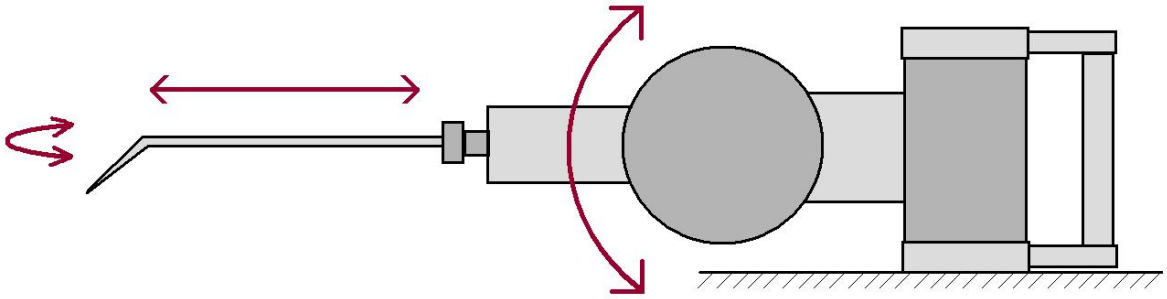

Figure 118 Schematic of nano-probe movements

Figure 118 shows a schematic of the range of nano-probe movements according to three separate drives. The principle components for these drives include a piezoelectric slider and stator [44]. The manipulators can be operated according to discrete steps within two modes, fine and coarse. Within fine mode exceptionally slight adjustments of the location of the slider upon the stator is controlled. This is brought about via the contraction and expansion of the piezoelectric components of the stator according to the nature of the applied voltage. The slider can remain fixed in position when idle through friction. For larger step movements than are achievable with fine mode, coarse mode can be used which relies on stick slip motion [44]. In this case a saw-tooth voltage waveform is introduced to the slider and stator previously used in fine mode. Using a sawtooth waveform leads to a gradual voltage increase followed by a sudden decrease resulting in one directional movement. During the portion of the waveform where the voltage changes quickly the piezo is unable to progress the slider back to its point of origin as a result of the change in peizo volume being so fast. This is due to the fact that the friction keeping the slider and stator mated is exceed, resulting in the slider failing to move entirely backwards [44]. A net slider movement is achieved by the repetition of this process. Nickel Chromium Probe tips

were prepared via electrochemical etching and introduced into the terminus of the nano probes.

Experiments were conducted upon three substrates, silicon, perspex and polished copper. Trials upon silicon were carried out in order to discern the dynamic movements of particles when motivated across a very flat, firm surface. Despite not being of representative hardness for oral tissue Silicon does provide a platform for particle motivation without the presence of confounding macroscopic asperities, which may interfere with particle movement. Trials were also conducted on Perspex. Being of a similar hardness to dentine and widely accessible, Perspex is often used as a substitute material. The hardness of a material and its resistance to deflection can have an important effect upon particle breakdown. Trials were also carried out upon polished copper in an attempt to study the surface markings produced by propagating particles. By polishing the copper to a very fine finish, in conjunction with copper being relatively soft, discernible surface damage can be assessed in order to support nano-manipulation observations on dynamic particle characteristics. The experimental procedure for trials upon polished copper was carried out using a modified CETR tribometer with a standard Unilever brush head interface. Linear reciprocation experiments were conducted using a load of 3N for a total of 10 brush passes at 2.5Hz.

Pure Copper samples were sectioned and set within Konductomet phenolic mounting compound (20-3375-016) and wet ground using a 'Bueler Automet 250' for 2 minutes using a pile coarseness of 120 microns, with a touch force of 20N, a head speed of 50 RPM and a platen speed of 240 RPM. Samples were then polished using a 0.25 micron diamond polishing slurry for 4 minutes; using a 20N touch force, head speed of 50 RPM and a platen speed of 140 RPM. The polishing process was progressed down to a 0.05 micron finish. Samples were ultrasonicated in distilled water for 5 minutes to clear the substrate of any remaining diamond particles (all shown below in Figure 119).

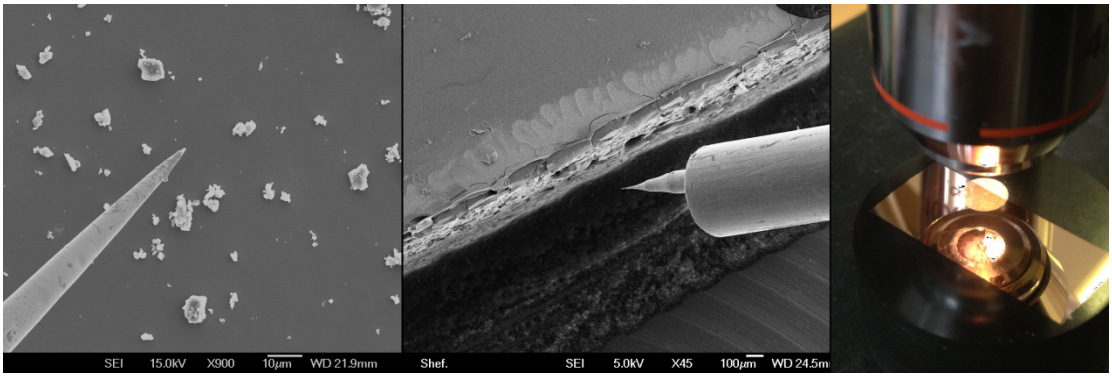

Figure 119 Left: Silicon, Middle: Perspex, Right: Polished Copper substrates

Due to its insulating properties perspex was gold sputter coated to avoid potential charging issues within the SEM. Silicon and copper remained uncoated to ensure no modification of

the substrate surface was introduced. Particles were administered dry to each substrate after sputter coating.

8.3 Results

Vicality Albafil

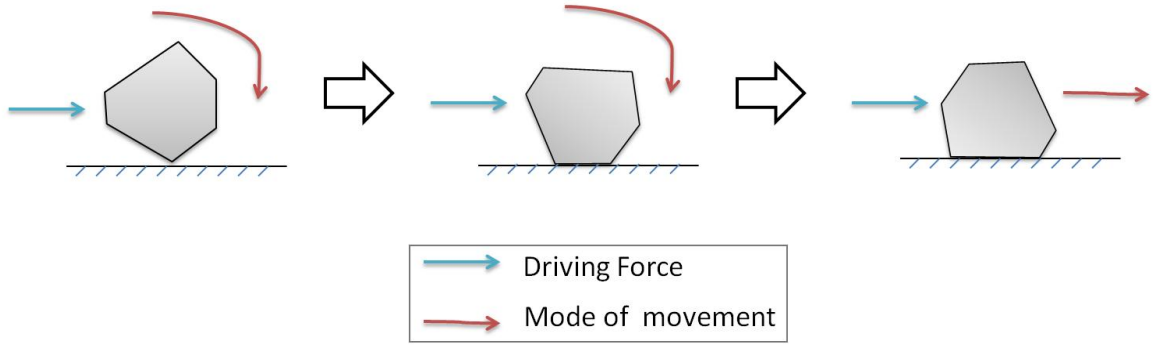

Figure 120 Schematic for the mechanistic movement of Vicality Albafil particles

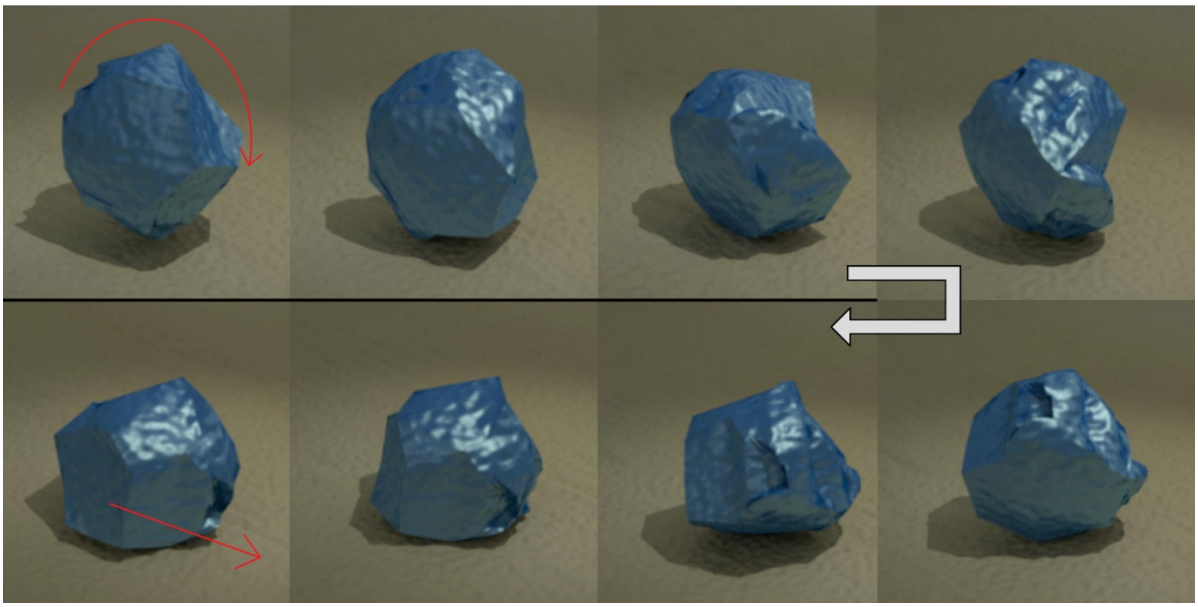

Figure 121 Simulated images of progressive particle movement for Vicality Albafil particles

SEM analysis of Albafil particles revealed multifaceted polyhedral geometry. Using manipulation probes to rotate particles so all sides could be studied there appears to be notable variance in the frequency of faces present. A common and significant feature of this particles geometry is the presence of a single face, or occasionally parallel pair of flat faces that are notably larger than all other faces.

Using the probes to load the particles, the structural resilience and particle fracture characteristics can be observed. Albafil particles demonstrate a strong resistance to breakdown with no observable particle fracture. Particles do not form structured agglomerations but do have a notable affinity to remain in contact with neighboring particles. Gathered particles are relatively easily separated with nano-probes showing inter-

particle adhesion to be reasonably weak. The small size of the particle and consequently the large net surface area does lead to accessible particle surface contact.

Trials manipulating Albafil upon the very flat Silicon substrate did reveal a pattern of behavior regarding the particles mechanism of movement (Figure 123 and Figure 124). The initiation of particle motivation invariably begins with planar rolling. A key feature of Albafil particles is the aforementioned presence of a larger face of the polyhedral structure. It was repeatedly observed that particles would roll across the shorter faces until this larger flat locates the substrate, whereupon the particle would continue to slide. Once this compliant position has been established it appears to be relatively difficult to encourage the particle to roll again upon Silicon. Conducting trials upon the softer Perspex substrate however did lead to an increased instance of particles being able to begin rolling again. Most likely a result of the increased permissible surface deflection with Perspex, there was a 'toeing in' effect where the preceding edge of the particle would dig in to the substrate surface and begin to roll. Usually particles re-locate a larger flat side and begin to slide again before long. Post processing analysis of trials upon copper, show surface marking which support this mechanistic movement.

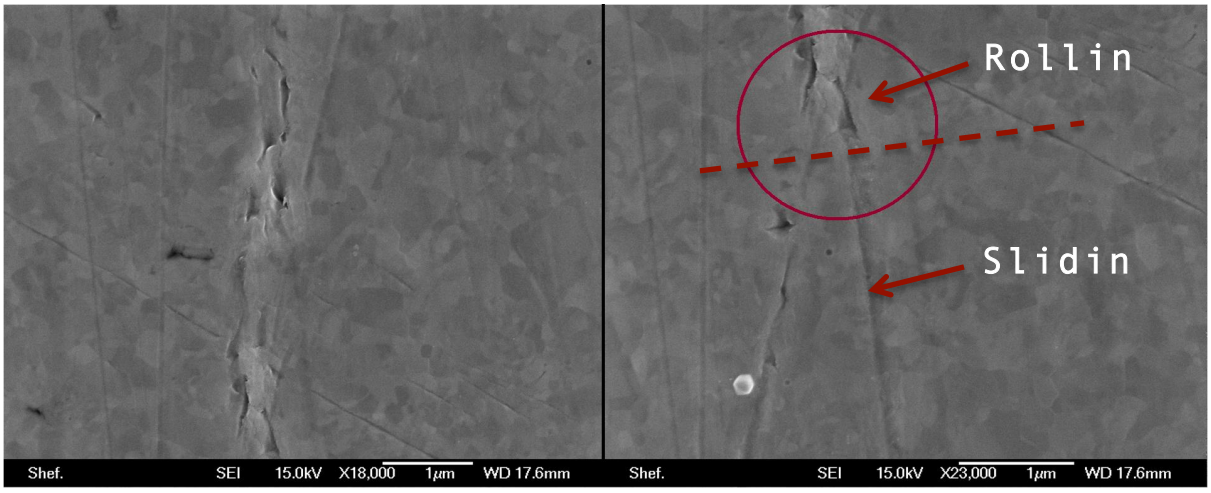

Figure 122 SEM images of surface markings from motivated Vicality Albafil particles on Copper (particle moving downwards)

Discrete marking can be seen in Figure 122 as a result of the Albafil particles rolling. Having defined angular sides this has led to the introduction of intermittent surface gouging. The right hand portion of the image highlights a transition from rolling to sliding. By comparison it seems sliding is less damaging to the substrate surface than rolling with Albafil particles.

S2E PCC

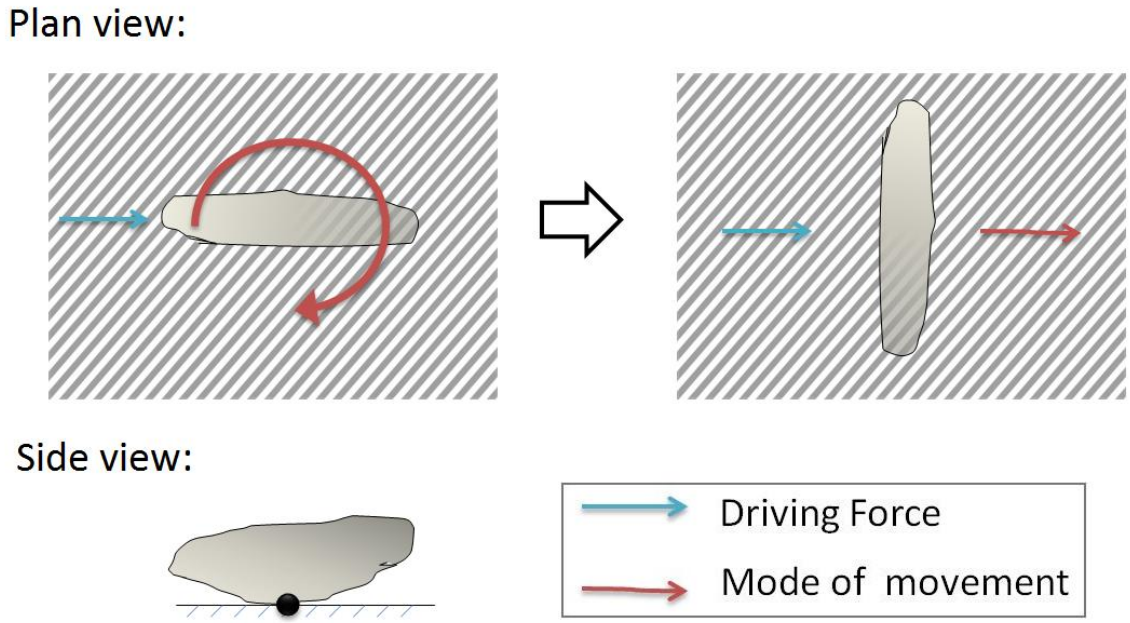

Figure 123 Schematic for the mechanistic movement of S2E particles

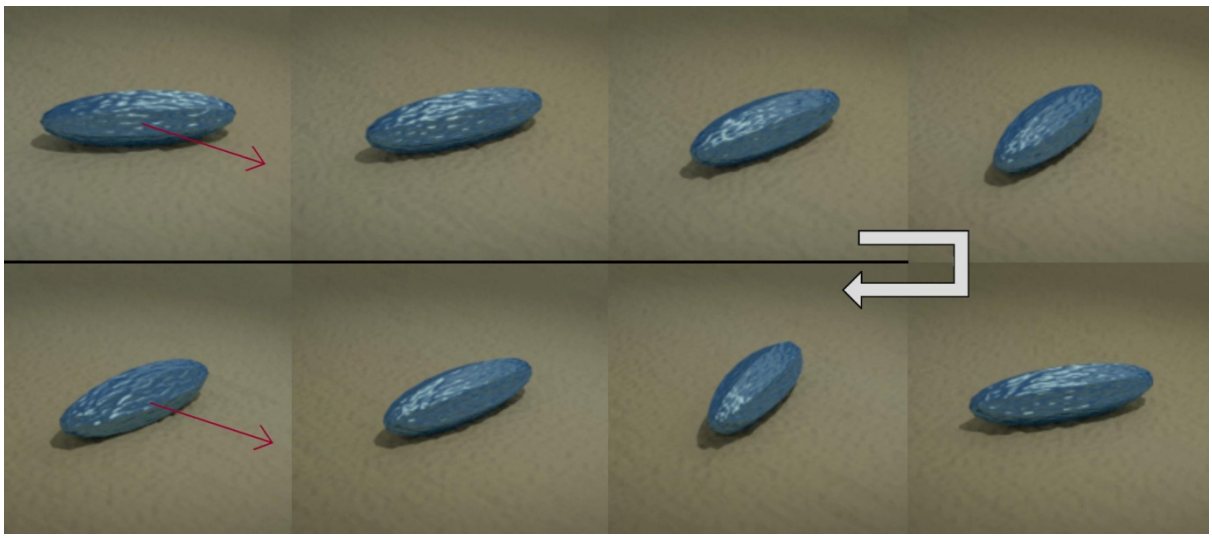

Figure 124 Simulated images of progressive particle movement for S2E particles

In contrast with the angularity of Albafil, S2E particles are smoother and more regular. SEM analysis shows particles to be oblong in shape with a wider, rounded midsection and relatively symmetrical tapering ends. Particle agglomerations are apparent but demonstrate no discernible shape or arrangement. Initial manipulation shows that particles are easier to part than observed with Albafil, with particle agglomerations easily divided with passive probe sweeps.

Analysing the mechanism of movement (Figure 123 and Figure 125) upon silicon suggests the predominant mode of movement appears to be sliding with intermittent rolling. The

initial roll seen when initiating Albafil particles was not a necessary feature with S2E. The obvious difference between the rolling characteristics of S2E compared to Albafil is that the improved symmetry and lack of sharp edges suggest that S2E particles are less likely to gouge the surface when moving. The wider center of the particle leads to predictable orientation when moved. The reduced particle-substrate contact is more representative of point contact, which causes the particle to readily rotate until perpendicular to the direction of movement regardless of the location of the impulse upon the particle. This is not seen with Rod particles, which have increased surface area contact, and were able to maintain original orientation when moved.

Trials conducted on both Silicon and Perspex both showed a subtle increase in particle fracture than that seen with Albafil. This fracture was relatively unpredictable and seemed most apparent when moving large agglomerations of particles. S2E are not as brittle as rod particles however and their smooth tapering shape does make them more likely to escape contact when loaded from above.

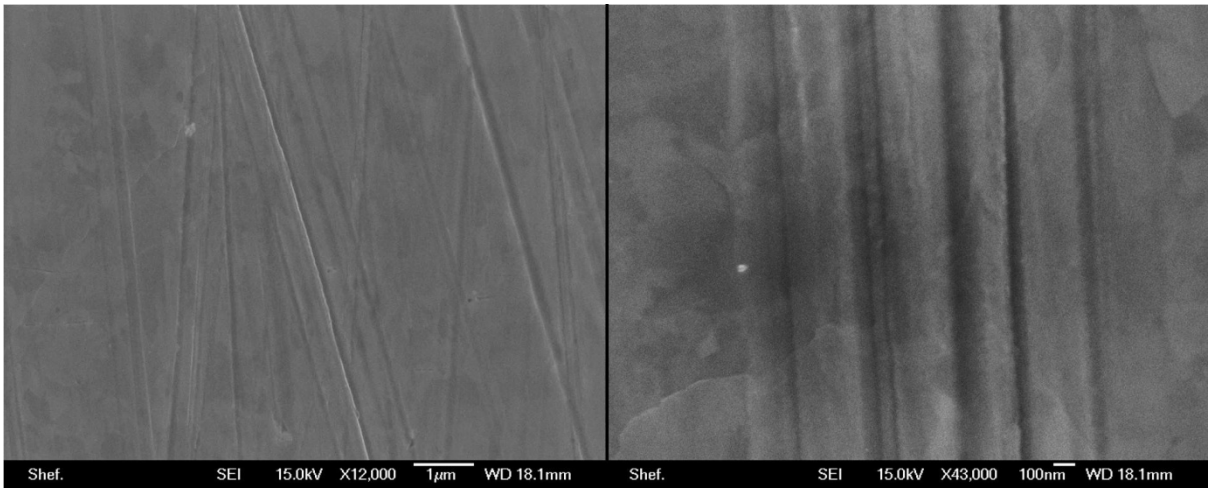

Figure 125 SEM images of surface markings from motivated S2E particles on Copper (particle moving downwards)

Analysis of surface markings derived from linear reciprocation experiments with S2E (Figure 125) show that the particle is indeed more sympathetic to the substrate surface. There are significantly few examples of intermittent gouging through particle tumbling with the observable scratches continuous in nature. Scratch frequency is not reduced, however the depth of observed scratches is notably shallow. The right hand portion of Figure 125 shows a highly magnified image of featured scratches on the scale of nanometers. The width and depth of these scratches are small and neat with no aggressive material removal. It would appear that the particles do not readily modify their position once moving.

Sturcal L

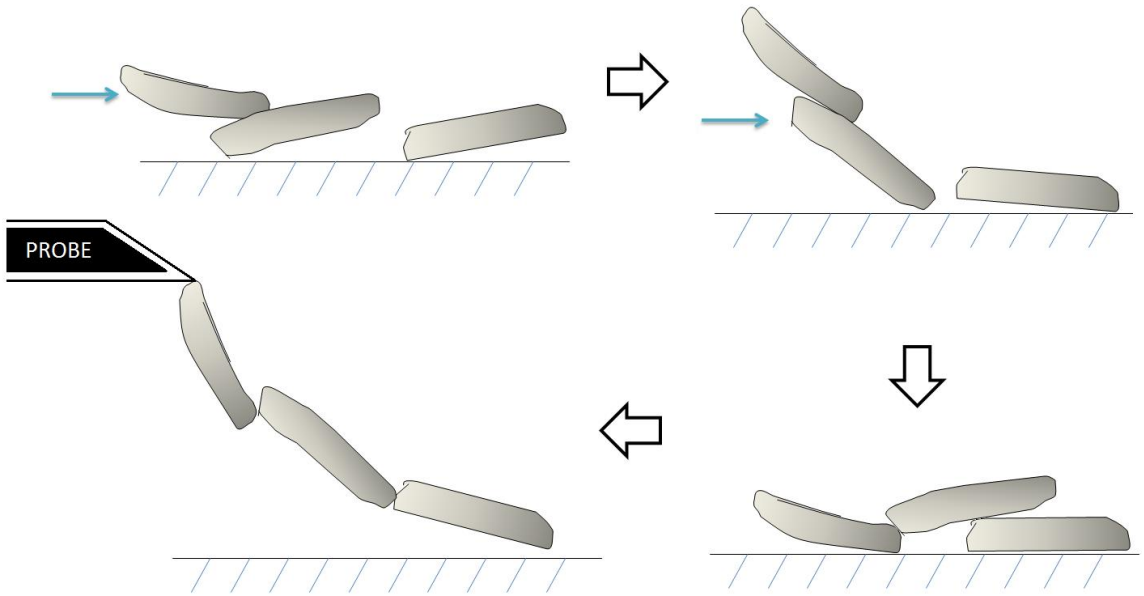

Figure 126 Schematic for the mechanistic movement of Sturcal L particles

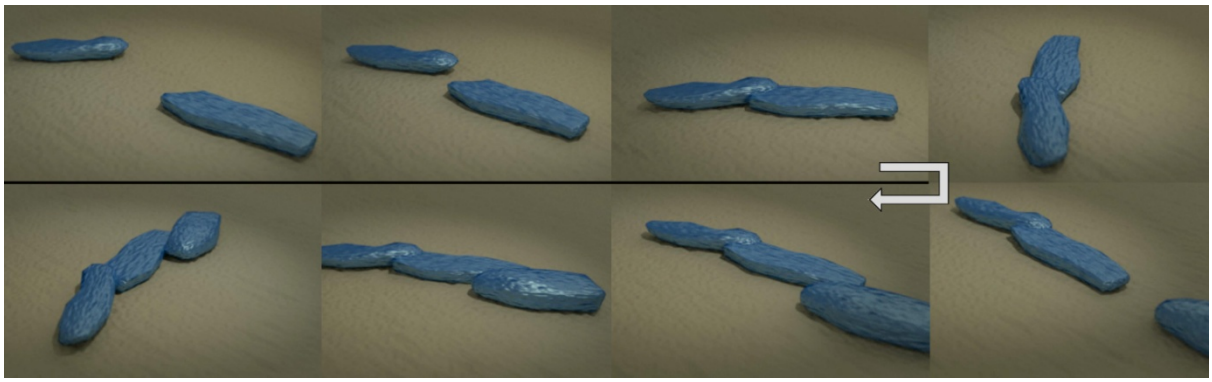

Figure 127 Simulated images of progressive particle movement for Sturcal L particles

Manipulation of individual Sturcal L particles on silicon shows no distinct recurring dynamic behavior. Particles display a range of movements including rolling and sliding and do not tend to favour a particular orientation. The characteristics of particle interaction however are notably different. Osculating particles, despite a small area of contact bond strongly to one another. Introducing particles leads to gradual agglomerations, which are considerably difficult to separate. Due to the strong shape of Sturcal L, loading of particles on both Silicon and Perspex led to little particle breakdown.

Recurrent agglomerative behavior was seen with both Sturcal L (Figure 128) and Sturcal F (in-keeping with findings throughout this thesis) however the size of resultant agglomerations with Sturcal L was notably larger with typical agglomerations around 15 microns in size. Agglomerations were spherical in shape with a high degree of directional

freedom making them easy to entrain and motivate. This was also observed in Chapter 9. The density of agglomerated particles was high with a subtly different arrangement in particles. Contained particles appear arranged pointing outwards rather than being a chaotic mass of particles. As a result little evidence of voids within the structures can be seen with loading and manipulation highlighting the strength of the agglomerations.

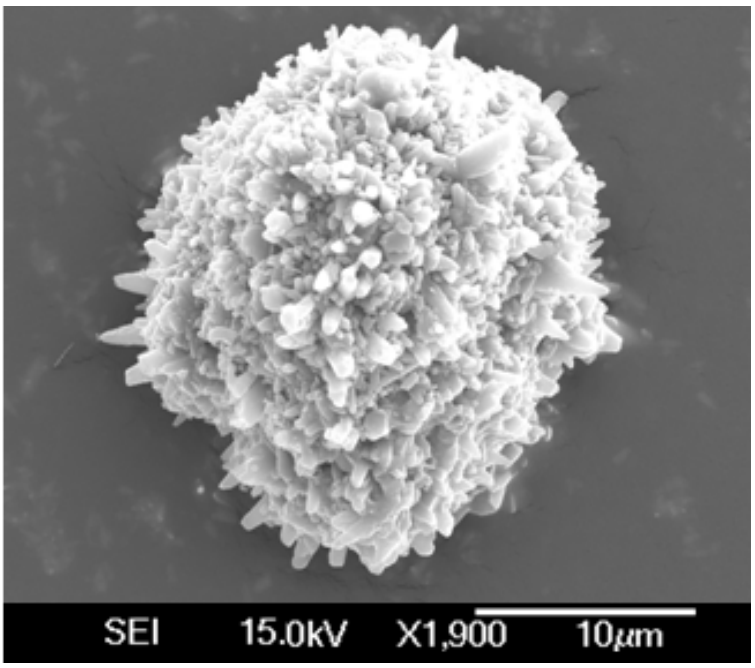

Figure 128 Scanning electron micrograph of typical Sturcal L agglomeration

Particles operating in isolation appear relatively sympathetic to the substrate surface. Particle agglomerations however being significantly larger and very difficult to breakdown pose more of a threat. Further to the size and strength of the agglomerations, the orientation of contained particles produce a series of projecting tips which appear to lead to notable substrate gouging.

Trials upon polished copper highlight just how damaging Sturcal L particles can be to a substrate surface. Figure 129 shows evidence of both small scale scratching from individual particles and more aggressive macroscopic galling and material removal from interaction with particle agglomerations. There also appear to be regions of clustered surface indentations from the projecting particle tips gouging the surface as the agglomerations roll. This fits neatly with suppositions made in Chapter 9, which observed the affinity of these particles to agglomerate and suggested that this was the main cause behind the particle ability to damage a substrate surface despite the particles relatively small individual size.

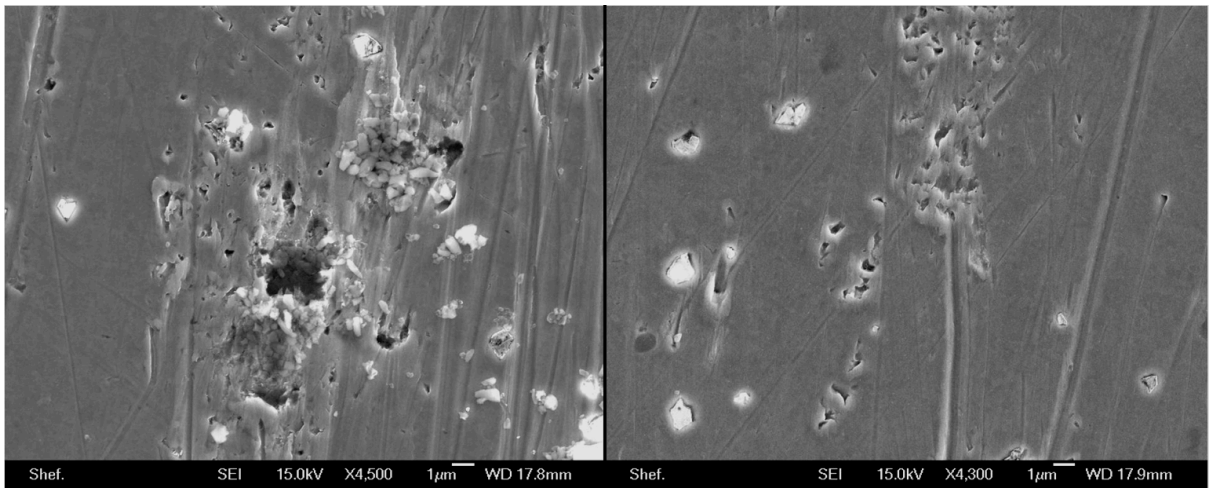

Figure 129 SEM images of surface markings from motivated Sturcal L particles on Copper (particle moving downwards)

Sturcal F

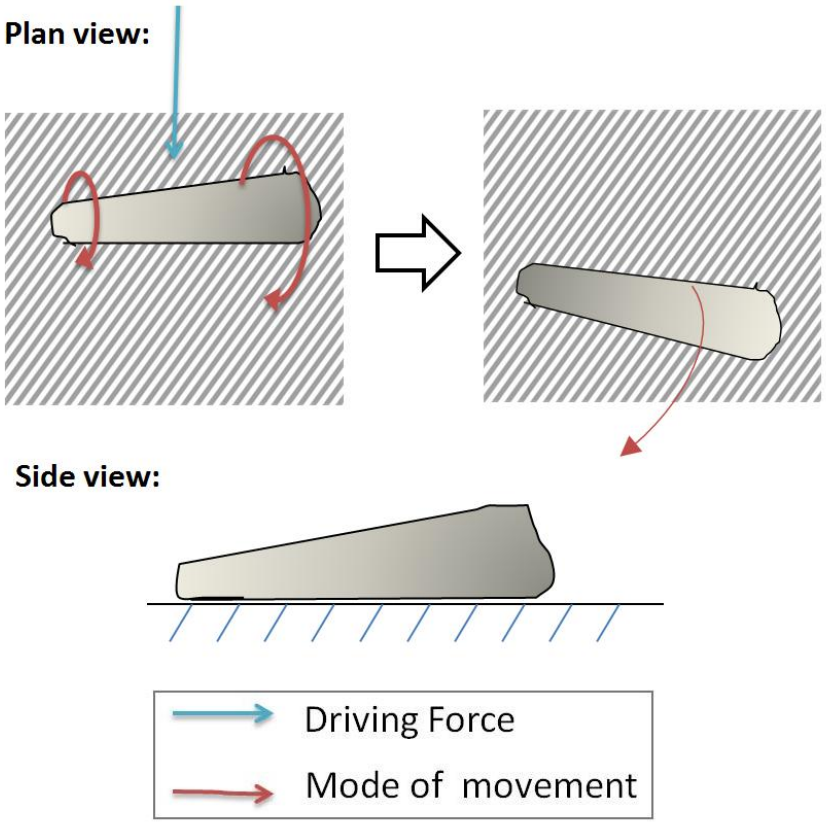

Figure 130 Schematic for the mechanistic movement of Sturcal F particles

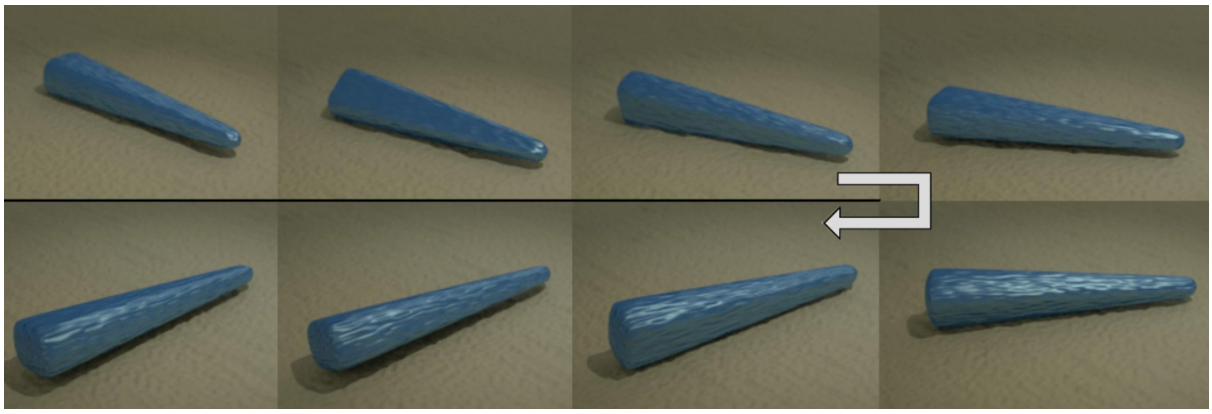

Figure 131 Simulated images of progressive particle movement for Sturcal F particles

Sturcal F particles, despite being smaller, can be most closely compared to Maruo Rods; upon closer inspection there are however subtle differences. The long sides of Sturcal F particles have a subtle taper which makes the overall geometry slightly wedge shaped. As a result of being much shorter the particles appear less fragile and more robust than Rods. This subtle dissimilarity in geometry leads to a significant change in the mechanism of movement. Trials upon silicon show that little sliding is seen with Sturcal F particles despite the presence of reasonably expansive flat sides. This contrasts with observations made with Rod particles, which invariably slide. The wedge shaped geometry of the particle dictates the characteristics of this roll. As the particle rotates the unevenness in end widths causes the particle to progress and turn in an arc across the substrate surface. Some sliding was observed however this was considerably more infrequent than rolling. The general form of Sturcal F particles is smooth with little presence of angular surface projections. Attempting to fracture particles upon a Perspex substrate showed Sturcal F to be much stronger than Rods, however particle breakdown was achievable. Particles loaded around the midsection did fracture in some cases with resultant faces of the fractured area relatively smooth with minimal sharp edges. Little evidence of particle fracture upon harder silicon was observed.

As with Sturcal L these particles extensively formed spherical agglomerations. The arrangement of particles within these agglomerations was less ordered than that seen with Sturcal L (particles largely projecting outwards) with contained particles forming a slightly more generic mass. Seemingly a result of the orientation of particles the Sturcal F agglomerations are more easily broken apart using manipulation probes than Sturcal L. The size of Sturcal F agglomerations is smaller than those seen with Sturcal L at around 7 microns in diameter.

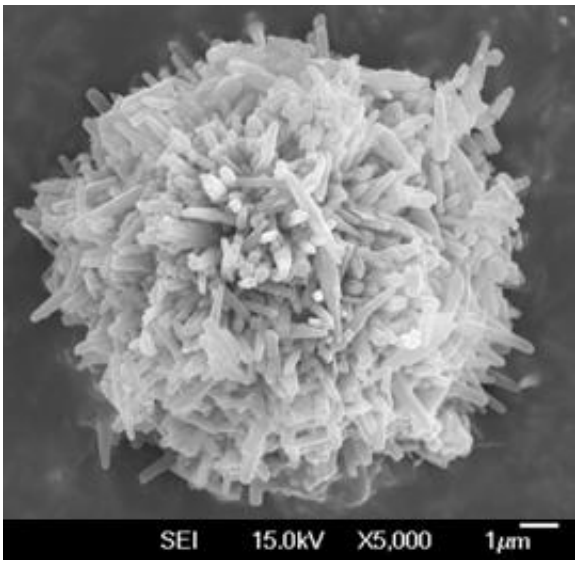

Figure 132 Scanning electron micrograph of typical Sturcal F agglomeration

Particle agglomerations (Figure 132) again show high directional freedom due to their spherical nature. Trials with polished copper showed a mixture of both individual scratches from isolated particles and intermittent pock marks most likely from rolling agglomerations. Immediately apparent from Figure 133 is the significant reduction in macroscopic surface damage compared to that seen with Sturcal L. This could be a result of both a reduction in the intractability of particle agglomerations and the arrangement of contained particles not leading to extensive projecting tips.

Close inspection of scratches caused by isolated particles reveals surface markings to be less smooth than that observed with other particles, which demonstrate sliding behavior (see Figure 133, right hand side). It would suggest that as particles are motivated they are less likely to remain in one fixed position. Instead, small discrete rotations of the particle as a result of it tapered geometry could be responsible for the jagged scratch walls.

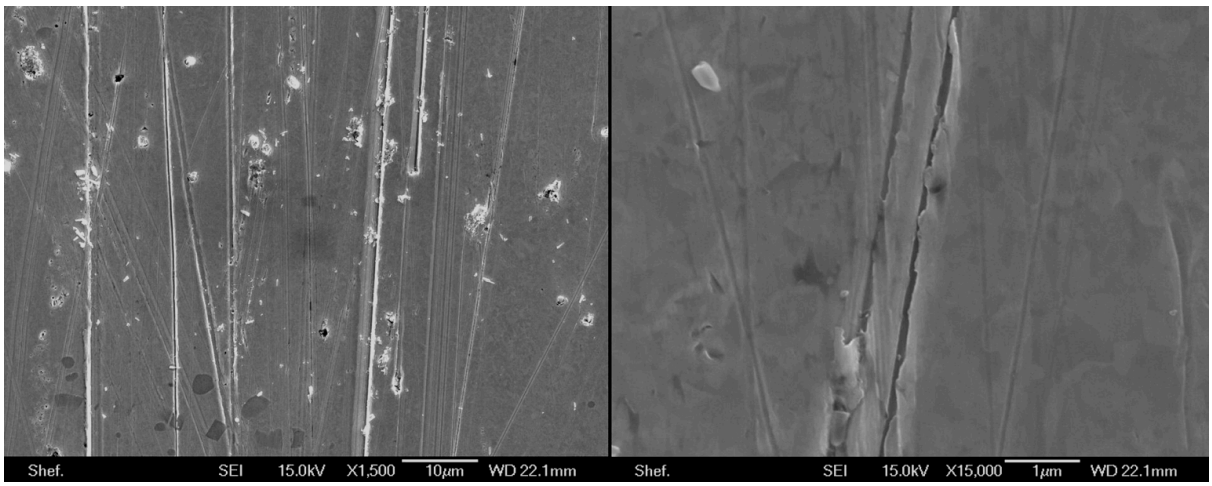

Figure 133 SEM images of surface markings from motivated Sturcal F particles on Copper (particle moving downwards)

Omya 5AV

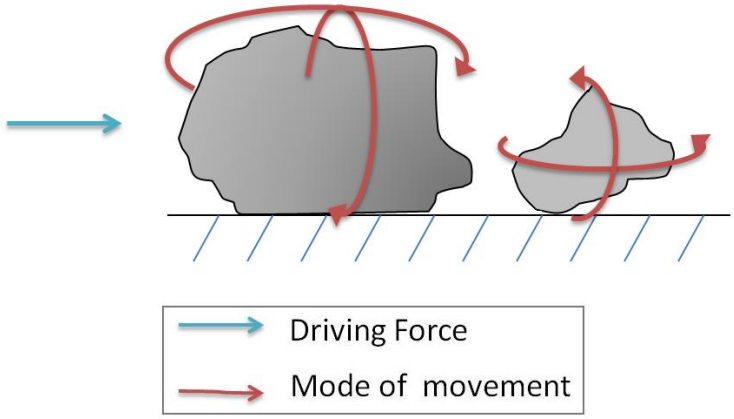

Figure 134 Schematic for the mechanistic movement of Omya 5AV particles

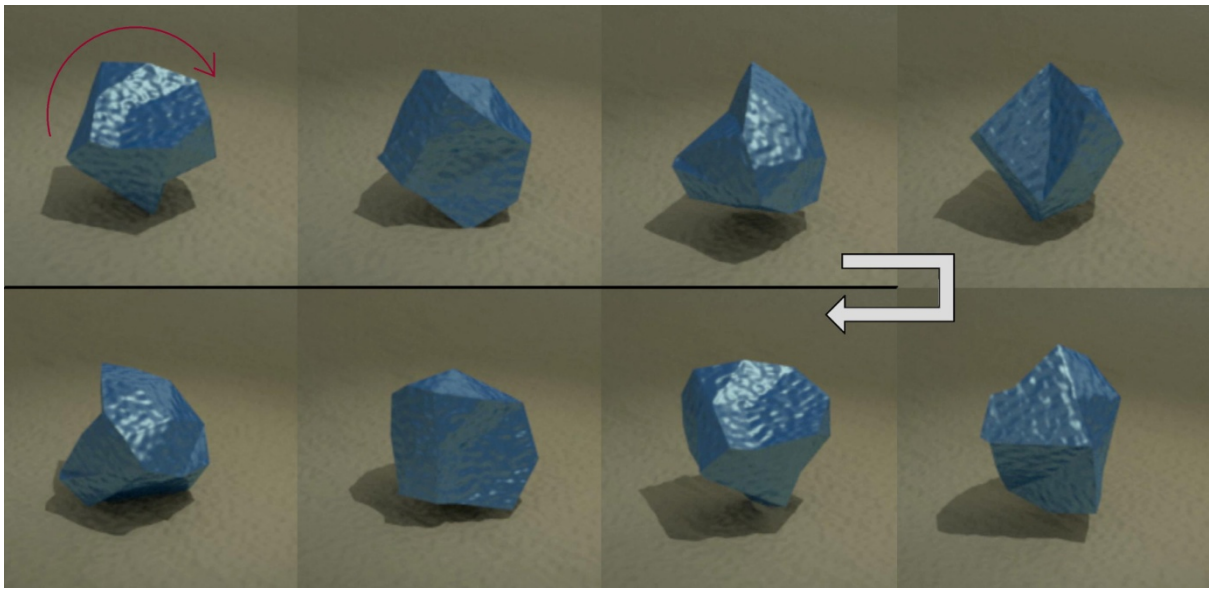

Figure 135 Simulated images of progressive particle movement for Omya 5AV particles

Particles show a significant increase in both the variance of particle size and shape compared to the vast majority of particles studied, particularly PCC's. A result of the method of manufacture (grinding), particles are miscellaneous in shape with unpredictable and varied directional freedom. Manipulation upon silicon shows particles are free to tumble across multiple axes showing few instances of sliding. Particularly evident on Perspex, the angular projections dig into the substrate leading to particles to begin rolling. As a result it is very difficult to encourage the particles to slide.

Omya 5AV appear to principally operate in isolation with little evidence of particle agglomeration. Particles demonstrate weak inter-particle adhesion and any instances of grouped particles are easily parted when manipulated.

Particle shape is are fairly robust and due to the rarity of flat parallel faces there is increased difficulty in the direct loading of particles; as a result breakdown of intact particles is infrequent. There is however a prevalence of cracks and partial fracture within some particles. Manipulating or loading these can lead to the division of the particle however it is difficult to know the degree to which the structure of a single particle has been compromised.

Figure 136 highlights the significant surface damage caused to the polished copper substrate as a result of interaction with Omya 5AV. Scratch frequency is the highest observed for all particles with the depth and directionality of scratches varied. Large-scale surface damage was also observed with instances of deep gouging and substrate material removal. Close inspection of surface scratches highlights the apparent turbulent nature of the entrained particle. Scratch walls are uneven suggesting the particle continues to roll.

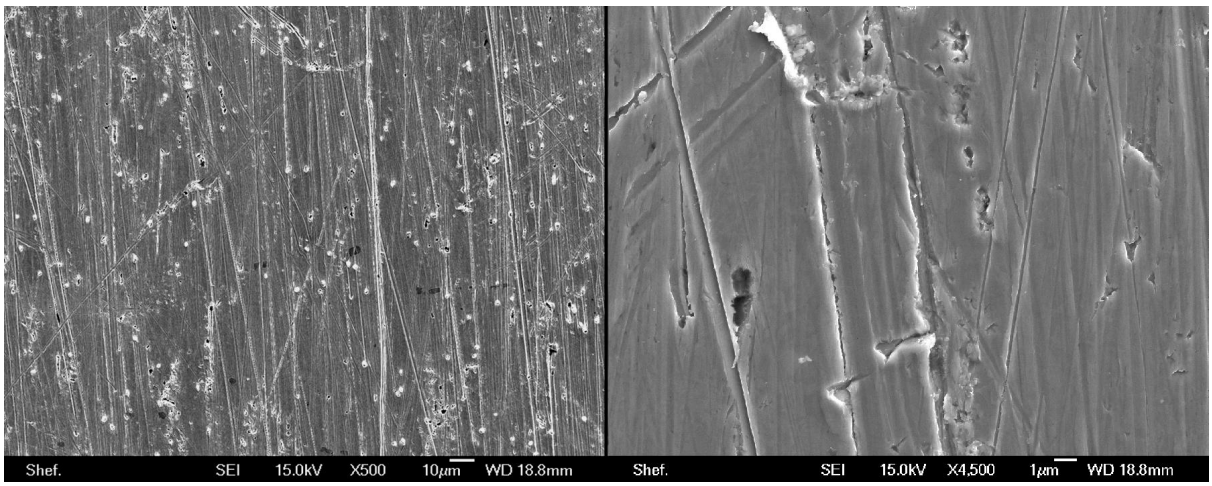

Figure 136 SEM images of surface markings from motivated Omya 5AV particles on Copper (particle moving downwards)

Maruo Rods

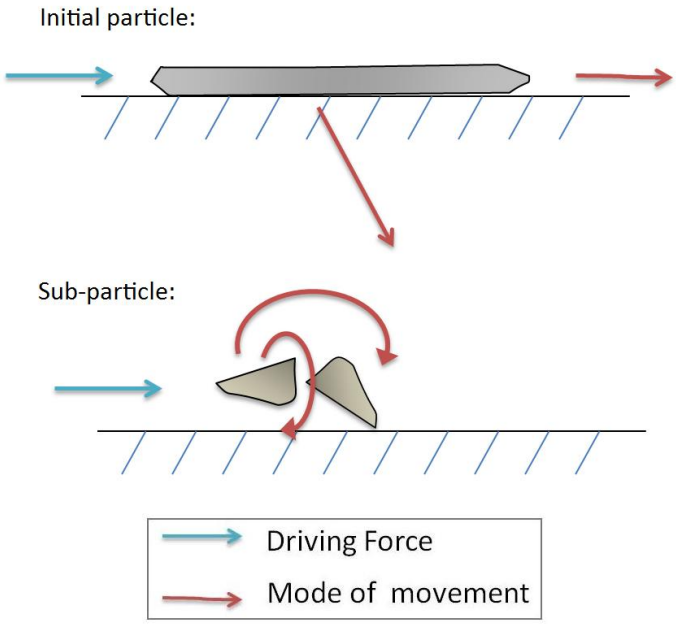

Figure 137 Schematic for the mechanistic movement of Rod particles

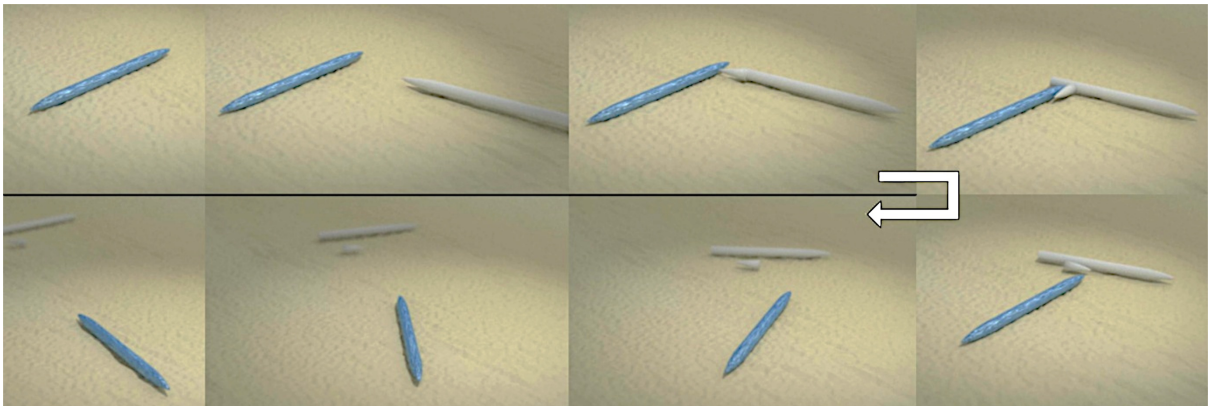

Figure 138 Simulated images of progressive particle movement for Maruo Rod particles

Motivation of Rod particles upon silicon shows that they are very difficult to encourage to roll; but rather move by sliding. The cross sectional shape of Rods contain upper and lower larger flat sides which span the length of the particle; these surfaces when in contact with the substrate are difficult to separate. Particles do not adhere to each other readily however the long slender shape of the particles does lead loosely interwoven lattices of particle agglomerations. When these agglomerations are motivated projecting particles are easily fractured. This ties in with observations and suppositions made in Chapter 10 for the occlusive behaviour of Rod particles within dentinal tubules.

A secondary sub particle can be observed with Rods of which the mode of movement differs from that of intact particles. The delicate tapering tips of Rods are susceptible to fracture and do so readily when particles interact or agglomerations are moved. Whereas intact particles only slide, the small particle tips operate in a similar fashion to Albafil particles and exhibit rolling behaviour. These 'sub-particles' led to the only damage observed with Rods, which was still relatively mild. Longer duration brush trials led to an increase in observable particles with tips missing (see Figure 139), increased presence of isolated particle tips and an increase in substrate damage.

Due to the extent in which Rod particles contact a flat surface, fracture of particles was particularly low on a silicon substrate. Any breakdown that was observed was erratic and unpredictable. With the introduction the softer Perspex substrate however particle fracture occurred relatively easily; this resultant fracture was recurrently neat with smooth opposing faces.

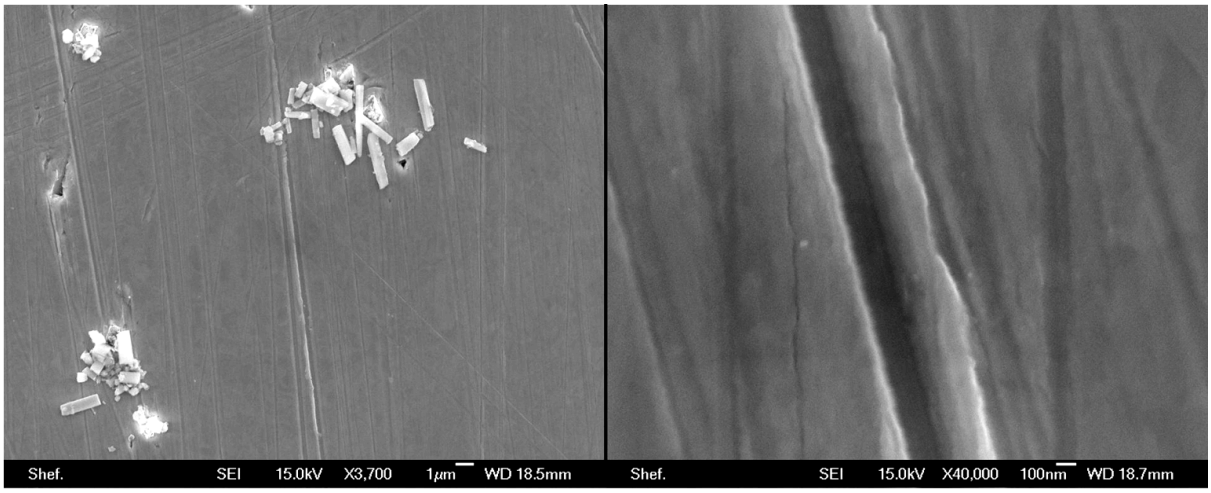

Figure 139 SEM images of surface markings from motivated Omya 5AV particles on Copper (particle moving downwards)

Figure 139 shows the sympathetic nature of Rod particles to the substrate surface. Scratch frequency is the lowest observed with all particles and the depth of observed scratches notably shallow. The regularity of featured scratches is high with the only surface gouging from isolated particle tips. Detailed analysis of scratches shows them to have neat walls with a smooth contoured profile. This would suggest that particles find a compliant position and remain as such throughout motivation.

Due to the extent in which Rod particles contact a flat surface, fracture of particles was particularly low on a silicon substrate. The softer Perspex surface however allows for more deflection and rotation about the ultimate point of fracture. The delicate nature of the particles geometry lends itself to accessible particle breakdown Figure 140 below compares

the typical fracture characteristics of Rod particles on both a harder silicon and softer Perspex substrates.

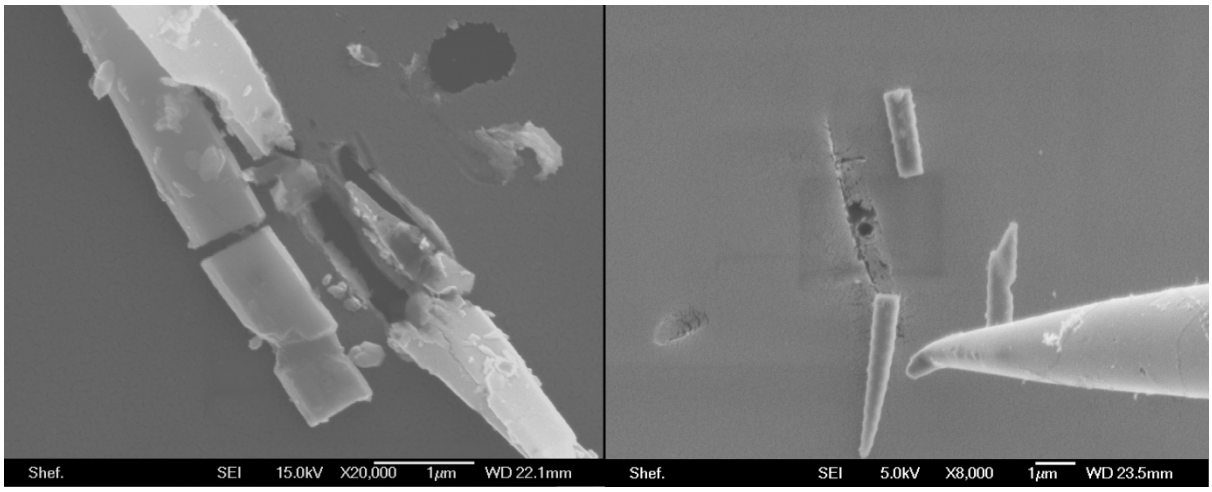

Figure 140 Comparison of fractured characteristics for loaded Rod particles upon Silicon (left) and Perspex (right)

8.4 Discussion

As a result of nano-manipulation testing across a variety of substrates it was determined that the $CaCO_3$ particles tested display dramatically different dynamic characteristics. Subtle variation in particle geometry can significantly influence both the mechanistic movement of that particle and the inter-particle and particle to substrate relationship. The two primary mechanisms observed were particle rolling and sliding. Analysis of the surface markings from the interaction between propagated particles and polished Copper reveals that particles that roll lead to significantly more substrate damage than that caused by particles prone to sliding. In some cases there is a duality of mechanistic particle behavior related to either the formation of smaller sub particles through fracture or the agglomerative nature of the particle.

Free body analysis of a typical particle-substrate interaction would suggest that multifaceted polyhedral particles with increased edges are likely to encounter the substrate in a scenario in which the majority of the contact is hinged around the meeting of two or more particle faces. This is an unstable system whereupon any further progression of the particle will create torque, which in turn will encourage additional rotation in this direction. The size of the particle perpendicular to the substrate surface will also affect the magnitude of this torque. A particle, which is able to be loaded at a greater distance from the substrate, will incur greater torque and thus is more likely to initiate a roll. As observed with the direct manipulation of particles, in order for a sliding mechanism to be adopted sufficient contact must be made between a particle face and the substrate surface. The maintenance of this pairing and thus the likelihood of continued sliding is closely related to the surface area of the particle face.

According to Evstigneev [at el] the maintenance of rolling motion is sustained through one pseudo-atom contacting the substrate acting as a pivot point. This process is only feasible if the substrate corrugation is high enough to overcome its adhesion [45, 46]. Further to this, there are predictable geometric criterions which can describe a particles affinity to roll or slide. When a particle engages the substrate in a fashion that may initiate a roll, leading to small scale rotation in the clockwise direction, this instantaneously creates a torque from the probe tip in the same direction perpendicular to the tip. Figure 141 shows simplified geometrical illustrations of the particles analysed within this study. The dashed line adjoins the point of contact between the nano-probe and the potential pivot point in contact with the substrate. The red arrows represent the normal force exerted by the probe tip upon the particle. If this force (represented by the red arrow) is located above the contact-pivot dashed line at the point where the tip meets the particle there is a negative torque and the particle is more prone to rolling. If the propagating force is located equal to or below this dashed line then the particle favours sliding [40]. Schematics were created according to observations made throughout extensive manipulation trials. Particles are depicted according to observed typical contact orientations.

SEM analysis of the probe tips used within manipulation trials revealed the portion of the tip terminus with potential to contact particles followed a taper of 60˚. The orientation of the probe was primarily administered normal to the substrate.

Figure 141 summarises the typical loading conditions according to each particle. In each case the generic profile of each particle is shown in contact with the probe tip, and the likelihood of the particle entering a rolling or sliding scenario assessed. As can be seen with Albafil, when the particle contacts the substrate through one of its smaller faces the normal to the probe tip lies above the ‘probe contact’ – ‘pivot point’ adjoining line which results in a negative torque and thus the particle is more likely to roll. When the particle locates a larger face and lies closer to the substrate surface the order of these lines is reversed resulting in a positive torque and particle sliding. This is what was observed in practice with Albafil usually rolling only across smaller facets and then sliding when a sufficiently larger particle face locates the substrate surface.

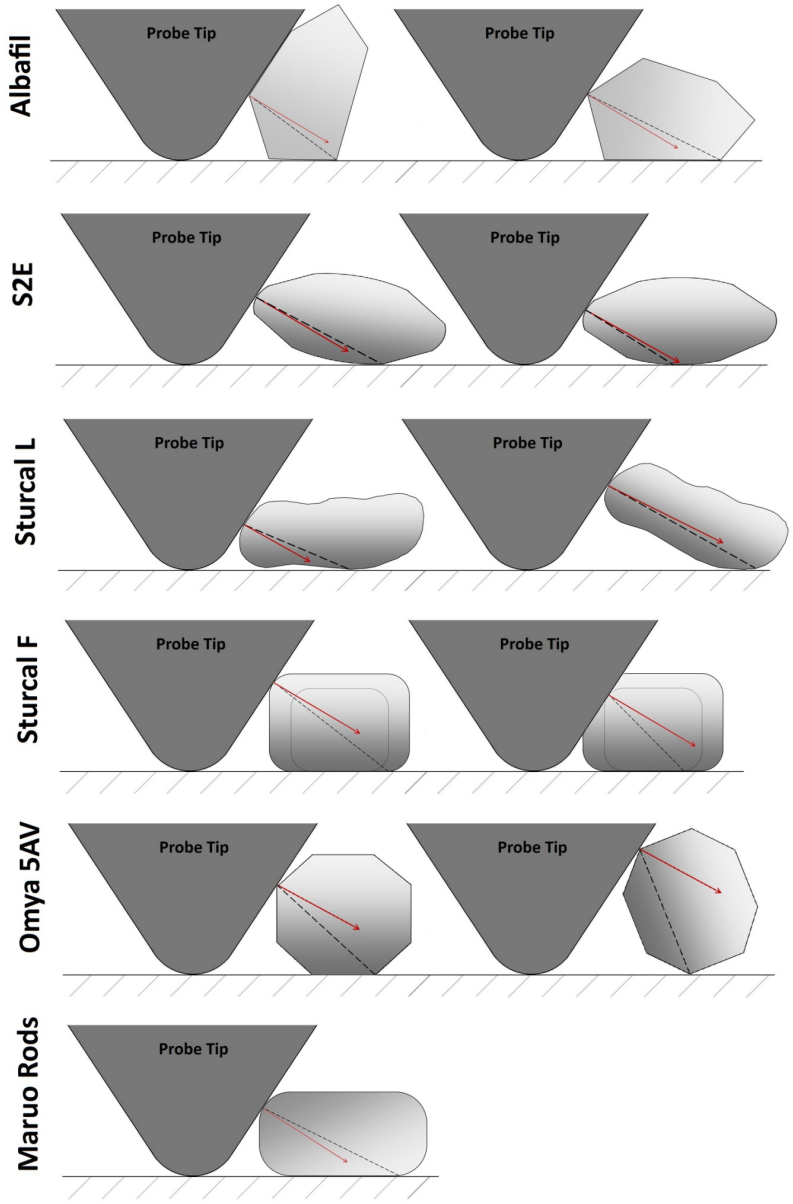

Figure 141 Free body schematics of particle-probe tip interaction

Figure 141 shows that according to typical particle geometry observed with Omya there is no scenario in which positive torque can be achieved, and therefore the particle is unlikely to slide. Close inspection of surface scratches shows evidence for particles rolling within contact when entrained. Comparing the results obtained with Omya with that of Vicality Albafil, another multifaceted particle, we can see a notable reduction in both scratch frequency and general surface damage with Albafil. This is most likely a result of two factors. Firstly Albafil being manufactured via a precipitation process, it is subject to greater control of particle attributes than Omya, which is ground. As a result the polyhedral faces of Albafil particles, despite the variation in number of faces and magnitude of face, are consistently flat. We therefore see rolling behavior as the particles progresses across the shorter faces (apparent in surface markings from copper substrate trials) before a larger flat

is ultimately located and the particle slides. Secondly the smaller size of the particle suggests that it is unlikely to experience the same moments when motivated as Omya 5AV particles, which project further from the particle-substrate interface.

The particles with the largest surface area were Maruo Rods. These particles were both consistent in shape and size whilst also demonstrating the largest flat faces observed. Analysis of these particles within Silicon manipulation trials highlighted the particles reluctance to roll, instead remaining in contact with the substrate through one face with yaw remaining unchanged and the particle sliding. Free body evaluation in Figure 141 evidences this with only one particle orientation analysed due to the particles reluctance to initiate separation with the substrate surface. This led to the lowest scratch presence and surface damage observed with all particles. The behavior was however limited to larger gross particles, which over time were prone to losing their tips through interaction with additional particles or via the motivation of cumulative particle masses with tips projecting. Yielded resultant sub-particles (tips), due to their stunted geometry tended only to roll. The surface markings derived through the entrainment of the Rod sub particles were minor however when compared to other particles which operate in similar fashion. It is possible that due to the small size of the resultant particle, that it is difficult to entrain and as a result escapes the contact area with limited interaction with the motivating body.

It is likely that the use of ground particles due to their varied structure and multifaceted geometry will lead to increased damage and material removal when used upon dentine for prolonged periods. Precipitated Calcium Carbonates on the other hand offer increased control over particle shape through modification of temperature and pressure during the reaction processes. In general PCC's possess smoother and flatter geometries, which increase the likelihood of particles adopting sliding mechanism as a result of good pairing of the substrate with a single large particle face. In theory this should result in PCC's posing less of a threat to dentine and other delicate surfaces when operating isolation. As seen in trials conducted within these experiments however, the most significant surface damage was the result of PCC operating as strong particle agglomerations. In order to minimise the likelihood of this agglomerative behavior the introduction of a surfactant may be beneficial, however further research would be required to validate this.

A summary of nano-manipulation observations is shown in Table 6:

Particle	Shape	Image	Size (µm)	Predominant movement	Likelihood of fracture	Affinity to agglomerate	Dentinal wear (x500)	Wear depth (µm)	Additional Observations
Albafil			3.6	Rolling then sliding	Low	Low		230	High speed encourages rolling
Rods			6 x 0.5	Slide	High (tips)	Medium		275	Fractured tips roll
Sturcal F		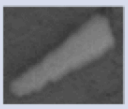	1.3	Roll about axis	Low	High	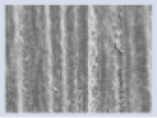	300	Very strong agglomerations
S2E			3.2	Slide	Medium	Medium	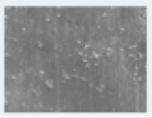	361	Rotate and slide
Sturcal L			7	Roll about axis	Low	High	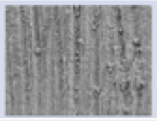	804	Very strong agglomerations
Omya			7	Roll	Low	Low	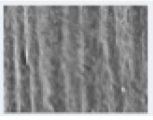	819	High directional freedom

Table 6 Summary of nan-manipulation observations

8.5 Conclusions

Within this study nano-manipulation technology was utitlised in order to analyse in real time the dynamic behavior of six Calcium Carbonate particles within a scanning electron microscope. Manipulation trials were carried out upon three substrates: Silicon, Perspex and Copper with the latter used to discern surface-marking characteristics derived through typical brushing conditions.

Subtle variation in particle geometry had a significant effect upon the dynamic mechanism adopted. Maruo Rod particles are visually similar in appearance to Sturcal F particles however subtle differences in the uniformity of the particle alters the mode of movement from a sympathetic sliding to more aggressive rolling mechanism. Similarly Omya 5AV particles and Albafil are both diverse multifaceted particles however the recurrent presence of one or more larger flat face with Albafil encourages the particle to cease rolling and begin sliding. As a result there are considerable differences in substrate damage.

There was a clear distinction between the likelihood of damage to the substrate surface caused by rolling particles and sliding particles. Rolling led to higher scratch frequency and depth than that observed with sliding particles.

The primary focus of this investigation has been on the dynamic properties of individual particles however the most significant substrate damage was introduced through particle agglomerations. Sturcal L and Sturcal F showed the greatest affinity to agglomerate with Sturcal L demonstrating significant inter-particle attraction and agglomerate resilience. Although the cause of this tenacious particle bonding is not apparent it is responsible for a significant increase in surface damage with Sturcal L. The particle most sympathetic to the substrate surface causing the least amount of damage within trials on polished copper was Maruo Rods.

As a result of the comparison of Precipitated Calcium Carbonates with Ground Calcium Carbonates it can be said that the typical geometry of GCC particles are varied and multifaceted. PCC's on the other hand offer more constrained geometry with a reduction in sharp edges. As a result PCC's are statistically less likely to roll than slide and therefore pose less of a threat to a substrate surface than GCC's.

9 PARTICLE AGGLOMERATION

SEM analysis of wear and scratching resulting from experiments in this thesis has suggested that some material removal is caused by particle agglomerations. This is known since the resultant micro-wear scars are larger than the individual particle size. The aim of this chapter is to determine the agglomerative behaviour of the different particles in an effort to better understand their dynamic properties and their affinity to agglomerate or remain in isolation when employed or motivated. It is important to understand this behaviour as the aggressive or sympathetic nature of the abrasive can easily be dictated by the affinity of the particle to agglomerate and the resultant shape of that agglomeration. Trials were conducted on six key particles to determine the extent to which agglomeration occurs, and the characteristics of the resultant agglomerations.

9.1 Introduction

A number of particles have been selected for this experimental analysis. The selection was made based on the particles that were of particular interest to the sponsor company. These were taken forward for a variety of reasons including low cost of manufacture, ease and speed of manufacture and precipitated calcium carbonates of novel geometry. The particles studied within the scope of this chapter are:

- Omya 5AV
- Vicality Albafil
- Maruo Rods
- S2E PCC
- Sturcal F
- Sturcal L

There are a number of proposed factors which can affect a particles affinity to agglomerate. Particle size and geometry was highlighted as an key factor in agglomerative behavior by Maskara and Smith [47] who studied the agglomerative strength of Silica particles using ultrasound. They found that the likelihood and resultant strength of agglomerations depends on the solubility (pH), the primary particle size and the solvent surface tension. It is of interest within this study to see how a subtle variation in particles geometry can lead to a change in the agglomerative behavior of that particle, and the shape and tenacity of that agglomeration. This may contribute an explanation as the particularly aggressive behavior of some particles compared to other that are relatively similar in size or shape but with subtle differences.

9.2 Analysis of agglomeration integrity by particle division trials

9.2.1 Experimental procedure

In order to observe the particle breakdown characteristics (if applicable) under repeat tensile loading the following experimental procedure was adopted. By studying multiple divisions, both tenacity and resilience of the agglomerations may be observed. In addition, this methodology aims to demonstrate that the mechanism of particle agglomeration varies between different particles and that some particles have a greater affinity to agglomerate.
Dry particles were first scattered onto clear adhesive tape. A secondary piece of adhesive tape was used to draw apart and separate the particles as shown in Figure 142. This process was repeated for 1, 4 and 6 divisions.

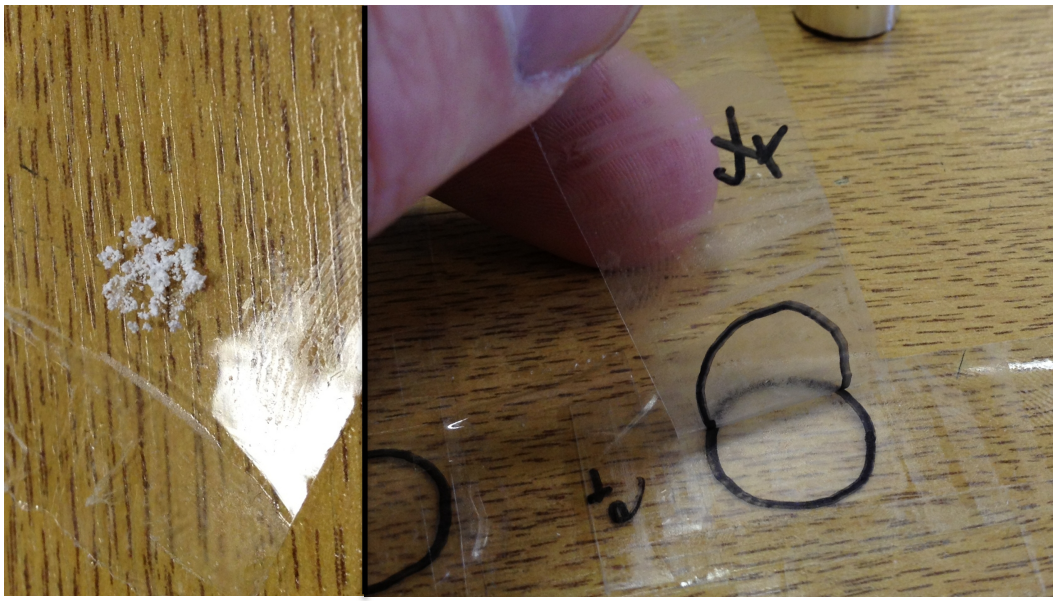

Figure 142 Division of particles for agglomeration study

Particles were then transferred to agar carbon tabs to be studied under scanning electron microscope (Figure 143).

Figure 143 Affixation of particles to carbon tabs for SEM analysis

Particles were distributed as evenly as possible to the tape and excess particles were removed using a blast of compressed gas. This process was repeated until the opacity of the tape was total i.e. there was a full and even coating of particles within the necessary application area. At no point were the tape or particles subject to contact by human hands or introduced to oils or moisture to ensure no exposure to contaminants that could affect the test results.

The particles were loaded by hand by smoothing the two tape counterparts together to remove the potential for trapped air and ensure complete contact for the area of interest. Care was taken to apply only the minimum force needed to achieve this so as to not risk

crushing the particles. Similarly, the rate and force by which the tape was drawn apart was considered and replicated as closely as possible so as to maintain inter-trial consistency.

9.2.2 Results and discussion

Table 7 compares SEM micrographs of the resultant particle formations after 1, 4 and 6 divisions.

	1 Division	4 Divisions	6 Divisions
Omya 5AV	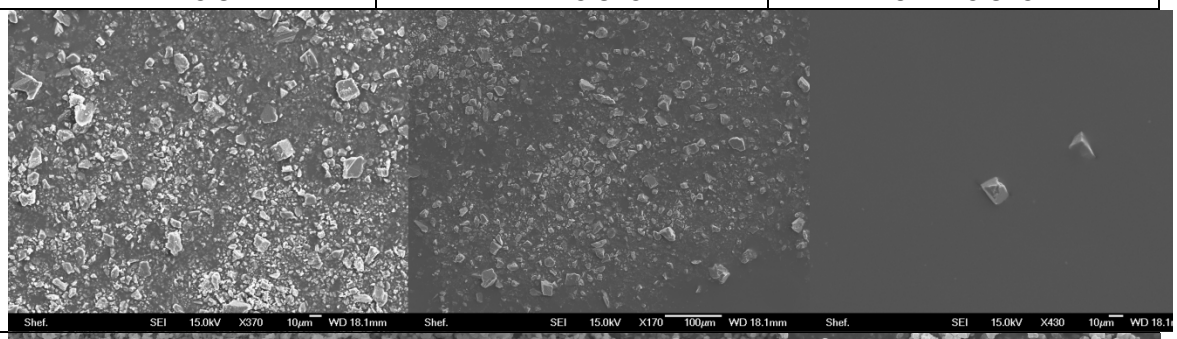		
Vicality Albafil	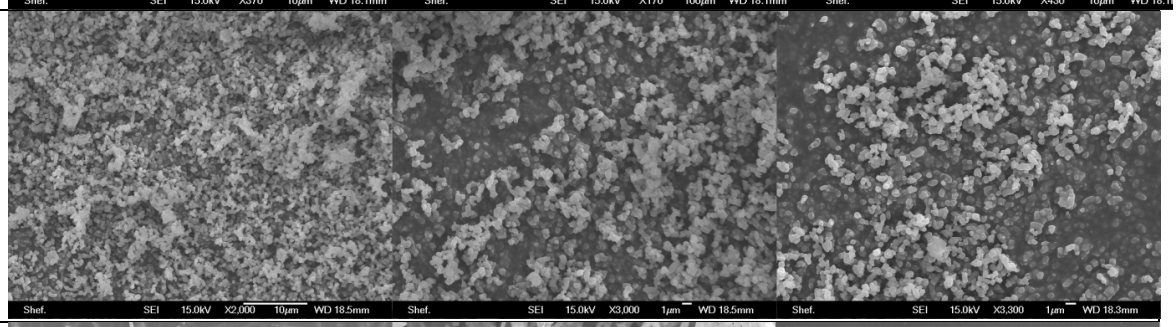		
Maruo Rods	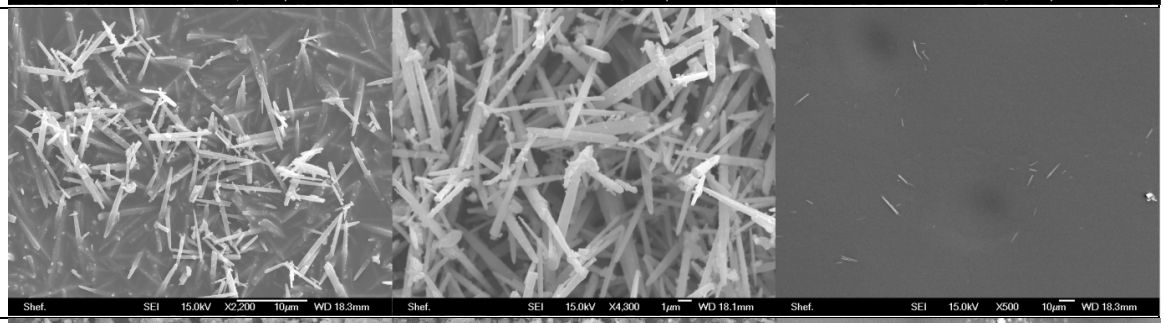		
S2E PCC	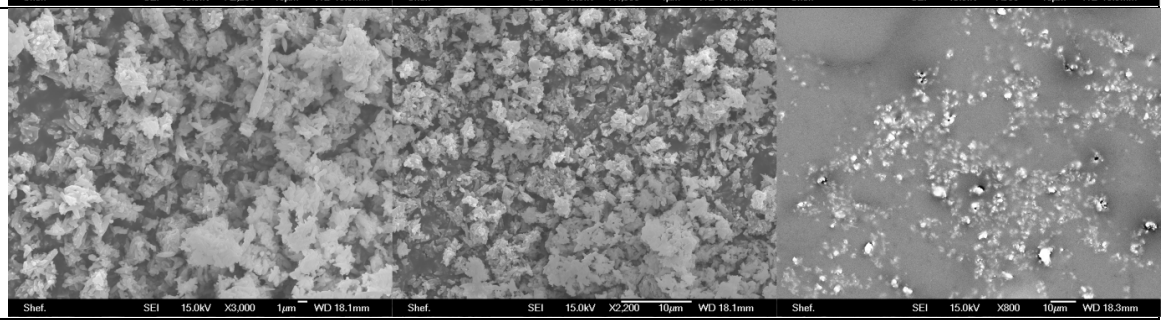		

Sturcal F	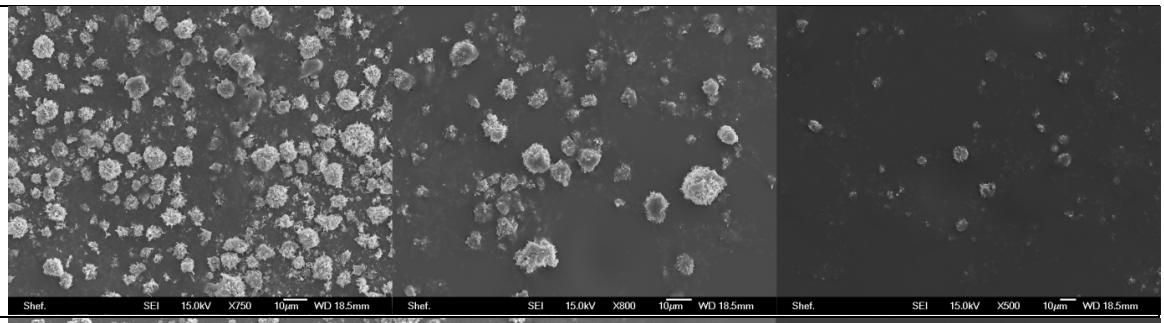
Sturcal L	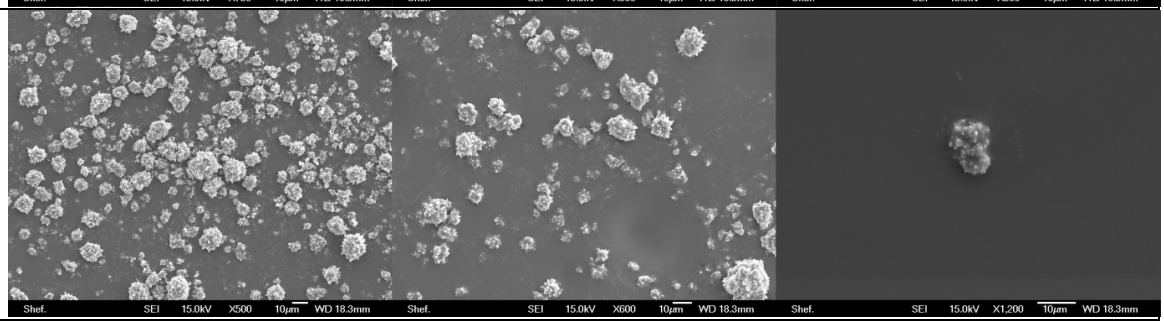

Table 7 SEM micrographs of remnant particle formations for 1, 4 and 6 divisions

Table 8 compares typical profile plots for surface scratching upon perspex for the 6 particles. These plots were acquired using atomic force microscopy as seen beforehand in this thesis.

	Typical surface damage profile plot
Omya 5AV	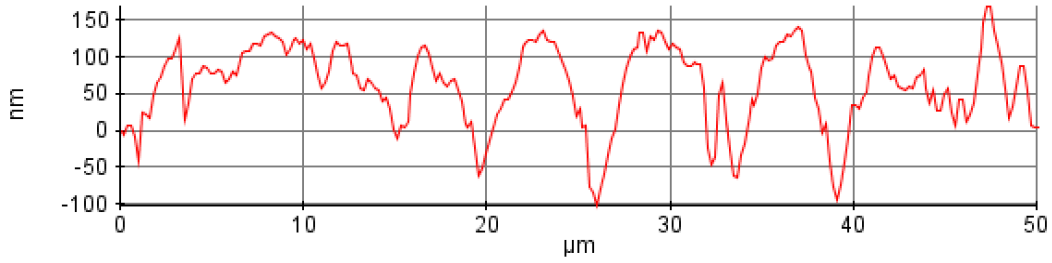
Vicality Albafil	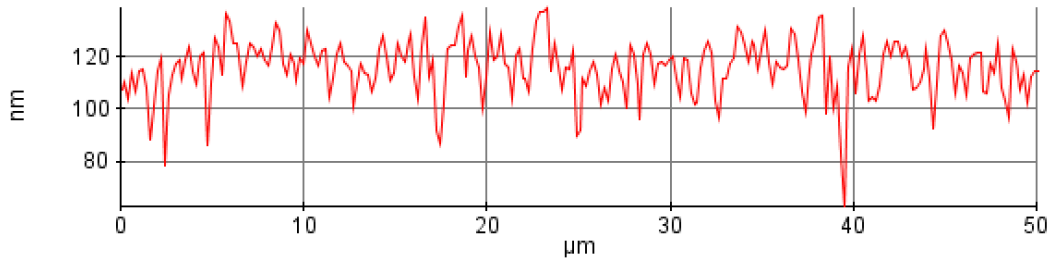
Maruo Rods	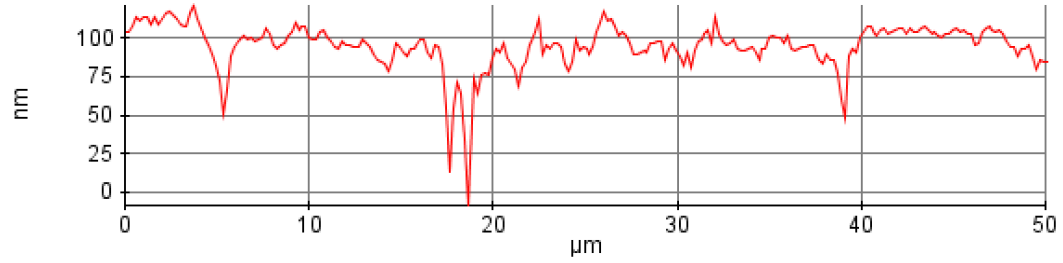

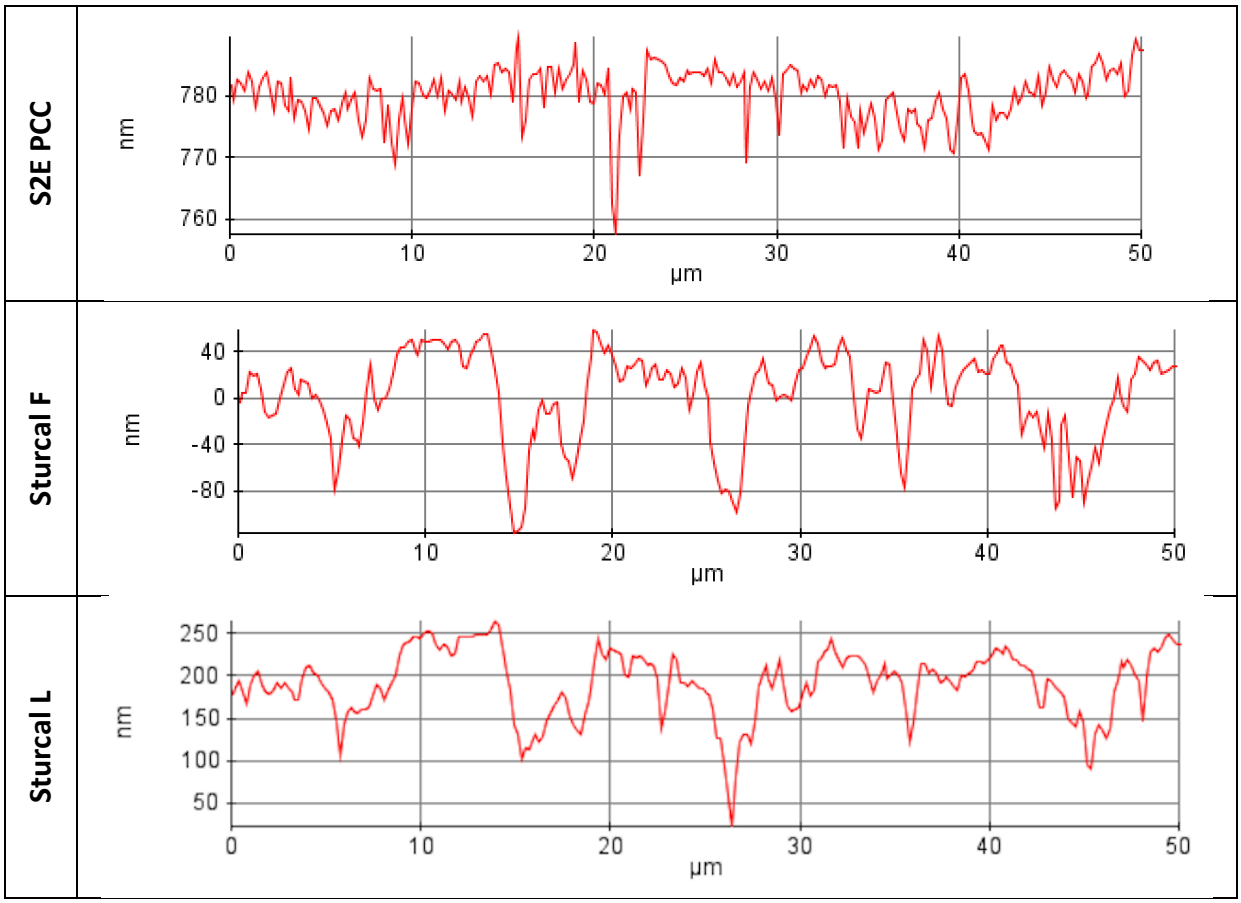

Table 8 surface profile plots for the 6 particles analysed upon perspex

For Omya 5AV we can see no obvious agglomerations between divisions, with the particles all remaining independent of one another. Particle presence decreases significantly during each progressive division. The lack of agglomeration of Omya 5AV particles was somewhat predictable based upon the wear scars observed during previous scratch testing. Figure 144 shows typical wear scars under SEM, generated by Omya 5AV particles with the magnitude of typical scratches from reciprocation trials shown in Table 8. Since scratch sizes are in general approximately equal to individual particles (around 7 microns), it can be concluded that the particles act as individuals rather than an agglomeration. Where scratch size is larger than particle size, it is likely that the mechanism is particle tracking within grooves formed by the trapping of particles and loose material.

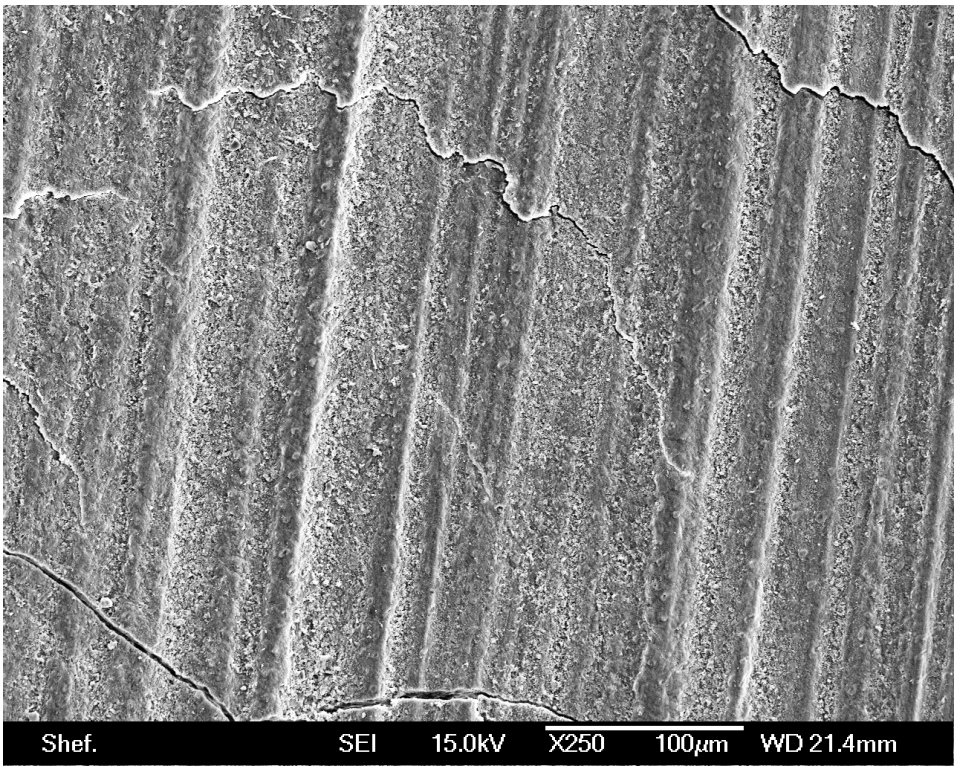

Figure 144 SEM micrograph of typical wear scars created by Omya 5AV particles upon human dentine

The behaviour of Vicality Albafil particles is similar to the Omya 5AV in that no obvious agglomeration is observable and that particles remain independent of each other. The particle presence decreases through each successive division (although there has generally been a lower rate of material removal from the process). The intractability of Vicality Albafil and its reluctance to be parted with the substrate surface is likely to be a result of its geometry. Comparing what has been observed previously with Omya 5AV in these trials and comparing the geometry of the particles derived from SEM analysis it can be seen that Omya 5AV is notably rounder than Vicality Albafil. Vicality Albafil is 3 dimensional polygonal in shape and as result has an increased number of flatter sides. Despite being smaller, It could be said that the Vicality Albafil particles are more likely to have an increased percentage of available surface area in contact with the adhesive tape than the Omya 5AV. This trend is again expected when considering the wear scars generated by this particle (Figure 145).

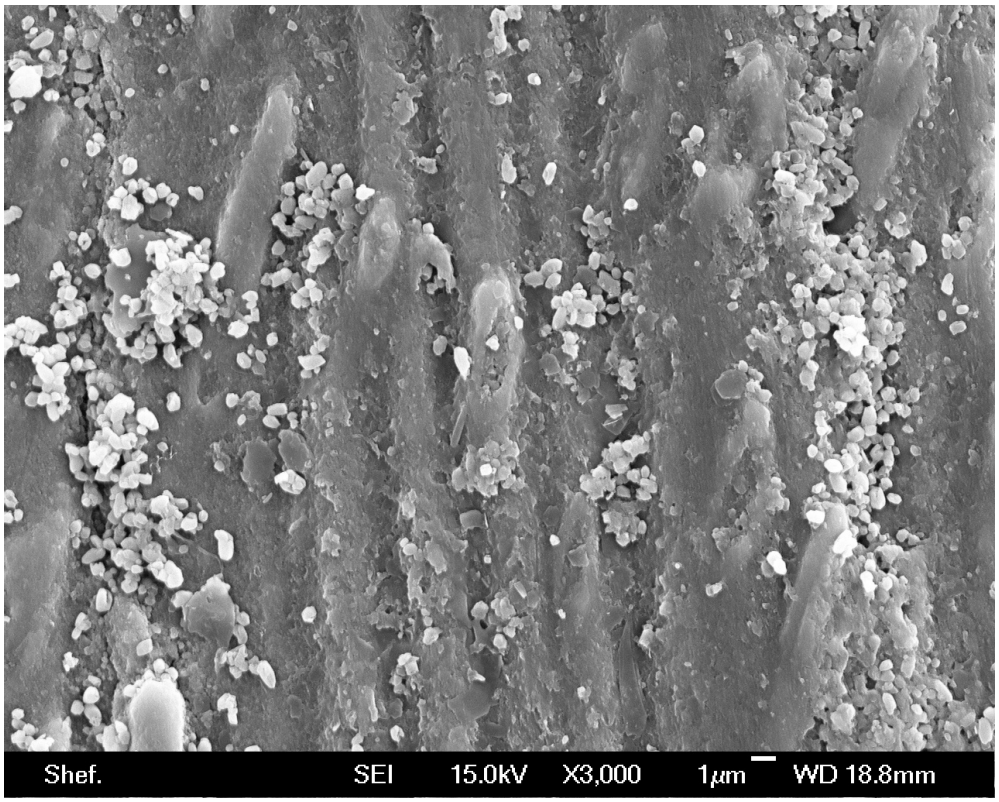

Figure 145 Typical wear scars generated by Vicality Albafil particles upon human dentine

The particle remnants seen above also indicate that the Vicality Albafil particles do not have a affinity to agglomerate. Larger scratch sizes than individual particle sizes, as with Omya 5AV particles are therefore due to particle tracking.

It can be seen from Table 8 that despite an increase in scratch frequency, the scratches reflect the magnitude of the individual particles (3-4 microns) supporting the notion that Vicality Albafil do tend to operate in isolation.

Initial scattering of Maruo Rod particles demonstrates they tend to become loosely interwoven due to their shape. Although this interaction is stronger than those observed with the rounder particles such as Vicality Albafil and Omya 5AV; i.e. many particles must be disturbed during any given particle motion, they are found to pull apart relatively easily by this method of division. This indicates that the particles are not bound together by anything other than geometric interaction.

Figure 146 shows typical scratches generated by Maruo Rods particles. The individual particles seen as remnants from the scratch test indicate no particle agglomeration. Similarly, the scratch widths are approximately equal to the particle widths or lengths.

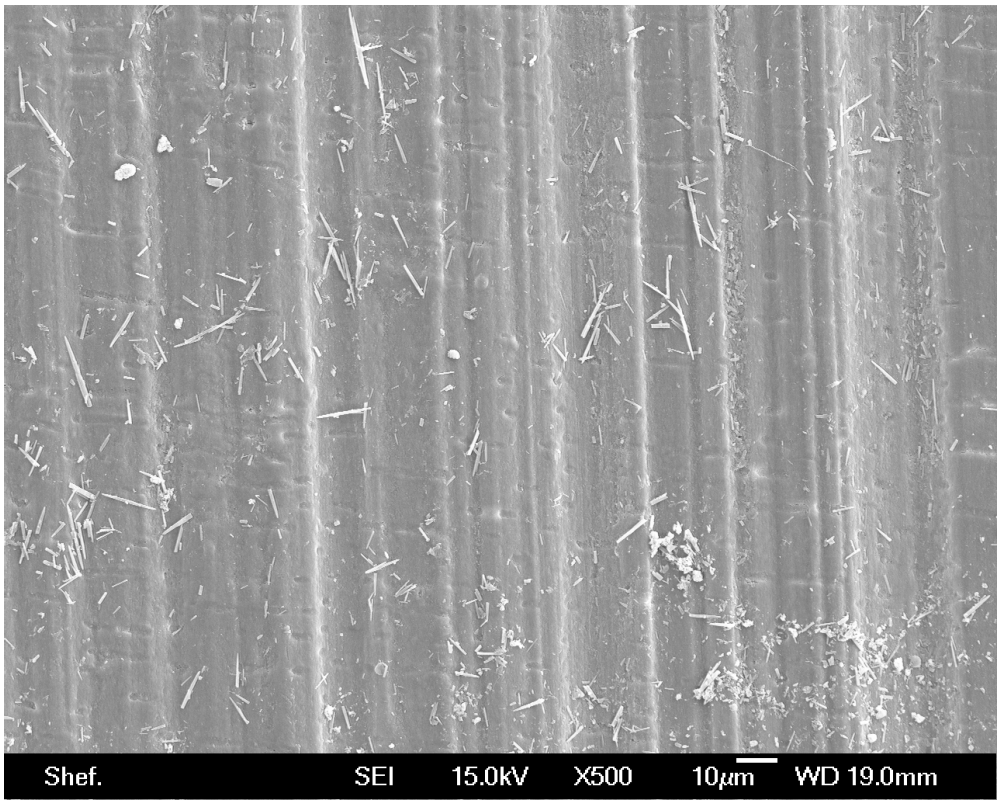

Figure 146 Typical scratch generation by Maruo Rods upon human denitne

The SEM images show the Maruo Rods to be more delicate to the substrate, with reduced evidence of particle tracking. When compared to rounder particles that apparently operate in isolation (Omya 5AV, Vicality Albafil) the resultant damage by Maruo Rods is less significant. There is perhaps a different mechanistic movement at play here, these behaviours are studied in more detail in Chapter 8.

We can see from Table 8 that scratches are lower in frequency compared to many particles (particularly Vicality Albafil), and suggest that the particles show very weak agglomerative behaviour. This is based upon the magnitude of the individual scratches tallying with the particle widths. There is some subtle surface roughening which may be from the motivation of loose agglomerations with projecting tips, however this material removal is not significant and would suggest the agglomerations are weak and short lived.

Some localised agglomeration can be seen with S2E PCC, however it is neither consistent in shape nor size. The agglomerations have no defined structure or form although generally the size decreases between progressive divisions suggesting that particles are easily removed from these formations. This result also fits in with the findings of the wear trials.

Figure 147 shows typical scratches generated by S2E PCC particles. The in-situ particles post-test indicate some degree of agglomeration whilst the majority of the work is done by

individual particles (since in general scratch size approximately equals individual particle size).

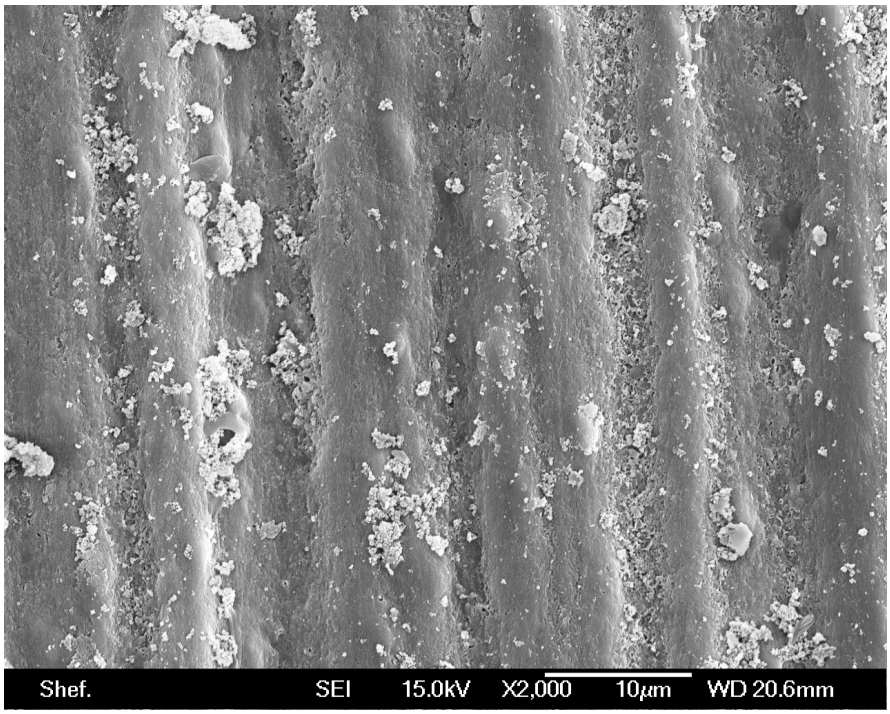

Figure 147 Typical wear scars generated by S2E PCC particles upon human dentine

Small-scale analysis of the wear characteristics in Table 8 shows that the majority of the scratches are seemingly introduced by individual particles (circa 4 microns). Macroscopic analysis of the wear regions however did show some larger undulations, which may be the result of agglomerative behaviour. These agglomerations if formed appear weak and with little order however.

For Sturcal F, the images give conclusive evidence of strong agglomerations. It is thought that this behaviour is due to its spherical arrangement leading to relatively large agglomerations with mode size around 7µm. It was also found that the agglomerations do not pull apart easily but get smaller throughout further divisions (losing exterior particles whilst maintaining form).

Figure 148 shows the affinity of the particles to agglomerate with few particles remaining in isolation upon the substrate surface after 1 division. Sturcal F is a notably small particle at a little over a micron in size, analysis of profile plots from scratch testing upon Perspex (Table 8) however show that defined individual scratches are being introduced of a larger magnitude. The width of these scratches is fairly comparable with the modal sizes of the agglomerations observed (7-15 microns).

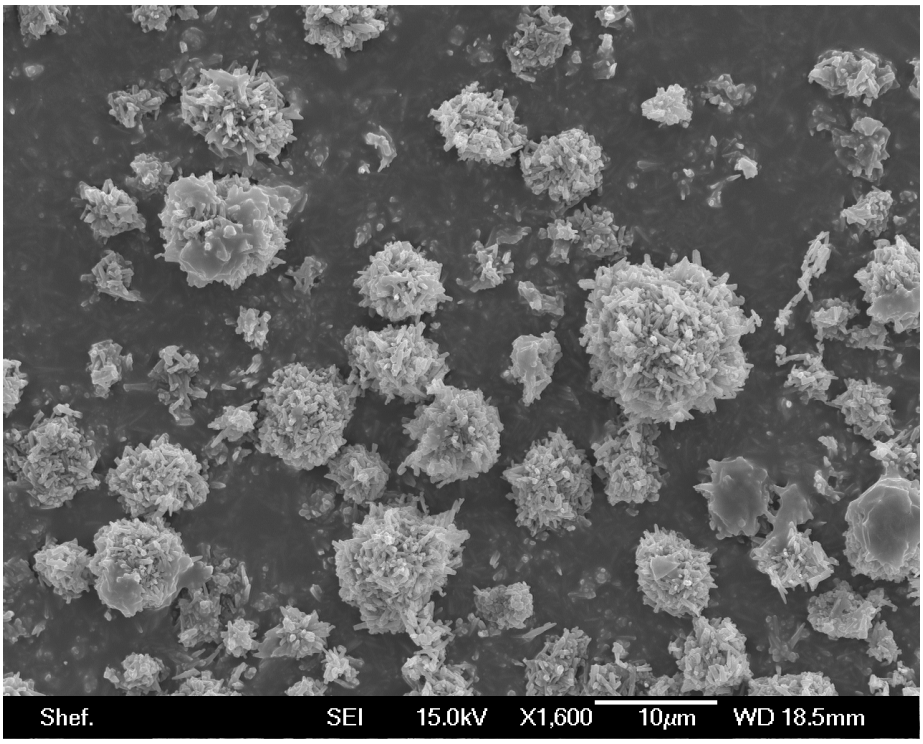

Figure 148 Agglomerations of Sturcal F particles after 1 division

The nature of the particle agglomeration is suggestive of the mechanism of Sturcal F's aggressive abrasive behaviour. Particles are found to project outwards from the main body of the agglomeration, which has the effect of rendering its shape relatively angular. It is thought that this contributes to the aggressive nature of these particles. Damage to dentine from using this particle was significant and extensive (Figure 149).

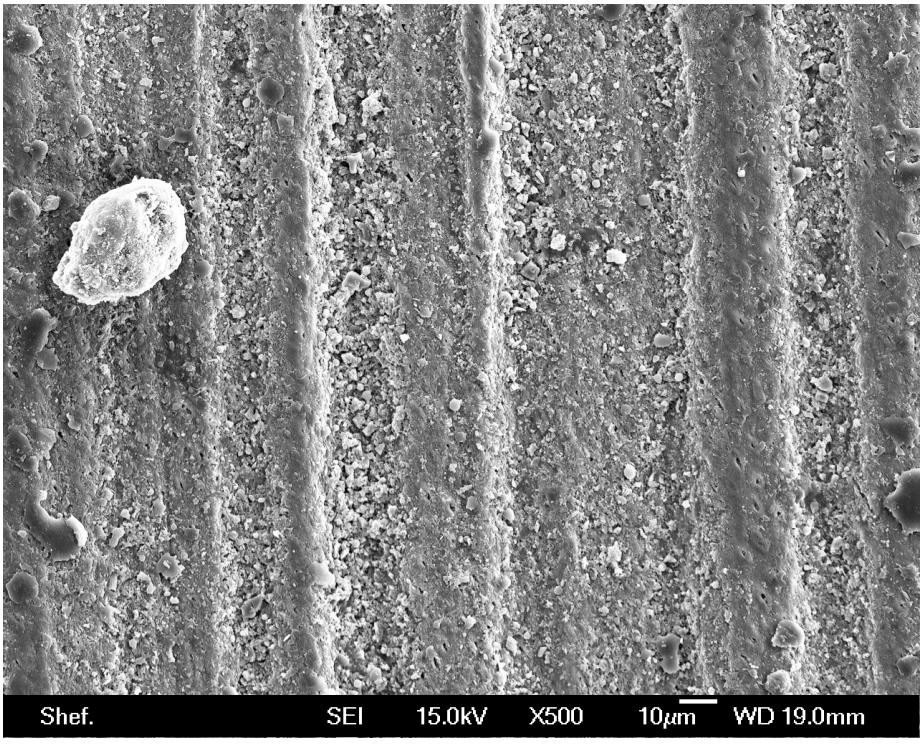

Figure 149 Typical wear scars generated by Sturcal F particles upon human dentine

The conformity of size between scratches and mode agglomeration size suggests that the strong agglomeration holds during abrasion and leads to the wear scars seen during testing.

Sturcal L particles were found to agglomerate in a very similar manner to the Sturcal F particles, with strong spherically arranged particles that do not pull apart easily. Mode agglomeration size was found to be consistently larger with Sturcal L particles than with Sturcal F at around 15 microns. Typical agglomerations for both particles are compared in Figure 153 Experimental setup for ultrasonic particle processing showing (a) schematic diagram and (b) experimental apparatus.

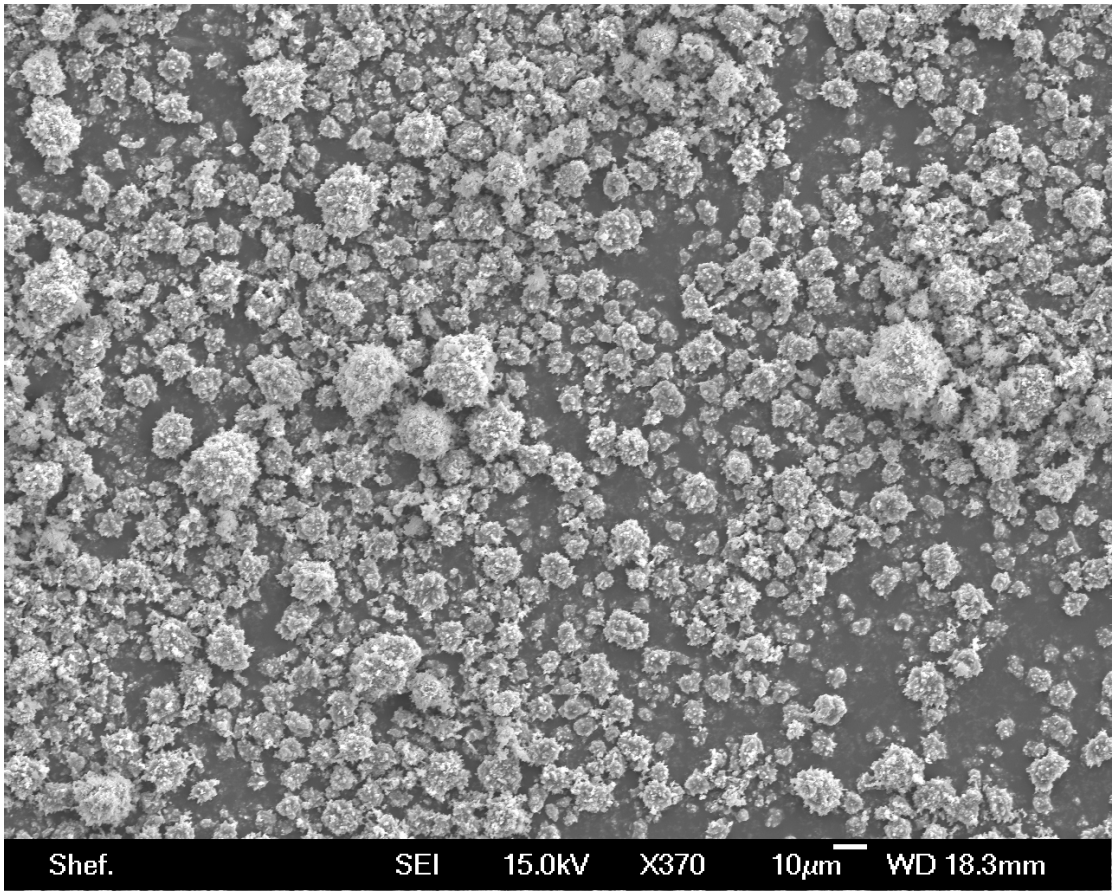

Figure 150 Agglomerations of Sturcal L particles after 1 division

Similar to Sturcal F particles, Sturcal L particles are arranged pointing outwards from the agglomeration centre giving an explanation of the aggressive wear behaviour of the particle. When comparing the grooves created during scratch testing of Sturcal L particles to the mode agglomeration size, it can be seen that there is conformity of size (Figure 151).

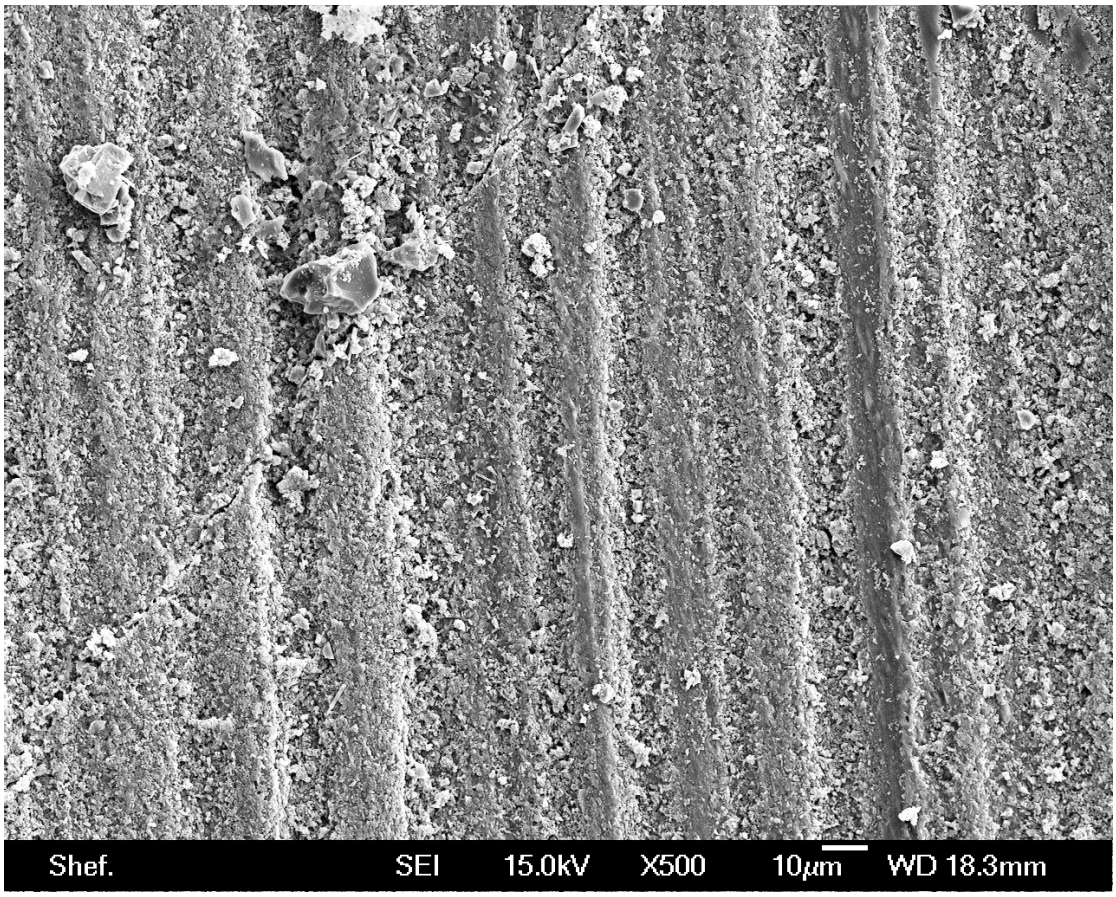

Figure 151 Typical wear scars generated by Sturcal F particles upon human dentine

Since there is conformity of scratch size and agglomeration size, it can be concluded that the agglomerations are responsible for the abrasive wear of the substrate. This result is interesting as it demonstrates that by careful selection of particles which agglomerate to greater or lesser extents, overall shape can be manipulated to give a higher or lower aggressiveness of wear.

9.2.3 Conclusions on sticky tape trials

Omya 5AV, Maruo Rods and Vicality Albafil particles have all shown little to no tendency to agglomerate. Comparing the observations with scratch test results confirm that these particles wear the surface more readily as individual particles than as a cluster.

Sturcal F and Sturcal L particles are shown to agglomerate readily. It is thought that this behaviour leads to scratching of a larger size than the individual particle. Agglomeration is also found between S2E PCC particles to some extent although the nature of the interaction is more chaotic with no discernable particle arrangement.

In other cases where strong agglomerations are not found, scratching can still be of a larger depth than individual particle sizes. In such cases particles can remain in grooves

throughout reciprocation trials, which can lead to larger than anticipated scratches relative to the particles size. In all cases careful irrigation was employed so as to avoid this.

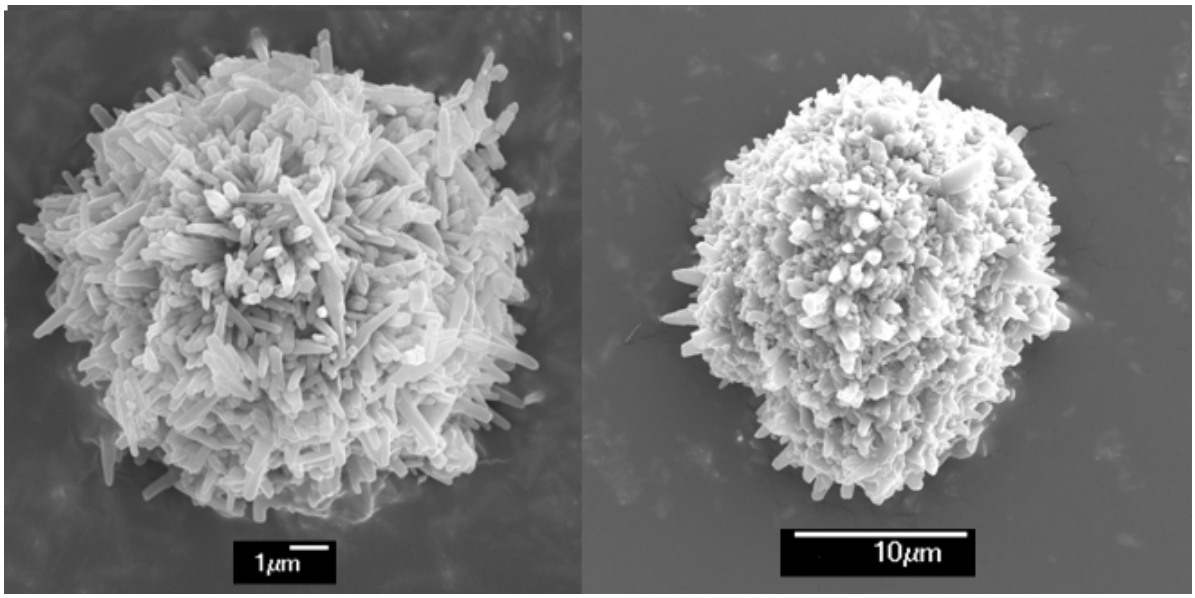

Figure 152 Agglomerations of Sturcal F (left) and Sturcal L (right)

Sturcal F is slightly less damaging than Sturcal L. The above comparison image (Figure 152) with particles at similar magnification shows just how densely packed the agglomerated Sturcal L particles are. This could be the reason behind its strength and aggressive nature. This supposition as to the increased density of Sturcal L particle arrangement's compared to Sturcal F is further investigated and validated using nano-manipulation analysis in Chapter 8.

9.3 Processing of particles in solution using ultrasound

Ultrasound is often used to dissipate particles evenly around a suspension using cavitation collapse as the mechanism of mixing. A method of measuring particles by laser diffraction can be used to determine modal size plots, however the nature of the particles are not fully understood by this method since it is not possible to state whether the measurements are of individual particles or agglomerations. It was therefore hypothesised that measuring the particles by laser, processing them with ultrasound and then measuring again would allow for analysis of agglomerations by inference from size distribution changes. In addition, it was thought that this may be a useful means of assessing which particles show more natural agglomerative behaviour in solution. In principle, it was thought that particles forming agglomerations would be dispersed by the propagating ultrasound energy, and so it would be expected that the modal sizing would decrease with processing.

9.3.1 Experimental procedure

Testing has been undertaken on particles to examine whether ultrasonic stimulation had an effect upon measured particle size, potentially leading to the breakdown of particles. 5g of each particle was suspended in 20ml of distilled H_2O for 3 minutes using a frequency of 27.8 KHz which was brought about the optimal cavitation activity. Figure 153 shows the experimental set up.

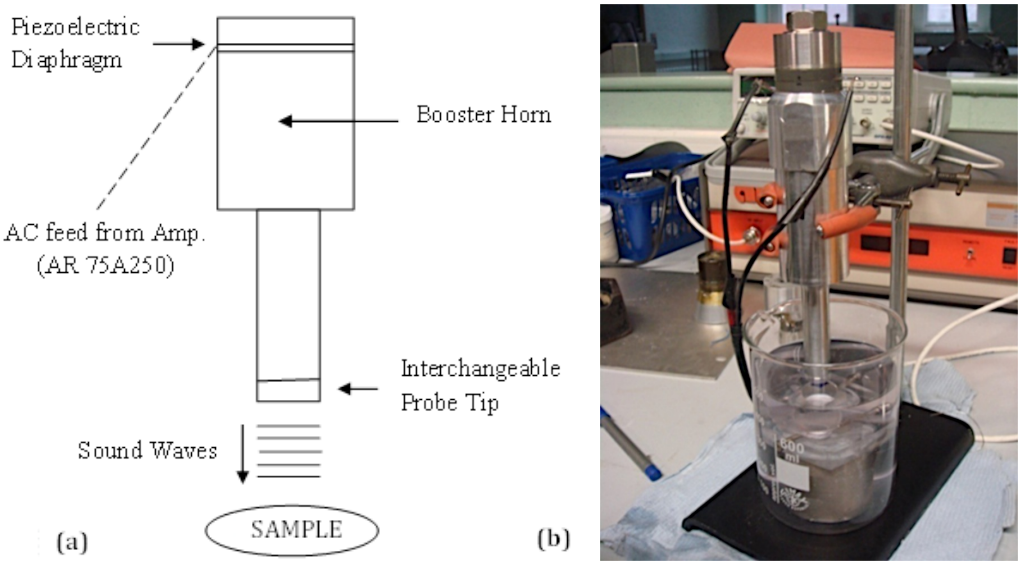

Figure 153 Experimental setup for ultrasonic particle processing showing (a) schematic diagram and (b) experimental apparatus

As above, the particles selected for this experiment have been chosen based on the interests of the sponsor company. These are as follows:

- Prologite Mica
- Vicality Albafil
- Attapulgite Clay
- S2E PCC
- MEV Vermiculite
- S20 Talc
- Omya 5AV
- Maruo Rods (after 24hr suspension)
- Maruo Rods (immediately sized)

9.3.2 Results

Prologite Mica

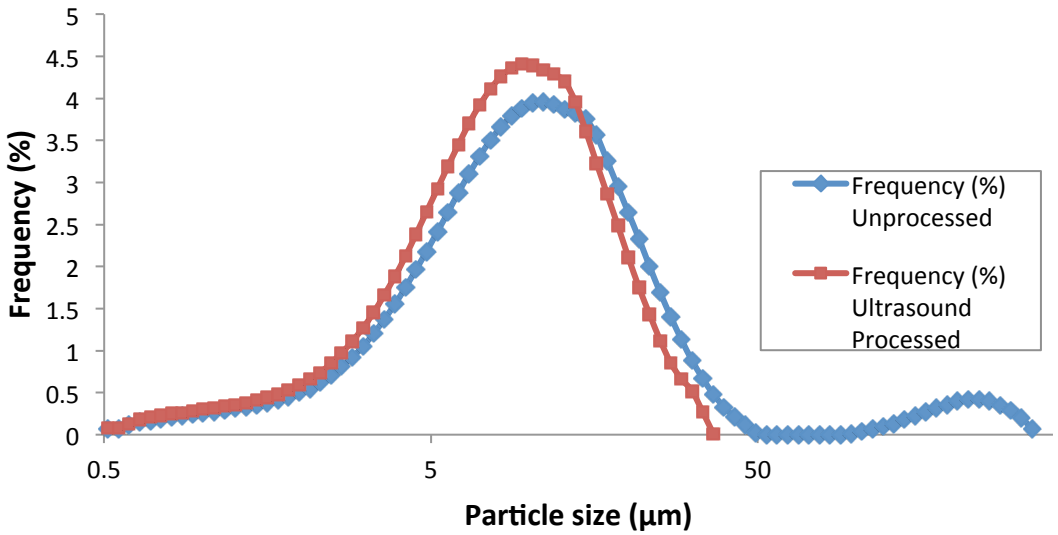

Figure 154 Particle size of processed and unprocessed Prologite Mica

Figure 154 shows the particle sizing measured before and after ultrasonic processing for Prologite Mica. Initial mode particle size was 9.50µm increasing to 11.04µm after processing. The particle sizing profiles generally match between unprocessed and processed particles, however the unprocessed particles have developed a low frequency of larger sizes. This suggests that the majority of particles are unaffected by the processing, however there may be a small number of agglomerated particles that are broken apart by the ultrasonic energy.

Vicality Albafil

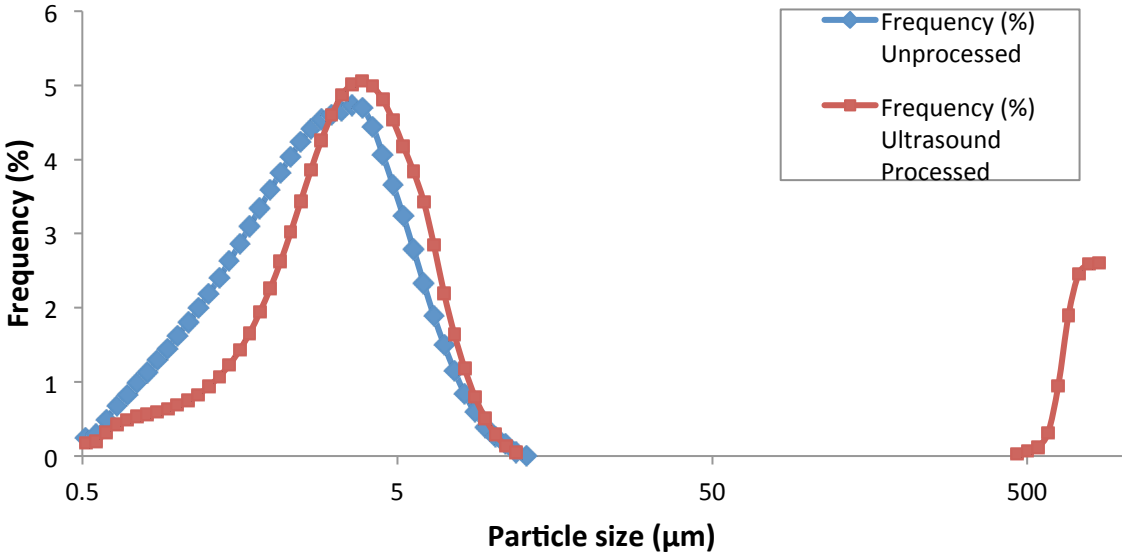

Figure 155 Particle size of processed and unprocessed Vicality Albafil

Figure 155 shows the particle sizing found before and after ultrasonic processing for Vicality Albafil. Initial mode particle size was 3.60µm increasing to 3.875µm after processing. Whilst the majority of the particles appear to be unchanged in size, and the distribution remains comparable, the appearance of a secondary peak of significantly larger particles (around 800µm in size) suggests that particles have been agglomerated by the process. The lack of particles sized between the primary and secondary peak suggests that the mechanism of agglomeration is by collection of further material by "seed" particles. This means that it is likely that particles are attracted more to other larger particles than to particles of the unprocessed size (and so the agglomerations continue to grow).

Attapulgite Clay

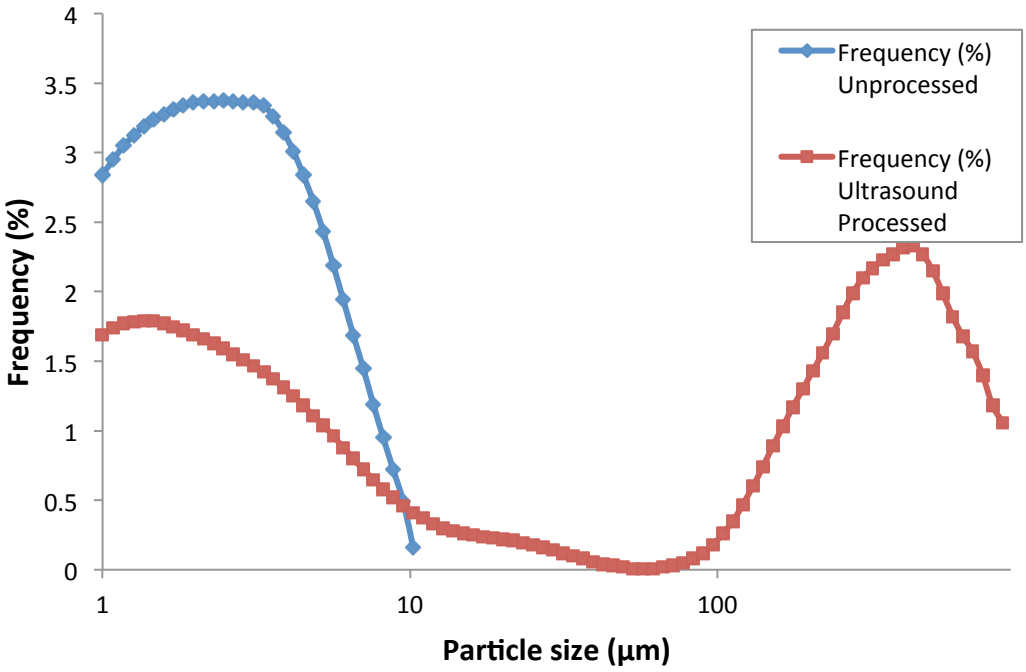

Figure 156 Particle size of processed and unprocessed Attapulgite Clay

Figure 156 shows the particle sizing found before and after ultrasonic processing for Attapulgite Clay. Initial mode particle size was 2.47µm increasing to 432µm after processing with a secondary peak at 1.41µm. The primary peak in this case is for much larger particles suggesting strongly that agglomeration has taken place between the particles and that the agglomerations take place readily. Furthermore, particles appear to favour being within an agglomeration than being individual particles since the modal particle size is much larger than the modal particle size of the unprocessed material.

S2E PCC

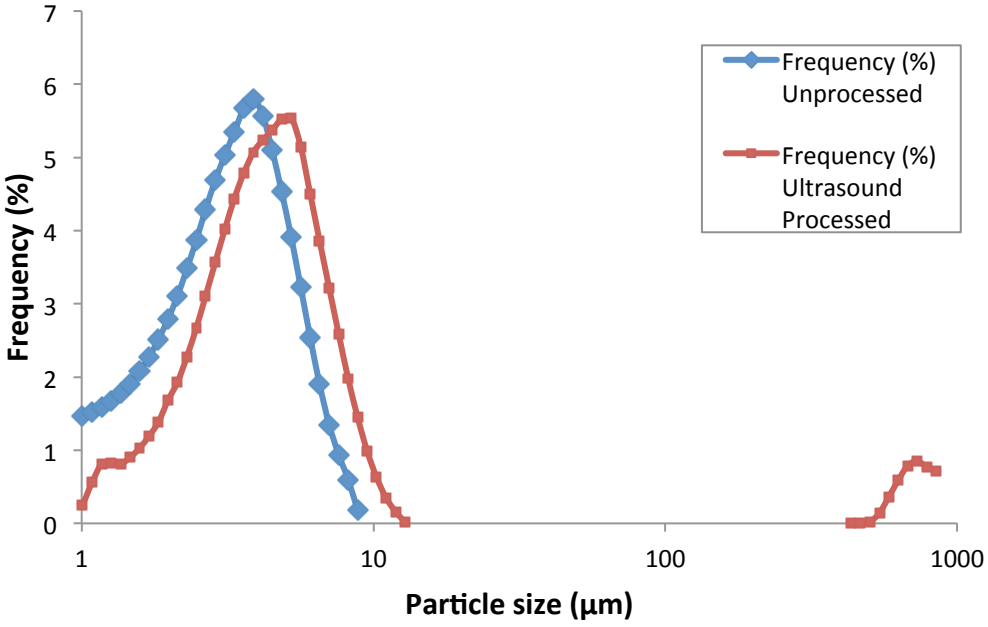

Figure 157 Particle size of processed and unprocessed S2E PCC

Figure 157 shows the particle sizing found before and after ultrasonic processing for S2E PCC. Initial mode partical size was 3.875µm increasing to 5.225µm after processing with a secondary peak at 729µm. As with Vicality Albafil the secondary peak of large agglomerations suggests that particles have an affinity to join to existing agglomerations.

MEV Vermiculite

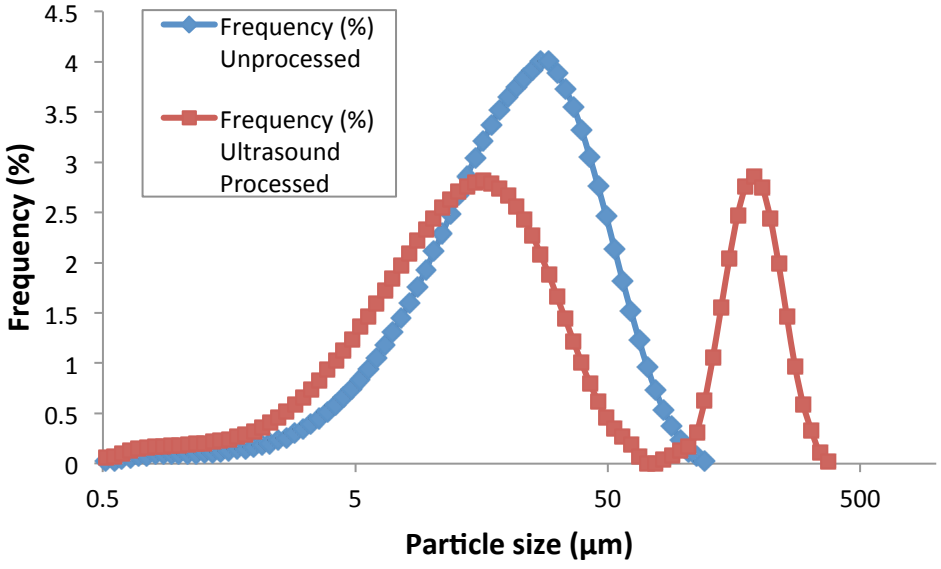

Figure 158 Particle size of processed and unprocessed MEV Vermiculite

Figure 158 shows the particle sizing found before and after ultrasonic processing for MEV Vermiculite. Initial mode particle size was 28.15µm decreasing to 16.05µm after processing with a secondary peak at 189.6µm. The distribution is consistent with Attapulgite Clay although the agglomerated processed particle sizes are much lower.

S20 Talc

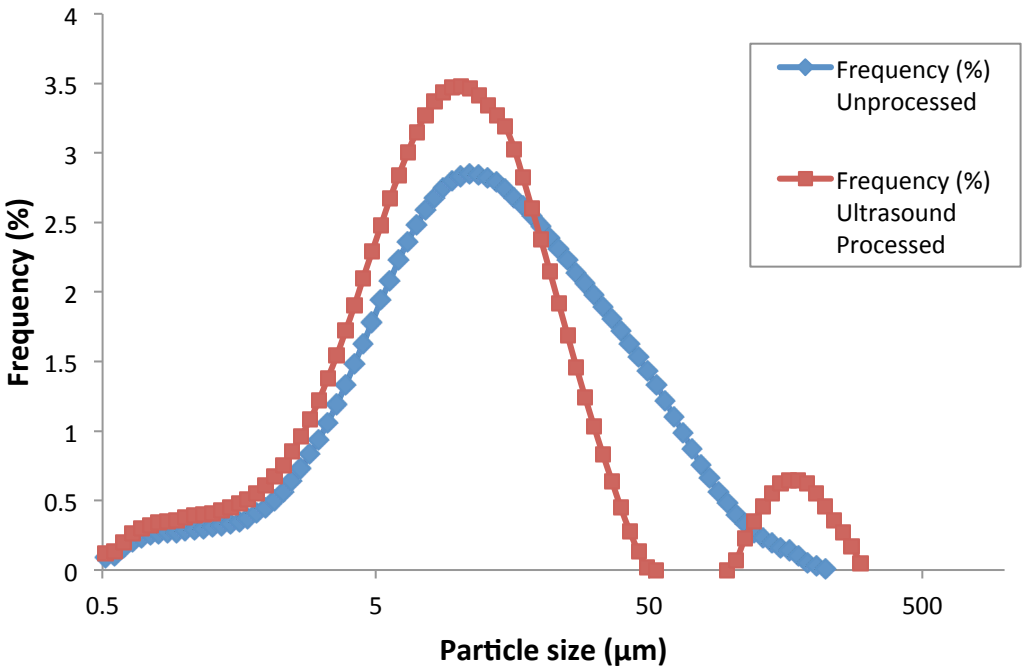

Figure 159 Particle size of processed and unprocessed S20 Talc

Figure 159 shows the particle sizing found before and after ultrasonic processing for S20 Talc. Initial mode particle size was 11.035µm increasing to 10.24µm after processing with a secondary peak at 169.3µm. This particle has shown signs of medium sized particles both joining and separating since there is a higher concentration of both in the processed sample. This suggests that there is a degree of agglomeration prior to processing which then both breaks apart and agglomerates further creating larger particles.

Omya 5AV

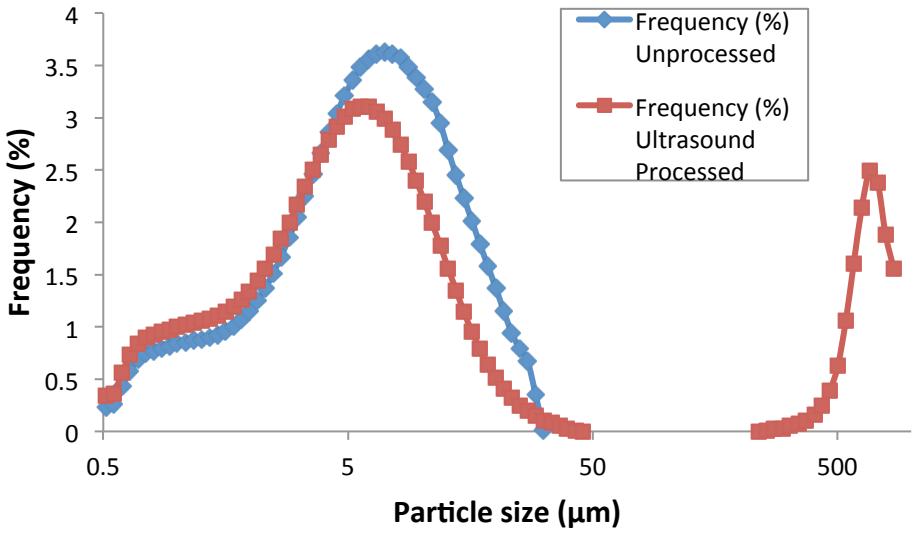

Figure 160 Particle size of processed and unprocessed Omya 5AV

Figure 160 shows the particle sizing found before and after ultrasonic processing for Omya 5AV. Initial mode particle size was 7.045µm decreasing to 5.63µm after processing with a secondary peak at 677µm. The unprocessed distribution of particle sizes remains similar post processing however there is development of a second peak indicating some degree of agglomeration.

Maruo Rods

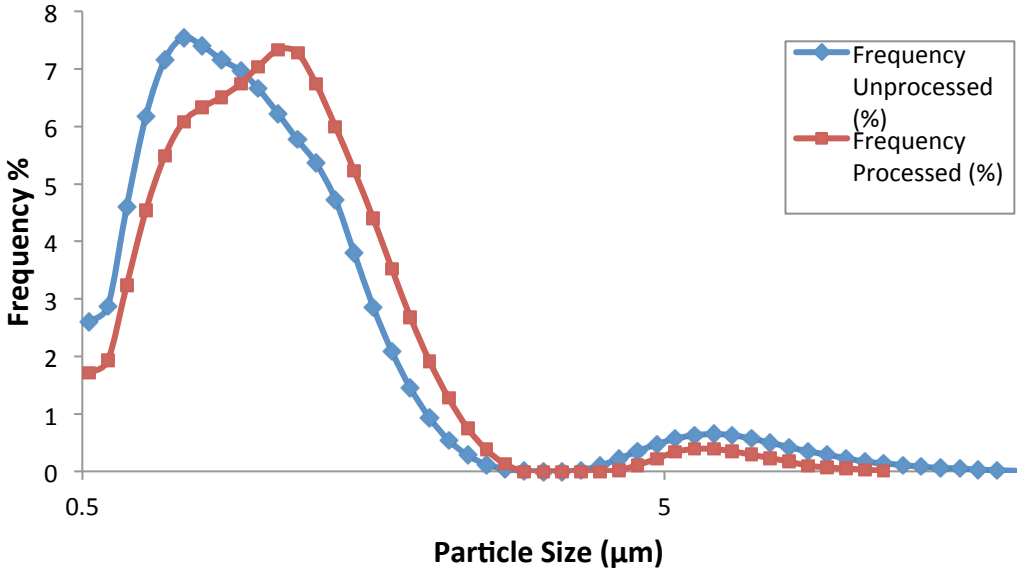

Figure 161 Particle size of processed and unprocessed Maruo Rods

Figure 161 shows the particle sizing found before and after ultrasonic processing for Maruo Rods (immediately sized). Initial mode partical size was 0.75µm increasing to 1.09µm after processing with secondary peaks at 6.07µm and 5.84µm respectively. There appears to be no significant change in distribution between the processed and unprocessed particles.

Maruo Rods (after 24 hour suspension)

When a sample is first introduced into the solution it forms layers of activity comprised of particles afloat on the surface, particles in suspension and particles on the container floor. Omya 5AV and Maruo Rods particles were found to not stay in suspension for long before sinking to the container floor (Maruo Rods longer than Omya 5AV but both less than 1 minute). Particles were then found to seldom leave the base of the container even when the sample was stimulated. Since particles were seen to sink after some time, it was thought that there may be an interaction between the particles and the water that changes over time. A further experiment was therefore carried out to observe the effect of allowing a settling time on Maruo Rods before processing. The particles were left in suspension for 24 hours before ultrasonic processing was undertaken as per the other samples.

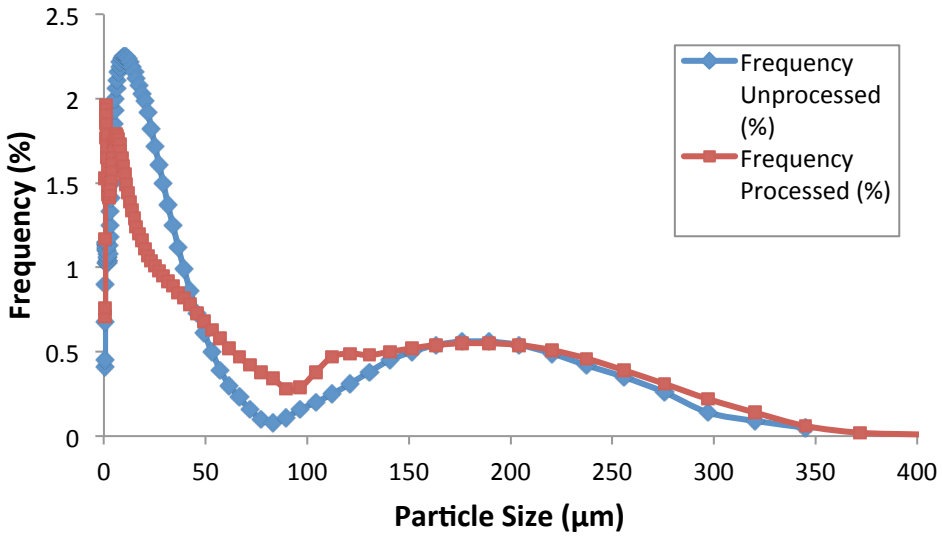

Figure 162 Particle size of processed and unprocessed Maruo Rods after 24hr suspension

Figure 162 shows the particle sizing found before and after ultrasonic processing for Maruo Rods after 24hr suspension. Initial mode particle size was 10.3µm with a secondary peak at 183µm decreasing to 1.00µm after processing with a secondary peak at 183µm. In contrast to the majority of the other samples tested, Maruo Rods after 24 hour suspension exhibit signs of agglomeration prior to processing. After processing these large agglomerations remain unaffected however some intermediate particle sizes are developed whilst smaller particles are reduced in frequency. This suggests an agglomeration of smaller particles rather than the nucleation to larger particles seen in other materials.

Since no agglomeration is seen without 24 hour suspension, it is suggested that there is a material characteristic change when Maruo Rods are suspended in solution. It is possible that this is due to moisture absorption, which may either affect the affinity of the particle to agglomerate, or may affect particle size. It is not possible to directly observe this distinction by electron microscopy because the potentially higher moisture content is not compatible with the testing requirements.

9.3.3 Conclusions for ultrasound trials

Prior to testing it was thought that particles forming agglomerations would be dispersed by the propagating ultrasound energy. The distribution of particle size observed during testing suggests that this is generally not the case. In nearly all cases the ultrasonic stimulation of particles in solution led to secondary peaks on the size distribution plots of a magnitude far greater than that of the original particle size (ranging from 11 to 200 times the size). This suggests that ultrasound may encourage particles to agglomerate. Further to this, it is observable that as particle size decreases, the magnitude of agglomeration increases.

Most particles show a secondary peak at larger sizes with lower frequencies of intermediate sizes. Therefore the proposed mechanism for the agglomeration in the majority of cases is nucleation to larger particles. Larger particles appear to more readily attract other individual particles to increase in size. For S20 Talc particles the sizing suggest that intermediate particles both agglomerate and break apart.

Some Prologite Mica particles are seen to break apart during ultrasonic processing reducing to the individual sizing. Rod particles appear to display some degree of natural agglomeration without encouragement and remain fairly unaffected by the introduction of ultrasonic energy. When left in suspension for 24 hours before sizing there is a rise in intermediate particle sizes.

Whilst the majority of particles showed an inclination to agglomerate by ultrasonic processing, it should be noted that the energy passed into the solution is very high and particle agglomeration may not occur as readily by other processes.

9.4 Summary of conclusions on agglomeration

Both of the experiments carried out give an indication of the agglomeration behaviour of the particles. Some particles are seen to agglomerate and remain together despite attempts to separate, whilst others are easily separated and don't show an affinity for union.

Both Sturcal particles were seen to agglomerate most readily generating clusters of outwardly pointing particles. Maruo Rods showed some degree of agglomeration by

ultrasonic excitation after being in solution for 24 hours but were reluctant to agglomerate otherwise. The other particles show some degree of agglomeration behaviour leading to changes in sizing distribution.

The primary mechanism for particle agglomeration was found to be nucleation to larger particles rather than repeated pairings of individual particles.

Comparing the agglomeration behaviour of the particles with the wear trials discussed previously helps to explain the mechanisms by which the particles develop more aggressive, angular shapes and hence increase wear rates or generate wear scars larger than individual particles.

10 PARTICLE INTERACTION WITH DENTINAL TUBULES

An important feature of dentine within human oral healthcare is dentinal tubules; these tubules are synonymous with sensitivity issues. The conventional role of particles within toothpaste is largely for tribological purposes. Abrasives are introduced to encourage the mechanical erosion and removal of surface detritus. Abrasives can however be employed to reduce the prevalence and severity of dental sensitivity by penetrating and sealing off tubule orifices. This chapter investigates the ability of bespoke abrasive particles in providing an extensive, consistent and structurally resilient seal within tubules. The particles studied in this chapter are Maruo Rods and Omya 5AV, details of which can be found in Table 2 in chapter 4.

10.1 Background

In vitro experimentation was undertaken in the form of constrained linear reciprocation brushing experiments and real-time scanning electron microscopy of direct particle manipulation. It was found that the proposed novel particle provided a significant improvement in the extent and resilience of tubule occlusions compared to conventional miscellaneous shaped ground particles of similar size and material. The efficacy of particle performance in this regard appears strongly dependent on the concentration of water present.

Dentinal tubules, often referred to as dental canalinculi are an important feature of dentine. These tubules appear as open pores and house the odontogenic process within dentinal fluid, which together are responsible for transmitting neural signals from the external surface of tooth to the pulpal core. These nerve impulses whilst useful in conveying external environmental conditions such as temperature, pressure and acidity can also lead to dental hypersensitivity, which can cause intense and acute discomfort. The control and regulation of these nerve impulses is of significance to dental professionals and the primary mode by which this is achieved is through the occlusion of exposed dentinal tubules.

Dentine forms one of the major components of teeth and is vital in both the provision of structure and foundation whilst also providing a medium through which neural communication can take place. There are three types of dentine; primary dentine is typically the most familiar located between the pulp chamber at the center of the tooth and enamel. Unlike primary dentine, which forms before the completion of the apical foramen, Secondary dentine develops throughout the lifetime of the tooth. Despite having a similar composition to that of primary dentine the rate of formation is slower and more varied with secondary dentine, which can lead to abrupt changes in tubule direction and lumen width. Tertiary dentine is formed in response to trauma and can be irregular and unpredictable. For the purposes of this study only primary mantle dentine has been analysed, as the associated tubules are representative of those likely to be exposed to external environment.

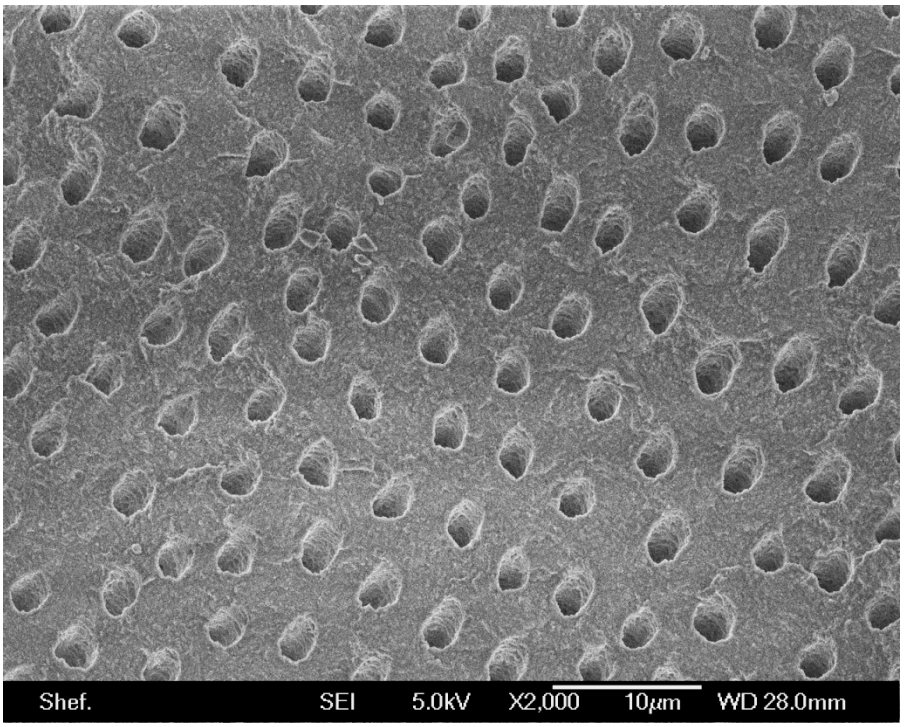

Figure 163 SEM micrograph of adult mantle dentine containing dentinal tubules. Image taken in close proximity to the sulcus

Figure 163 shows a scanning electron micrograph of a typical prepared sample. Primary dentine is largely composed of circumpulpal dentine surrounding the pulp chamber, with mantle dentine forming the outermost layer beneath the amelodentinal junction (DEJ). Sumikawa et al [48] investigated the change in tubule density, tubular diameter, and peritubular width according to progressive distances from the DEJ. They concluded that numerical density consistently decreased with distance from the DEJ along with an increase in diameter. A typical tubule diameter for human dentine is around 1 micron at the outermost surface. Subtle variations in lumen geometry can have a significant effect on the occlusive performance of particles, for this reason samples were only taken from locations in close proximity to the DEJ.

Dentine is usually shielded from external stimuli by protective enamel. This can however become compromised or diminished throughout everyday life leading to exposure of areas of mantle dentine. The most common way in which dentine can become exposed is through gum recession, which is a common and widespread occurrence. As the depth of enamel tapers towards gum level (the sulcus) whereupon the root is protected by a layer of cementum, there is an area of transition within which dentine can become readily exposed. Samples were acquired within close proximity to this region.

Extensive research into dentinal tubule characterisation has in the past been carried out upon bovine dentine; this is largely due to the accessibility and low cost of the tissue.

Schilke et al [29] reports that although there is not a significant difference in tubule density and diameter in coronal dentine, there is increased variance in bovine root dentine.

Many studies are carried out for the purposes of investigating the performance of adhesive restorations. In these cases the overall frequency and cumulative orifice area is of importance; whereas subtle differences in lumen shape and size are often inconsequential. Camargo et al [49] investigated the number and the diameter of dentinal tubules in root canals, in the cervical, middle, and apical thirds, of human and bovine teeth. They concluded that statistically significant differences were found both for the frequency and the diameter of dentinal tubules between the two tissues. It is for this reason only human dentine is analysed within this chapter.

Tubule infiltration using particles is an area which has been extensively researched. The objective of this process is to limit or prevent sensitivity issues by impeding the transmission of nerve impulses by blocking tubule lumen. Tubule geometry and its associated components play an important role in understanding and predicting the occlusive process. Figure 164 shows the structure of an odontogenic process and its arrangement within dentinal tubules. Commonly in adults the odontoblast process extends less than one quarter of the tubule length and it is dentinal fluid that communicates between the outer surface and the process itself. There is still relatively little known about what comprises dentinal fluid. Stedman's medical dictionary defines it as a lymph or transudate of extracellur fluid, mainly comprised of a cytoplasm of odontoblastic processes [50].

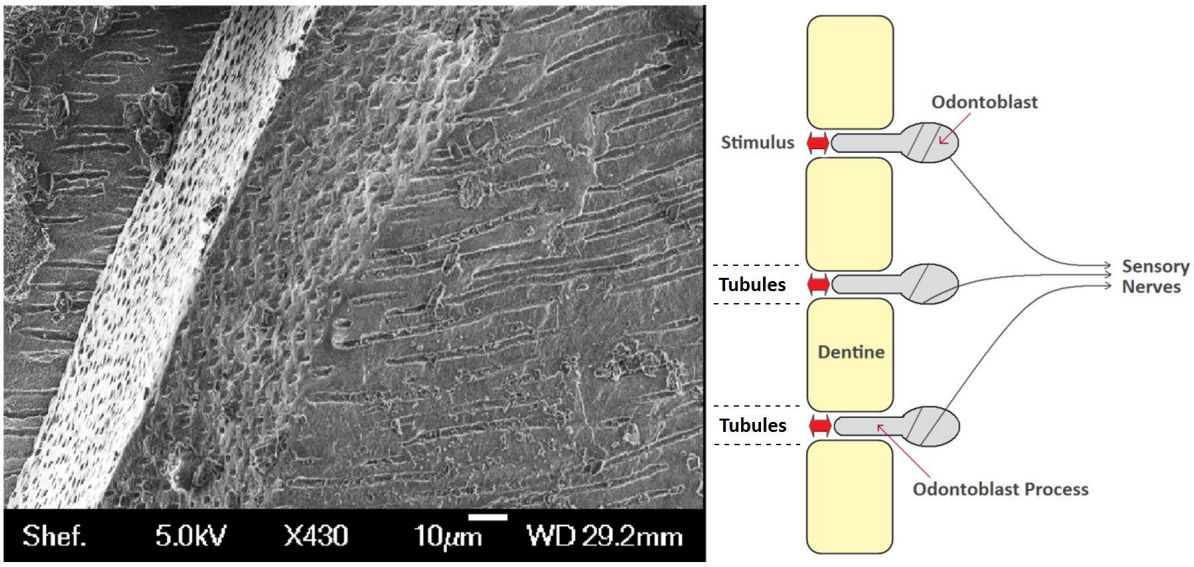

Figure 164 Left: SEM micrograph of sectioned dentine showing pathways of tubules, Right: schematic of odontoblast process and tubule assembly

There are several mechanisms proposed to explain the transmission of stimulus to the sensory nerves. One such mechanism is the hydrodynamic process proposed by Brännström and Åström [51]. Variance in the flow of plasma like dental fluid leads to the triggering of

mechanoreceptors located on the nerves within the pulpal core, this in turn induces a pain response. This process can be activated by air pressure, temperature fluctuation, dehydrating chemical and forces acting on the tooth. An alternative mechanism is modulation theory which suggests that damaged or coarsely stimulated odontoblasts release specialised pain inducing proteins along with neuro-transmitting agents [52] which in turn generate a pain response through cell membrane receptors. Alternatively Transducer Theory centres on the synergistic relationship between the terminal nerve endings and the odontoblastic process, a similar configuration to that of a conventional synapse. The validity of this theory is uncertain due to the physical lack of substances common in aiding in the transmission of neural sensations such as acetylcholine. Gate Control Theory proposed by Melzack and Wall [53] puts forward the idea that the perception of pain is relative to the interaction between separate neurons and not just as a result of the direct stimulus of pain receptors. Using the spinal cord as a means of modulation, the so called “gate”, incoming signals can be blocked or allowed to pass subject to the differentiation between the characteristics of the fibres responsible for the signal.

The most widely accepted of these mechanisms for dental pain communication is hydrodynamic theory. This mechanism neatly accounts for both the instantaneous generation of pain signals through direct mechanoreceptor stimulation via invasion of the tubule lumen, as well as the effects of thermal stimuli on the production of pain signals. Introducing both hot and cold stimuli to dentine can lead to the expansion and contraction of dentinal fluid respectively which in turn can lead to the stimulation of mechanoreceptors. Thirdly the hydrodynamic mechanism also accounts for the stimulation of pulpal nerves via contact with salty or sugary substances. Dentinal fluid is usually of low osmotic concentration and thus readily propagates towards substances of higher osmotic concentration; this dynamic flow can lead to the stimulation of mechanoreceptors.

Abrasive particles can be employed as means of lowering the prevalence of dental hypersensitivity by impeding the stimulation of dentinal fluid. They achieve this by penetrating and filling the orifices of the tubule, creating a barrier between potential external stimuli and the dentinal fluid. Some dentifrices rely on active agents for example potassium and fluorides as a means of blocking tubules via internal seeding and crystalline expansion. Arrais et al [54] compares the occlusive efficacy of dentifrices reliant on precipitation constituents or by stimulating the formation of secondary dentine, and dentifrices which block tubules via direct particle occlusion. It was concluded that the three dentifrices studied all increased tubule occlusion compared to the control studies using only brushing with filaments and no brushing. The statistical difference between the occlusive performances of the three approaches is difficult to differentiate, further to this the tenacity and resilience of the resultant obstruction cannot easily be known.

Typically the mode of tubule impregnation using particle infiltration is random with little purposeful design. In these instances particles which are small enough to enter tubules do so sporadically when motivated across lumen during the brushing process, until a partial or complete blockage of the orifice is formed. The structural integrity and resilience of these barriers is often varied and unpredictable. A benefit of the formation of a lumen barrier via abrasive particle infiltration is that the occlusive process is unaffected by subtle chemical and environmental conditions. Dentifrices relying on active agents may vary in performance as a result of variation in buccal conditions. This chapter focuses on the affinity of specialised tailored particles to interact with and effectively seal tubule lumen compared to particles of similar material and magnitude but produced via standardised milling processes.

10.2 Experimental Methods

10.2.1 Dentine Samples

Samples were sourced and prepared as described in Chapter 4.2.1. Both mantle and circumpulpal dentine were prepared and studied. Although both are examples of primary dentine subtle differences can be observed. Mantle dentine typically borders the amelodentinal junction and is representative of tubules likely to be exposed through gum recession or acid erosion. It can be said that mantle dentine is more mineralised than circumpulpal dentine with a difference in associated collagen fibres. For the purpose of this investigation however the geometry and frequency of the dentinal tubules is paramount with tissue composition less important. Figure 165 highlights in red the approximate locations within which tubules were analysed. These locations are in close proximity to where the sulcus would be situated before extraction.

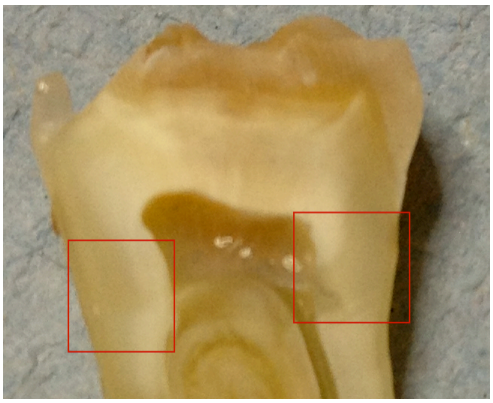

Figure 165 Overview of sample locations on bisected adult 3rd molar

10.2.2 Experimental setup

The dynamic and occlusive behaviour of Rod particles was analysed both in isolated trials and in comparison with Omya 5AV ground calcium carbonate particles. The aforementioned linear reciprocation setup was employed for trials administering particles via filament entrainment. In all brush trials a standard Unilever toothbrush was used under a load of 3N for a duration of 30 seconds. Trials were conducted both dry and in the presence of distilled

water. Wet trials were carried out using varying quantities of water in order to study the effect of water presence on the occlusive process. Rod particles were also analysed in the form of a more viscous anhydrous Rod paste. Trials were conducted at different dilutions using distilled water and administered using a linear reciprocation nylon brush rig.

The occlusive efficacy of rod particles is related both to its geometry and its dynamic behaviour both in isolation and as a cumulative agglomeration. In order to better understand this dynamic behaviour in-situ nano-manipulation experiments were undertaken within a JEOL 6500F scanning electron microscope. Particles were manipulated using Nickel/Chromium nano-probes with a polished Silicon substrate in order to both understand and predict motivational mechanisms and characteristics of fracture.

Nano-manipulation analysis was also employed as a tool for assessing the structural integrity of resultant tubule occlusions. Nickel-Chromium nano-wires (Figure 166) were prepared and introduced to the terminus of probes in order to directly manipulate microscopic bodies atop and amidst the substrate. Probes were hand controlled by an operator in order to both derive a visual understanding of the structural resilience of particles as well as discern the dynamic behaviour of individual particles and agglomerations when motivated. Although probe load data is not directly quantifiable object resilience can be gauged through visual assessment of probe flexure when attempting to motivate.

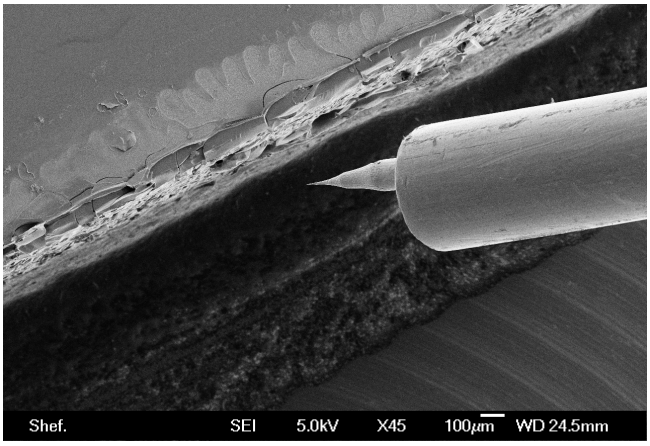

Figure 166 Nickel/Chromium nano-manipulation probe being introduced to substrate

10.3 Results

10.3.1 Dry Abrasive Particles

Brushing with dry particles led to significant and extensive tubule occlusion. SEM Analysis of the inter-tubule dentine revealed no evidence of surface degradation or scratching. Particle presence within tubules comprises of smaller particle fragments fractured from larger intact

particles. In many cases these fragments appear to be the tips of particles, identifiable by the acute taper in particle width (see Figure 167).

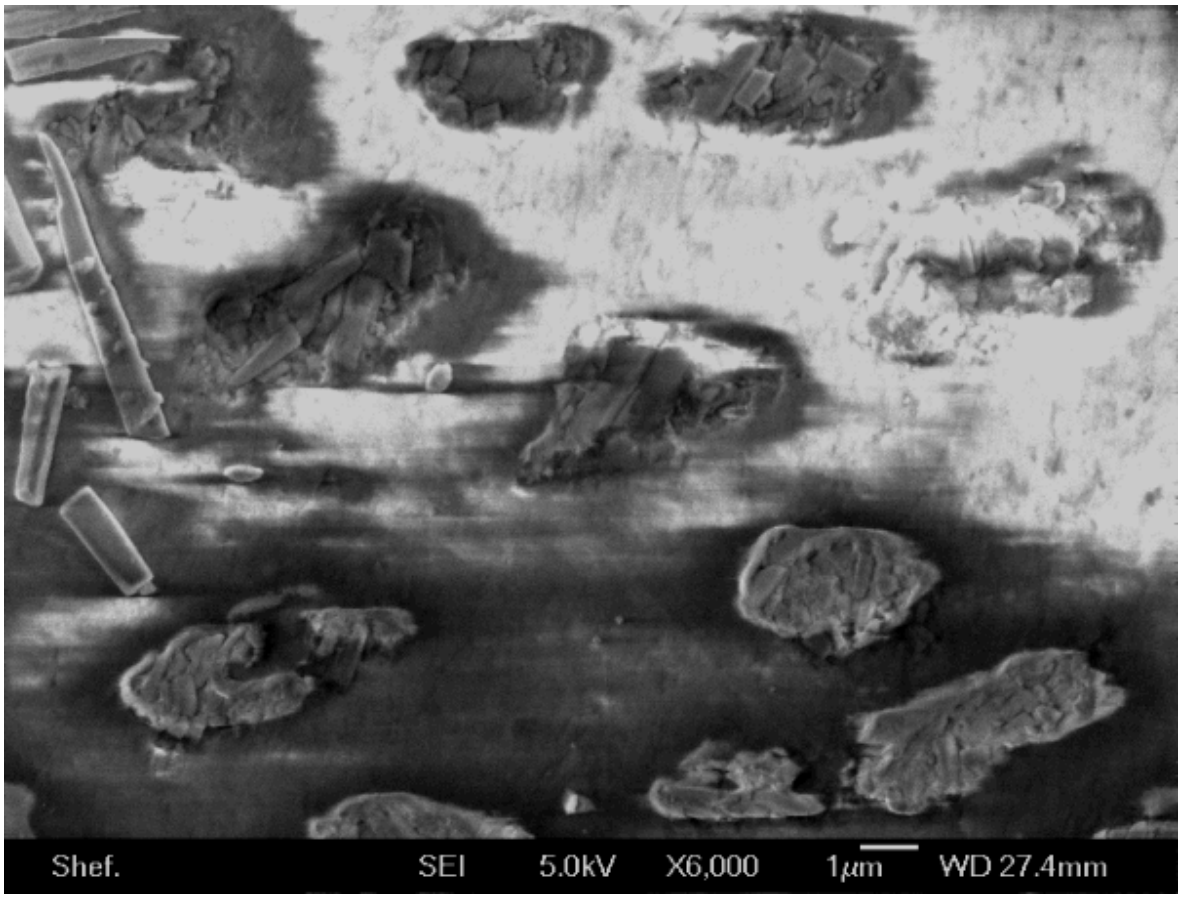

Figure 167 Scanning electron micrograph of occluded tubules after brushing with dry Rod particles

The density of particle fragments within tubule lumen is high with particles filling tubules entirely to the substrate surface. These particle fragments tessellate relatively neatly with very few instances of voids.

There is a distinct reduction in the frequency of occluded tubules when brushing with dry Omya 5AV particles compared to that observed using Rod particles. Figure 168 and Figure 169 demonstrate this, showing a fairly even distribution of filled and unfilled tubules. Analysis of tubules containing particles show present particles are not densely packed as seen with Rods and do not appear to provide a comprehensive barrier against external stimulus.

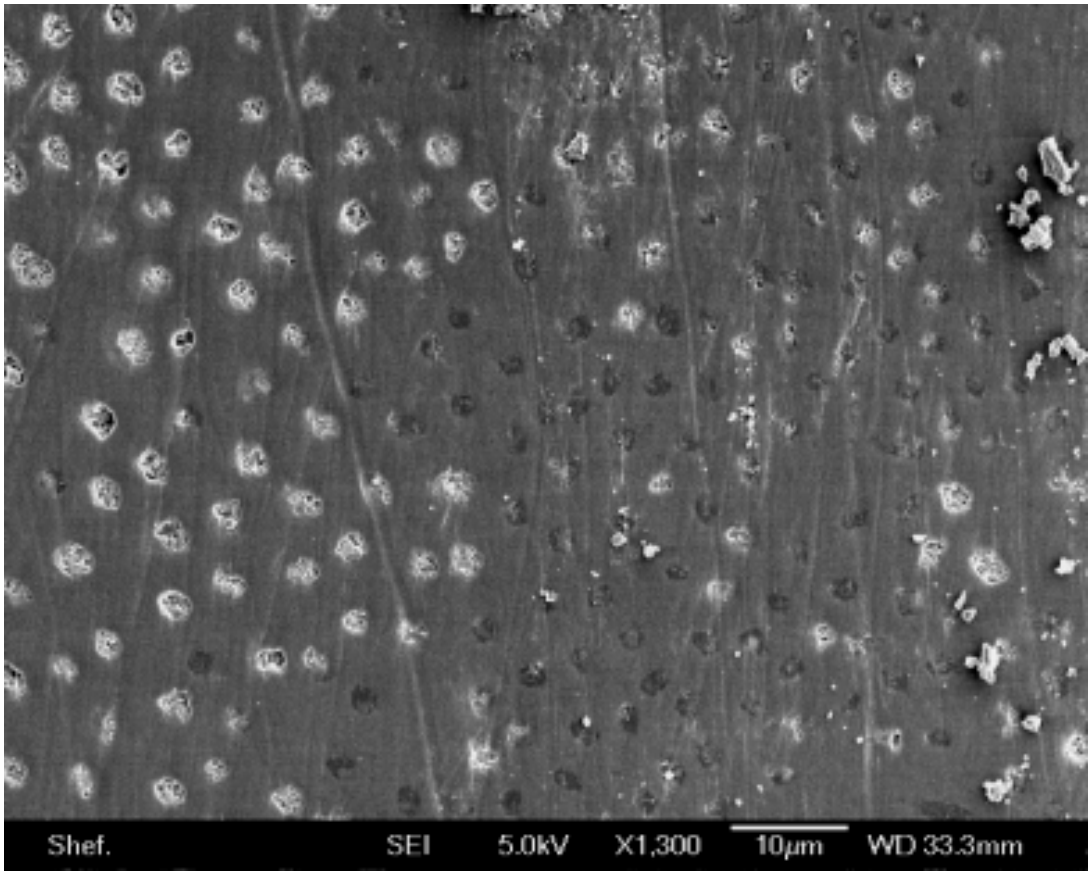

Figure 168 Scanning electron micrograph of occluded tubules after brushing with dry Omya 5AV particles

Close inspection of inter-tubule dentine reveals a notable increase in surface damage and abrasive scratching compared to equivalent Rods trial; this was observable within Chapter 7 also.

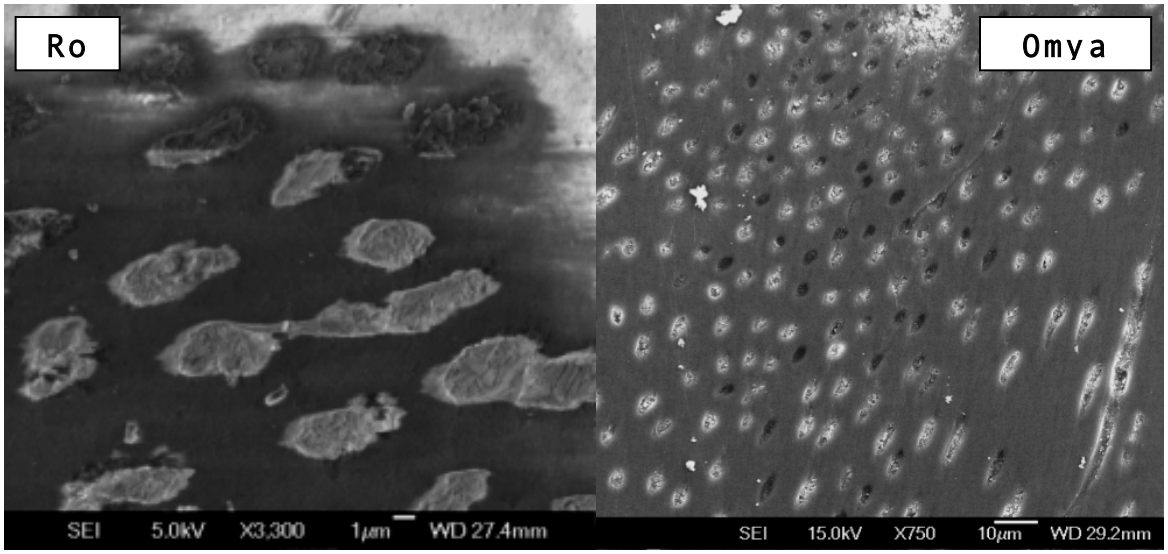

Figure 169 Comparative SEM images of occluded tubules after brushing with dry Rods and Omya 5AV particles respectively

10.3.2 Wet Abrasive Particles

Using the same reciprocation setup as previous trials, particles were brushed in a suspension of pure distilled H_2O under the same operating conditions. SEM analysis showed almost all exposed tubules remained entirely vacant. The introduction of water appears to have a dramatic effect on the efficacy of particles to interact and penetrate tubules. Further to impeding particle-tubule interaction brushing in suspension leads to a much lower incidence of particle fracture. As can be seen in Figure 170 particles appear to be relatively intact with few smaller fragments of particle or clear examples of particle breakdown. Care was taken when concluding brushing trials to ensure the substrate surface remained undisturbed. Samples were not aggressively rinsed post trial in order to minimise potential evacuation and removal of small particle fragments. The notable presence of remaining idle particles suggests that particles were not illegitimately removed from within the sample.

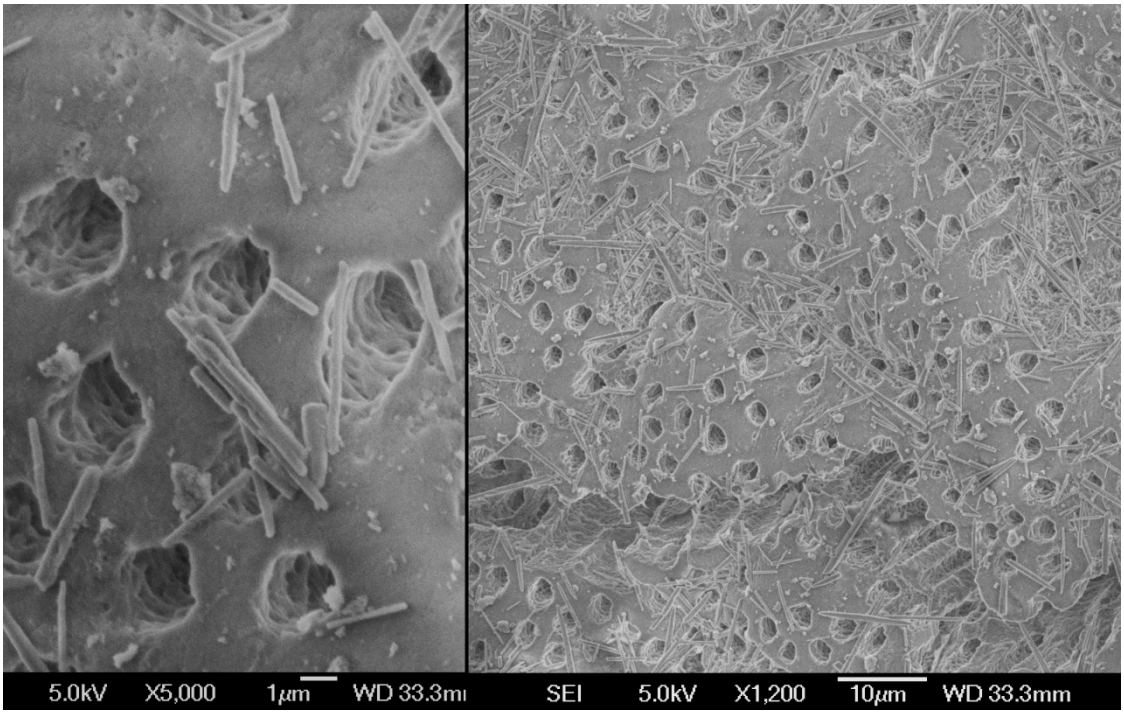

Figure 170 Scanning electron micrographs of dentinal tubules after brushing with Rod particles in a suspension of distilled H_2O

As seen in trials utilising dry Rod particles, there is little evidence of dentine scratching or surface damage. There is a potential argument, based upon visual feedback on processed regions (and proposed elsewhere in this thesis) that the use of Rod particles may introduce a smoothing effect upon the substrate surface. Further work would be required to support this claim.

Similar observations were made with Omya 5AV to that observed with Rod particles with the introduction of water leading to an impedance of particles into tubules. This is not solely a result of particle size as small fragments capable of tubule penetration were observed in

close proximity to tubule lumen, but little evidence of particles within tubules. Particle breakdown appears limited however this is difficult to distinguish due to the broad range in particle size as a result of the manufacturing process.

Contrary to findings with Rod particles (both dry and in solution) is the continued presence of surface damage. In this case, brushing with Omya in solution led to extensive roughening of the dentine surface. Perceptible scratches are no longer a feature as seen in dry trials, however Figure 171 and Figure 172 illustrates the typical surface roughening observed across the majority of the sample.

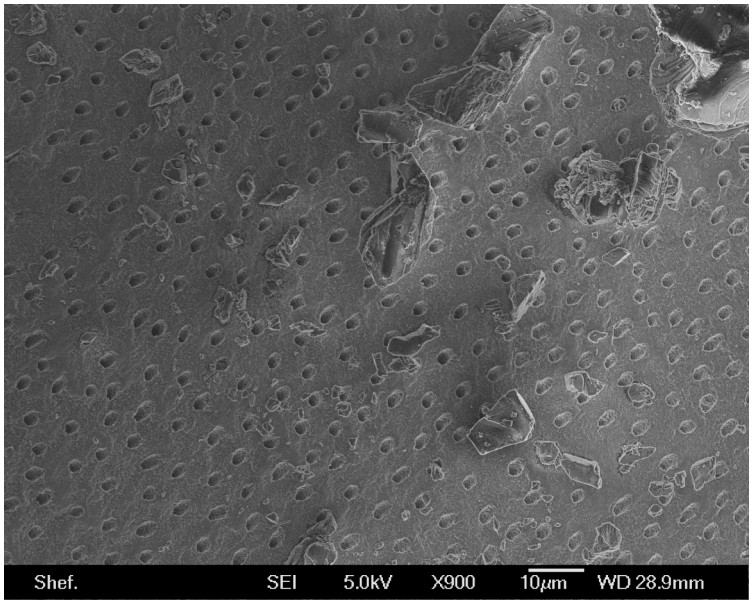

Figure 171 Scanning electron micrograph of dentinal tubules after brushing with Omya 5AV particles in a suspension of distilled H_2O

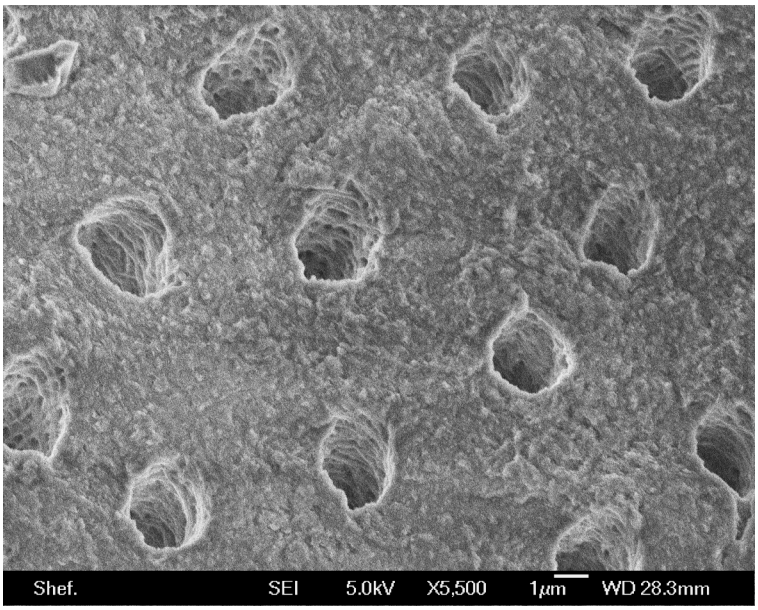

Figure 172 Example of surface roughening observed through brushing with Omya 5av in water suspension

10.3.3 Anhydrous Paste and the Effect of Water Content

Condition (water : paste)	Image
Dry	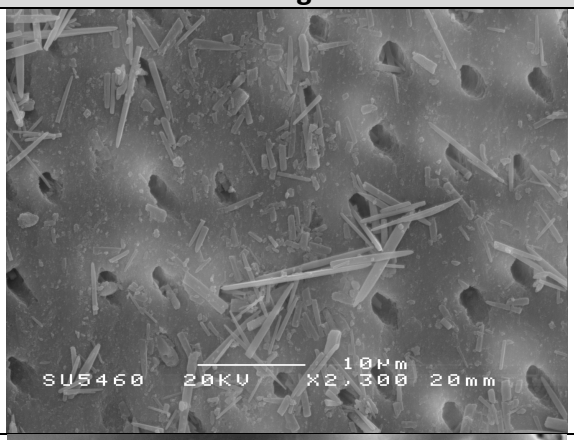
3:1	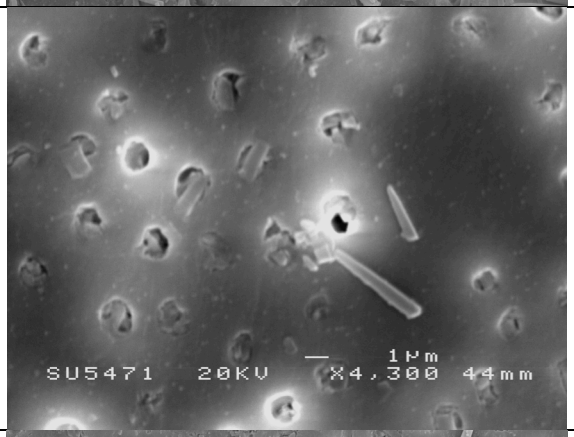
2:1	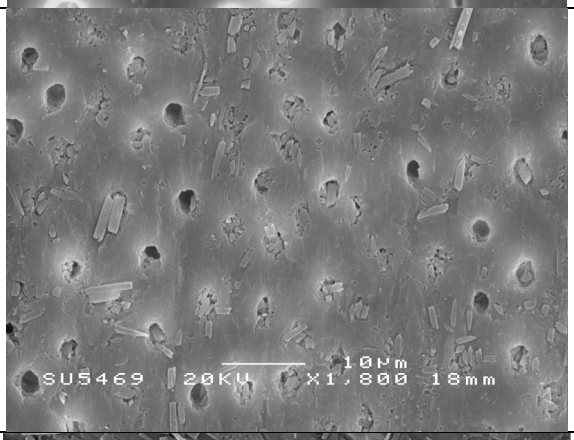
1:1	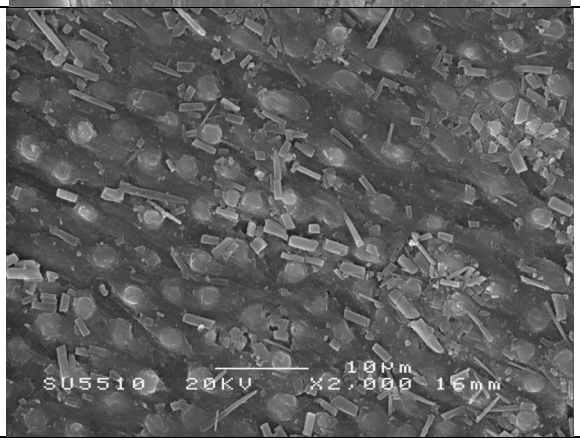

Table 9 Anhydrous paste and the effect of water content

Dry

Trials conducted with solely anhydrous Rod paste without added water led to ineffective tubule capping. Unlike trials conducted using dry particle in a distilled water suspension there does appear to be instances of particles loosely invading tubules, however these are infrequent. There does appear to be a notable increase in particle breakdown with many smaller particle fragments visible after trial. These particle fragments however are largely found around the substrate surface and are seldom seen within tubule lumen. In keeping with other Rod trials there is little evidence of surface damage.

3:1 Ratio

Diluting the anhydrous rod paste using distilled water to a 3:1 ratio led to an increase in particle presence within tubules. As can be seen from Table 9, the frequency of vacant tubules has significantly decreased with a fairly even distribution of filled and unfilled tubules. The density of invading particles is lower than that seen with dry rod particles however the introduction of water to rod paste has led to both an increase small particle fragments and an increase in these fragments being encouraged into tubule lumen. The degree to which tubules are filled cannot however be considered and effective seal. As with other Rod particle trials there appears to be no obvious damage to surface dentine.

2:1 Ratio

A lesser dilution of anhydrous rod paste led to an increase in particle fragments found within dentinal tubules. Further to this increase in occlusive frequency there is an observable increase in the density of particles contained within the tubule lumen. Few tubules remain unfilled post trial and although a complete seal is not achieved the proportion of vacant tubules is now a minority.

Inspection of shape and size of resultant particles suggest that, as seen in dry Rods trials, tips are being fractured away from particles and it is these tips that are being entrained into tubules leading to obstruction. Table 9 shows the contrast in remaining particle size. Some infrequent instances of surface roughening or isolated de-lamination can be found as a result of these trials however these are minimal.

1:1 Ratio

Brushing with an equal ratio of rod paste to distilled water led to the most significant result in terms of tubule occlusion. Tubules were almost entirely sealed with the tubule lumen wholly concealed. Particle breakdown appears extensive similar to trials conducted with dry particles however unlike dry trials the boundaries of tessellating particle fragments are not

visible. In this case a smooth consistent layer spans the tubule lumen. Closer inspection of the sample (Figure 173) shows that the surface has not been coated in an outermost smear layer. Dentine between tubules is still visible however the tubules themselves are occupied and coated by material. It was not obvious from these images as to the structure of these occlusions and whether below this smooth outer barrier there lies a foundation of particle fragments, or if the extent of this protective obstacle is a thin shell. Further work was carried out utilising nano-manipulation technology to investigate this.

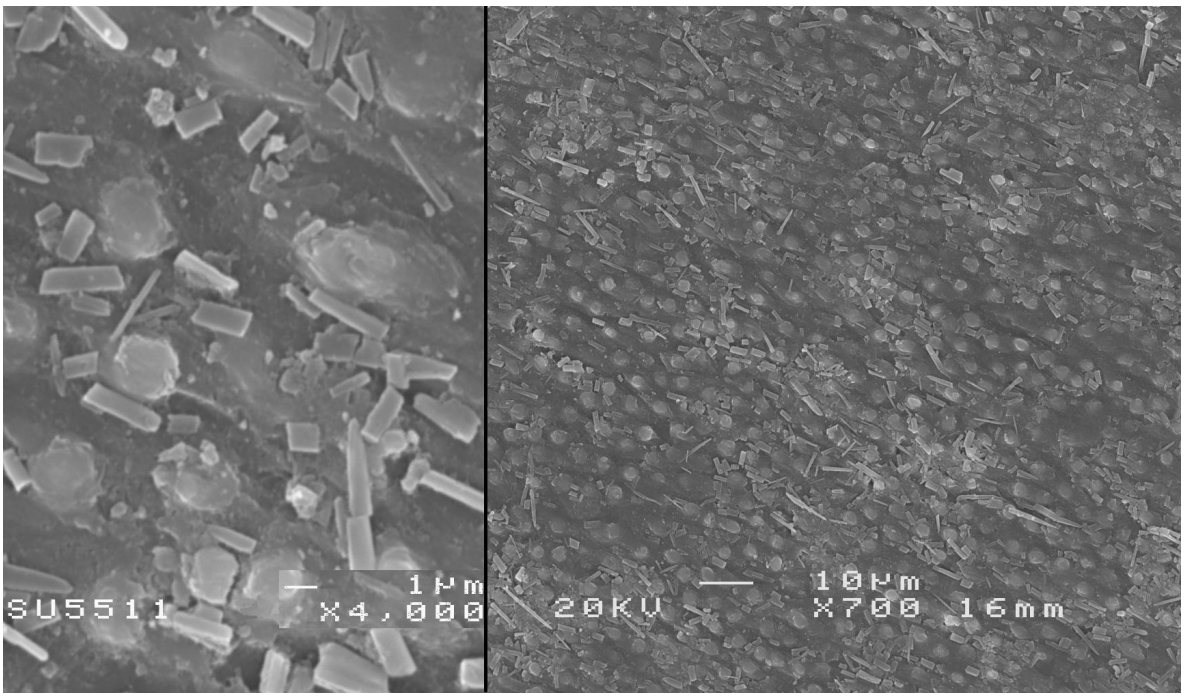

Figure 173 Scanning electron micrograph of dentinal tubules after brushing with Anhydrous Rod paste with distilled water (1:1 – Water : Paste)

10.3.4 Nano-manipulation analysis

Using nano-probes to investigate the comparative resilience of the resultant barriers formed within dental tubules, the efficacy of each experimental scenario can be examined. In the case of Omya 5AV it was found that regardless of the degree to which tubules were infiltrated by particles, that the resultant barrier was not of a solid nature. Particles were relatively loose and could easily be moved within and encouraged out of tubules. Trials conducted using Rod particles yielded varied results with some trials carried out in the presence of water preventing tubule-particle interaction. Those trials which did lead to particle infiltration demonstrated increased particle intractability with particles much more difficult to remove from tubules than Omya 5AV. As seen in Figure 174 with dry trials, the particle fragments are arranged relatively densely. It was not possible to remove these particles from the resultant mosaic nor was there any deflection when the particle layer was loaded using nano-probes. The intractability of the Rod particles is likely to be related to its reliably uniform cross section and the increased precision of tessellation. However the

affinity of the Rod particles to invade tubules is associated with its dynamic and agglomerative characteristics when motivated. (see Figure 175)

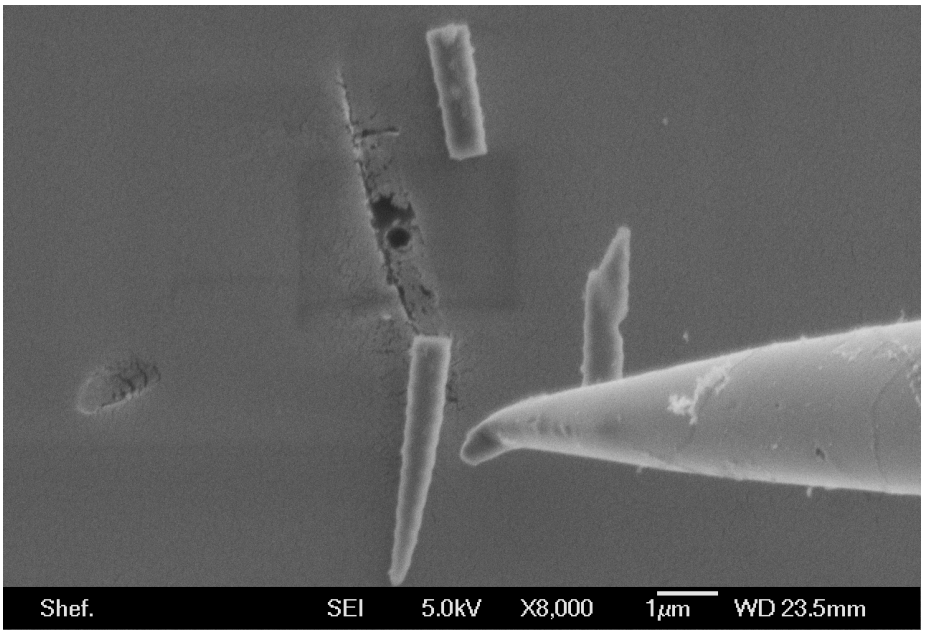

Figure 174 Image of fractured Rod particle being motivated by nano-manipulation probe

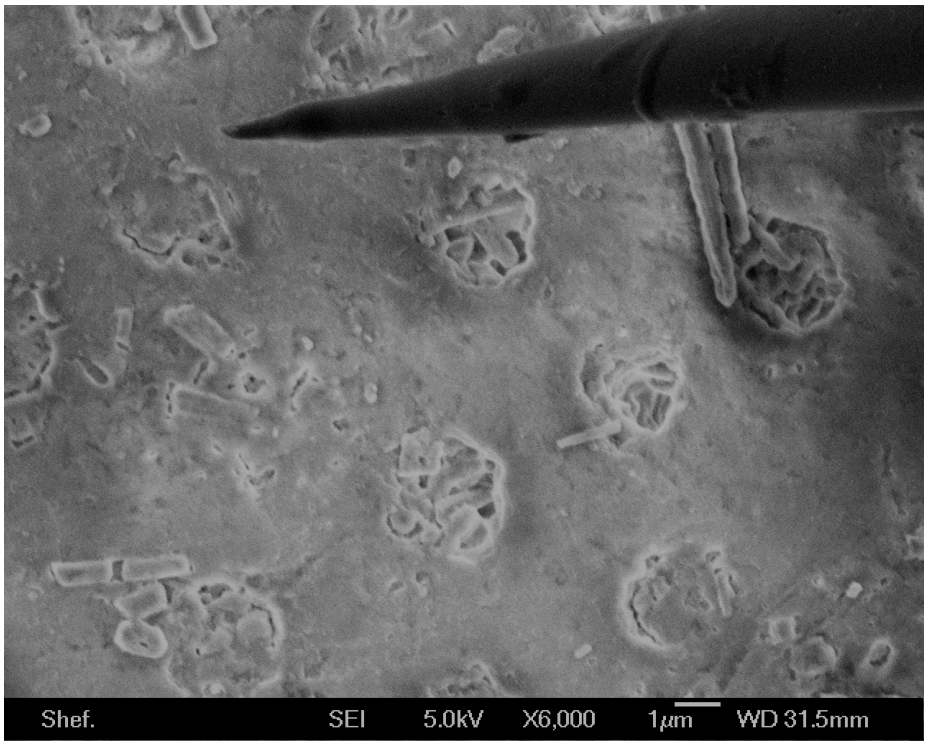

Figure 175 Nano-manipulation of occluding Rod fragments within tubule lumen (Anhydrous Rod paste with water trial, 2:1 ratio)

Omya 5AV particles had significant directional freedom and were prone to rolling about across multiple axes. Showing little agglomerative behaviour they operated primarily as a mass of individual particles. Rods however ardently remained in contact with the substrate

surface with a larger contacting surface area than possible with Omya. Rod particles were rarely found in isolation but rather formed loose agglomerations with particles demonstrating weak adhesion to neighbouring particles (as seen in Chapter 9). Rod particles were also easier to fracture than Omya, which were robust in shape. The increased ease of this particle breakdown is related to substrate hardness, with softer surfaces allowing increased deformation and thus rotation about the point of fracture. Trials conducted on substrates of similar hardness to dentine (Perspex) led to more extensive particle breakdown with characteristically neat edges at the point of fracture. On harder Silicon substrates the mode of fracture was more irregular requiring higher loads to achieve. Fracture characteristics observed in brushing trials upon dentine showed similar characteristics to those observed upon softer substrates (Perspex) in nano-manipulation trials (Figure 176 and Figure 177).

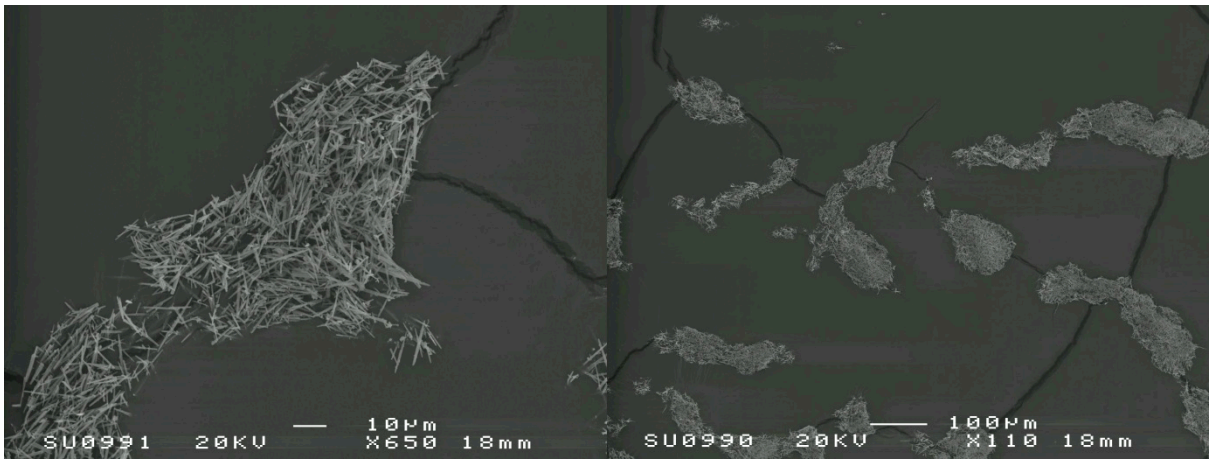

Figure 176 Typical agglomerative formations observed with Rod particles

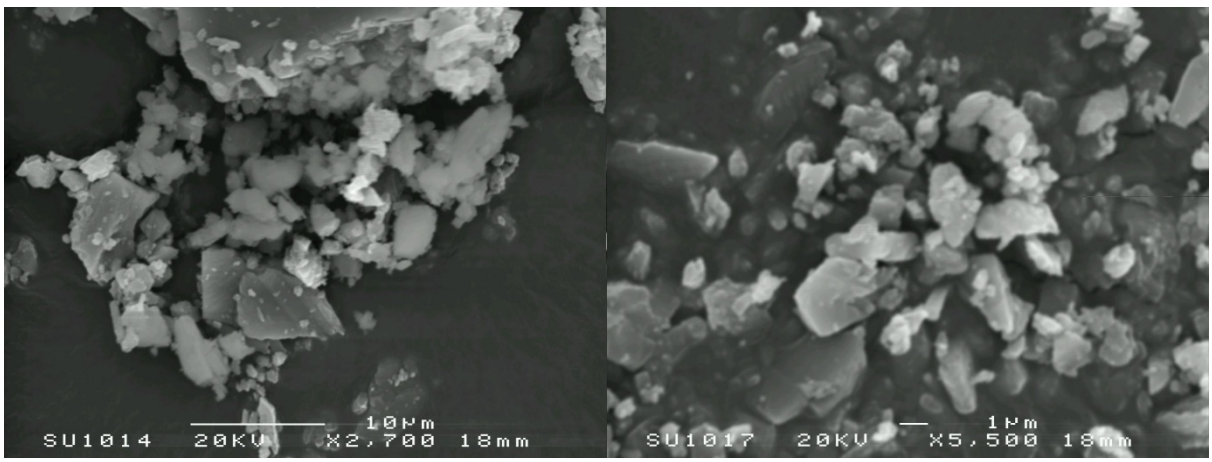

Figure 177 Omya 5AV particles demonstrating little agglomerative behaviour

Motivation of Rod particle agglomerations often led to loose cumulative particle movement rather than separation of particle masses. The orientation of contained particles has little order with many projecting tips loosely interwoven. When particle agglomerations progress over undulations and recessed features in the substrate surface these projecting tips are fractured away, often remaining within the surface feature.

10.4 Discussion

The mode of tubule occlusion investigated within this study differs from some conventional methods, relying primarily on efficient and extensive obstruction of the tubule lumen using particle fragments. Analysis of dentinal tubules after brushing trials showed that Rod particles demonstrated a significantly higher affinity to infiltrate and remain within tubules than the comparison 'standard particle' Omya 5AV. This ability appears delicately related to the magnitude of fluid presence in the brushing scenario.

Particles fully suspended in water were clearly impeded from entering tubules leaving them extensively vacant. This could be a result of particles being suspended in fluid and rarely contacting the substrate surface or effectively being entrained by brush filaments. Initial optical microscope analysis of Rod and Omya 5AV particles in suspension support that Rod particles do remain in suspension for longer than Omya 5AV particles when undisturbed. Taking account of the generic shapes of each particle, Omya being roughly spherical and Rods an elongated cuboid; Omya would have a considerably low surface area to volume ratio. Rods on the other hand, having a high surface area to volume ratio implies the particle will descend more slowly through a fluid medium. Due to the dynamic and turbulent nature of the fluid medium this is likely to further contribute to less Rod particles being in contact with the substrate surface than more spherical particles such as Omya 5AV. As a result there will be less particle entrainment at the point of filament-substrate contact and thus less particle fracture.

SEM analysis of remaining particles supports the resilience of Rod particles with increased fluid content showing very little evidence of particle breakdown. Another possibility is that an increase in fluid presence can lower the prevalence of particle agglomerations with Rods, which in turn could retard the proposed mechanism of particle tip fracture from propagating particle agglomerations. This mechanism fits with nano-manipulation observations, which demonstrated that tips readily fracture away from particles when moving agglomerations leading to many small particle fragments. These fragments were comparable in size to those typically residing in tubules after brushing trials. Nano manipulation observations did show that the tenacity of these Rod agglomerations was very low with weak inter-particle adhesion. This could mean that a subtle increase in fluid is enough to cause these weak agglomerations to disperse, or prevent them from effectively forming in the first place.

In moderation the introduction of water had a beneficial effect on tubule occlusion leading to both increased particle fragment presence within tubule lumen and more comprehensive sealing of the tubule orifice. Part of this improved tubule sealing was the result of a thin layer of deposited material on the surface of the dentine. This additional layer was present only at 1:1 water to particle ratio and using nano-manipulation techniques to excavate,

appeared to have a foundation of solid particle fragments below. This outer layer was approximately one to three microns thick, relatively brittle and difficult to remove. Too higher presence of water however had an acute and detrimental effect on the ability of particles to invade dentinal tubules. This was progressively observed at water-to-particle ratios of 2:1 and 3:1 respectively. The frequency and efficacy of particles in tubules decreased with a greater presence of water; beyond a ratio of 3:1 the effects were similar to that observed with particles in full water suspension.

Further to investigating the efficacy of Rod particles in invading dentinal tubules the robustness and resilience of the resultant seal was also scrutinised. The frequency and density of Rod particles contained within tubules was consistently higher than observed with Omya 5AV particles. Using nano-manipulation the intractability of the contained particles was qualitatively assessed with Rod particles showing significantly more resistance to movement and removal. This is likely to be a result of the neat tessellating nature of Rod particles within the tubule. The orientation of these fragments is most commonly arranged in plane, concurrent with the substrate. Very few particles are seen projecting out from the particle lattice, which could be a result of continued fracture and smoothing during the brushing process. The resultant lattice contains particles, which both overlap and at the circumference of the tubule dig into the tubule walls. The combination of these features is likely to be responsible for the resilience of the tubule blockage with Rods. Omya 5AV particles on the other hand having a larger variance in size and shape do not effectively or neatly arrange themselves within tubules. It is likely that Omya particles contained within tubules are more easily removed by interacting fluid, such as saliva, than Rod particles.

Experiments with Rods both dry and in the form of a more viscous anhydrous Rod paste were both affected in performance by the presence of water. Tubule occlusion through fractured tips increased with the introduction of water up to roughly a 3:1 (water to particle) ratio, after which the occlusion of tubules stopped. One difference between the two systems was that dry rod particles were fairly adept at infiltrating and blocking tubules whereas anhydrous Rod paste on its own was relatively poor. This could be a result of the presence of thickening agents inhibiting the proposed mechanism of particle penetration and occlusion; results from these trials show very little particle breakdown. The introduction of water appears to alter the rheological properties of the paste sufficiently so as to remove this impedance of particle breakdown. The main benefits associated with the use of anhydrous Rod paste are ease of application and the advantageous smooth ‘shells’ forming atop tubule occlusions. Despite most likely not introducing much defensive strength they work in conjunction with a particle fragment foundation, which does provide fairly established support. These outer layers help to more effectively seal the tubule, which should help to reduce odontoblastic stimulus via chemical processes.

10.5 Conclusions

Experiments were undertaken to visualise and understand the invasive efficacy and occlusive capabilities of two abrasive particles with dentinal tubules. The abrasives studied were Maruo Rod particles and Omya 5AV.

There is a clear difference in the occlusive performance of the Rod particles compared to a standard abrasive of generic shape (Omya). Rod particles proved more adept at infiltrating and remaining within tubule lumen that Omya 5AV in all experiments.

The efficacy of the occlusive process for all particles was delicately related to the magnitude of water present. Full water suspension led to almost no tubule infiltration by particles whilst a narrow spectrum of water dilution dramatically augmented the occlusive process. An equal ratio of water to particle led to the most extensive and complete blocking of tubules for Rod particles.

The robustness and resilience of the resultant occlusions using Rod particles are significantly higher than that achieved through using standard comparative particles (Omya 5AV). Optical analysis shows both a neater tessellation and higher density of particles with nano-manipulation able to demonstrate the intractability of contained particles.

With Rods, the primary mechanism behind the occlusive process appears to be from the fracturing of protruding particle tips from agglomerations moving across open tubules. This was supported by nano-manipulation analysis to directly observe this effect. The mechanistic movement and infiltration into tubules with Omya 5AV appears random.

Rod particles appear more sympathetic to dentine than Omya 5AV with no incidence of surface roughening or scratching. Conversely Omya 5AV particles led to often-extensive dentine roughening, apparent in a number of brushing trials.

11 CONCLUSIONS

This chapter discusses conclusions from all testing conducted within this thesis. The three main perspectives for experimentation are addressed: wear behaviour of particles, nano-manipulation findings and dental hypersensitivity.

11.1 Original Objectives

The aim of this work was to investigate the efficacy of novel abrasive particles in oral hygiene. It was important to fully characterise and visually understand the individual particles and their geometric characteristics and how this relates to the way they scratch dental material, for the purposes of improved toothpaste design.

Through a range of experimentation, an understanding of the effect of the particles upon substrates representative of dentine, and using genuine dentine was sought. As part of this testing the primary objectives were:

- To conclusively determine the dynamic characteristics of particles and their mechanistic movements
- To discern the affinity of particles to operate as individuals or to form and remain in agglomerations. To carry out wear experiments to investigate the aggressive nature of the particles as agglomerations and formulate a hierarchy of the particles that pose the greatest threat to Odontogenic tissue.
- To relate the findings from nano-manipulation investigations to observations from wear experiments and gain an understanding of how material damage and surface markings are introduced.
- To gain an understanding of the effect of particle breakdown and fracture characteristics upon the abrasive and interactive properties of the particles
- To analyse the interaction of particles with dentinal tubules and investigate the affinity of bespoke particles (Rods) to aid dental sensitivity.
- To identify optimum abrasives for toothpastes

11.2 Particle conclusions

When considering very small abrasives that are only a few microns or less in size, one may assume that there is little difference from one particle to the next, other than the overall size of the particle. It has been demonstrated from the findings presented that this is not the case and that very subtle differences can have a dramatic effect upon the abrasive performance (and potential damaging behaviour) of the particle.

Using scanning electron microscopy a visual understanding of the aesthetic differences between the particles can be gained, which shows just how varied these particles are. There was a clear contrast in between the physical properties of the Calcium Carbonates manufactured through precipitation processes compared to those produced through grinding. The precipitated particles demonstrate much improved control of size and quality. Quality in this case describes the uniformity and general integrity of the particles. Comparing Maruo Rods and Sturcal particles (precipitates) with Omya 5AV (ground), we can

see that the former has reliably smooth surfaces with few instances of structural imperfections or internal fissures or voids. This is not the case with ground particles. This improved control uniformity does come at cost however with precipitation process being notably more expensive that grinding.

The effect of the different crystal structure upon particles in terms of natural particle shapes when manufactured through grinding is difficult to discern. The chaotic nature of the grinding process is likely to eclipse any natural shape bias caused by crystal structure however precipitated particles are more likely to be effected.

The largest particles considered were bamboo particles shortly followed by polyester resin particles, with the smallest sturcal f and attapulgite clay. Within these investigations the relationship between particle size and the aggressiveness of that particle towards material removal was examined. It could be said that a larger particle does not necessarily suggest that it will be more adept and detrital removal or more likely to cause substrate damage. From testing it was shown that the Sturcal particles were in fact the most aggressive particles tested, with the largest particles (bamboo and polyester resin) being relatively sympathetic to the substrate surface. The aggression of these particles was found to be closely related to how the particles interact with each other, and the degree to which they operate as individuals or as agglomeration.

11.3 Review of nano-manipulation findings

One of the most important objectives of this thesis was to visualise and understand the dynamic particle behavior in situ as it happens. Many experiments were carried to compliment this work however the wear and scratch observations derived through testing and post processing analysis can show only the ultimate result of the particle behavior, and not specifically how this behavior was realised. Emphasis was focused on the 6 high value Calcium Carbonate particles of greatest interest to the sponsor company. Manipulation trials were carried out upon three substrates: Silicon, Perspex and Copper with the latter used to discern surface-marking characteristics derived through typical brushing conditions.

One of the main observations was the clear distinction in the likelihood of damage to the substrate surface caused by rolling particles and sliding particles. Rolling particles led to higher scratch frequency and depth than that observed with sliding particles. The particle that showed the greatest affinity to slide was Maruo rod particles, which, due to its geometry, readily mated flush with the substrate surface and was difficult to remove from contact. This supports the theory of rod particles being both sympathetic to the substrate surface and potentially introducing further positive effects in the form of smoothing effects. As rod particles were invariably motivated flush in contact with the substrate surface it is possible that the rod particle achieve their smoothing ability by contact with and removal of

scratch shoulders. When scratches form there is both a combination of material removal and plastic deformation of the substrate surface relative to the ductility of the material being scratched. The introduction of these pronounced scratch shoulders can cumulatively alter the aesthetic properties of a material making it look rougher or less reflective; within the field of oral care this is an important consideration. We have seen using visualization techniques that Rod particles do indeed move in this way and we have also demonstrated that the addition of Rod particles to Omya 5AV particles (a particle which much more damaging) that it the resultant damage is notably lessened (Chapter 7.3.2.6).

Subtle variation in particle geometry had a significant effect upon the dynamic mechanism adopted. Maruo Rod particles are visually similar in appearance to Sturcal F particles however subtle differences in the uniformity of the particle alters the mode of movement from a sympathetic sliding to more aggressive rolling mechanism. Similarly Omya 5AV particles and Albafil are both diverse multifaceted particles however the recurrent presence of one or more larger flat face with Albafil encourages the particle to cease rolling and begin sliding. As a result there are considerable differences in substrate damage.

The primary focus of this investigation has been on the dynamic properties of individual particles however the most significant substrate damage was introduced through particle agglomerations. Sturcal L and Sturcal F showed the greatest affinity to agglomerate with Sturcal L demonstrating significant inter-particle attraction and agglomerate resilience. Although the cause of this tenacious particle bonding is not apparent it is responsible for a significant increase in surface damage with Sturcal L. The particle most sympathetic to the substrate surface causing the least amount of damage within trials on polished copper was Maruo Rods. The analysis of the motivation of agglomerations of Rod particles was also key in formulating explanation as to the efficacy of Rod particles as an effective agent against dental hypersensitivity; this is discussed in more detail in Chapter 11.5.

The manipulation experiments in this investigation were conducted dry, both to gain insight into the dynamic properties of the particles without bias; but also due to the necessity for the SEM environment to remain free of moisture. This will undoubtedly lead to different environmental conditions to that found in the mouth and further research would need to be conducted to discern the affect of water on the particles dynamic and interactive behaviour. The main aim of section of research was to gain an understanding of how the basic geometric and physical properties for the particles, and the subtle variation in these particles can lead to dramatically different results in terms of potential damage and possible material removal. It was then possible to use these findings to draw conclusions as to how these properties might be exploited to introduce positive effects within oral care procedures.

11.4 Review of particle wear behaviour

A number of experimental procedures were adopted in order to study the scratch and wear characteristics of the different particles. As expected there was significant variation in both the appearance and the severity of the wear behaviour between particles.

Linear reciprocation trials showed some particles to demonstrate low scratch frequency and depth suggesting they are sympathetic to the substrate surface. This is not necessarily a reflection upon the particles efficacy as an abrasive. The geometry and dynamic characteristics of these 'gentle' particles when motivated may well make them adept at removing surface detritus and macroscopic asperities without marking the substrate surface. Hubersorb 600 had both the lowest average scratch frequency and scratch depth despite being similar in size to Omya 5av, which was relatively aggressive.

It is apparent that a subtle change in size or shape can have a dramatic effect on the aggressiveness of the particle to the substrate surface. This could be contributed to a number of factors including a change in the in the agglomerative behaviour of the particle. This ties in with observations made in Chapter 7. There was little relationship between particle size and scratch frequency above 10µm, however there was a more legible relationship between particle size and scratch depth observed.

The particle the highest average scratch frequency was Vicality Albafil (3.6 microns) and the particle with greatest average scratch depth was FM1000 (7.6microns). FM1000 particles are by no means the largest of the tested particles and therefore a particles affinity to scratch is subject to other variables. We can see from Chapter 6, we can see that FM1000 demonstrated one of the most significant 'angle of repose' results of all the particles.

It was important to conduct testing upon genuine Odontogenic material in to observe the particles behaviour within representative conditions. Using computer controlled Tribometer setups and adjusting associated variables it was possible to appreciate the effect of these variables upon the abrasive performance of the particle. Particle behaviour was seen to vary depending on the speed and load applied. Complemented by nano-manipulation observations we can see that this is usually a result of a change in mechanistic movement for the particle; In some cases a transition from sliding to rolling or vice versa.

It was clear that entrainment speed had a greater effect on wear than load. Maruo Rods and Sturcal L particles were observed to be the only samples with which speed had little effect on wear rate. Trials without particles at the contact (water only) produced no noticeable wear demonstrating that it is the effect of the particles that is being observed during this testing.

In some cases, the mixing of particles led to a synergistic change in wear performance, most significantly with Maruo Rods, where the wear was greater than for the two individual particles combined. Other particles such as Sturcal L in mixture however led to a reduction in wear. When introduced with Omya 5AV particles, Maruo Rods showed polishing effects on the small scale scratching.

It was shown that a modification of the viscosity properties of the abrasive slurry can modify the abrasive performance of the particle. In this case experimentation using a agar based binding agent was carried out. Review of the COF data for the particles showed that in many cases the introduction of a binding agent increased the friction properties whilst reducing the observed surface damage. It could be that this may make for an effective balance between stain removal and remaining sympathetic to the substrate surface.

The importance of particle agglomeration was highlighted during wear trials, with the affinity of the particle to operate as an individual or as an agglomeration was shown to have a dramatic effect upon the likelihood of the particle to lead to surface damage. The particles, which showed the greatest affinity to agglomerate was Sturcal L and Sturcal F, these particles also lead to the most aggressive wear observed. Chapter 9 investigates the geometrical properties of these particles, where it was found that the spherical shape of the agglomeration and the notable order with which the particles were arranged (in the case of Sturcal L presenting multiple sharp particle tips) contributed to the aggressive nature of the particle. The primary mechanism for particle agglomeration was found to be nucleation to larger particles rather than repeated pairings of individual particles.

11.5 Review of Dental Hyper-sensitivity findings

Experiments were undertaken to visualise the invasive efficacy and occlusive capabilities of two abrasive particles with dentinal tubules. The abrasives studied were Maruo Rod particles and Omya 5AV.

There is a clear difference in the occlusive performance of the rod particles compared to a standard abrasive of generic shape (Omya). Rod particles proved more adept at infiltrating and remaining within tubule lumen that Omya 5AV in all experiments.

The efficacy of the occlusive process for all particles was delicately related to the magnitude of water present. Full water suspension led to almost no tubule infiltration by particles whilst a narrow spectrum of water dilution dramatically augmented the occlusive process. An equal ratio of water to particle led to the most extensive and complete blocking of tubules for rod particles. Without further investigations it is difficult to know for sure the reasoning behind why the efficacy of the process is sensitive to water presence. One explanation could be related to the prevalence of fractured tips available. As observed in

both brushing trials and Nano manipulation trials, Rod particles gather up relatively easily and move as a mass or lattice with many projecting tips. As these particle masses progress over open tubules the particle tips break off and remain within the lumen, ultimately sealing it off. Water presence might impede this in two ways, firstly if the water discourages the particles from forming these localised agglomerations; and secondly by remaining in tubules and impeding the particle fragments from infiltrating. Just the right ratio of water to particle slurry however may encourage this process thus leading to the optimum results we observed with a 1:1 ratio.

The robustness and resilience of the resultant occlusions using Rod particles are significantly higher than that achieved through using standard comparative particles (Omya 5AV). Optical analysis shows both a neater tessellation and higher density of particles with nano-manipulation able to demonstrate the intractability of contained particles.

With Rods, the primary mechanism behind the occlusive process appears to be from the fracturing of protruding particle tips from agglomerations moving across open tubules. This was supported by nano-manipulation analysis to directly observe this effect. The mechanistic movement and infiltration into tubules with Omya 5AV appears random.

11.6 Recommendations and industrial application of findings

As a result of the comparison of Precipitated Calcium Carbonates with Ground Calcium Carbonates it can be said that the typical geometry of GCC particles are varied and multifaceted. PCC's on the other hand offer more constrained geometry with a reduction in sharp edges. As a result PCC's are statistically less likely to roll than slide and therefore pose less of a threat to a substrate surface than GCC's. Further to this the shape and size can be modified by revising conditions in the manufacturing process, such as temperature or pressure. From observations gained through nano-manipulation experiments it could be proposed that the optimum desirable shape for the precipitate would be to modify the shape of Rod particles according to the following amendments:

- Maintain the flatness of the upper and lower face but increase the width of the particle. This would serve to maximise the potential of the particle to remain in contact with the substrate surface whilst improving the potential of the abrasive to remove surface build-up and scratch shouldering effects.
- To decrease the length of the particle. By lowering the aspect ratio of the particle and making them less needle like they are less likely form loose interwoven agglomerations which introduce projecting tips into and away from the substrate surface. This would also serve to improve the overall strength of the particle decreases breakdown. This was observed with Sturcal F particles, which were notably stronger and resistant to breakdown when loaded.

- To limit the tapering tips. The delicate nature of the pointed tips of the Rods made them very easy to break off, forming a particle with an entirely different mechanistic movement; one which almost entirely rolled leading to higher substrate damage. This may have proven beneficial in tubule infiltration studies (Chapter 10) however in applications where dentinal tubules do not feature, this is not a necessary benefit.

Many experimental findings within this thesis suggest that a subtle variation in the physical properties of a particle can have a dramatic effect on the abrasive performance of that particle. As a result, by augmenting the precipitation process it may be possible to gain control of the ultimate efficacy of the particle. By playing with the associated variables, the manufacture process can be changed to meet the needs of the cleaning process. For example, to encourage agglomeration in cleaning scenarios where the substrate is not delicate and maximum detrital removal is desirable.
In order to investigate this, subtle variations of an individual particle would need to be produced. These variants can then be studied using nano-manipulation techniques, and the findings related back to wear observations (much like the experimental process for work in this thesis). By analysis of enough particle permutations, trends can be observed which may lead to more considered manufacture processes for precipitated Calcium Carbonates.

It has been demonstrated that the implementation of some particles as mixtures can have a positively synergistic effect on the wear behaviour (in the case of the work conducted here this was the addition of Rod particles leading to improved substrate smoothing). It would be of interest to investigate the formulation of combination paste slurries, with the strengths of two particle traits. Particle combinations could be used in industry with the following potential benefits:

- Combining the abrasive aggression of some particles (Omya 5AV, Sturcals) to remove surface detritus, and the smoothing potential of rods to improve substrate aesthetics.Although, when mentioned earlier in this thesis, the synergistic relationship of particles when used in tandem did in some cases lead to increased aggression; This was only an result in some cases. In other there was instances of the particles introducing smoothing affects, such as the case in question here, with Rod particles leading to substrate smoothing. The point being made is that the results show that with careful consideration we can augment the behaviour and synergistically improve the performance of particles with some combinations. More work would be required to clarify and quantify this effect.
- Combining particles that demonstrate effective tubule infiltration and sealing (maruo rods) with potentially cheaper particles that abrasively competent. This way a cost effective paste can be produced with positive claims towards aiding dental hypersensitivity.

- Introducing paste inclusions that capitalise on the agglomerative affinity of some particles. Particles such as Maruo rods sturcal L and F readily form and are motivated as agglomerations. Many natural materials (potentially waste products from other manufacturing processes) could be introduced which are likely to be readily entrained by these agglomerations (facilitating the abrasive process). An example might take the form of dry shards of rind or peel from fruits. These inclusions would have form and geometry sufficient to become easily entrained. These inclusions would need to adhere to toxicology guidelines and ideally be readily available and cheap to source. These are often benefits associated with naturally source materials.

11.6.1 Key benefits of this research to end users

Oral care is a fiercely competitive industry, with manufacturers investing significant sums of money into research, which potentially may reveal a competitive edge, or a better understanding of the mechanistic characteristics of their cleaning products.

The research that was tasked began with the very broad focus of analysing materials common to existing products, and trying to qualitatively and quantitatively gauge the abrasive performance of these particles. It quickly became apparent that there were areas that would be of key importance for scrutiny, including: the affect of particle size and shape, the agglomerative behaviour of the particles, and the affinity of particles to infiltrate and remain in tubules.

The latter of the above areas of research (tubule infiltration) led to one of the most significant contributions as well as a patent for a new sensitivity aid. This work is discussed in Chapter 10, but the main findings centred on both the importance of particle shape, and the sensitive relationship with the presence of water. Commonly formulas that are designed to be presented as dental sensitivity aids rely on either random particle infiltration or seeded crystal growth to occlude tubules. With this in mind, particles are often sought that are small and smooth so that the potential for them to drop into tubules unimpeded is maximised. What was found within this research however is that long angular particles (Rods), which ordinarily may not be considered due to their size being larger than the tubules they are trying to infiltrate, can be utilised according to different mechanisms which prove adept and sealing off the tubule orifice. A further benefit of this is that PCC particles allow for the potential to dictate particle size and shape by augmenting the precipitation conditions, which will allow for variations in particle form to be studied.

Although it was already understood that the inclusive particles have a profound affect on the abrasive performance of a paste, this work has highlighted how a very subtle change in particle size and geometry can have a notable affect on the agglomerative behaviour of that particle, and thus a potentially dramatic effect on wear rate. As a result the sponsor company now gives careful consideration to this affect and further work is being conducted in an effort to exploit this. For example in third world countries, particularly regions of India, the most popular formulations of those with very coarse inclusions which make the user

able to really feel the active agents at work. Some larger particles can prove expensive relative to the more budget components in these formulations. As a result of supporting work within this thesis different approaches are entertained, including adopting smaller particles (which may have better individual abrasive properties) but augmenting the agglomerative behaviour of these particles to lend the texture of a coarse paste.

11.6.2 Critical Review of this research

This work has set the stage for further research to look in more detail at questions that have been raised during the course of these experiments:

- Can modifications in the precipitation process give control of particle size and shape and thus can the efficacy of abrasive particles be controlled?
- I have shown that synergistic particle combinations can be employed. The detailed interaction of particles when working in tandem is an interesting and broad opportunity for further investigation.
- Much work here has value in how it compares the dynamic behaviour of particles. Whilst a multitude of wear experiments have been conducted within this research, it would be of value to conduct direct nano-manipulation experimentation of particles when in a fluid medium. The research conducted here begs the question of how the dynamic behaviour of particles changes and differs when in fluid.

The following critical reflection on this work is conducted from 4 key perspectives:

1. **The suitability of the research**

The subject matter of oral care very is prevalent in research currently with large sum of money invested in products and research into their performance and development. The work conducted in this thesis was done so using the latest particles of interest to the sponsor company and covered a spectrum of characteristics from budget to bespoke particles.

Experimentation was conducted both with the various aims of a manufacturing company in mind; not just the effectiveness of an abrasive particle but also factors related to each particle such as cost of manufacture and availability amongst others.

This work has provided the sponsor company with specific insight into the dynamic properties of the particles, something that has been lacking in literature, which focuses more on the affect of particle size on wear characteristics.

2. **The effectiveness of the data collection process**

Throughout this work consideration has been given to the variability in dentine and how this may skew results by offering variation in substrate material properties. This is but one consideration demonstrating the meticulous nature to which data was acquired. Trials were conducted multiple times, as minimum in triplicate, but if the associated setup was considered at all unpredictable often up to ten times, in order to improve the reliability of results.

3. The validity of the sample selection process

Prior experimentation was conducted to see how representative bovine dentine is as a human dentine substrate, it was determined that this was not in fact a satisfactory substitute. As a result all experiments were conducted on human dentine making the results further validated

Consideration was given to both the donor from which samples were acquired, as well as stringent constraints applied to the sample storage and preparation processes. Stringent constraints were applied to sample donors. Samples were acquired only from adult humans all above the age of 18. Sourced teeth were removed for orthodontic purposes and were free of caries and of sound oral health

4. The appropriateness of the research methodology to the research subject

Experimental setups were designed to be as representative as possible to a realistic brushing scenario. It was appropriate however to consider the reproducibility of experiments, and the variability of brush filaments was in some cases confounding. For that reason, in experiments focusing on subtle wear effects the interface between the particles and the substrate was simplified (for example to that of a solid nylon ball). Although dissimilar to a conventional brushing setup the results can still be compared and contrasted satisfactorily, but with the added benefit of a solid reliable contact not being susceptible to variation which may confound results.

Experimentation was conducted on regions of dentine which was representative of that which would become exposed naturally through gum recession and other regularly occurring processes. Although there is only negligible difference in the mechanical properties of the different dentine's, it was deemed probable that the difference in tubule frequency could affect proceedings when interacting with particles and particle agglomerations (particularly with respect to tubule infiltration trials). This attention to detail regarding the representativeness of setup was extended to all aspects of experimental procedure.

12 REFERENCES

[1] Daily Fact Fix. 2011. factfixx.com. [ONLINE] Available at: http://www.factfixx.com/2011/06/28/invention-of-the-toothbrush/. [Accessed 08 November 13]

[2] F. Bernardini, C. Tuniz, A. Coppa, L. Mancini, D. Dreossi, D. Eichert. "Beeswax as Dental Filling on a Neolithic Human Tooth," PLoS ONE, vol. 7, pp. 188-197, 2012.

[3] Edward Byrne BDS DGDP. 2002. edwardbyrne.com. [ONLINE] Available at: http://www.edwardbyrne.com/erosion.htm. [Accessed 16 November 13]

[4] B. James, J. William Robbins, R. S. Schwartz. "Fundamentals of Operative Dentistry: A Contemporary Approach." 2nd edition. Carol Stream, Illinois, Quintessence Publishing Co, Inc, p. 128. ISBN 0-86715-382-2, 2001.

[5] Brighton Implant Clinic. 2010. brightonimplantclinic.co.uk. [ONLINE] Available at: http://www.brightonimplantclinic.co.uk/periodontal-disease-photos/. [Accessed 22 November 13]

[6] E. M. Wilkins, "Clinical practice of the dental hygienist " vol. 11th Edition, Special Care in Dentistry, pp. 274–275, doi: 10.1111/j.1754-4505.1983.tb00117.x, 2012.

[7] R. Eric, C. Reynolds, "Contents of toothpaste – safety implications," Australian prescriber, vol.17, pp. 49-51, 1994.

[8] A. Lovdal, A. Waerhaug, "Incidence of clinical manifestations of periodontal disease in light of oral hygiene and calculus formation," Journal of the American Dental Association, vol. 56, Issue 1, pp.21-33, 1958.

[9] A. M. Helmenstine. 2014. chemistry.about.com. [ONLINE] Available at: http://chemistry.about.com/od/geochemistry/a/mohsscale.htm. [Accessed 17 December 13]

[10] R. Lewis, S. C. Barber, and R. S. Dwyer-Joyce, "Particle motion and stain removal during simulated abrasive tooth cleaning," Wear, vol. 263, pp. 188-197, 2007.

[11] D. Stachowiak, "Simulation of three-dimensional abrasive particles," Wear, vol. vol.258, pp. 208-216, 2005.

[12] C. Arrais, "Occluding effects dentrifices on dentinal tubules," Journal of Dentistry, vol.31, pp. 577-584, 2003.

[13] Z. Wang, Y. Sa, S. Sauro, H. Chen, W. Xing, X. Ma, "Effect of desensitising toothpastes on dentinal tubule occlusion: A dentine permeability measurement and SEM in vitro study," Journal of Dentistry, vol. 38, pp. 400-410, 2010.

[14] Oxford University Press, "Oxford Dictionary of English (3 ed.)", Print ISBN-13: 9780199571123, DOI: 10.1093/acref/9780199571123.001.0001, 2010.

[15] I. M. Hutchings, "Tribology, Friction and Wear of Engineering Materials", Publisher: Edward Arnold, ISBN 034056184X, 9780340561843, 1992.

[16] N. P. Suh, "The delamination theory of wear," Wear, vol.25, pp. 111-124, 1973.

[17] N. P. Suh, "An overview of the delamination theory of wear," Wear, vol. 44, pp. 1-16, 1977.

[18] J. Gates, "Two-body and three body abrasion: a critical discussion," Wear, vol. 214, pp. 139-146, 1998.

[19] ASM Handbook Comittee (2002), "Friction Lubrication and Wear Technology," ASM Handbook, U.S.A, ASM International, vol. 18, pp. 18-21, 2002.

[20] M. Levy, "The effect of erodent particle characteristics on the erosion of metals," Wear, vol.151, pp. 381-390, 1991.

[21] A. L. P. Chhik, "The effects of erodent composition and shape on the erosion of steel", Wear, vol. 89, pp. 151-162, 1983.

[22] F. I. Misra A, "On the size effect in abrasive and erosive wear," Wear, vol. 65, pp. 359-373, 1981.

[23] R.L. Aghan, "Mechanisms of abrasive polishing," Wear, vol.16, pp. 293-301, 1970.

[24] F. J. R. Tegethoff, E. Kroker, "Calcium carbonate : from the Cretaceous period into the 21st century,", ISBN 9783764364250, Basel : Birkhauser, pp. 78-82, 2001.

[25] R. Lewis, R.S. Dwyer-Joyce, "Fluid/Solid Interactions in Abrasive Cleaning", Department of Mechanical Engineering, University of Sheffield, Internal report, p.19, June 2000.

[26] N. S. H. Sin, N.P. Suh, "Abrasive wear mechanisms and the grit size effect," Wear, vol. 55, pp. 163-190, 1979.

[27] A. M. E. Rabinowicz, "Effect of abrasive particle size on wear," Wear, vol. 8, pp. 381-390, 1965.

[28] S. Yin, L.K. Ives, "Abrasive machining of porcelain and zirconia with a dental handpiece," Wear, vol. 225, pp. 975-989, 2003.

[29] R. Schilke et al, "Comparison of the number and diameter of dentinal tubules in human and bovine dentine by scanning electron microscopic investigation," Archives of Oral Biology, vol. 45, pp. 355-361, 2000.

[30] M. S. Helfer, H. Schilder, "Determination of the moisture content of vital and pulp less teeth," Oral Surg Oral Med Oral Pathol, vol. 34, pp. 661-670, 1972.

[31] W. G. Matthews, C. D. Showman, and D. H. Pashley, "Air blast-induced evaporative water loss from human dentine, in vitro," Archives of Oral Biology, vol. 38, pp. 517-523, 1993.

[32] R. Lewis, R.S. Dwyer-Joyce, "Fluid/Solid Interactions in Abrasive Teeth Cleaning", University of Sheffield, Internal Report, pp. 7-14, 2001.

[33] R. Lewis, and R. S. Dwyer-Joyce. "Interactions between toothbrush and toothpaste particles during simulated abrasive cleaning." Proceedings of the Institution of Mechanical Engineers, Part J: Journal of Engineering Tribology, vol. 220, Issue 8, pp. 755-765, 2006.

[34] C. Chuenarrom et al, "Effect of Indentation Load and Time on Knoop and Vickers Microhardness Tests for Enamel and Dentin," Materials Research, Vol.12, pp. 473-476, 2009.

[35] I. Slutzky-Goldberg, M. Maree, R. Liberman, L. Heling, "Effect of Sodium Hypochlorite on Dentin Microhardness," Journal of Endodontics, Vol. 30, pp. 880-882, 2004.

[36] Z. Liu, "Measuring the angle of repose of granular systems using hollow cylinders", PhD Diss, University of Pittsburgh, 2011.

[37] A. J. Baker, "A study of tribological processes during the milling of rice", PhD Diss, University of Sheffield, p. 76, 2014.

[38] A. Kishen, "Mechanisms and risk factors for fracture predilection in endodontically treated teeth," Endodontic Topics 2006, vol. 13, pp. 57–83, 2006.

[39] S. Ito et al. 2003. Wiley InterScience. [ONLINE] Available at: http://onlinelibrary.wiley.com. [Accessed 27 January 14].

[40] M. Sitti, H. Hashimoto, "Controlled pushing of nanoparticles: modelling and experiments," IEEE/ASME Transactions on Mechatronics, vol. 5, pp. 199-211, 2000.

[41] Z. W. Jing Hou, L. Liu, Y. Yang, "Modelling and analyzing nano-particle pushing with an AFM by using nano-hand strategy," Nano/Micro Engineered and Molecular Systems (NEMS), 5th IEEE International Conference on. IEEE, pp. 518-523, 2010

[42] A. F. Lixin Dong, T. Fukuda, "Nanorobotic manipulation of nano-order objects inside SEM," Micromechatronics and Human Science (MHS), Proceedings of 2000 International Symposium on. IEEE, pp. 151-156, 2000.

[43] M. Sitti, "Survey of nanomanipulation systems," Nanotechnology, IEEE-NANO, Proceedings of the 2001 1st IEEE Conference on. IEEE, pp. 75-80, 2001.

[44] K. Nanotechnik, "MM3A Micromanipulator System Manual ", Version 4.03, 2005.

[45] M. Evstigneev, K. Mougin and P. Reimann, "Modelling of nanoparticle manipulation by AFM: Rolling vs. sliding regimes," EPL (Europhysics Letters), vol. 101, number 6: 66002, March 2013.

[46] D. Keeling, R. Fawcett, P. Beton, C. Hobbs, L. Kantorovich, "Bond breaking coupled with translation in rolling of covalently bound molecules." Physical review letters vol.94, number 14: 146104. 2005.

[47] A. Maskara, D.M. Smith, "Factors Affecting Strength of Agglomerates Formed During Spray Drying of Nanophase Powders," MRS Proceedings, vol. 346. Cambridge University Press, p.637, 1994.

[48] D. A. Sumikawa, "Microstructure of primary tooth dentin," American Academy of Pediatric Dentistry, vol. 21, Issue 7. pp.439-444, 1999.

[49] C. Camargo, M. Siviero, S. Camargo, S. De Oliveira, C. Carvalho, and M. Valera, "Topographical, Diametral, and Quantitative Analysis of Dentin Tubules in the Root Canals of Human and Bovine Teeth," Journal of endodontics, vol. 33, pp. 422-426, 2007.

[50] Stedman, "Definition of dentinal fluid," Stedman's medical dictionary, 26th edition, Lippincott Williams and Wilkins Edition, p. 665, ISBN: 0-683-40007-X ,1995.

[51] M. Brännström, A. Åström, "A Study on the Mechanism of Pain Elicited from the Dentin," Journal of Dental Research, vol. 43, pp. 619-625, 1964.

[52] M. N. Turker, "A Method for Studying the Peripheral Mediators of the Dental Pain Induced by Electrical Stimulation," Archives Of Physiology And Biochemistry, vol. 83, pp. 553-561, 1975.

[53] R. Melzack, P. D. Wall, "Pain Mechanisms: A New Theory," Survey of Anesthesiology, vol. 11, pp. 89-90, 1967.

[54] C. Arrais, C. D. Micheloni, M. Giannini, and D. Chan, "Occluding effect of dentifrices on dentinal tubules," Journal of Dentistry, vol. 31, pp. 577-584, 2003.

13 APPENDICES

Appendix 1

Tubule density:

	Bovine Dentine	Human Dentine
No. of measurements	200	200
Average distance (µm)	7.05	3.04
Standard deviation	2.47	0.87
Student T Value	$5.936E^{-53}$	

Figure A3.1.

Tubule width:

	Bovine Dentine	Human Dentine
No. of measurements	200	200
Average width (µm)	1.84	3.10
Standard deviation	0.365	0.374
Student T Value	$6.12E^{-14}$	

Figure A3.2.

Density	Width
• Null hypothesis - There is no statistical difference between data sets • Critical value P = 0.05 >0.05 accept null hypothesis <0.05 accept null hypothesis **In this case (Tubule distance from neighbour) the differences between Bovine Dentine and Human Dentine were very significant: P = 5.94E-53**	• Null hypothesis - There is no statistical difference between data sets • Critical value P = 0.05 >0.05 accept null hypothesis <0.05 accept null hypothesis **In this case (Tubule diameter) the differences between Bovine Dentine and Human Dentine were significant:** **P = 6.115E-14**

Figure A3.3.

Appendix 2 – Common crystal systems

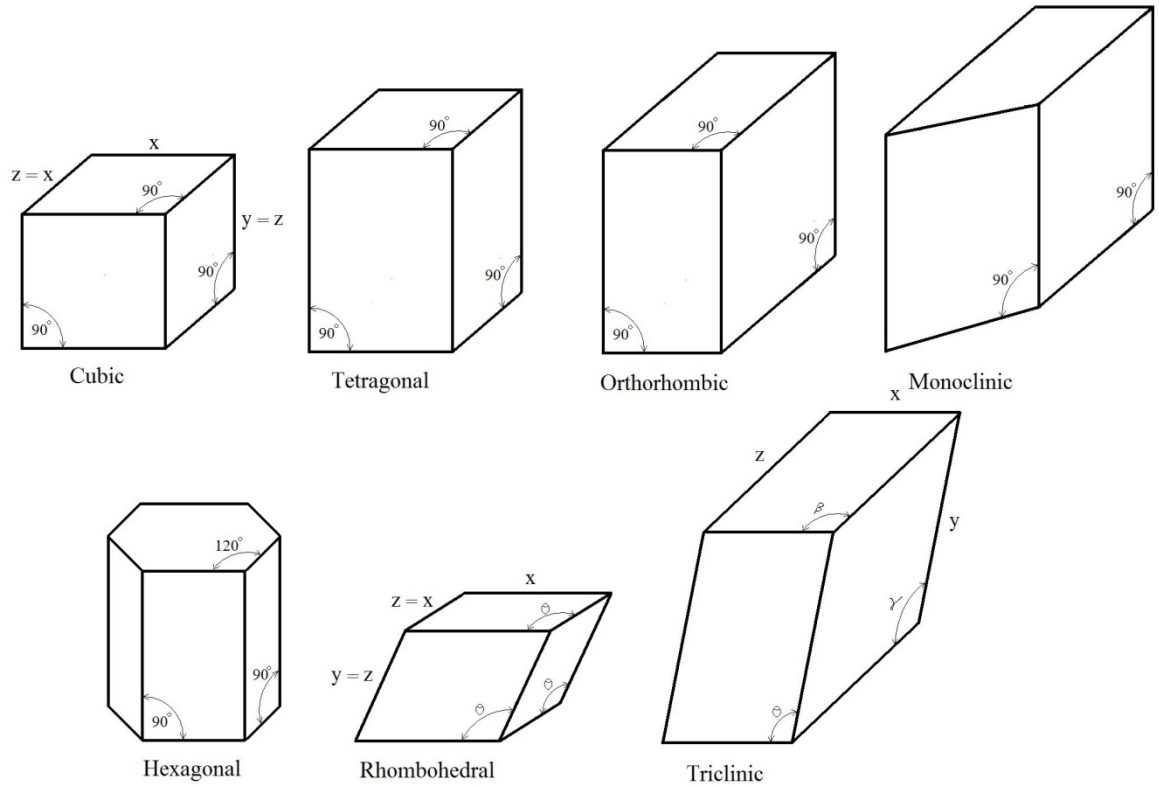

Figure A4.1.

Appendix 3 - Table of measured values derived from AFM surface scans of scratched Perspex for different particles

Particle	Size (microns)	Start (20°)	Middle (35°)	End (70°)	Average scratch frequency (µm)	Greatest Scratch Depth (nm) (Start)	Greatest Scratch Depth (nm) (Middle)	Greatest Scratch Depth (nm) (End)	Average scratch depth (nm)	Ra (start) (nm)	Ra (Middle)(nm)	Ra (End) (nm)	Average Ra (nm)
Bamboo	345	18	22	19	20	205	122	66	131	23	28	9	20
PE Resin	255	23	25	25	24	109	105	61	92	9	38	9	19
Hub.5121	125	14	27	14	18	72	108	66	82	8	14	13	12
Hub. 250	83.5	22	12	11	15	76	69	43	63	8	6	4	6
Perlite	33	33	22	28	28	266	568	302	379	28	89	26	48
MEV Vermiculite	28.15	17	22	20	20	205	168	149	174	29	30	11	23
S20 Talc	11.04	23	26	21	23	275	360	266	300	47	82	31	53
B200 Prologite Mica	11	19	20	18	19	215	236	244	232	23	29	25	26
FM1000	7.595	12	15	18	15	633	485	323	480	100	104	49	84
Omya 5AV	7	24	14	27	22	263	241	170	225	34	40	36	37
Hub. 600	6.065	15	13	17	15	5.6	8.3	5.2	6	2	4	7	4
Rods	6	18	18	18	18	59	35	40	45	6	6	7	6
Barralev A	5.225	24	25	29	26	62	83	63	69	4	11	8	8
S2E PCC	3.88	33	29	39	34	58	60	21	46	6	9	3	6
Vicality Albafil	3.6	38	42	33	38	45	58	71	58	8	9	8	8
SC103 Attapulgite Clay	2.47	44	34	27	35	59	101	48	69	11	16	4	10
Sturcal F	1.3	44	29	32	35	77.3	178	161	139	13	31	20	21
		24.76	**23.24**	**23.29**		**157.9**	**175.6**	**123.5**		**21**	**32**	**16**	

Figure A5.1.

Appendix 4 – Graphs comparing the 'roundness' of particles with both scratch frequency and scratch depth

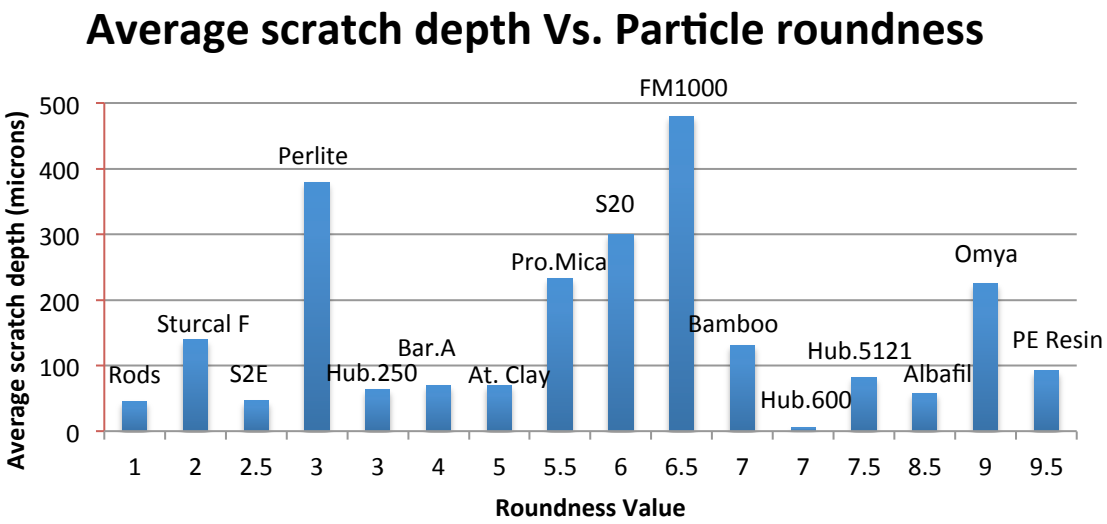

Figure A5.2.

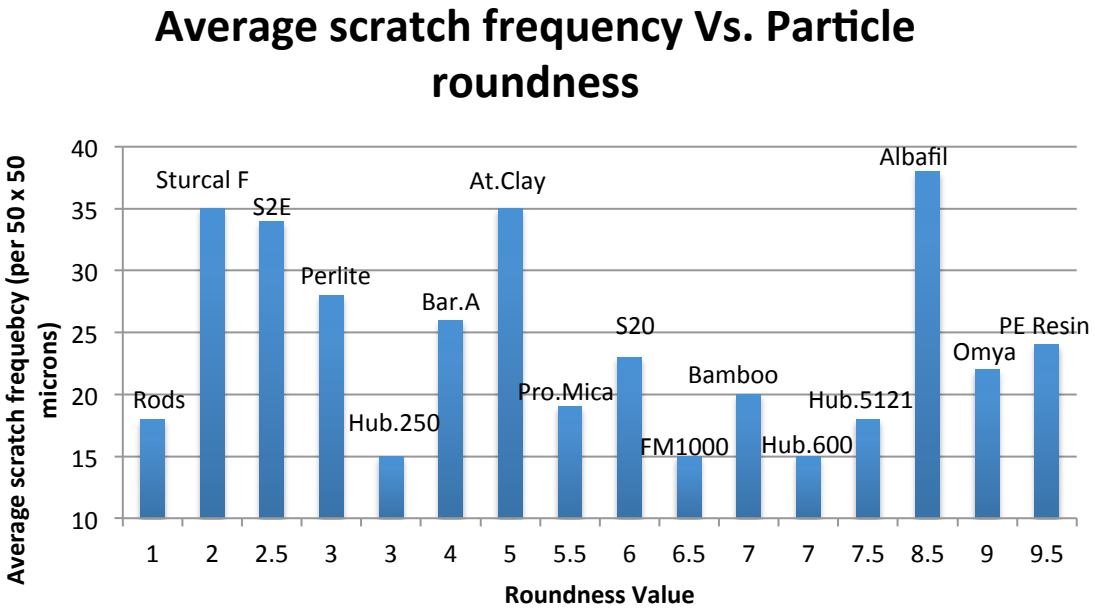

Figure A5.3.